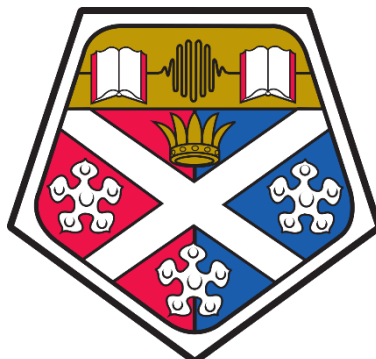


University of Strathclyde
Department of Pure and Applied Chemistry



Metal-Free C-H Functionalisation Methods

*A thesis submitted to the University of Strathclyde in part fulfilment of regulations for
the degree of Doctor of Philosophy in Chemistry.*

Tomasz Mirosław Kubczyk

Supervised by Professor Nicholas C. O. Tomkinson

2016

Declaration

This thesis is the result of the author's original research. It has been composed by the author and has not been previously submitted for examination which has led to the award of a degree.

The copyright of this thesis belongs to the author under the terms of the United Kingdom Copyright Acts as qualified by University of Strathclyde regulation 3.50. Due acknowledgement must always be made of the use of any material contained in, or derived from, this thesis.

Signed

Date

Abstract

This thesis describes the development of two metal-free C–H functionalisation methods which encompass oxidations of sp^3 - and sp^2 -hybridised C–H bonds.

Chapter 1 provides a brief introduction to the rapidly growing area of C–H functionalisation and outlines selected metal-catalysed and metal-free C–H functionalisation methods.

Chapter 2 describes the development of a novel metal-free C–H functionalisation method of alkanes, from concept, through initial investigations, optimisation and substrate scope to mechanistic studies.

Chapter 3 gives a detailed account of the development and mechanistic investigations of peroxide-mediated C–H functionalisation method exclusive to aromatic C–H bonds.

Chapter 4 presents the experimental data obtained in the process of developing the new methodologies described herein.

Chapter 5 contains an appendix.

Chapter 6 contains a bibliography.

Acknowledgements

First and foremost, I would like to express my sincere gratitude to my Ph.D. supervisor, Professor Nick Tomkinson, for giving me the opportunity to undertake novel and interesting projects for the Ph.D. programme of study. His great mentorship and continuous support, patience, motivation, enthusiasm, as well as immense knowledge let me thrive as a researcher.

The work, at times, would have been much less enjoyable were it not for the people, past and present, involved in the Tomkinson group. Special shouts go to Dr Mike Rawling, Dr Julian Rowley from Swindon, Lola ‘Demonio’ Beltran, Andrei ‘Pula’ Dragan and ‘Ma Chérie’ Camille Indey, who have shared more of my ups and downs than most. Many cheers go to Stuart Davidson and Liam McCarron for being outstanding hosts in the great country of Scotland. Muchos gracias to Carla ‘La Colchonera’ Ferrer for teaching me a bit of Spanish. I also owe a special thank you to Andrei Dragan who was a great project partner.

I would also like to thank the post-doctoral co-workers, Dr Justyna Wojno, Dr Heulyn Jones, Dr James Tellam, Dr Stefano Bresciani, and all the technical staff at the University of Strathclyde, whom I had the pleasure of working with.

I am immensely grateful to Dr Filipe Vilela, Dr Stephen Sproules, Dr Alan Kennedy and Dr John Parkinson, who have proven to be exceptional collaborators.

Finally, I would like to thank my wife for her tremendous support and encouragement over the last three years, without which the completion of this thesis would not have been even remotely possible.

Table of Contents

Declaration	II
Abstract.....	III
Acknowledgements	IV
Table of Contents	V
Abbreviations	XI
1. Introduction	1
1.1. Transformations in Organic Chemistry	1
1.2. Challenges in C–H Functionalisation	1
1.3. Nature’s solution to C–H Functionalisation	4
1.4. Synthetic Strategies towards C–H Functionalisation	4
1.4.1. C–H Activation Induced by Heterogeneous Metal Catalysts.....	5
1.4.2. C–H Activation Induced by Homogeneous Metal Catalysts.....	8
1.4.2.1. Oxidative Addition-Reductive Elimination.....	9
1.4.2.2. σ -Bond Metathesis.....	9
1.4.2.3. 1,2-Insertion-Elimination	10
1.4.2.4. Homolytic Cleavage by Two Metalloradicals.....	10
1.4.2.5. Electrophilic Activation.....	11
1.4.2.6. Indirect Activation by Metal Complexes	12
1.4.3. Enzymatic Systems.....	12
1.4.4. Metalloporphyrins	14
1.4.5. Non-Heme Catalysts.....	16
1.4.6. Functional Group-Directed C–H Functionalisation	18
1.4.7. Metal-Free C–H Activation and Functionalisation	19
1.4.7.1. Dioxiranes 83	20
1.4.7.2. Oxaziridines 84	21

1.4.7.3. Perhydrates 85	22
1.4.7.4. Peracid-Induced C-H Functionalisation	22
1.5. Conclusions	23
1.6. Project Overview	24
2. Functionalisation of sp ³ C-H Bonds	25
2.1. Early Concepts.....	25
2.2. Reaction Monitoring.....	26
2.3. Initial Investigations	29
2.4. Keto-Enol Peracid Equilibria	31
2.5. Quantitative Reaction Monitoring	35
2.6. Optimisation of the Reaction System	36
2.6.1. The Role of Atmospheric Oxygen.....	36
2.6.2. Source and Quantity of Hydrogen Peroxide 58	37
2.6.3. Reaction Time	43
2.6.4. Effect of Temperature.....	44
2.6.5. Effect of Stirring.....	45
2.6.6. Effect of Light	45
2.6.7. Solvent System	46
2.6.8. Concentration Range	50
2.6.9. Generation of Water	51
2.6.10. Alternative Peroxide Sources	52
2.6.11. <i>In Situ</i> Generation of Diphenylketene 120	54
2.6.12. Isocyanate and Isothiocyanate Substrates	55
2.6.13. Alternative Ketenes	56
2.6.14. Summary.....	60
2.7. Substrate Scope	60

2.7.1. Cycloalkanes.....	60
2.7.2. Saturated Heterocycles	62
2.7.3. Aryl Substrates	63
2.7.4. Linear Alkanes.....	65
2.7.5. Future Directions	66
2.8. Mechanistic Studies.....	67
2.8.1. Control Reactions	67
2.8.2. First Proposed Mechanism	68
2.8.3. Second Proposed Mechanism.....	69
2.8.4. Deuterium Studies	70
2.8.5. Singlet vs. Triplet Oxygen.....	81
2.8.6. ¹⁸ O- Labelling Studies	84
2.8.7. Further ¹⁸ O- labelling Studies.....	90
2.8.8. Generation of ¹⁸ O-Labelled Hydrogen Peroxide 58-¹⁸O	94
2.8.9. Generation of Hydroperoxy Radical 170	96
2.8.10. α -Lactone Intermediate.....	97
2.8.11. Co-product Identification	100
2.8.12. Over-oxidation.....	106
2.8.13. Reactions with Peracids.....	107
2.8.14. Revision of Reaction Mechanism 2.....	109
2.9. Concluding Remarks and Future Directions	111
3. Functionalisation of sp ² C–H Bonds	114
3.1. Introduction	114
3.2. Attribution	114
3.3. Initial Investigations	115
3.4. Substrate Scope	116

3.5. Mechanistic Considerations.....	120
3.5.1. The Radical Mechanism.....	121
3.5.2. Single Electron Transfer (SET) Mechanism	122
3.5.3. The Ionic Mechanism.....	124
3.5.4. Initial Observations	124
3.5.5. Preliminary Experiments.....	124
3.5.6. Mechanistic Studies.....	125
3.5.6.1. Acid Catalysis.....	126
3.5.6.2. Effect of Water	129
3.5.6.3. Reaction Kinetics.....	132
3.5.6.4. Hammett Study.....	134
3.5.6.5. Isotopic Labelling Studies	137
3.5.6.6. Mechanistic Probes.....	140
3.5.6.7. Electron Paramagnetic Resonance Studies.....	148
3.6. Conclusions	150
4. Experimental.....	152
4.1. General Experimental Details.....	152
4.2. Synthesis of Carboxylic Acids	154
4.3. General Procedure 1: Acid Chloride Synthesis.....	157
4.4. Synthesis of diphenylketene 120 ¹¹⁹	159
4.5. Synthesis of diphenylacetic anhydride 214 ¹²⁰	160
4.6. General Procedure 2: Ester Synthesis.....	161
4.7. General Procedure 3: Ester Synthesis 2 ⁵³	161
4.8. General Procedure 4: sp ³ C–H Bond Oxidation.....	171
4.9. General Procedure 5: Internal Standard Checks.....	171
4.10. Synthesis of Carbamates and Thiocarbamates	172

4.11. General Procedure 6: Diester Synthesis	174
4.12. General Procedure 7: Keto-enol Studies	178
4.13. General Procedure 8: Isotopic Labelling Studies Using $^{18}\text{O}_2$ Gas	178
4.14. Synthesis of $\text{D}_2\text{O}_2\cdot\text{urea}$ 122-D	180
4.15. General Procedure 9: Deuterium Studies	180
4.16. General Procedure 10: Payne Epoxidation ⁸³	181
4.17. Preparation of 4,7-diphenylbenzo[<i>c</i>]-1,2,5-thiadiazole 182 ¹²³	181
4.18. Singlet Oxygen Experiments	182
4.18.1. Trapping Singlet Oxygen ⁷⁸	182
4.18.2. Generation of Singlet Oxygen	183
4.18.2.1. Method 1 ⁷⁹	183
4.18.2.2. Method 2 ⁸¹	183
4.19. Generation of hydrogen peroxide 58 ⁸⁴	184
4.20. Generation of <i>t</i> -butyl hydroperoxide 126 ⁸⁵	185
4.21. General Procedure 11: Derivatisation of cyclohexyl 2,2-diphenylacetate 110	186
4.22. Synthesis of cyclopropane-1,1-dicarboxylic acid 280 ¹²⁵	186
4.23. Synthesis of cyclopropyl malonoyl peroxide 241 ⁹⁷	187
4.24. General Procedure 12: Oxidation of Arenes	188
4.25. General Procedure 13: Aminolysis of Esters.....	192
4.26. Synthesis of 1-(3,5-dimethylphenyl)-2-phenylacetylene 303 ¹²⁸	193
4.27. Synthesis of Alkenes	194
4.28. General Procedure 14: Cyclopropanation	196
4.29. General Procedure 15: Hammett Analysis	198
4.30. Synthesis of <i>N</i> -sulfonyl imine 297 ¹³²	200
4.31. Synthesis of 307-trans	201

4.32. Synthesis of 310-trans	201
4.33. General Procedure 16: Effect of Water	202
4.34. General Procedure 17: EPR Experiments.....	203
4.34.1. Control Reactions	203
4.34.2. Purification of DMPO 312	204
4.34.3. Sample Preparation for EPR Studies.....	204
5. Appendix	206
5.1. X-Ray Crystallographic Data	206
5.2. Selected ¹ H NMR Spectrometric Data	242
5.3. Selected Mass Spectrometric Data	246
6. References	255

Abbreviations

Various abbreviations have been used throughout this thesis that may not be familiar to the reader. These abbreviations are listed below:

Å	Ångström
AcOH	acetic acid
atm.	atmospheric
APCI	atmospheric pressure chemical ionisation
aq.	aqueous
Ar	aryl
b.p.	boiling point
BPMCN	<i>N,N'</i> -bis(2-pyridylmethyl)- <i>N,N'</i> -dimethyl-1,2-cyclohexanediamine
BPMEN	<i>N,N'</i> -bis(2-pyridylmethyl)- <i>N,N'</i> -dimethyl-ethylene-1,2-diamine
BP	British Petroleum
br	broad
Bu	butane
Bz	benzoyl
cal	calories
cod	1,5-cyclooctadiene
CI	chemical ionisation
cm	centimetre(s)
Cp	cyclopentadienyl
c-Pr	cyclopropyl
C	Celsius
CETOH	2-chloroethanol
CIEEL	chemically initiated electron-exchange luminescence
conv.	conversion
Cy	cyclohexyl
CyH	cyclohexane
d	doublet

DCC	<i>N,N'</i> -dicyclohexylcarbodiimide
dd	doublet of doublets
ddd	doublet of doublets of doublets
DEG	diethylene glycol
dm	decimetre(s)
dt	doublet of triplets
DMAP	4-dimethylaminopyridine
DME	1,2-dimethoxyethane
DMF	dimethyl formamide
DMPO	5,5-Dimethyl-1-pyrroline- <i>N</i> -oxide
dr	diastereomeric ratio
<i>ee</i>	enantiomeric excess
Et	ethyl
equiv.	equivalent(s)
EI	electron impact
EPR	Electron Paramagnetic Resonance
ESI	electrospray ionisation
EtOAc	ethyl acetate
EtOH	ethanol
FG	functional group
g	gram(s)
GC	gas chromatography
GC-MS	gas chromatography-mass spectrometry
h	hour(s)
HC	hydrocarbon
hept	heptet
HFIP	1,1,1,3,3,3-hexafluoroisopropanol
HRMS	high-resolution mass spectrometry
Hz	Hertz
IR	infra-red
<i>J</i>	coupling constant
J	joules

kcal	kilocalories
kJ	kilojoules
kton	kilotons
lit.	literature
LRMS	low-resolution mass spectrometry
<i>m</i>	meta
m	multiplet
M	molar
MA	maleic anhydride
Me	methyl
med	medium
mg	milligram(s)
MHz	megahertz
min	minute(s)
mL	millilitre(s)
μL	microliter(s)
mol	mol(es)
mm	millimetre(s)
MMO	methane monooxygenase
mmol	millimole(s)
m.p.	melting point
MS	mass spectrometry
<i>m/z</i>	mass-to-charge ratio
nbe	norbornene
nm	nanometre(s)
NMR	nuclear magnetic resonance
Nu	nucleophile
NSI	nano-electrospray
<i>p</i>	para
PCA	pyrazine-2-carboxylic acid
PFB	perfluoro- <i>tert</i> -butanol
Ph	phenyl

POM	polyoxometalate
Porph	porphyrin
Ph	phenyl
ppm	parts per million
Pr	propyl
q	quartet
recryst.	recrystallised
<i>rel</i>	relative
r.t.	room temperature
select.	selectivity
TCE	2,2,2-trichloroethanol
TEMPO	2,2,6,6-Tetramethylpiperidine 1-oxyl
TFA	trifluoroacetic acid
TFE	2,2,2-trifluoroethanol
THF	tetrahydrofuran
Tip/tipyl	2,4,6-triisopropylphenyl
TLC	thin layer chromatography
TMG ₂ dien	2',2-(2-2'-(methylazanediyl)-bis(ethane-1,2-diyl))bis(1,1,3,3-tetramethylguanidine
TMG ₃ tren	tri(2-(<i>N</i> -tetramethylguanidyl)ethyl)amine
TON	turnover
TPA	tris(2-pyridylmethyl)amine
td	triplet of doublets
tt	triplet of triplets
UV	ultraviolet
VPO	vanadium phosphorus oxide
vs	versus
wk	weak
Z	charge
2D	two-dimensional

Chapter 1: Introduction

1. Introduction

1.1. Transformations in Organic Chemistry

Organic compounds either form the basis of, or are important constituents of, many products including medicines, perfumes, paints, petrochemicals, and food.¹ Their properties are determined by the spatial arrangement and types of chemical groups, known as functional groups, which these molecules contain. Typically, the introduction of a desired functional group into a molecule relies on the modification of pre-existing functionality, e.g. conversion of cyclohexyl chloride **1** into cyclohexanol **2** (**Figure 1.1a**). However, this approach can involve many steps, making it costly and time-consuming. An alternative approach that shows great promise is C–H activation and functionalisation. This strategy converts a C–H bond into a useful functional group, for example cyclohexane **3** into cyclohexanol **2** (**Figure 1.1b**). By employing this approach additional synthetic steps may be avoided, thus improving the step, atom and redox economy of the synthetic process.²

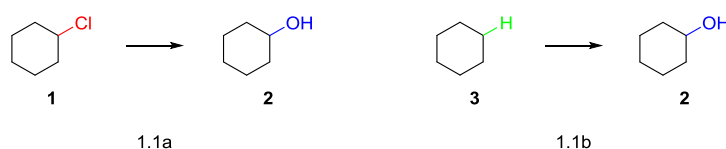


Figure 1.1. Traditional (1.1a) and alternative (1.1b) approach to functionalisation.

1.2. Challenges in C–H Functionalisation

Most organic compounds, particularly alkanes, have numerous C–H bonds. Although these bonds are considered to be one of the least reactive groups, they have attracted much attention because alkanes are readily available from natural gas and crude oil, and are inexpensive. Thus C–H activation and functionalisation is often branded as the ‘Holy Grail’ of synthetic organic chemistry. However, the deliberate and selective transformation of C–H bonds into useful functional groups has been a challenge in synthetic organic chemistry for over 100 years. In the late nineteenth century, Hoffman³ reported a direct halogenation of unactivated C–H bonds but it was not until 50 years later

that the area of C–H activation really began to flourish. One reason for this was that alkanes are fairly unreactive because the C–C and C–H bonds are relatively strong.⁴ For example, the bond dissociation energy of a primary, secondary and tertiary C–H bond in 2-methyl butane **4** is about 101, 98, and 96 kcal mol⁻¹, respectively. The bond dissociation energy of the sp² C–H bond on a benzene ring is 113 kcal mol⁻¹, and the methyl C–H bond in toluene **5** is 90 kcal mol⁻¹. The bond dissociation energy of the C–C bond in ethane **6** is 88 kcal mol⁻¹ (**Figure 1.2**).

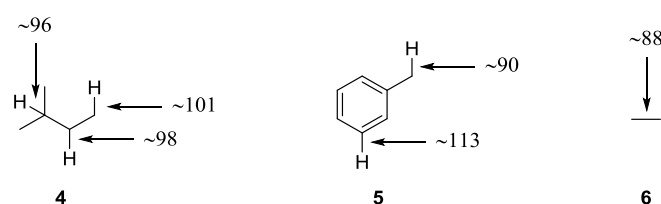
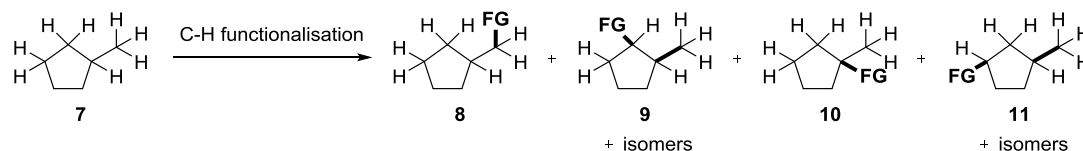


Figure 1.2. Bond dissociation energies (kcal mol⁻¹) of selected hydrocarbons.

Another potential problem in establishing C–H functionalisation as a structural synthetic method is the ubiquity of C–H bonds in organic molecules. Complex molecules often contain multiple C–H bonds which have different levels of reactivity and some oxidation systems cannot discriminate between individual primary, secondary and tertiary C–H bonds (**Scheme 1.1**). The low reactivity of alkanes also means that either severe reaction conditions or highly reactive reagents must be used to functionalise these substrates. In either case, more than one possible product can be formed, which further decreases selectivity. For example, oxidation of simple hydrocarbons, such as methylcyclopentane **7**, can lead to as many as ten different mono-functionalised products including **8**, **9**, **10**, and **11**.



Scheme 1.1. An example of regioselectivity challenge in C–H functionalisation.

In addition, targeting a specific molecule in a mixture of chemical substances can be difficult, let alone a specific site in a molecule. The presence of two or more C–H bonds of the same type at different positions in a molecule but in similar chemical environments

is frequently encountered. For example, oxidation of dihydrojunenol **12** to either 4-epiajanol **13** or dihydroxyeudesmane **14** may be desirable, yet represents a formidable synthetic challenge (**Figure 1.3**).

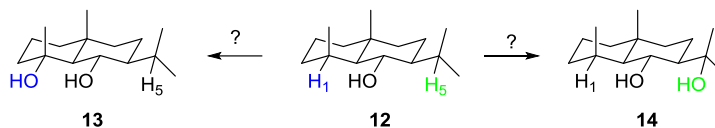
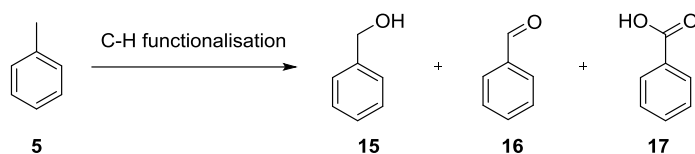


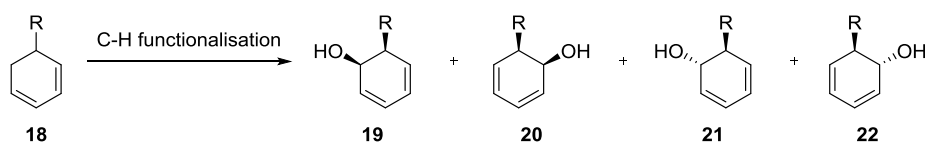
Figure 1.3. An example of site-selective oxidation challenge in C–H functionalisation.

An additional challenge in C–H functionalisation arises when stopping a reaction at the correct oxidation level and thus achieving good chemoselectivity is required. Ideally, the oxidation system should deliver a single product. Failure to prevent the desired product from over-oxidation often results in unwanted co-products. Likewise, incomplete oxidation may produce extraneous co-products. For example, oxidation of toluene **5** may lead to three possible products: benzyl alcohol **15**, benzaldehyde **16**, and benzoic acid **17** (**Scheme 1.2**).



Scheme 1.2. An example of chemoselectivity challenge in C–H functionalisation.

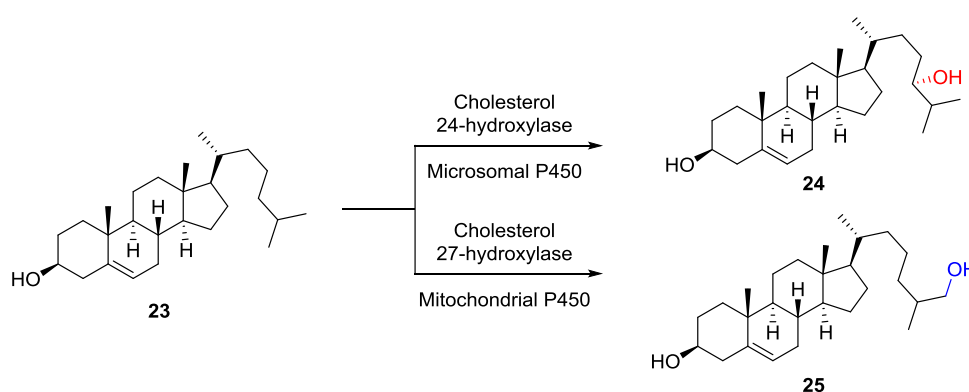
Finally, achieving high levels of stereoselectivity and/or enantioselectivity in C–H functionalisation adds to the array of challenges synthetic chemists must address. For example, the oxidation of **18** may lead to the products **19–22** (**Scheme 1.3**).



Scheme 1.3. An example of stereoselectivity challenge in C–H functionalisation.

1.3. Nature's solution to C–H Functionalisation

Nature has overcome many challenges related to C–H functionalisation by using enzymes, which act as catalysts in hydrocarbon oxidation. The combination of molecular recognition, such as size and/or shape selectivity, substrate orientation and catalytic metal centres allows excellent chemo-, regio- and stereoselectivity to be achieved.⁵ The ability of enzymes to catalyse the hydroxylation of saturated C–H bonds, the epoxidation of double bonds, the oxidation of heteroatoms, dealkylation reactions, oxidative deamination and many others,⁶ is crucial in important biochemical processes. An example of selective oxidation is the hydroxylation of cholesterol **23** by the cytochrome P450 24-hydroxylase (found almost exclusively in brain) and 27-hydroxylase (found in organs and tissues) to 24-hydroxycholesterol **24** and 27-hydroxycholesterol **25**, respectively (**Scheme 1.4**).⁷



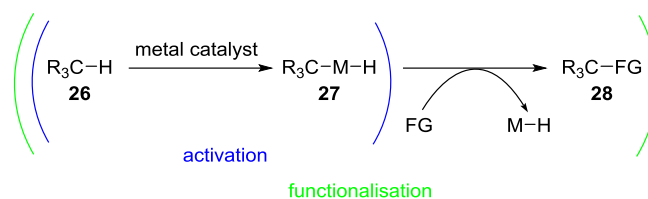
Scheme 1.4. An example of site- and stereoselectivity in C–H functionalisation.

In these and other biochemical reactions, a C–H bond on the substrate is selectively oxidised to give a product, which can undergo further transformations or have a specific biological effect.

1.4. Synthetic Strategies towards C–H Functionalisation

The inert nature of saturated hydrocarbons makes the transformation of most C–H bonds into useful functional groups challenging. Therefore, scientists have been trying to discover and develop strategies to overcome the difficulty associated with this problem.

It is important to distinguish between C–H activation and C–H functionalisation at this stage as these terms are sometimes used interchangeably and incorrectly. The term ‘activation’ is used within this thesis to mean that the reactivity of a C–H bond has been increased. This often involves replacement of a carbon–hydrogen bond **26** with a carbon–metal complex **27**. Subsequent cleavage of the C–M bond may or may not lead to the desired product **28** (**Scheme 1.5**).



Scheme 1.5. General scheme of metal-catalysed C–H activation and functionalisation.

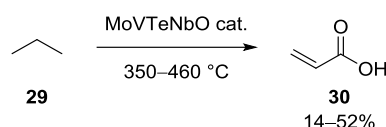
The term ‘functionalisation’ is used to describe replacement of hydrogen in a C–H bond **26** with a functional group, e.g. **28**. This may be achieved by means other than metal-catalysed activation.

To date, numerous methods of C–H functionalisation have been developed and it is helpful to divide them into major subfields based on the C–H activation approach: heterogeneous metal catalysis, homogenous metal catalysis, enzymatic and biomimetic methods, strategies using metalloporphyrins and non-heme catalysts, and functional group directed and metal-free approaches. A brief overview of the salient features of these strategies is presented in this introduction. For simplicity, only methods capable of converting sp^3 C–H bonds into C–O bonds are discussed. The methodologies described within this introduction are exemplary only and are not exhaustive. Numerous other methods exist and the reader is referred to comprehensive reviews and other publications relating to C–H functionalisation such as .

1.4.1. C–H Activation Induced by Heterogeneous Metal Catalysts

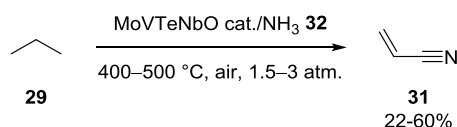
The application of heterogeneous metal catalysts in C–H functionalisation is a very attractive goal. However, few reactions have been successfully employed on the industrial scale.

Candidates for the selective oxidation of alkanes include mixed-metal oxide complexes, often containing vanadium as one of the elements. The potential of molybdenum- and vanadium-based mixed oxides as oxidation catalysts was reported by Bartek *et al.*⁸ in 1993 but the catalysts generally produced low to moderate yields of the product. A few years later Ushikubo *et al.*⁹ and Lin and Linsen¹⁰ reported Mo-V-Te-Nb-O catalysts which oxidised *n*-propane **29** to acrylic acid **30** in up to 52% yield (**Scheme 1.6**).



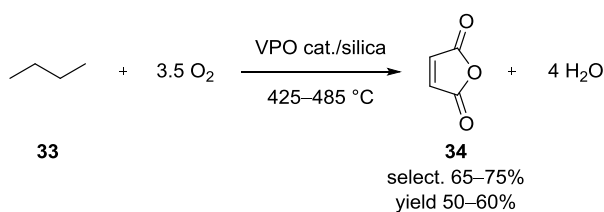
Scheme 1.6. Conversion of *n*-propane **29** to acrylic acid **30** using MoVTeNbO catalysts.

Interestingly, these catalysts were also effective at oxidising *n*-propane **29** to acrylonitrile **31** when ammonia **32** was present (**Scheme 1.7**).¹¹



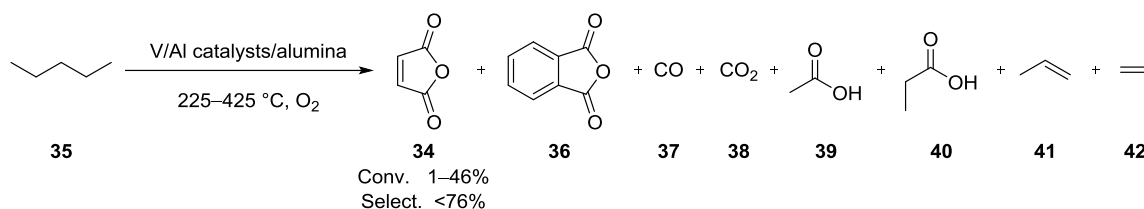
Scheme 1.7. Conversion of *n*-propane **29** to acrylonitrile **31** using MoVTeNbO catalysts.

Another series of catalysts of the V-Sb-O family found industrial applications when in 1997 BP opened a unit for the production of acrylonitrile **31** from propane **29** *via* a process referred to as ammoxidation.¹² Scientific studies followed and soon it became clear that the catalytic properties could be altered by modifying the elements in the vicinity of vanadium. As a result, a family of vanadium phosphorus oxide (VPO) catalysts ensued. They are currently used to catalyse the oxidation of *n*-butane **33** to maleic anhydride **34** with high selectivities (65–75%) and moderate yields (50–60%) on the industrial scale (500 kton of MA annually) (**Scheme 1.8**).¹³



Scheme 1.8. Commercial conversion of *n*-butane **33** to maleic anhydride **34**.

High selectivities were achieved in similar transformations by adjusting the ratio of metals comprising the catalysts, as was shown in the V/Al-catalysed oxidation of *n*-pentane **35** to maleic anhydride **34** (Scheme 1.9).¹⁴ Yields in the range of 1–46% and good selectivities (up to 76%) were achieved with phthalic anhydride **36**, carbon monoxide **37**, carbon dioxide **38**, acetic acid **39**, propanoic acid **40**, propene **41** and ethene **42** as the co-products.



Scheme 1.9. Commercial conversion of *n*-pentane **35** to maleic anhydride **34**.

Another class of heterogeneous catalysts capable of selective oxidation of alkanes and other hydrocarbons is the polyoxometalate (POM) group. Most notable examples include the oxidation of isobutane **43** to methacrolein **44** (conv. 1–5%, select. 3–80%) and other products (methacrylic acid **45**, carbon monoxide **37**, carbon dioxide **38**, and acetic acid **39**) using $\text{H}_3\text{PMo}_{12}\text{O}_{40}$ and vanadium substituted derivatives,¹⁵ oxidation of propane **29** to acrylic acid **30**,¹⁶ and oxidation of methane **46** to formic acid **47**¹⁷ (conv. <1%) using Pd-Cs salts of $\text{PVMo}_{11}\text{O}_{40}$ (Figure 1.4).

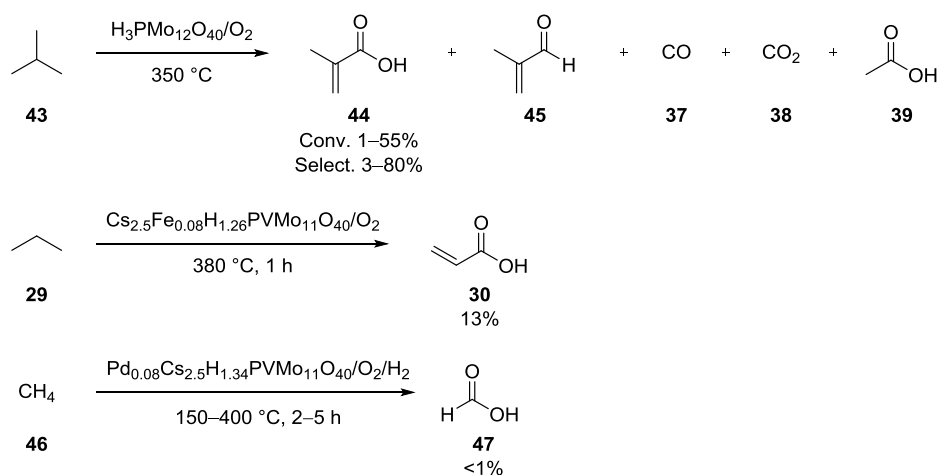


Figure 1.4. Examples of C–H functionalisation by the POM group of catalysts.

In summary, the attractiveness of this approach is recognisable as it makes the separation and re-use of catalysts simple and cheap as they are recycled by filtration. On the other hand, harsh reaction conditions result in less economic processes and therefore production plants are often built in locations where energy is inexpensive. Additional drawbacks are the lack of applicability to solid substrates and heat transfer problems that may be encountered.¹⁸ Lack of fundamental mechanistic understanding allowing an empirical and logical improvement of heterogeneous catalysts has been a major barrier to their development and wider application.

1.4.2. C–H Activation Induced by Homogeneous Metal Catalysts

The exact nature of C–H activation promoted by metal complexes varies depending on the substrate, solvent, transition metal and ligands in the metal complex. However, C–H activation induced by homogenous catalysts can be divided further based on the character of interaction between metal and alkane into: oxidative addition-reductive elimination, σ -bond metathesis, 1,2-insertion-elimination, homolytic cleavage by two metalloradicals, electrophilic activation, and indirect activation by metal complexes (**Figure 1.5**).¹⁹

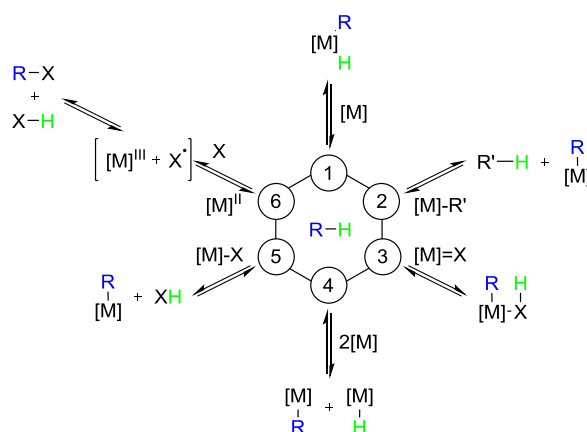
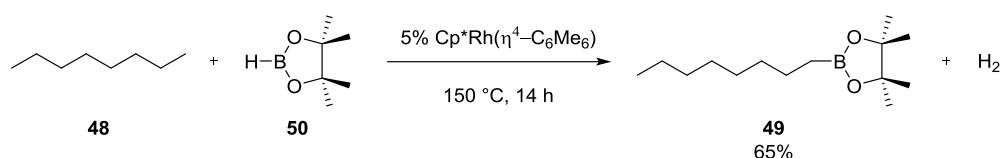


Figure 1.5. A simplified representation of commonly invoked C–H bond activation mechanisms:

- (1) oxidative addition-reductive elimination, (2) σ -bond metathesis, (3) 1,2-insertion-elimination, (4) homolytic cleavage by two metals, (5) electrophilic activation, (6) indirect activation by metal complexes.¹⁹

1.4.2.1. Oxidative Addition-Reductive Elimination

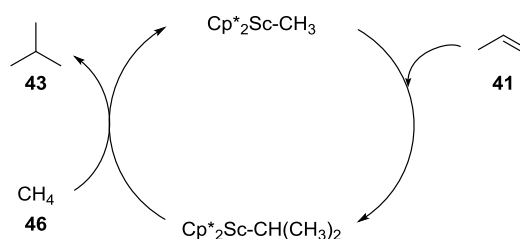
Oxidative addition-reductive elimination is the most common mechanism, in which the metal directly interacts with alkane breaking the C–H bond and making the M–C and M–H bond. The reactive metal fragment frequently has cyclopentadienyl (Cp), phosphine or CO ligands. Typical metals are second and third row transition metals, and either weak oxidants or no oxidants are used due to oxidative degradation of these metal complexes. This approach exhibits the inversion of selectivity typical of radical and electrophilic pathways in which C–H bonds tend to be oxidised in the following order: tertiary > secondary > primary. An example in which this approach was successfully applied in the functionalisation of unreactive C–H bonds was reported by Hartwig *et al.*,²⁰ who oxidised octane **48** to alkylborane **49** in the presence of pinacolborane **50** and a rhodium catalyst (Scheme 1.10).



Scheme 1.10. Preparation of linear alkylborane **49** from unactivated alkane **48** via oxidative addition-reductive elimination mechanism.

1.4.2.2. σ -Bond Metathesis

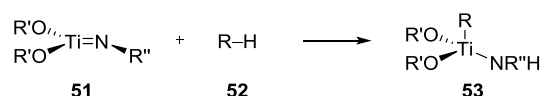
σ -Bond metathesis is a one-step reaction by which two σ bonds are broken and two new σ bonds are formed in a concerted manner without change of the metal oxidation state. For redox-inactive metals with d^0 electronic configuration and the f-block (groups 3 and 4, lanthanides and actinides), an oxidative process is not possible, and the preferred mechanism is σ -bond metathesis. The commonly accepted intermediate is formed by electrophilic attack of the metal. σ -Bond metathesis is usually used with unsaturated reagents for an efficient process (Scheme 1.11). For example, Barros and others combined propene **41** and methane **46** to make isobutane **43** in up 99% by using a scandium catalyst.²¹



Scheme 1.11. Hydromethylation of propene **41** via σ -bond metathesis mechanism.

1.4.2.3. 1,2-Insertion-Elimination

When an early transition metal is coordinated to a ligand with π -bonding capability (e.g. alkoxide, amide, imide, etc.), the unsaturation at the metal centre is stabilised through π -donation from the ligand. The M=X functionality (X = OR, NR, NR₂, CR, CR₂) adds to the C–H bond, and the 1,2-addition product M(XH)R results. **Scheme 1.12** shows such an addition of (OR')₂Ti=N-R'' **51** (R' = H, SiH₃, SiMe₃, Si^tBu₃) to reagent **52** (R = Me, Et, vinyl, c-Pr, Cy, Ph, Bz) to give (OR')₂TiR(NR''H) **53**.²²

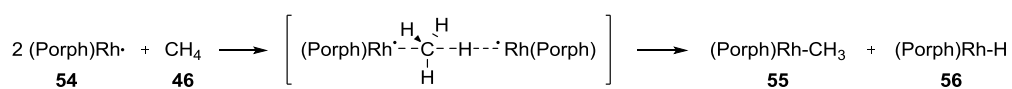


Scheme 1.12. Formation of (OR')₂Ti–NRH complex **53** via 1,2-insertion mechanism.

Reductive elimination can then lead to a hetero-functionalised hydrocarbon. If the regeneration of the M=X group could be made catalytic, this would constitute a major advance.

1.4.2.4. Homolytic Cleavage by Two Metalloradicals

In 1991, Wayland and his group found that porphyrin Rh(II) complexes such as **54** react with methane **46** (and other hydrocarbons) in the temperature range of 23–120 °C to give equimolar amounts of (Porph)Rh–CH₃ **55** and (Porph)Rh–H **56** (**Scheme 1.13**).²³



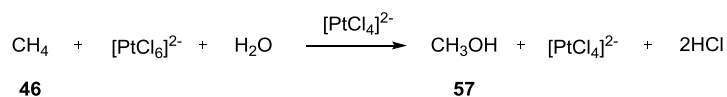
Scheme 1.13. Activation of C–H bond in methane **46** via homolytic cleavage by two metalloradicals.

There is strong evidence that these reactions take place in a linear fashion, in which one metal centre attacks the methane carbon and the other abstracts a hydrogen atom. The resulting products can potentially lead to organic products and regeneration of the catalyst but more research is needed to achieve this ultimate goal.

1.4.2.5. Electrophilic Activation

Despite slight progress of the first four C–H activation mechanisms in selective C–H functionalisation, none of these systems is close to commercialisation. Catalysts capable of inducing oxidative-reductive elimination and homolytic cleavage by two metalloradicals are oxidatively unstable, and those capable of inducing σ -bond metathesis and 1,2-insertion-elimination form prohibitively strong metal–OR bonds, thereby inhibiting further functionalisation.

In contrast, electrophilic activation by late transition metals, such as Pt(II), Pd(II), Tl(III), and Hg(II) provides one of the most promising systems. Discovered in the early 1970's by Shilov and his group,²⁴ the oxidation of methane **46** to methanol **57** (Scheme 1.14) is yet to be improved.

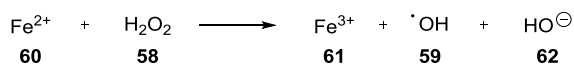


Scheme 1.14. Oxidation of methane **46** by the Shilov system – example of electrophilic activation.

Although none of the systems developed to date is in commercial use, the remarkable selectivity of these systems is encouraging. Noticeably, a primary C–H bond is more reactive than a C–H bond neighbouring a functional group, such as a hydroxyl group. In fact, the order of reactivity for alcohols and ethers is $\alpha\text{-C-H} < \beta\text{-C-H} < \gamma\text{-C-H} < \delta\text{-C-H}$, and for carboxylic acids, sulfonic acids and phosphonic acids, it is $\alpha\text{-C-H} < \beta\text{-C-H} < \gamma\text{-C-H} \approx \delta\text{-C-H}$.²⁵ Recent developments are encouraging for an eventual application on an industrial scale.²⁶

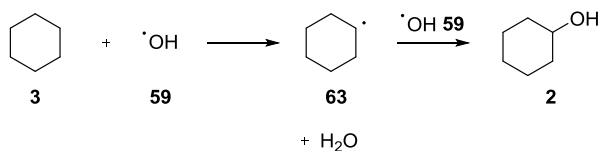
1.4.2.6. Indirect Activation by Metal Complexes

Another type of activation is when a metal complex promotes the formation of a reactive species, which then attacks the C–H bond. The mechanisms described earlier require a contact between the metal and the C–H bond, whereas complexes falling into this category initially activate another reactant, i.e. O₂ or H₂O₂ **58**, to form a reactive species that attacks the C–H bond. Such species are usually radicals, such as hydroxyl radicals **59**. An example of this is the Fenton reaction.²⁷ Treatment of an Fe(II) salt **60** with aqueous hydrogen peroxide **58** results in the oxidation of **60** to Fe(III) **61**, and the decomposition of **58** to hydroxyl radicals **59** and hydroxyl anions **62** (Scheme 1.15).



Scheme 1.15. Indirect activation by metal complexes – the Fenton reaction.

Hydroxyl radicals **59** can then react with an alkane, such as cyclohexane **3**, to form cyclohexyl radicals **63**, which may go on to give other products, e.g. cyclohexanol **2** (Scheme 1.16).

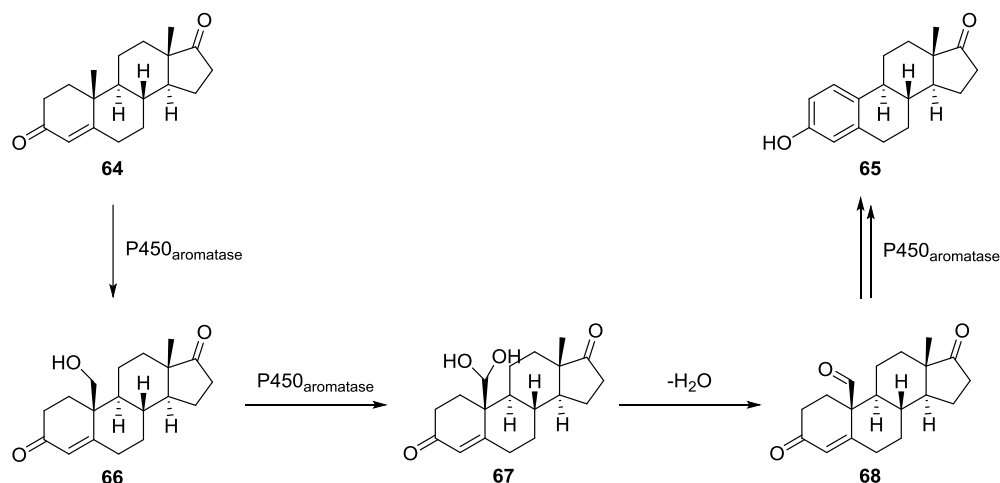


Scheme 1.16. Indirect activation of cyclohexane **3** by hydroxyl radicals **59**.

1.4.3. Enzymatic Systems

Natural enzymes catalyse a variety of C–H bond functionalisations. Their efficiency in these processes facilitates their increased use as biocatalysts. The biggest advantage of enzymes is their unparalleled selectivity, which is often utilised when control of chemo-, regio- or enantioselectivity in chemical transformations is required. In many cases, >99% enantiomeric excess (*ee*) can be achieved when enzymes are used. An example showcasing the extraordinary selectivity of enzymes is the conversion of androst-4-ene-3,17-dione **64** into estrone **65** catalysed by human placental aromatase

(Scheme 1.17).²⁸ This reaction involves three consecutive oxidative steps: two hydroxylations at the 19-methyl group to give **66** and **67** and a final oxidative decarbonylation of the intermediate aldehyde **68**. All three reactions are stereospecific.



Scheme 1.17. Conversion of androst-4-ene-3,17-dione **64** into estrone **65** catalysed by human placental aromatase.

In addition, enzymes are highly active under mild conditions such as temperature, pressure and pH, which renders them extremely useful on both small and industrial scale. Another benefit is that reactions are preferentially carried out in aqueous media. Using water as solvent is desirable within an industrial setting as it is more environmentally-friendly and attains sustainable development. A further advantage is the broad diversity of reactions that can be catalysed by enzymes, which means their application on the industrial scale is progressively increasing.

Irrespective of the advantages, there are also certain drawbacks to using enzymes. The availability of enzymes for commercial exploitation has been limited due to a lack of in-depth characterisation of many enzymes. This often means that although theoretically a wide range of reactions can be catalysed by enzymes, only certain substrates can be directly used due to the size-selection preferences of a given enzyme. Enzymes also require co-substrates and co-factors, which may translate into higher costs. More importantly, they sometimes lack stability in varying conditions and desirable media. When harsher temperatures, pressures or pH are required to maximise efficiencies and yields, the stability of enzymes is rather limited and often leads to their deactivation.

Furthermore, it is difficult to develop simple synthetic analogues of natural enzymes because the whole enzyme structure, and not just the active site, often determines its reactivity. Therefore, the grand challenge to a synthetic chemist lies in the preparation of model compounds that sufficiently mimic the steric and electronic effects of enzymes, and can catalyse a variety of reactions under varying conditions. For a more thorough understanding, the reader is referred to comprehensive reviews on enzymatic C–H functionalisation, such as that of Arnold *et al.*²⁹ or Hollman *et al.*³⁰

1.4.4. Metalloporphyrins

Most research inspired by enzymatic C–H functionalisations has been focused on mimicking biological systems, for example by using iron, manganese and ruthenium as the metal centre in a porphyrin frame. This approach has been called ‘biomimetic’.

Iron-containing enzymes comprise a large group of enzymes, which can be divided into two subgroups based on the active site structures, i.e. heme and non-heme containing enzymes. In 1979, Groves and his group, inspired by the presence of an iron porphyrin at the active site in cytochrome P450 enzymes, reported the first example of metalloporphyrin-catalysed hydroxylation of saturated C–H bonds.³¹ They demonstrated the oxidation of cyclohexane **3** and adamantane **69**. Typically, iodosyl benzene **70** was added over 30 min to a solution of the catalyst and hydrocarbon substrate in dichloromethane. The reactions carried out at room temperature and under a nitrogen atmosphere gave cyclohexanol **2** or 2-adamantol **71** and 1-adamantol **72** in 8, 1, and 12% yield, respectively (**Figure 1.6**).

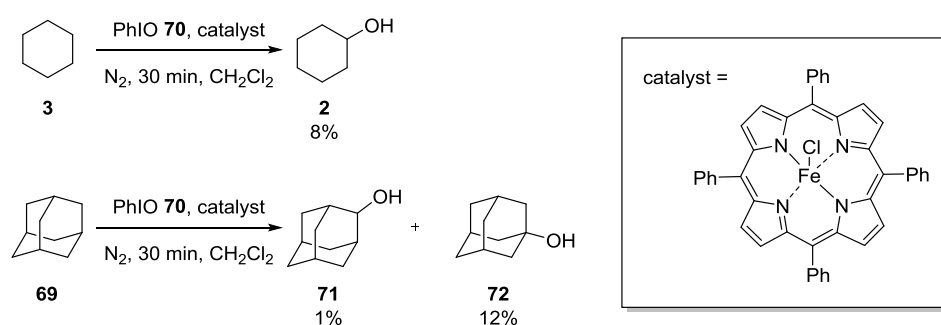


Figure 1.6. Hydroxylation of cyclohexane **3** and adamantane **69**.

groups³³ have achieved regioselective oxidation with porphyrin-based catalysts but their substrates were attached to the catalysts through covalent bonds, which prevented turnover and generally showed a trend towards stoichiometric rather than catalytic oxidation. (3) Porphyrin ligands are thermally labile and thus prone to oxidative self-degradation, and (4) often require an expensive oxidant such as iodosyl benzene **70**. Although metalloporphyrin-catalysed oxidations of alkanes have been intensively studied and significant progress in addressing the challenges associated with them has been made, there is a growing interest in catalysis by other types of metal complexes.

1.4.5. Non-Heme Catalysts

Alongside the ubiquitous P450-based enzymes with an iron-porphyrin in the active site, non-heme iron enzymes have emerged as an important class of enzymes in the past decade. Like their heme counterparts, they promote a number of important biological reactions, including desaturation, cyclisation, hydroxylation, dihydroxylation, epoxidation and sulfoxidation reactions.³⁴ Biomimetic systems that model non-heme iron enzymes are sought-after because these enzymes are excellent at oxygen and peroxide activation.

Non-heme metal catalysts can be classified as mononuclear or binuclear depending on the number of metal ions. Mononuclear non-heme iron catalysts perform a diverse array of transformations including functionalisation of C–H bonds. They do so by involving either high-spin ferrous (Fe^{2+}) ions or high-spin ferric (Fe^{3+}) active centres. The most effective non-heme iron catalysts that oxidise alkane substrates are usually

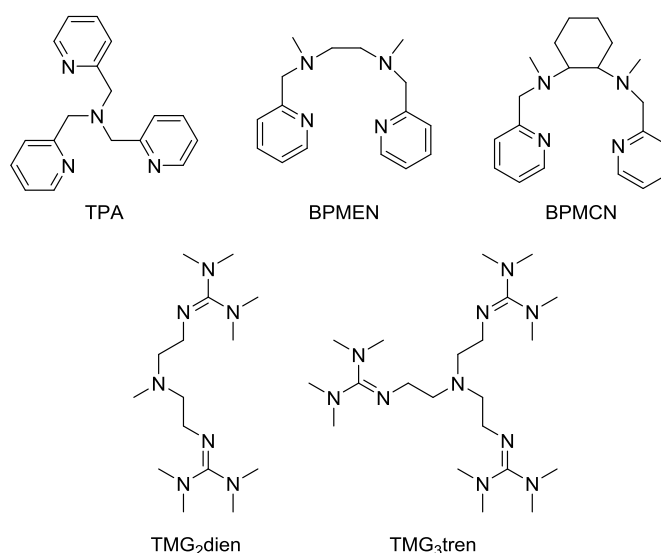
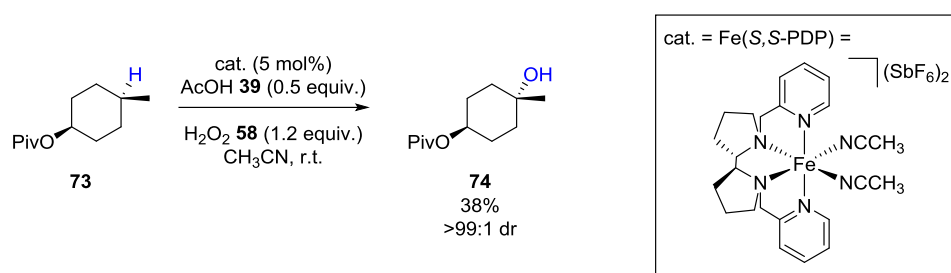


Figure 1.8. Commonly used ligands in mononuclear non-heme iron catalysts.

mononuclear iron catalysts with neutral, multidentate ligands such as TPA, BPMEN and BPMCN, tetramethylguanidines and their derivatives (**Figure 1.8**).

A prime example is the oxidation of pivalate **73** to the hydroxylated product **74** reported by Chen and White (**Scheme 1.18**).³⁵ The iron complex with a PDP scaffolding effectively used hydrogen peroxide **58** and acetic acid **39** to achieve a yield of 38% of the oxidised product with an excellent diastereomeric ratio (>99:1 dr).



Scheme 1.18. Hydroxylation of **73** with a non-heme iron catalyst.

Non-heme iron catalysts have shown a great promise for oxidations of unactivated sp^3 C-H bonds but their applications have been somewhat limited due to the required large substrate to oxidant ratio, low catalyst turnover numbers, and poor selectivities for product formation. Attempts have been made to overcome and improve some of these drawbacks by developing catalysts with different metal ions. The most commonly encountered metals are manganese and copper. The oxidation chemistry of manganese complexes has developed rapidly since Hage published in *Nature* the very high bleaching catalytic effect of some manganese complexes, such as **75–79** (**Figure 1.9**).³⁶

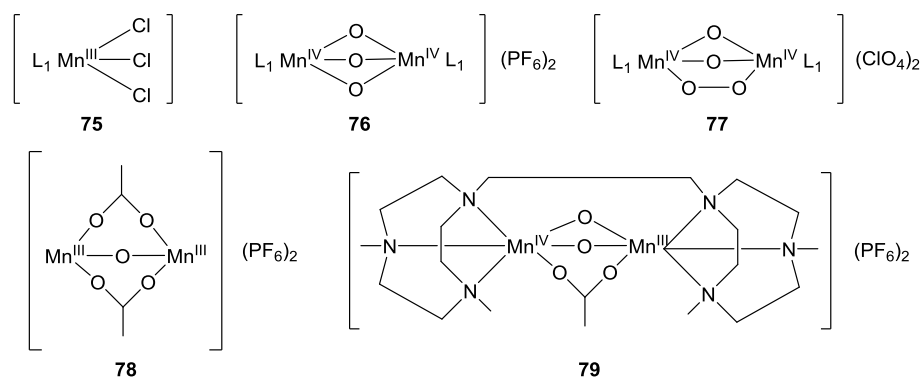
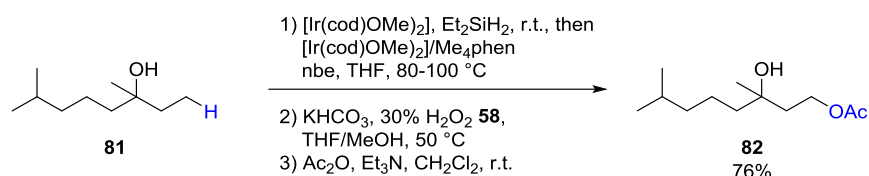


Figure 1.9. Mn complexes with high catalytic bleaching effect.

new methods that would make use of functional groups that exist in the target molecule. An excellent example is the work of Simmons and Hartwig.⁴¹ Iridium-catalysed silylation of 3,7-dimethyl-octan-3-ol **81** to 3,7-dimethyl-1-acetate-1,3-octanediol **82** was achieved by adding methanol **57**, KHCO_3 and H_2O_2 **58** to the crude silylation mixture, heating to $50\text{ }^\circ\text{C}$, and acylating to give product **82**, which was easily purified by silica gel chromatography (**Scheme 1.20**).



Scheme 1.20. C–H bond functionalisation directed by an alcohol group.

1.4.7. Metal-Free C–H Activation and Functionalisation

The usual catalyst in C–H transformations contains a transition metal, which activates a suitable oxygen source and allows functionalisation of the C–H bond. Such catalysts have to withstand harsh conditions (high temperatures and pressures) typically employed in the industry but oxidative degradation renders some catalysts inefficient. An alternative approach is to use oxidatively resistant organic systems which would achieve C–H functionalisations without the need of metal complexes. Non-metal organic oxidants, notably dioxiranes **83**, oxaziridines **84**, perhydrates **85**, oxaziridinium salts **86** and oxoammonium salts **87** have become available in recent years (**Figure 1.10**).

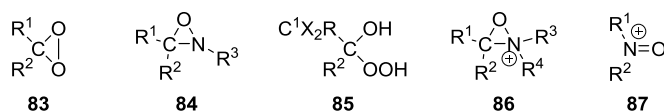


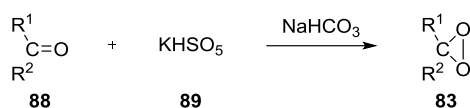
Figure 1.10. Dioxirane **83**, oxaziridine **84**, perhydrate **85**, oxaziridinium salt **86** and oxoammonium salt **87**.

Perhydrates **85** are only briefly discussed below due to their similarity to peracids and their potential in C–H functionalisation, while oxaziridinium salts **86** and oxoammonium salts **87** are not due to lack of scientific literature on their functionalisation of unactivated

C–H bonds. Activation by halogen radicals is deliberately omitted as this method is well-established in the scientific literature.⁴²

1.4.7.1. Dioxiranes **83**

Dioxiranes **83** are three-membered ring peroxides, which are easily synthesised from ketones **88** and Oxone[®] (**Scheme 1.21**), whose active species is potassium monoperoxysulfate (KHSO₅) **89**, a readily available and cheap industrial chemical.⁴³



Scheme 1.21. Preparation of dioxiranes **83**.

The carbon atom can be replaced by a heteroatom to give heteroatom-containing dioxiranes (**Figure 1.11**), where X can be P, N, Si, S, Se, Ge, Sn, Pb or Te.⁴⁴

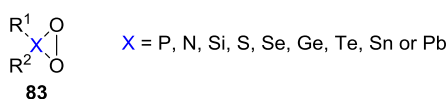
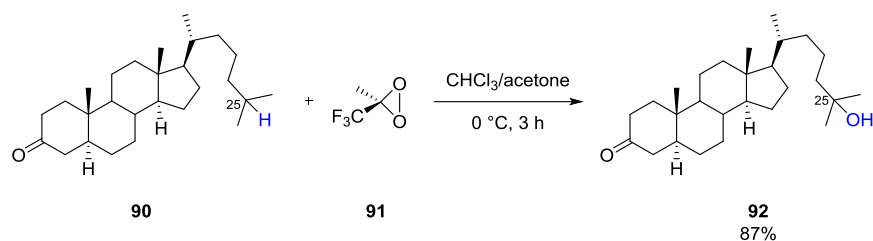


Figure 1.11. Heteroatom-containing dioxiranes **83**.

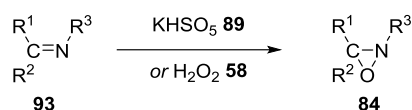
During the past twenty years, the successful use of dioxiranes as a class of powerful and versatile oxygen-transfer reagents has been demonstrated for a variety of substrates.⁴⁵ Although epoxidations have received the greatest focus, dioxiranes have been shown to be capable of C–H functionalisations, often exhibiting remarkable selectivity. An excellent example is that published by Bovicelli *et al.*,⁴⁶ in which a tertiary C–H bond at C₂₅ of **90** was selectively oxidised to a hydroxyl group using dioxirane **91** to give steroid **92** (87%) (**Scheme 1.22**).



Scheme 1.22. Selective hydroxylation using methyl(trifluoromethyl)dimethyldioxirane **91**.

1.4.7.2. Oxaziridines **84**

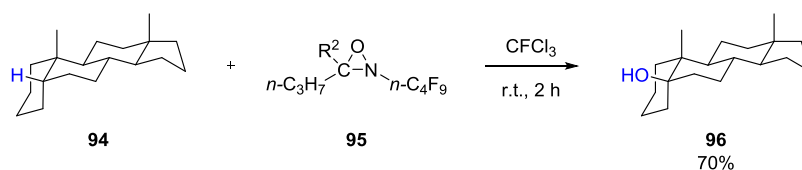
Oxaziridines **84** represent a class of three-membered heterocyclic compounds containing oxygen, nitrogen and carbon. They can be prepared in a similar manner to dioxiranes by the addition of potassium monoperoxysulfate **89** or hydrogen peroxide **58** to an imine **93** (**Scheme 1.23**).



Scheme 1.23. Preparation of oxaziridines **84**.

Although generally less reactive than dioxiranes **83**, oxaziridines **84** are powerful oxidants due to the three-membered ring strain and the relatively weak N–O bond ($\sim 53 \text{ kcal mol}^{-1}$).⁴⁵

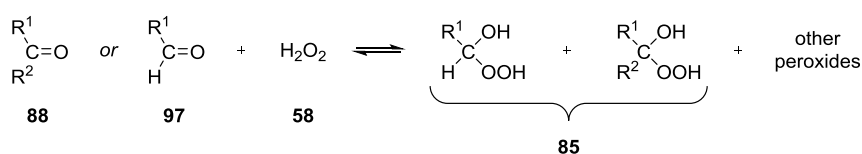
Among oxaziridines, perfluorinated oxaziridines deserve a special mention due to their oxidising power. This class of oxidant has proven efficient in the regioselective and often diastereoselective hydroxylation of various hydrocarbon substrates. An illustrative example of that was reported by Arnone.⁴⁷ Treatment of the unfunctionalised steroid **94** with perfluoro-*cis*-2-*n*-butyl-3-*n*-propyloxaziridine **95** gave **96** in 70% yield after just 2 h at room temperature (**Scheme 1.24**).



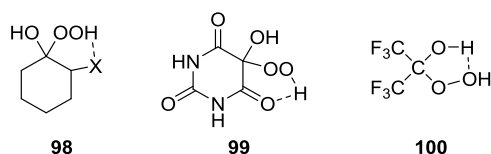
Scheme 1.24. Selective hydroxylation using perfluorinated oxaziridine **95**.

1.4.7.3. Perhydrates **85**

Perhydrates **85**, also called α -hydroperoxides, are derivatives of ketones **88** and aldehydes **97**, from which they are ordinarily prepared by the addition of hydrogen peroxide **58** (Scheme 1.25).

Scheme 1.25. Preparation of perhydrates **85**.

Other methods for the synthesis of this class of compound involve photooxygenation of non-tertiary alcohols and the ozonolysis of alkenes in the presence of water or alcohol.⁴⁵ They are relatively unstable species and tend to revert to the starting materials, with a few exceptions, such as **98–100**, that are more stable probably due to intramolecular hydrogen bonding (Figure 1.12).

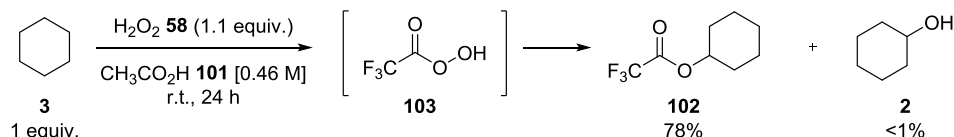
Figure 1.12. Stable perhydrates reported in the literature.⁴⁵

The perhydrate of hexafluoroacetone **100** is most reactive among perhydrates and is a strongly electrophilic oxidant, which effectively oxidises a variety of organic compounds.⁴⁵ They hold great potential as effective C–H functionalisation reagents due to the weak O–O bond, just like those found in peracids, but their potential in C–H functionalisation is yet to be fully exploited.

1.4.7.4. Peracid-Induced C–H Functionalisation

Reports of peracid-induced C–H functionalisations are scarce. In 1976, Deno and Messer reported a successful hydroxylation of cyclohexane **3** with hydrogen peroxide **58** and

trifluoroacetic acid **101** as the reaction medium.⁴⁸ Although a mixture of products (**102** and **2**) was obtained, the reaction proceeded at room temperature within 24 h (**Scheme 1.26**).



Scheme 1.26. Peracid-induced C–H functionalisation of cyclohexane **3**.

This reaction provided important mechanistic implications pointing to trifluoroacetic peracid **103** as the reactive species and set an important precedent. Astonishingly, this transformation passed largely unnoticed and remained conceptually underdeveloped. A few attempts have been made to improve yields and selectivities using metal catalysts⁴⁹ but analogous catalytic metal-free methods have not been developed.

1.5. Conclusions

Transition metal C–H activation and subsequent functionalisation reactions have attracted enormous interest due to several aspects that make those transformations attractive. The inherently low reactivity of saturated alkanes is usually easily overcome by the replacement of a C–H bond with a C–M bond, and quite often can be done in a predictable fashion. Their reactivity can be altered by modifying the shape and nature of ligands, which may result in good to excellent stereoselectivity. Some metals are easily accessible (e.g. iron is the fourth most abundant element in the Earth’s crust) and are relatively cheap. However, most metals are expensive and toxic, and metal catalysts often require complicated synthetic preparations, bespoke supporting ligands, high temperatures and pressures, and costly waste water treatment. They can be more difficult to handle and may be air- or/and water-sensitive. Furthermore, upon activation they may form a complex that is too stable to react further, and consequently inhibit subsequent functionalisation.

Enzymatic and biomimetic systems have also been studied, developed and utilised in C–H functionalisation but an alternative route, which would generate a reactive species capable

of reacting with the hydrocarbon independent of any participation of the metal complex, is highly desirable.

1.6. Project Overview

New methodologies which functionalise C–H bonds with a high level of precision and predictability in the absence of a transition metal are highly desirable and needed. Some organic oxidation systems, such as dioxiranes **83** or oxaziridines **84**, have been successfully used to a certain degree but the spectrum of possibilities for metal-free C–H functionalisation is immense and has not been explored to the full.

Our approach to the design of novel sustainable C–H functionalisation methods was based on the following guiding principles: (1) reactions should proceed at room temperature, (2) in the presence of moisture and air, (3) and reagents should be available in no more than three synthetic steps.

The desire to use a readily accessible and cheap oxidant was inspired by biological systems and directed our search towards simple functionalisation methodologies capable of oxidising unactivated alkanes.

Chapter 2: Functionalisation of sp^3 C–H Bonds

2. Functionalisation of sp^3 C–H Bonds

2.1. Early Concepts

The foundation of this project was molecular modelling by Carpenter⁵⁰ who found that homolytic cleavage of the O–O bond of acetic peracid **104k** to give radical **105** and hydroxyl radical **59** required around 43 kcal mol^{-1} of energy. Generally, in carbonyl chemistry, enol tautomers are thermodynamically less stable than the corresponding keto tautomers.⁵¹ Therefore, it was reasonable to hypothesise that enol tautomers of carboxylic peracids would be less stable than the corresponding keto tautomers. Carpenter found that the energy difference between the keto tautomer **104k** and the enol tautomer **104e** of acetic peracid was around 16 kcal mol^{-1} . He also calculated that radicals **106** and **59**, formed upon homolytic cleavage of the O–O bond of **104e**, would be *ca.* 20 kcal mol^{-1} lower in energy than radical **105** and **59**. Putting all this information together yielded strong predictions that if conditions favouring the equilibrium towards peracid enol tautomer **104e** could be found, an energy input of around 7 kcal mol^{-1} would be needed to break the weak O–O bond and thereby generate hydroxyl radical **59** and radical **106** (Figure 2.1).

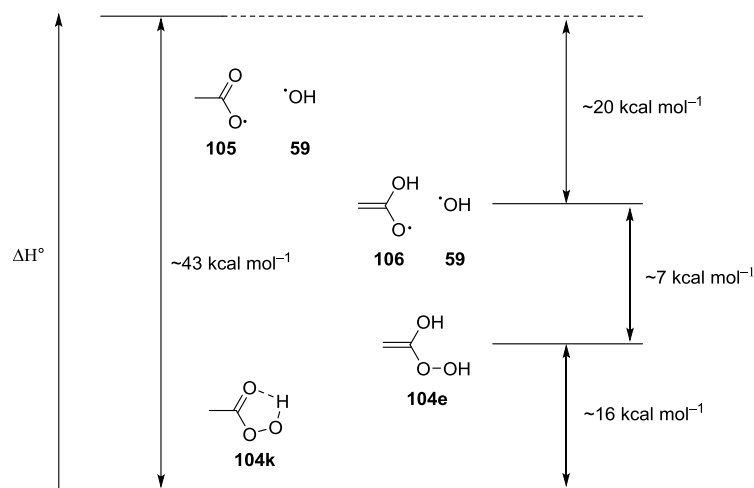
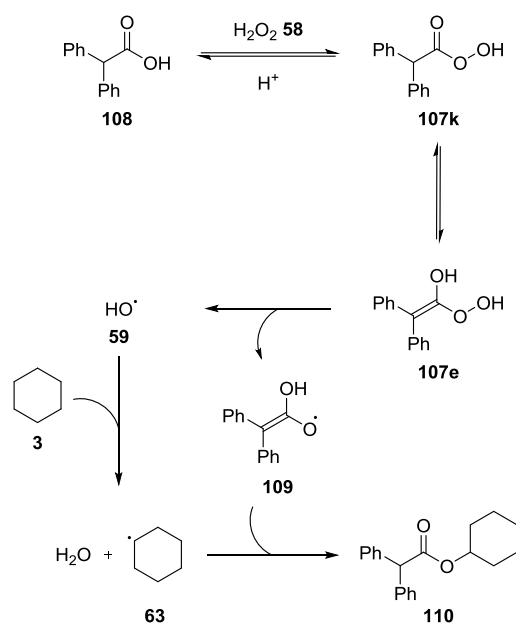


Figure 2.1. Relative energies of keto and enol acetic peracid tautomers **104k** and **104e** and radicals arising from the homolytic O–O bond cleavage.

On the basis of these calculations, we envisaged that the oxidation of unactivated alkanes, such as cyclohexane **3**, could be achieved by an *in situ* formation of peracid, e.g.

diphenylacetic peracid **107k**, from its parent acid, diphenylacetic acid **108**, and hydrogen peroxide **58** in the presence of a catalytic amount of a strong acid. Assuming that peracid **107k** would be in equilibrium with its enol tautomer **107e**, the weak O–O bond of **107e** should spontaneously break, thereby generating hydroxyl radical **59** together with radical **109**. The very reactive hydroxyl radical **59** could, in turn, abstract a hydrogen atom from a molecule of cyclohexane **3** to give cyclohexyl radical **63** and a molecule of water. Recombination of cyclohexyl radical **63** with radical **109** would give ester **110** upon tautomerisation (**Scheme 2.1**).



Scheme 2.1. Proposed pathway for the oxidation of alkanes.

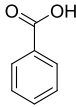
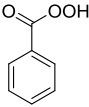
Based upon this modelling and initial scheme we set out to discover if we could bring about reaction of diphenylacetic acid **108** and cyclohexane **3** to form ester **110** in the presence of hydrogen peroxide. In principle, this would deliver a new C–H functionalisation protocol that generates water as the sole co-product of the reaction.

2.2. Reaction Monitoring

Before any practical work could begin, a method of monitoring the reaction, and more specifically, the formation of peracids and their respective tautomers had to be developed. Quantitative analysis of peracids is typically achieved by iodometric titration, while a

qualitative analysis can be accomplished by investigating NMR spectra as shown by Tuttle *et al.*⁵² A noticeable difference in the obtained ^1H NMR (~ 12 ppm; ~ 13 ppm), ^{13}C NMR (167 ppm; 169 ppm), and ^{17}O NMR (252 ppm; 317 and 275 ppm) chemical shift of benzoic acid **17** and benzoic peracid **111**, respectively, was reported by this group (**Table 2.1**).

Table 2.1. The most distinctive ^1H NMR, ^{13}C NMR and ^{17}O NMR chemical shifts of benzoic acid **17** and benzoic peracid **111**.

		
	17	111
^1H NMR/ppm	12.0 ± 0.5 (OH)	13.2 ± 0.5 (OOH)
^{13}C NMR/ppm	167 (C=O)	169 (C=O)
^{17}O NMR/ppm	252 (OOH)	317, 275 (OOOH)

To validate these findings and explore their potential in reaction monitoring, a commercially available sample of an acetic peracid **104** solution containing approximately 45% of acetic acid **39** was analysed by ^1H and ^{13}C NMR spectroscopy. The ^1H NMR spectrum showed a singlet for acetic acid **39** at δ 2.09 ppm (confirmed by spiking) and a singlet for acetic peracid **104** at δ 2.03 ppm (**Figure 2.2**), while ^{13}C NMR spectrum showed acetic acid **39** peaks at δ 20.6 ppm and 177.3 ppm, and acetic peracid **104** peaks at δ 17.0 ppm and 171.6 ppm (**Figure 2.3**). The difference in chemical shift between acetic acid **39** and peracid **104** was unequivocal and presented a potential tool for distinguishing between carboxylic acids and their corresponding peracids.

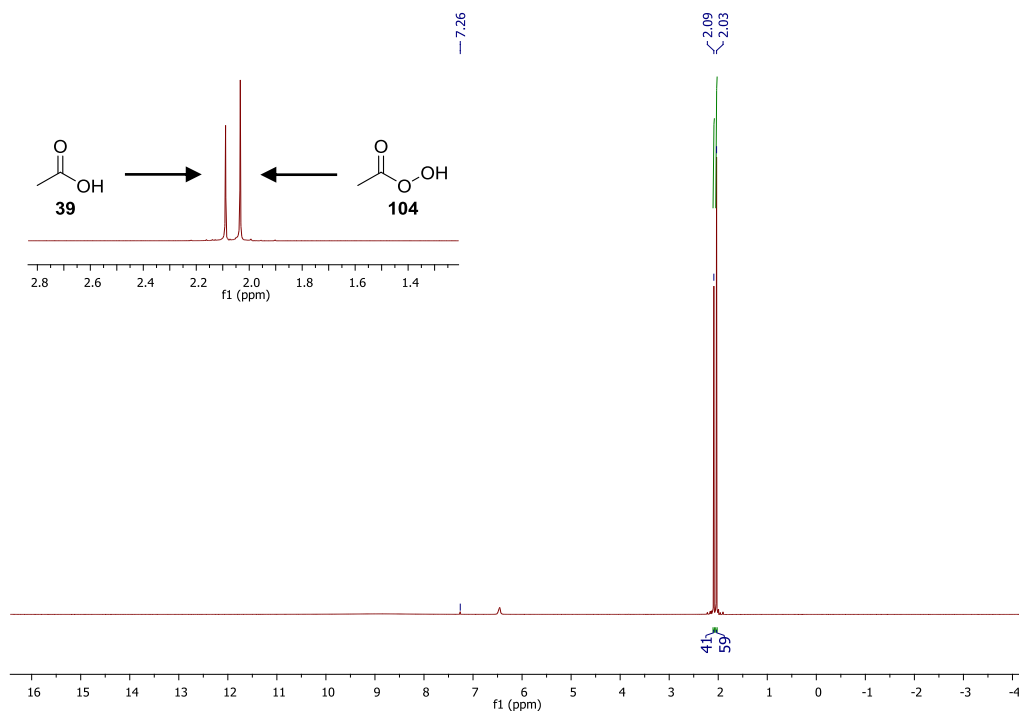


Figure 2.2. ^1H NMR spectrum of acetic peracid **104** solution containing acetic acid **39**.

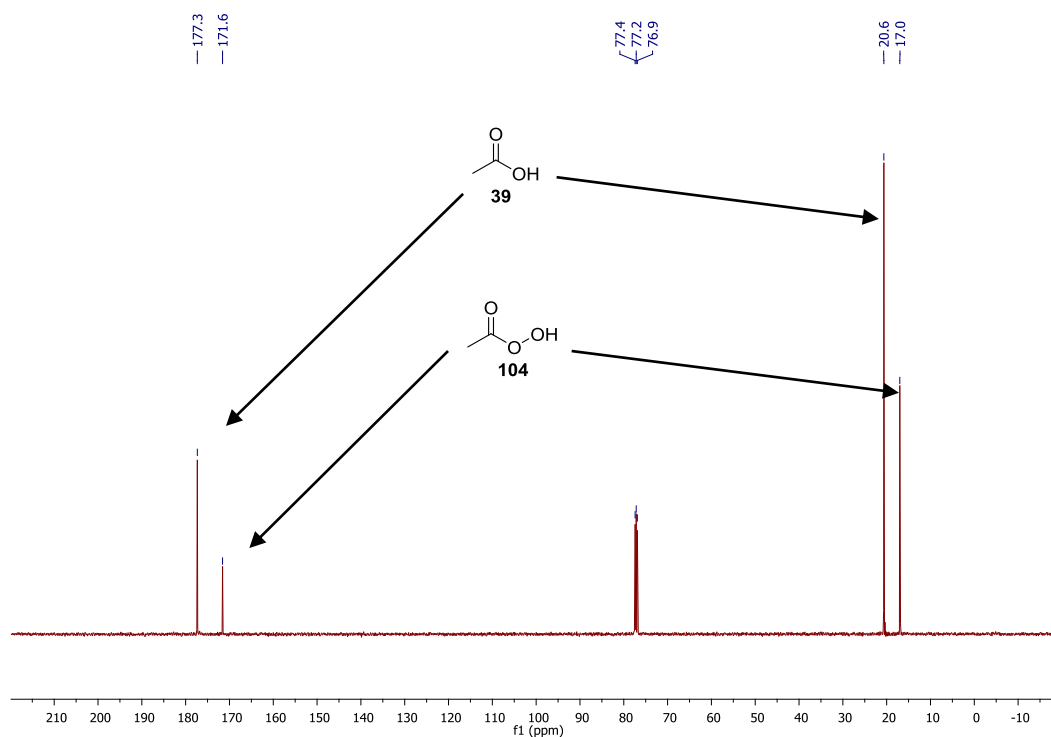


Figure 2.3. ^{13}C NMR spectrum of acetic peracid **104** solution containing acetic acid **39**.

Since iodometric titration is labour-intensive and time-consuming, and a change in ^1H and ^{13}C NMR chemical shift between an acid and a peracid was evident, it was decided

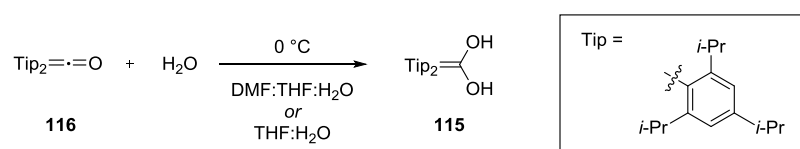
hydrogen peroxide **58** (30% w/w) could achieve equilibrium within 24 h at 30 °C in the presence of sulfuric acid (1–1.5 mol%).⁵⁷ Each of these methods was briefly examined but no clear indication of the formation of **110** or **112** was seen when the reaction was conducted in the respective hydrocarbon solvents.

Analysis of the reaction by thin layer chromatography showed no additional spots, which seemed to indicate that peracid **107** either did not form, which would be consistent with ¹H NMR analysis, or decomposed on the silica plate.

2.4. Keto-Enol Peracid Equilibria

We considered our lack of success could have been due to three possible reasons: (1) the desired peracid **107k** was not being formed; (2) tautomerisation of the keto tautomer **107k** to the enol tautomer **107e** of diphenylacetic peracid was not taking place; (3) cleavage of the O–O bond was not occurring under the reaction conditions. Since preparation methods of peracids are well established, and the energy barrier of ~ 7 kcal mol⁻¹ is relatively small, it was hypothesised that tautomerisation of **107e** to **107k** could be faster than the homolytic cleavage of the O–O bond.

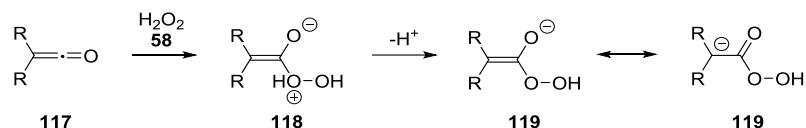
To the best of our knowledge, no quantitative data on peracid keto-enol equilibria have been reported in the scientific literature. However, several enols of carboxylic acids (1,1-enediols) have been observed. Notably, Frey and Rappoport⁵⁸ reported the generation of solutions of $\geq 98\%$ of 2,2-ditipylethene-1,1-diol **115** (tipyl = Tip = 2,4,6-triisopropylphenyl), which could be stored at –18 °C for one week. The enediol **115** was prepared by hydration of ditipylketene **116** in a mixture of DMF:THF:H₂O in a 42:3:5 ratio (alternatively THF:H₂O in a 9:1 ratio) at 0 °C (**Scheme 2.5**).



Scheme 2.5. Formation of 2,2-ditipylethene-1,1-diol **115**.

Co-solvent(s) had to be used since ditipylketene **116** was insoluble in water. The authors listed a number of prerequisites that the ideal co-solvent should fulfil: (1) it must dissolve the ketene; (2) be water miscible; (3) be unreactive towards the ketene; (4) be commercially available in its polydeuteriated form to enable NMR study; (5) be a good hydrogen-bond acceptor since the analogous 1,1-enediols are stabilised by hydrogen-bond accepting solvents.

In order to observe 1,1-enediols, their generation had to be much faster than their tautomerisation to the keto form. It can be reasonably assumed that the same applies to peracid enols. Hence, accelerating the nucleophilic attack by hydrogen peroxide **58** on a ketene or decreasing the ketonisation rate should increase the lifetime of the desired intermediates. A close look at a plausible mechanism of peracid formation reveals that a reaction between hydrogen peroxide **58** and a ketene **117** gives rise to a zwitterionic species **118** first, and then to a carbanion **119** whose charges are delocalised on C_β (**Scheme 2.6**). Consequently, electron-withdrawing substituents on C_β should stabilise the transition state and accelerate the reaction.



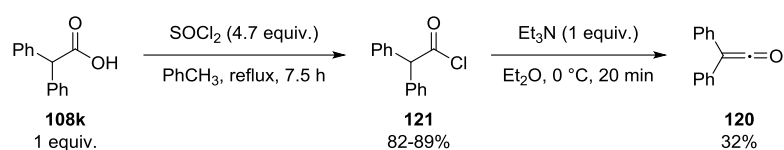
Scheme 2.6. Nucleophilic attack of hydrogen peroxide **58** on a ketene **117**.

At this stage we were clearly having problems with forming the peracid **107k**. Whilst this was frustrating, it was not considered crucial to the investigation where we wished to establish if **107e** was an efficient source of hydroxyl radical **59**. Drawing inspiration from the work of Rappoport^{58a} we decided to investigate the addition of peroxide to a ketene in order to form an enol peroxide directly (**Scheme 2.6**). If success was achieved, it was intended to revisit direct formation of the peracid at a later stage in the investigation.

The steric and electronic properties of ditipylketene **116** would make it a good substrate for our reaction if it was not for the potential radical side-reactions of the primary and (especially) tertiary C–H bonds of the isopropyl groups of **116** that could take place. Diphenylketene **120**, on the other hand, offered similar structural and electronic

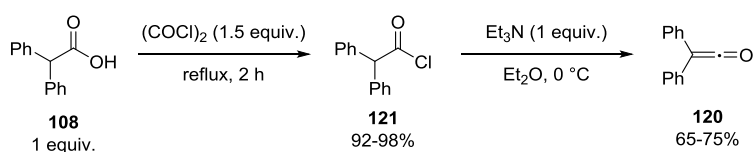
characteristics without the risk of instigating side reactions, which made it our preferred choice.

Diphenylketene **120** was initially prepared by the method of Taylor and co-workers.⁵⁹ Conversion of diphenylacetic acid **108k** (1 equiv.) to diphenylacetyl chloride **121** by treatment with thionyl chloride (4.7 equiv.) followed by a drop-wise addition of base (1 equiv.) gave **120** in 32% yield (**Scheme 2.7**).



Scheme 2.7. Diphenylketene **120** preparation by Taylor's method.⁵⁹

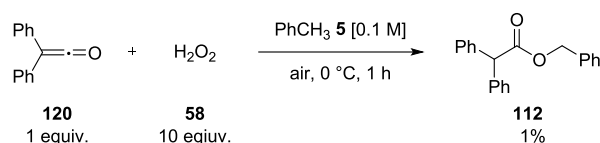
Better yields (65–75%) were obtained with shorter reaction times (2 h) when oxalyl chloride (1.5 equiv.) was used instead of thionyl chloride (4.7 equiv.) (**Scheme 2.8**). This approach further benefited from the removal of toluene **5** as the reaction solvent. Recrystallisation from petroleum ether (30–40 °C) yielded the acid chloride **121** in the range of 92–98%, which could be stored for more than a month at 19 °C without significant decomposition. Dropwise addition of base and subsequent distillation led to the formation of **120**. Kügelrohr distillation proved to be superior to short-path distillation in terms of time and yield, and was performed throughout these studies for best results.



Scheme 2.8. Modified preparation method of diphenylketene **120**.

Once diphenylketene **120** was successfully synthesised, its use in alkane oxidation was investigated. To gain evidence for the formation of **107e** a series of experiments were performed in an NMR tube. In order to provide direct access to the desired tautomer **107e**, diphenylketene **120** (1 equiv.) was placed in an NMR tube containing a deuterated solvent [0.1 M], and the nucleophile (1 equiv.) was added (**Table 2.2**). Water was also studied as the nucleophile to see if 2,2-diphenylethane-1,1-diol **108e** could be observed

Observation of an intermediate is affirmative of its formation but its absence does not always exclude the possibility of formation. Although **108e** and **107e** were not observed, their formation could not be ruled out. The question whether homolytic cleavage of the O–O bond was faster, if occurring at all, than the destruction by tautomerisation was not answered. Therefore, diphenylketene **120** (1 equiv.) and hydrogen peroxide **58** (aq. 30% w/w, 10 equiv.) were stirred in toluene **5** [0.1 M] for 1 h at 20 °C (**Scheme 2.9**).



Scheme 2.9. First successful oxidation of toluene **5**.

Quenching the reaction with saturated sodium metabisulfite and extracting with ethyl acetate followed by flash chromatography (toluene elution) led to an encouraging yield of 1% of benzyl 2,2-diphenylacetate **112**. This important result showed that the proposed reaction scheme was plausible although no indication of a mechanistic course was provided by this result. Prompted by this result we decided to investigate optimal reaction conditions and probe the substrate scope.

2.5. Quantitative Reaction Monitoring

Cyclohexane **3** was chosen as the next hydrocarbon to be examined because the resulting product **110** had a characteristic ^1H NMR spectrum with the multiplet at δ 5.1 ppm, which greatly simplified the problem of quantification. For the ease of monitoring the reaction and performing quantitative analysis, 1,4-dinitrobenzene was chosen as an internal standard because it has only one singlet at δ 8.43 ppm in the ^1H NMR spectrum, which did not overlap with any other peak of the proposed reaction mixture. This approach had the additional advantage in that it did not require the desired product to be isolated by column chromatography thus enabling fast reaction screening/optimisation.

To validate this method and evaluate its accuracy, the internal standard was added to a known amount of the authentic sample of **110**, worked-up by the reported procedure, and analysed by ^1H NMR spectroscopy. **Figure 2.4** shows the relative ratio of cyclohexyl

2,2-diphenylacetate **110** to 1,4-dinitrobenzene. In three separate experiments, ester **110** was weighed out as 1%, 8%, and 15% of the theoretical yield that could be obtained from diphenylketene **120** (300 mg) in a typical experiment (3 h, air atmosphere). No loss of **110** occurred during the work-up and the method was shown to be accurate to 1%.

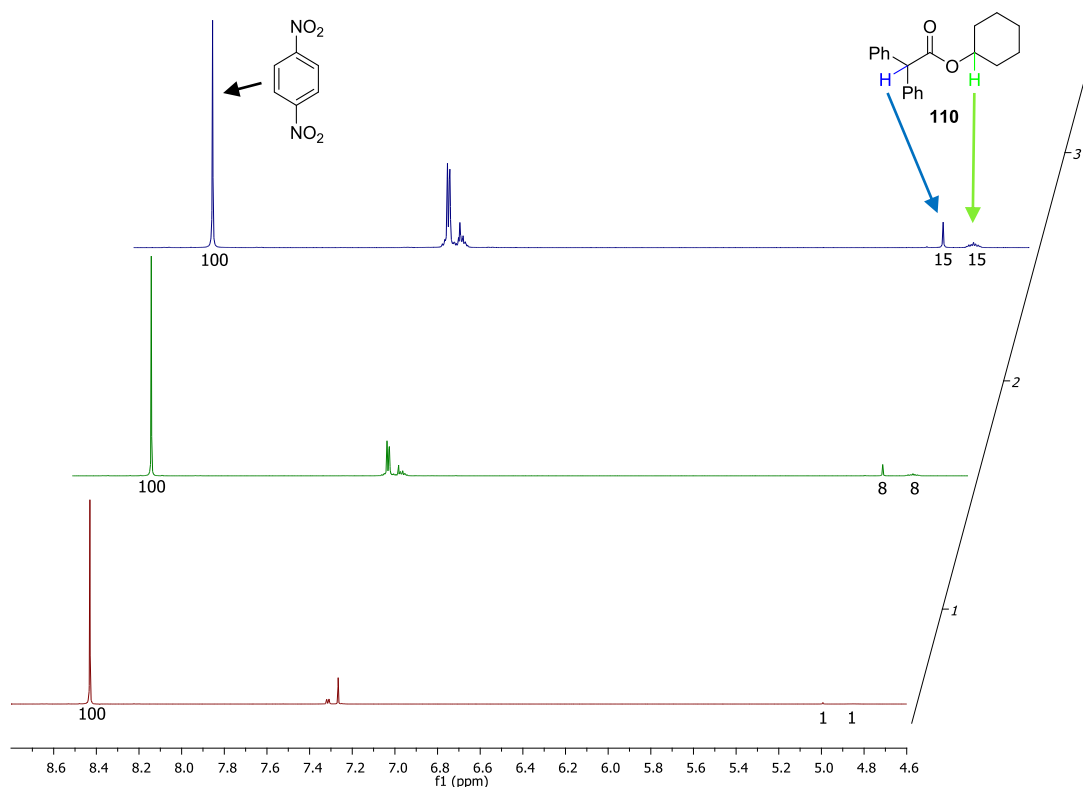


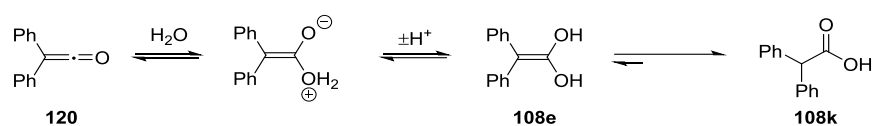
Figure 2.4. Stacked ^1H NMR spectra of ester **110** (relative to 1,4-dinitrobenzene).

2.6. Optimisation of the Reaction System

2.6.1. The Role of Atmospheric Oxygen

Stirring diphenylketene **120** (1 equiv.) and hydrogen peroxide **58** (aq. 30% *w/w*, 10 equiv.) in toluene **5** [0.1 M] for 1 h resulted in the formation of ester **112** in 1% yield (Section 2.4, Scheme 2.9). These experiments were carried out in a stoppered flask under an air atmosphere. Because the conversions were proving capricious, a control reaction was conducted under an inert atmosphere (N_2) (Scheme 2.10).

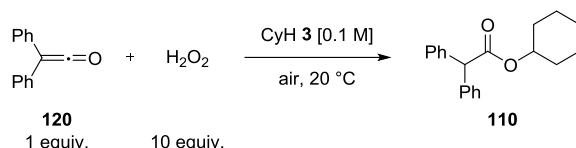
tautomerise to **108k** (Scheme 2.12), which is detrimental to the overall process of C–H functionalisation within our reaction system.



Scheme 2.12. Nucleophilic attack of water on diphenylketene **120**.

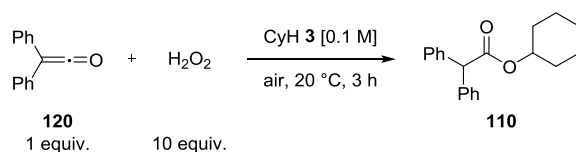
In order to minimise the extent of hydrolysis we investigated alternative sources of hydrogen peroxide **58**, namely urea hydrogen peroxide adduct **122** ($CO(NH_2)_2 \cdot H_2O_2$), sodium percarbonate **123** ($Na_2CO_3 \cdot 1.5H_2O_2$) and sodium perborate **124** ($NaBO_3 \cdot nH_2O$, $n = 1-4$). Urea hydrogen peroxide **122** is inexpensive, stable, safe and easy to handle. It also has a relatively high proportion of hydrogen peroxide **58** (~35%),⁶¹ which we thought might offer some advantages over aqueous hydrogen peroxide **58** (30% *w/w*) in our reaction. Sodium percarbonate **123** is another easy to handle and concentrated source of hydrogen peroxide **58** whose content exceeds 30% (by weight). The non-toxic, inexpensive and readily available peroxygen compound sodium perborate **124** is also a good substitute for potentially hazardous concentrated hydrogen peroxide **58**.

To evaluate the performance of urea hydrogen peroxide adduct **122** over aqueous hydrogen peroxide **58** (30% *w/w*), a series of experiments were carried out (Table 2.3). These involved addition of a hydrogen peroxide source (10 equiv.) to a solution of diphenylketene **120** (1 equiv.) in cyclohexane **3** [0.1 M], and stirring the mixture at 25 °C over time.

Table 2.3. Comparison of H_2O_2 •urea **122** and aqueous H_2O_2 **58**.

Entry	Source of H_2O_2	Time [h]	Conversion [%]
1	30% H_2O_2	1	6
2	H_2O_2 •urea	1	8
3	30% H_2O_2	3	6
4	H_2O_2 •urea	3	8

To our gratification, H_2O_2 •urea **122** performed not only as well as aqueous hydrogen peroxide **58** (30% *w/w*) but even slightly better giving an 8% conversion after 1 h and 3 h. However, no further increase in the conversion upon extension of the reaction time and the disappearance of the yellow colour (associated with the presence of diphenylketene **120**) after about 1.5 h raised our concerns. We hypothesised that diphenylketene **120** was being consumed in a non-productive fashion. Therefore, it was decided that the previous experiments should be repeated with a dropwise addition of **120** over 3 h (using a syringe pump) to a flask containing hydrogen peroxide **58** (10 equiv.) and cyclohexane **3** [0.1 M] (**Table 2.4**).

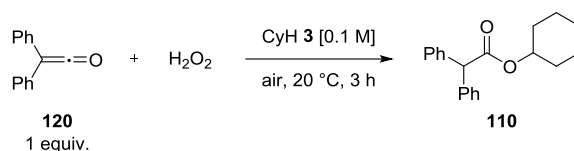
Table 2.4. Addition of diphenylketene **120** over 3 h using a syringe pump.

Entry	Source of H_2O_2	Time [h]	Conversion [%]
1	30% H_2O_2	3	12
2	H_2O_2 •urea	3	17

The conversion doubled for both the aqueous hydrogen peroxide **58** (30% *w/w*) and H_2O_2 •urea **122** reactions, rising from 6% to 12% (**Table 2.4, Entry 1**) and 8% to 17% (**Table 2.4, Entry 2**), respectively. The higher conversion obtained upon switching from

At this point, it was clear that increasing the amount of H_2O_2 •urea **122** from 1 equivalent (Table 2.6, Entry 3) to 10 equivalents (Table 2.6, Entry 4) did not improve the conversion to **110** beyond 17%. The same observation was made when 1 equivalent (Table 2.6, Entry 5), 2 equivalents (Table 2.6, Entry 6), and 10 equivalents (Table 2.6, Entry 7) of aqueous hydrogen peroxide **58** (30% w/w) were used in the reaction. A 12 % conversion to **110** was observed in all instances. Likewise, both the reaction with 1 equivalent (Table 2.6, Entry 8) and 10 equivalents (Table 2.6, Entry 9) of sodium percarbonate **123** resulted in a 3% conversion. Identical conversions (3%) were observed when sodium perborate **124** was used as the peroxide source (Table 2.6, Entries 10 and 11).

Table 2.6. Investigations into different amounts of H_2O_2 sources.

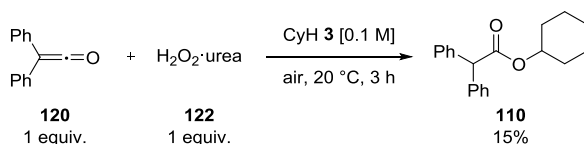


Entry	Source of H_2O_2	Amount of H_2O_2 [equiv.]	Conversion [%]
1	H_2O_2 •urea	0.01	4
2	H_2O_2 •urea	0.1	13
3	H_2O_2 •urea	1	17
4	H_2O_2 •urea	10	17
5	30% H_2O_2	1	12
6	30% H_2O_2	2	12
7	30% H_2O_2	10	12
8	Na_2CO_3 •1.5 H_2O_2	1	3
9	Na_2CO_3 •1.5 H_2O_2	10	3
10	$NaBO_3$ •4 H_2O	1	3
11	$NaBO_3$ •4 H_2O	10	3

These results reassured us that stoichiometric amounts of hydrogen peroxide **58** were sufficient for the reaction to proceed, and we did not regard increasing the amount of H_2O_2 •urea **122** above 10 equivalents to be either practical or economical.

What we considered to be an interesting question from a mechanistic point of view was how low the H_2O_2 •urea **122** loading could be before the reaction would cease. Therefore, it was decided that sub-stoichiometric amounts of **122** would be used in a series of experiments. Interestingly, the conversion was only slightly lower (13%) when 0.1 equivalents of **122** were used (**Table 2.6, Entry 2**) compared to the reaction with 1 equivalent of **122** (17%) (**Table 2.6, Entry 3**). The lower conversion may be explained by the fact that **122** is insoluble in most reaction solvents and vigorous stirring is required. This, in turn, meant that once **122** was washed up on the side of the flask it did not experience much interaction with the reaction mixture. While this may indeed be an influential factor, the lower conversion (4%) in the reaction with 0.01 equivalents of **122** (**Table 2.6, Entry 1**) seemed to refute that theory. A more detailed mechanistic understanding is needed before definite conclusions can be drawn from this series of experiments.

To test for a non-productive decomposition of hydrogen peroxide **58** into water and oxygen gas during the course of the reaction another experiment was carried out. Diphenylketene **120** (1 equiv.) was added over 3 h to cyclohexane **3** [0.1 M], while H_2O_2 •urea **122** (1 equiv.) was added in portions at regular intervals (0.2 equiv. every 10 min) (**Scheme 2.13**).



Scheme 2.13. Investigation of potential H_2O_2 **58** decomposition.

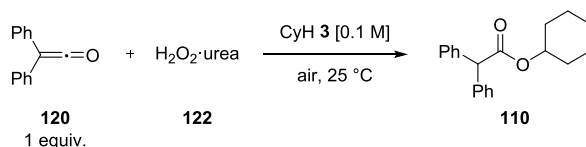
The conversion (15%) was slightly lower than that of the control reaction (17%), which indicated that **122** did not decompose (or did so to a negligible level) to unwanted co-products under the reaction conditions.

We concluded that H_2O_2 ·urea **122** exhibited a better activity than aqueous hydrogen peroxide **58** (30% w/w), sodium percarbonate **123** or sodium perborate **124** in the reaction, and that a stoichiometric amount of **122** was sufficient for the reaction to proceed. Hence, it was decided that 1 equivalent of **122** should be used in all subsequent reactions.

2.6.3. Reaction Time

The experiments carried out thus far showed that a prolonged time of reaction through the addition of diphenylketene **120** over time had a positive impact on the conversion to **110**. These reactions were run for either 1 h or 3 h. Therefore, diphenylketene **120** (1 equiv.) was added to the mixture of H_2O_2 ·urea **122** and cyclohexane **3** [0.1 M] over 6 h and 24 h. The summary of results is presented in **Table 2.7**.

Table 2.7. Effect of time on the reaction.



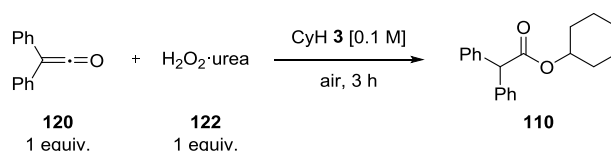
Entry	Amount of H_2O_2 [equiv.]	Time [h]	Conversion [%]
1	1	1	8
2	1	3	17
3	1	6	20
4	1	24	24
5	0.01	3	4
6	0.01	6	6
7	0.1	3	13
8	0.1	6	17
9	10	3	17
10	10	6	20

It was apparent that regardless of the amount of **122**, extending the reaction time led to an increase in conversion. The highest conversion (24%) was achieved when **120** was added to a mixture of **122** and **3** over 24 h. Although that represented a significant 41% increase in conversion, it was decided that the optimal reaction conditions would be further investigated over a reaction period of 3 h for practical reasons.

2.6.4. Effect of Temperature

The C–H functionalisation of cyclohexane **3** was also monitored as a function of temperature. The reaction appeared to work well in the range of 19–25 °C. However, it is often desirable to carry out a reaction at elevated temperatures to shorten reaction times. On the other hand, the rate of decomposition of diphenylketene **120** would be slower at lower temperatures. With this in mind, we decided to study the effect of low and high temperatures on the reaction (**Table 2.8**). The reactions were carried out by adding diphenylketene **120** (1 equiv.) to a flask containing H_2O_2 ·urea **122** (1 equiv.) and cyclohexane **3** [0.1 M] immersed either in an ice bath or an oil bath. The range of temperatures that could be tested was limited by the melting point of cyclohexane **3** (7 °C) and diphenylketene **120** (5–8 °C) in the lower temperature region, while the upper limit was set by the boiling point (80 °C) of cyclohexane **3**.

Table 2.8. Effect of temperature on the reaction.



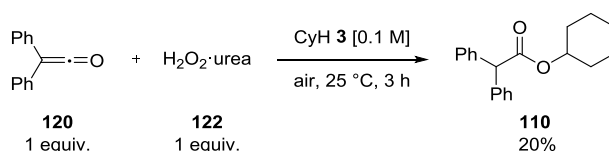
Entry	Temperature [°C]	Conversion[%]
1	10	8
2	19	18 ¹
3	25	18 ²
4	35	21 ³
5	50	21 ³

¹average conversion of 11 experiments; ²average conversion of 50+ experiments; ³reaction carried out in duplicate.

The data presented in **Table 2.8** showed that a rise in temperature did not have a significant impact on the conversion but a decrease in temperature slowed the reaction considerably.

2.6.5. Effect of Stirring

Studies have shown that heterogeneous reactions are influenced strongly by the type of stirring and the speed (or power) of stirring. To determine whether stirring had any effect on the reaction, different speeds of stirring were examined. There was no difference in the conversion when the reaction was stirred slowly or vigorously. In addition, a flask containing H_2O_2 •urea **122** (1 equiv.) and cyclohexane **3** [0.1 M] was sonicated while diphenylketene **120** (1 equiv.) was added over 3 h (**Scheme 2.14**).



Scheme 2.14. Oxidation of cyclohexane **3** in a sonicator.

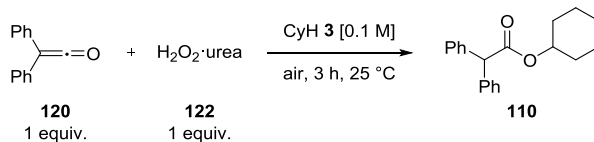
It was found that the conversion to **110** (20%) was identical to that of the control reaction (20%), and that sonication did not have any significant influence on the reaction. Although H_2O_2 •urea **122** is insoluble in most, if not all hydrocarbon solvents, **122** interacted with the reaction mixture even with minimal stirring.

2.6.6. Effect of Light

It has been established that light can act as a radical reaction initiator.⁶² Often, all that is required is illumination by diffuse daylight or by ceiling lights to bring about a radical process. Hence, the effect of light on our reaction was also studied. Three experiments were carried out simultaneously. One reaction was conducted in a flask wrapped in aluminium foil in darkness (**Table 2.9, Entry 1**), a second reaction was exposed to sunlight (**Table 2.9, Entry 2**), and a third was a control reaction exposed to fumehood

light (**Table 2.9, Entry 3**). All reactions involved a 3 h addition of diphenylketene **120** (1 equiv.) to a mixture of H_2O_2 •urea **122** (1 equiv.) and cyclohexane **3** [0.1 M] at 25 °C.

Table 2.9. Effect of light on the reaction.



Entry	Source of light	Conversion [%]
1	No light	17
2	Sunlight	17
3	Fumehood light	17

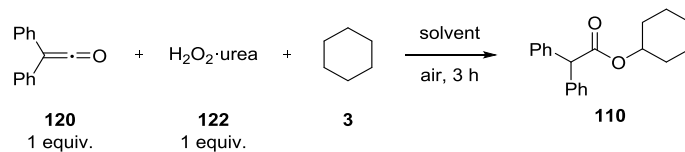
Our primary conclusion from this series of experiments (**Table 2.9**) was that light had neither a negative nor a positive impact on the reaction suggesting that any potential radical formation was not induced by light.

2.6.7. Solvent System

The reactions carried out up to this point could be regarded as solvolysis processes since the hydrocarbons that were functionalised were used as solvents. The reactions were biphasic when aqueous hydrogen peroxide **58** (30% w/w, 1 equiv.) was used. This was subsequently replaced by urea hydrogen peroxide **122** to minimise the extent of hydrolysis of the diphenylketene substrate **120**. An opportunity existed to improve the overall stoichiometry of the reaction through the introduction of a solvent and using cyclohexane **3** as a stoichiometric reagent. Therefore, a series of solvents were examined within the reaction (**Table 2.10**).

The ideal solvent should be chemically inert towards the reagents and should dissolve them readily. In our system, use of a single solvent was restricted by the solubility of the reaction components. Although diphenylketene **120** was soluble in most hydrocarbon solvents, urea hydrogen peroxide **122** displayed poor solubility in hydrophobic media.

The solubility of **122** was first examined in cyclohexane **3** [0.1 M] at 25 °C by submitting it to sonication for 1 h. Semi-quantitative analysis by Merckoquant[®] Peroxide Test strips showed no presence of **58** in cyclohexane **3**. Hydrogen peroxide **58** was also extracted from a hydrogen peroxide **58** solution (30% w/w) with dichloromethane but solubility of **58** was low (10 mg/L as indicated by Merckoquant[®] Peroxide Test strips). Despite these discouraging results, the solubility and reaction of **120**, **3** and **122** was investigated in a number of organic solvents (**Table 2.10**).

Table 2.10. Screening of common reaction solvents.

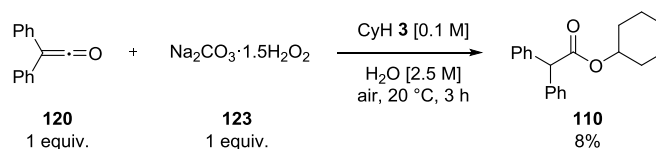
Entry	Amount of cyclohexane 3 (equiv.)	Solvent	Concentration [mol dm ⁻³]	Conversion [%]
1	55	toluene	0.05	8
2	1.5	benzene	0.1	0
3	10	benzene	0.1	2
4	10	quinoline	0.1	0
5	10	carbon tetrachloride	0.1	2
6	91	1,4-dioxane	0.5	4
7	55	1,4-dioxane	0.05	1
8	90	acetonitrile	0.77	3
9 ¹	90	acetonitrile	0.77	3
10	90	water	0.005	13
11 ²	90	water	0.005	16
12	90	water	1.5	14
13	10	chloroform	0.1	0
14	10	dichloromethane	0.1	2
15	10	acetone	0.1	2
16	10	1,2-dichloroethane	0.1	1

¹ reaction carried out at reflux; ² reaction carried out for 6 h.

Despite relatively good solubility of **122** in acetonitrile, a subsequent 3 h addition of diphenylketene **120** resulted in a conversion to **110** of only 3% (**Table 2.10, Entry 8**). Performing the reaction under reflux conditions did not improve the conversion (3%)

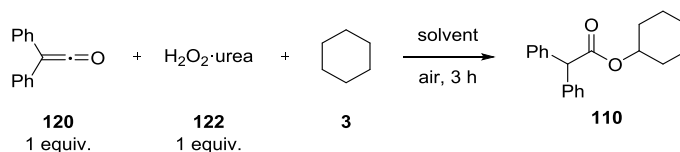
(Table 2.10, Entry 9). Urea hydrogen peroxide **122** was not soluble in other solvents and conversions in the range 0–8% were observed (Table 2.10, Entries 1–7 and 13–16.). It was clear that water dissolved **122** readily but large amounts of water were not desirable in our reaction. Consequently, an attempt was made to dissolve **122** in the minimum amount of water in order to enable transfer of hydrogen peroxide **58** from the complex ($\text{CO}(\text{NH}_2)_2 \cdot \text{H}_2\text{O}_2$) into the organic layer (cyclohexane **3**) (Table 2.10, Entries 10 and 11). However, conversions were either lower (13–14%) or comparable (16% upon extending reaction time up to 6 h) to reactions that were performed under anhydrous reaction conditions (17–20%).

A similar effect was also demonstrated for sodium percarbonate **123** as the peroxide source. Addition of a small amount of water to a mixture of sodium percarbonate **123** in cyclohexane **3**, followed by addition of diphenylketene **120** over 3 h increased the conversion from 3% to 8% (Scheme 2.15).



Scheme 2.15. Releasing H_2O_2 **58** from sodium percarbonate **123**.

It has been reported that the solubility of oxygen is greatly enhanced in fluorinated solvents.⁶³ In addition, fluorinated solvents exhibit a high ionising power, strong hydrogen–donor ability, and, in particular, low nucleophilicity.⁶⁴ Therefore, a number of fluorinated solvents were also screened for their compatibility with our reaction process (Table 2.11).

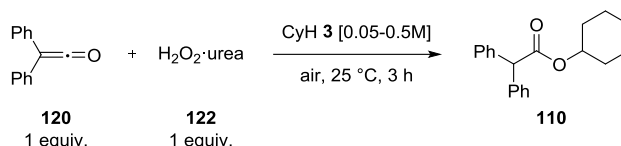
Table 2.11. Investigations into fluorinated solvents.

Entry	Concentration of cyclohexane 3 [mol dm ⁻³]	Solvent	Concentration [mol dm ⁻³]	Conversion [%]
1	0.2		0.2	0
2	0.05		0.05	8
3	0.05		0.05	6
4	0.05		0.05	0
5	0.05		0.05	0

To our disappointment the fluorinated solvents that were examined did not induce better conversions even when excess cyclohexane **3** (relative to **120**) was used. Furthermore, their use proved to be problematic due to solubility issues. Diphenylketene **120** was neither soluble nor miscible with perfluorohexane (**Table 2.11, Entry 3**), was insoluble in 1,1,1,3,3,3-hexafluoro-2-propanol (**Table 2.11, Entry 4**), and only partially soluble in 2,2,2-trifluoroethanol (**Table 2.11, Entry 5**). Therefore, it was concluded that fluorinated solvents were not a good medium for the reaction.

2.6.8. Concentration Range

We next investigated the effect of the concentration of cyclohexane **3** on the reaction. Diphenylketene **120** (1 equiv.) was added over 3 h to a flask containing H₂O₂·urea **122** (1 equiv.) and various concentrations of cyclohexane **3** at 25 °C (**Table 2.12**).

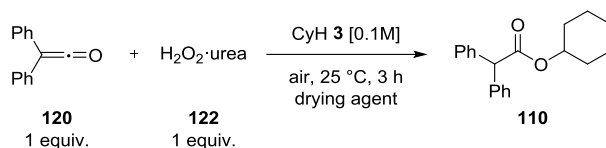
Table 2.12. Effect of cyclohexane **3** concentration on the reaction.

Entry	Concentration [mol dm ⁻³]	Conversion [%]
1	0.05	17
2	0.1	17
3	0.5	17

Surprisingly, the concentration of diphenylketene **120** in the range of 0.05–0.5 mol dm⁻³ had no impact on the conversion to **110**, with identical reaction outcomes being achieved (**Table 2.12, Entries 1–3**). This suggests the overall kinetics of the reaction is rapid when compared to the timeframe being examined in our reaction (3 hours).

2.6.9. Generation of Water

If the reaction mechanism proposed in **Section 2.1 (Scheme 2.1)** was correct, one molecule of water was generated for every molecule of the target ester **110**. If water then reacted with diphenylketene **120**, the enol tautomer of diphenylacetic acid **108e** would be formed. Under the reaction conditions, the keto tautomer of diphenylacetic acid **108k** would be favoured. As a consequence, theoretically, the maximum conversion to ester **110** could be only 50%. To provide a potential solution to this problem two reactions were set up. The first with 3Å molecular sieves and the second with magnesium sulfate in which diphenylketene **120** (1 equiv.) was added to a mixture of H₂O₂·urea **122** (1 equiv.) and cyclohexane **3** [0.1 M] at 25 °C (**Table 2.13**).

Table 2.13. Effect of desiccants on the reaction.

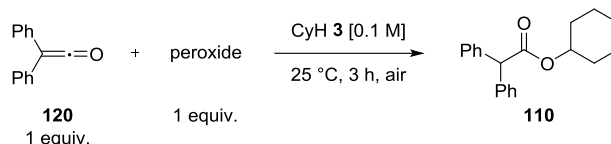
Entry	Drying agent	Conversion [%]
1	3Å molecular sieves	10
2	magnesium sulfate	13
3	none	17 ¹

¹average conversion of 30 reactions

The attempts to remove water from the reaction resulted in lower conversions to **110** and hence the idea of using drying agents was abandoned.

2.6.10. Alternative Peroxide Sources

In our search for the most efficient source of hydrogen peroxide **58** we examined aqueous hydrogen peroxide **58** (30% *w/w*), $\text{H}_2\text{O}_2 \cdot \text{urea}$ complex **122**, sodium percarbonate **123** and sodium perborate **124**. The effect and reactivity of structurally different, commercially available peroxides was also examined. Initially, benzoyl peroxide **125** and *tert*-butyl hydroperoxide **126** were tested in the reaction with diphenylketene **120** and cyclohexane **3** under the reaction conditions shown in **Table 2.14** (**Entries 1 and 2**).

Table 2.14. Effect of alternative peroxides on the reaction.

Entry	Peroxide	Conversion [%]
1	 125	0
2	 126	6
3	 127	0
4	 128	10

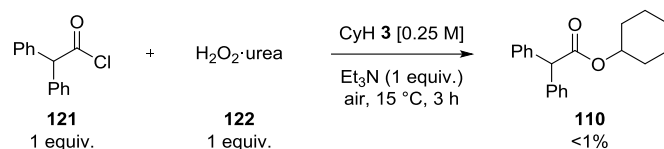
The replacement of $\text{H}_2\text{O}_2\cdot\text{urea}$ **122** by benzoyl peroxide **125** did not result in the formation of ester **110**. This is unsurprising since high temperatures (100–150 °C) are typically required to cleave the O–O bond and generate the corresponding radicals.⁶⁵ On the other hand, *tert*-butyl hydroperoxide **126** gave a 6% conversion to **110** (Table 2.14, Entry 3). It was therefore possible that the use of other hydroperoxide compounds in the reaction could result in better conversions. Cumene hydroperoxide **127** and 2-butanone peroxide **128** were among the commercially available hydroperoxides and were also studied (Table 2.14, Entries 3 and 4). Surprisingly, **127** did not lead to the formation of **110** but replacing urea hydrogen peroxide **122** with 2-butanone peroxide **128** resulted in a 10% conversion to ester **110**.

Despite the curious results, none of the commercially available peroxides paralleled the ability of urea hydrogen peroxide **122** to oxidise cyclohexane **3**. It was not clear why some hydroperoxides did not have the same effect as **122** while others seemed to facilitate the reaction to some extent raising further mechanistic questions. Although the range of

commercially available peroxides is limited, it could be expanded through the individual preparation of bespoke peroxides if desired, although this could detract from the attractiveness of the process.

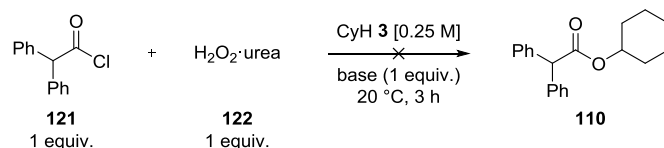
2.6.11. *In Situ* Generation of Diphenylketene **120**

In order to circumvent the multi-step synthesis of diphenylketene **120**, we attempted to generate it *in situ* from available starting materials. A solution of diphenylacetyl chloride **121** (1 equiv.) in cyclohexane **3** [0.25 M] and urea hydrogen peroxide **122** (1 equiv.) was treated with triethylamine (1 equiv., added over 3 h) (**Scheme 2.16**). The reaction was carried out at 15 °C and resulted in a <1% conversion to **110**.



Scheme 2.16. Attempted in-situ generation of diphenylketene **120**.

The low conversion could be potentially caused by reaction of triethylamine with urea hydrogen peroxide **122** to give triethylamine *N*-oxide **129**.⁶⁶ Although we have found no evidence for the formation of **129**, we decided to examine different bases to avoid this potential problem. To a flask containing $\text{H}_2\text{O}_2\cdot\text{urea}$ **122** (1 equiv.), cyclohexane **3** [0.25 M] and base (1 equiv.) was added a solution of diphenylacetyl chloride **121** (1 equiv.) in cyclohexane **3** over 3 h (**Scheme 2.17**).



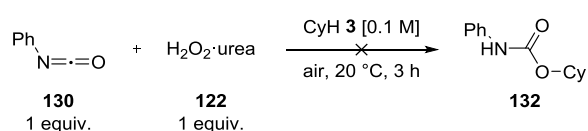
Scheme 2.17. Attempted in-situ generation of diphenylketene **120** using different bases.

Sodium carbonate, sodium hydroxide, and sodium hydride were used as alternatives to triethylamine in a series of experiments but none of the reactions produced the target ester **110**, as determined by examination of crude reaction mixtures by ^1H NMR spectroscopy.

2.6.12. Isocyanate and Isothiocyanate Substrates

Structurally similar but significantly more stable isocyanates and isothiocyanates were thought to be potentially capable of oxidising unactivated hydrocarbons as an alternative to diphenylketene **120**. Therefore, it was of interest to us to compare these families of compounds with ketenes and test their reactivity in the oxidation reaction. Phenyl isocyanate **130** and phenyl isothiocyanate **131** were chosen as the representative substrates.

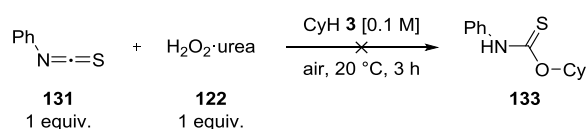
The reactions were carried out under similar reaction conditions as those with diphenylketene **120**. Phenyl isocyanate **130** (1 equiv.) and H_2O_2 ·urea **122** (1 equiv.) were stirred in cyclohexane **3** [0.1 M] for 3 h in an open flask (**Scheme 2.18**).



Scheme 2.18. Testing the reactivity of phenyl isocyanate **130** in the oxidation reaction.

Comparison of ^1H NMR spectra of the reaction mixture with that of phenyl isocyanate **130** and an authentic sample of carbamate **132** revealed that only the starting material was present. No detectable desired reaction occurred even after the reagents were stirred for 6 days. Only the starting materials were recovered.

In parallel, phenyl isothiocyanate **131** (1 equiv.) was stirred with H_2O_2 ·urea **122** (1 equiv.) in cyclohexane **3** [0.1 M] for 3 h (**Scheme 2.19**).



Scheme 2.19. Testing the reactivity of phenyl isothiocyanate **131** in the oxidation reaction.

Similarly to the phenyl isocyanate **130** reaction above, phenyl isothiocyanate **131** did not react to give thiocarbamate **133**. Only the starting material was observed by ^1H NMR and IR spectroscopy.

These results demonstrated that despite structural similarities, isocyanates and isothiocyanates did not share the reactivity of ketenes in the oxidation of hydrocarbons.

2.6.13. Alternative Ketenes

In the design of this reaction the choice of ketene was directed by the fact that ketenes can be stabilised both by conjugation and by bulky substituents, and each of these factors contributed to the stability of diphenylketene **120**. Additionally, the absence of sp^3 C–H bonds and a reliable, highly yielding preparation method made **120** an attractive candidate for the desired oxidation reaction (Section 2.4, Scheme 2.9). After the initial success in developing the reaction, a possibility existed to achieve higher conversions through structural modifications of the ketene backbone. Several ideas were explored and are described further.

Substituents exert major effects on ketene stabilisation and properties. Smaller substituents drastically decrease the stability of ketenes. In fact, difluoroketene **134** and dichloroketene **135** are amongst the least stabilised ketenes that have been prepared to date (Figure 2.5).

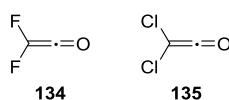
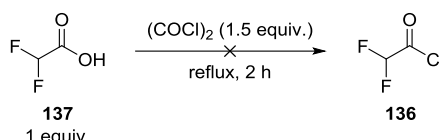


Figure 2.5. Structures of difluoroketene **134** and dichloroketene **135**.

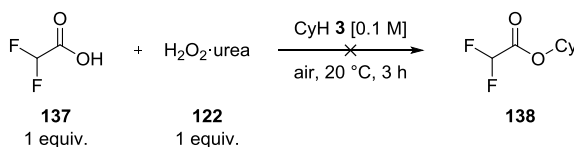
The low steric hindrance experienced by these ketenes could contribute to increased reactivity and higher conversions in our reaction system, although it could favour competing reactions instead. It could also be that through the polarization of the C–X σ bond (due to the electronegativity of fluorine or chlorine) the O–O bond could be weakened. This weakened bond would therefore be further activated for homolytic cleavage and potentially lead to higher conversions. The preparation methods of difluoroketene **134** and dichloroketene **135** are scarce. Both ketenes have been reported to be unstable and were typically prepared and observed *in situ*.⁶⁷

Building on the successful synthesis of diphenylketene **120**, an attempt was made to prepare ketene **134** and **135** using the same method. Difluoroacetyl chloride **136** was not commercially available and was therefore prepared by refluxing difluoroacetic acid **137** (1 equiv.) in oxalyl chloride (1.5 equiv.) but this method proved to be unsuccessful (**Scheme 2.20**). ^1H NMR analysis and comparison with the starting material revealed only the presence of unreacted difluoroacetic acid **137**.



Scheme 2.20. Attempted formation of difluoroacetyl chloride **136**.

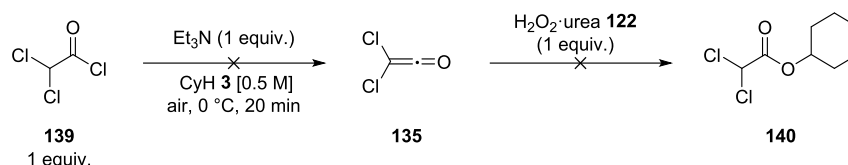
In a separate experiment, acid **137** (1 equiv.) was stirred with urea hydrogen peroxide **122** (1 equiv.) in cyclohexane **3** [0.1 M] in an effort to form cyclohexyl difluoroacetate **138** *in situ* (**Scheme 2.21**).



Scheme 2.21. Attempted oxidation of cyclohexane **3** with difluoroacetic acid **137**.

Interestingly, inspection of the ^1H NMR spectrum revealed that although ester **138** did not form, aromatic protons were present in the crude reaction mixture. Unfortunately, the very low mass recovery (4 mg of unidentified product out of 1 g of **137** used) effectively discouraged us from further investigation of this process.

An *in situ* generation of dichloroacetyl chloride **135** and oxidation of cyclohexane **3** was also examined as an alternative process. Dropwise addition of triethylamine (1 equiv.) to a cooled solution of dichloroacetyl chloride **139** (1 equiv.) in cyclohexane **3** [0.5 M] was followed by addition of urea hydrogen peroxide **122** (1 equiv.) (**Scheme 2.22**).



Scheme 2.22. Attempted formation of **140** through in-situ generation of dichloroketene **135**.

Stirring the mixture at 25 °C for 3 h produced a number of unidentified products (^1H NMR spectroscopy) but ester **140** was not present in the crude reaction mixture.

Following the unsuccessful synthesis of halogenated ketenes, attention was turned to making structural changes to diphenylketene **120**. Addition of either electron-donating or electron-withdrawing substituents to the phenyl rings could have a considerable impact on the reactivity of the resulting ketene. Upon a literature search, a handful of research articles were found that reported synthesis of derivatives of diphenylketene **120** which fulfilled the original selection criteria (**Section 2.4**). Bis(4-chlorophenyl)ketene **141** (**Figure 2.6**) was chosen owing to the accessibility of starting materials.

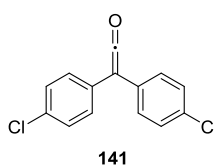
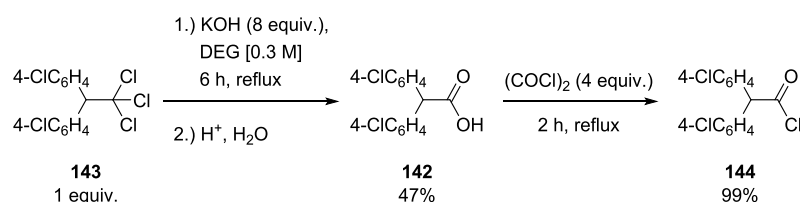


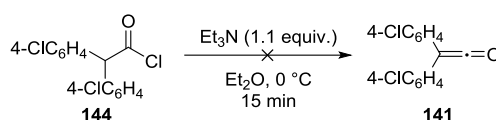
Figure 2.6. Structure of bis(4-chlorophenyl)ketene **141**.

Bulk preparation of bis(4-chlorophenyl)acetic acid **142**⁶⁸ from 4,4'-DDT **143** was more economically viable despite commercial availability of **142** and was carried out as shown in **Scheme 2.23**. Following recrystallisation of **142**, bis(4-chlorophenyl)acetyl chloride **144** was made in excellent yield (99%) by the method described in **Section 2.4** (**Scheme 2.7**).



Scheme 2.23. Preparation of starting material **142** and **144**.

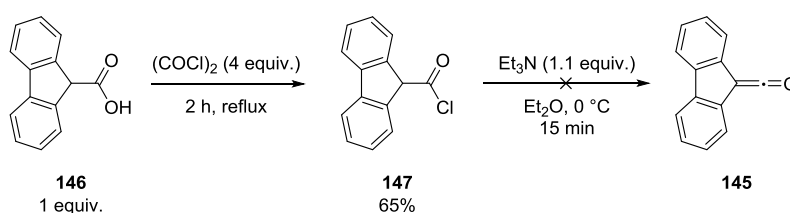
Following the reported synthesis, triethylamine (1.1 equiv.) was added over 15 min to a cold solution of **144** (1 equiv.) (**Scheme 2.24**). Prior to distillation, IR analysis was performed but did not show the expected characteristic stretch of ketene **141** (2103 cm^{-1}).⁶⁹



Scheme 2.24. Attempted formation of ketene **141**.

Although a couple of synthesis reports of bis(4-chlorophenyl)ketene **141** are present in the literature, the compound has never been isolated.⁶⁹⁻⁷⁰ The reason for this may be the high reactivity of ketene **141**, which could be undergoing subsequent reactions such as hydrolysis.

A conceptually interesting idea that was examined involved a ketene with a fused fluorenyl core, 9-carbonyl-fluorene **145** (**Scheme 2.25**). The additional rigidity that would be induced in ketene **145** could result in its decreased reactivity and increased stability. Refluxing 9-fluorenylcarboxylic acid **146** in oxalyl chloride (4 equiv.) gave 9-fluorenylcarboxylic acid chloride **147** in a good yield (65%) but formation of ketene **145** was unsuccessful under our standard reaction conditions (**Scheme 2.25**).



Scheme 2.25. Attempted formation of ketene **145**.

As was the case with ketene **141**, IR data did not reveal a peak that would be characteristic of a ketene. Lack of results, and inability to analyse the reactions and monitor ketene formation by other means (NMR spectroscopy or mass spectrometry) resulted in pursuit of alternative methods to understand our novel oxidation process further.

2.6.14. Summary

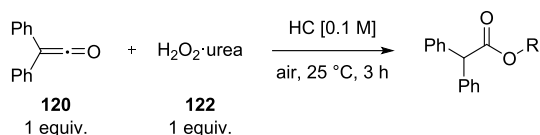
The initial reaction conditions were modified according to the results obtained after an extensive optimisation study. To date, the preferred reaction conditions are: 25 °C, air as a source of oxygen, H_2O_2 •urea **122** as a hydrogen peroxide source, and the syringe-pump addition of diphenylketene **120** over 3 h. For better conversions freshly distilled diphenylketene **120** was used. Readily available isocyanates and isothiocyanates could not replace ketenes, and all attempts to synthesise alternative ketenes were unsuccessful. Minor differences in conversions (16–20%) for reactions carried out under the same reaction conditions (25 °C, 3 h, air) cannot yet be explained by reasons other than experimental error.

2.7. Substrate Scope

With these optimised conditions, the substrate scope was investigated by submitting a series of hydrocarbons to the reaction conditions developed.

2.7.1. Cycloalkanes

At this stage, our investigation was narrowed to symmetrical alkanes to avoid selectivity issues. As summarised in **Table 2.15**, the conversions of seemingly similar cycloalkanes: cyclopentane **148** (**Entry 1**, 2%), cyclohexane **3** (**Entry 2**, 17%), cycloheptane **149** (**Entry 3**, 17%) and cyclooctane **150** (**Entry 4**, 2%) - varied greatly.

Table 2.15. Oxidation of various cycloalkanes.

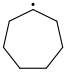
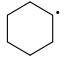

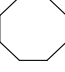
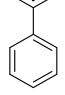
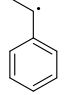
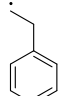
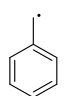
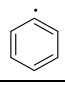
Entry	R	Conversion [%]
1		2 ^a
2		17 ^b
3		17 ^c
4		2 ^c

^a average of 3 reactions; ^b average of 30 reactions; ^c average of 2 reactions.

It was not obvious how a conformational effect influenced the reaction and the resulting conversions. One possibility was that the higher conversions of cyclohexane **3** (17%) and cycloheptane **149** (17%), and the lower conversions of cyclopentane **148** (2%) and cyclooctane **150** (2%) were associated with the enthalpies of formation of free radicals (Table 2.16).⁷¹ It has been reported that cyclohexane **3** and cycloheptane **149** require less energy ($\sim 14 \text{ kcal mol}^{-1}$ and $\sim 12 \text{ kcal mol}^{-1}$, respectively) to form free radicals than cyclopentane **148** ($\sim 26 \text{ kcal mol}^{-1}$), which suggested a direct relationship between reactivity and bond strength. Unfortunately, the enthalpy of formation of the respective radical of cyclooctane **150** could not be compared as it has not been reported in the literature.

Although it was too early to draw definite conclusions, a promising suggestion arose that enthalpies of formation of free radicals could potentially be a good predictor of the reactivity of a given hydrocarbon in the reaction. Therefore, whilst it was surprising that functionalisation of toluene **5** under the reaction conditions developed was limited (Table 2.17, Entry 4), this observation was consistent with the higher enthalpy of formation of the associated radical (Table 2.16, Entry 8).

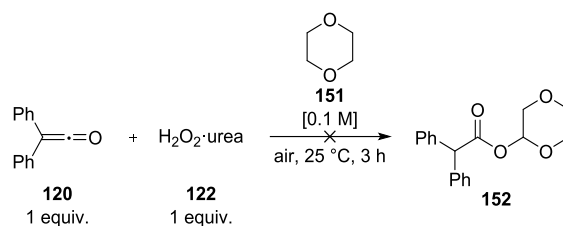
Table 2.16. Enthalpies of formation of free radicals of some hydrocarbons.

Entry	Radical	$\Delta_f H^\circ_{298}/\text{kcal mol}^{-1}$
1		12.2 ± 1^{71}
2		13.9 ± 1^{71}
3		25.6 ± 0.6^{71}
4		- ^a
5		32.2^{71}
6		40.4^{71}
7		- ^a
8		49.7 ± 0.6^{71}
9		80.8 ± 0.7^{71}

^a not reported

2.7.2. Saturated Heterocycles

In line with the concept of oxidising symmetrical alkanes, and to examine the effect of electronegative atoms on the reactivity of substrates, 1,4-dioxane **151** was chosen as a representative of saturated heterocycles and used as solvent in the reaction (**Scheme 2.26**).



Scheme 2.26. Attempted oxidation of 1,4-dioxane **151**.

The desired ester **152** was not observed as 1,4-dioxane **151** proved to be completely inert under the reaction conditions. This surprising result negated the idea that the presence of a lone pair of electrons of the adjacent heteroatom could help stabilise the expected radical **153** (**Figure 2.7**),⁷² which could undergo further reactions.

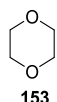
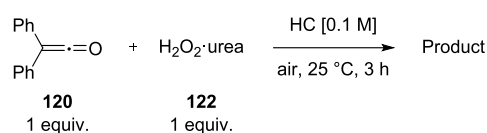


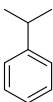
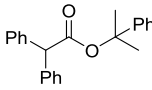
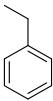
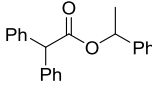
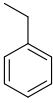
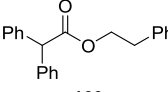
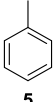
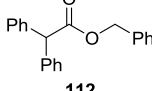
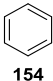
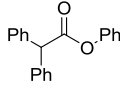
Figure 2.7. 1,4-dioxane radical **153**.

Although saturated heterocycles are common structural motifs in Nature, this discouraging result directed our attention towards investigating other substrates.

2.7.3. Aryl Substrates

Toluene **5** was the first hydrocarbon that was successfully oxidised within this investigation. Its high enthalpy of formation of free radicals (~ 49.7 kcal mol⁻¹, **Table 2.16, Entry 8**) was reflected in the observed yield of 1%. Likewise, benzene **154** required a large input of energy (~ 81 kcal mol⁻¹, **Table 2.16, Entry 9**) so it was not surprising that its oxidation to phenyl 2,2-diphenylacetate **155** was unsuccessful even when benzene **154** was refluxed for 7 days (**Table 2.17, Entry 5**).

Table 2.17. Oxidation of benzylic hydrocarbons.

Entry	HC	Product	Conversion [%]
1	 156	 157	0
2	 158	 159	8
3	 158	 160	0
4	 5	 112	1 ^a
5	 154	 155	0 ^b

^a average of 5 reactions; ^b reaction conditions: reflux, 7 days.

It was expected that oxidation of cumene **156** should give **157** in high yield due to the relatively low enthalpy of formation of the corresponding radical (~ 32 kcal mol⁻¹, **Table 2.16, Entry 5**). The reason why **157** did not form (**Table 2.17, Entry 1**) was unclear but could be explained by the fact that methyl groups made cumene **156** inaccessible to bulky radicals, such as **109** (**Section 2.1, Scheme 2.1**), and prevented the reaction. This theory was further supported by the fact that ethylbenzene **158** was oxidised to **159** in 8% yield despite having a higher enthalpy of radical formation (~ 40 kcal mol⁻¹, **Table 2.16, Entry 6**). Unfortunately, comparison with the other possible product **160** (**Table 2.17, Entry 3**) was not possible because data on enthalpy of radical formation was not reported in the

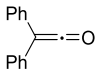
literature (**Table 2.16, Entry 7**). Alternatively, it is possible that the expected products were not stable under the reaction conditions and reacted further to form other products.

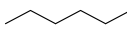
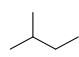
These results indicated that this methodology may favour oxidation of secondary over primary benzylic C–H bonds. Such selectivity would be typical of a radical process, in which C–H bonds react in the following order: $3^\circ > 2^\circ > 1^\circ$.⁷³ More examples of oxidation trends between various C–H bonds were needed to interpret our data further. Therefore, our attention was turned to linear alkanes.

2.7.4. Linear Alkanes

The alkanes, hexane **161** and 2-methylbutane **162**, were investigated under the reaction conditions (**Table 2.18**) to contrast and compare the selectivity of different C–H bonds (primary, secondary, tertiary).

Table 2.18. Oxidation of linear alkanes.

 120 1 equiv.	+ H ₂ O ₂ ·urea 122 1 equiv.	$\xrightarrow[\text{air, 25 }^\circ\text{C, 3 h}]{\text{alkane [0.1 M]}}$	Product(s)
---	---	---	-----------------------

Entry	Alkane	Conversion [%]
1	 161	0
2	 162	0

Upon inspection of ¹H NMR spectra and comparison with authentic samples, it was found that none of the possible products of either alkane were formed. With respect to regioselectivity, it was surprising that even the weaker (secondary and tertiary) C–H bonds were inert to oxidation under the reaction conditions examined (**Table 2.18**). These results, along with the differences in conversion between cyclopentane **148** and ethylbenzene **158**, provided evidence that the presence of an electron-donating substituent was required in order for the molecule to be functionalised. This requirement presents an

opportunity for selective oxidations, which may be achieved either by installation and removal or use of existing substituents.

2.7.5. Future Directions

The difference in conversion of cyclopentane **148** (2%) and ethylbenzene **158** (8%) showed that the enthalpy of formation of free radicals (~ 26 and 40 kcal mol $^{-1}$, respectively) was not a good prediction method of the relative reactivity of hydrocarbons. Complete inertness of linear alkanes **161** and **162** towards oxidation provided further support to that observation. Other factors, therefore, must play a more important role in reactivity and determining the factors governing the reaction will be key to unlocking its potential.

Additional insights into selectivity and reaction requirements, *i.e.* presence of electron-withdrawing or electron-donating substituents, could be gained by oxidising a number of compounds, e.g. propylbenzene **163**, indane **164** or 1,2,3,4-tetrahydronaphthalene **165** (Figure 2.8).

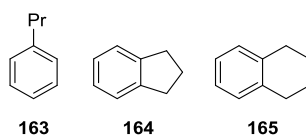


Figure 2.8. Potentially interesting hydrocarbons.

Further work could also involve oxidations of substrates with substituents of varying electron-withdrawing capacities, e.g. halogens, nitrile, nitro, etc. Heterocycles other than 1,4-dioxane **151** could also be investigated to learn more about the effect of heteroatoms which are built into the ring. Tetrahydrofuran **166**, piperidine **167** or thiane **168** may be some interesting examples to further interrogate this intriguing transformation (Figure 2.9).

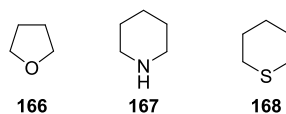


Figure 2.9. Potentially interesting heterocycles.

2.8. Mechanistic Studies

Since the optimisation studies did not lead to discovering conditions that would result in a dramatic improvement in conversion, we turned our attention to acquiring information about the mechanism of the process. We were hoping that an insight into the reaction mechanism would enable us to direct the reaction along the desired reaction pathway. We began our investigation by conducting a series of control experiments.

2.8.1. Control Reactions

Before the crucial role of oxygen in the reaction became evident, it was thought that the O–O bond of diphenylacetic peracid **107k** would form as a result of the nucleophilic attack of hydrogen peroxide **58** on diphenylketene **120** (Section 2.4, Figure 2.6). Unexpectedly, the target molecules did not form under an inert atmosphere. This finding posed a compelling question about the role of hydrogen peroxide **58**, if any, in the process. Hence, the first control reaction was carried out without urea hydrogen peroxide **122**. Diphenylketene **120** (1 equiv.) was simply added over 3 h to an open flask containing cyclohexane **3** [0.1 M] (Scheme 2.27).

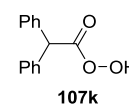
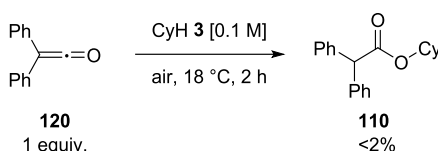


Figure 2.10.

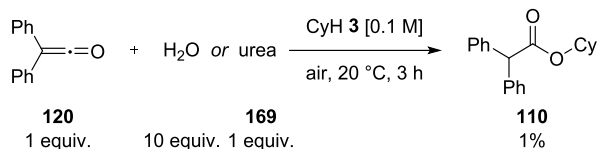


Scheme 2.27. Oxidation of cyclohexane **3** without any source of hydrogen peroxide **58**.

In the absence of a hydrogen peroxide source, a 2% conversion to ester **110** was observed by ^1H NMR spectroscopy of the crude reaction mixture. Although the reaction proceeded without hydrogen peroxide **58**, higher conversions were achieved using **58** and **122**, suggesting it could function as an initiator in the reaction or offer an alternative pathway to the product.

As concentrated hydrogen peroxide **58** is explosive, it is sold as aqueous solutions or as a complex, e.g. urea hydrogen peroxide **122**. In order to account for any influence that

water or urea **169** could exert on the reaction, control reactions were carried out by adding diphenylketene **120** (1 equiv.) over 3 h to cyclohexane **3** [0.1 M] in the presence of water (10 equiv.) or urea **169** (1 equiv.) at 20 °C (**Scheme 2.28**).

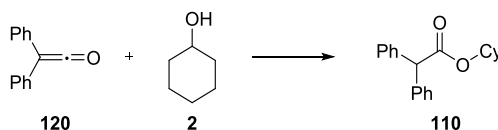


Scheme 2.28. The effect of water and urea **169** on the reaction.

As anticipated, neither water nor urea **169** positively influenced the conversion to **110**. While some conversion was observed with both additives, this did not exceed 1% and most likely resulted from the auto-oxidation of diphenylketene **120**.

2.8.2. First Proposed Mechanism

Ketenes undergo a variety of addition reactions with nucleophilic species. Therefore, it was hypothesised that cyclohexane **3** was oxidised to cyclohexanol **2**, which underwent a nucleophilic attack on diphenylketene **120** (**Scheme 2.29**).



Scheme 2.29. Formation of **110** through nucleophilic attack of **2** on **120**.

The formation of cyclohexanol **2** could arise through formation of cyclohexyl radical **63**, which, in turn could form through abstraction of a hydrogen atom from cyclohexane **3** by molecular oxygen (**Figure 2.11**). Recombination of cyclohexyl radical **63** and hydroperoxy radical **170** would give cyclohexyl hydroperoxide **171**. Subsequent homolytic cleavage of the O–O bond could result in the formation of cyclohexyloxy radical **172** and hydroxyl radical **59**. A second hydrogen atom abstraction from water would then lead to cyclohexanol **2**.

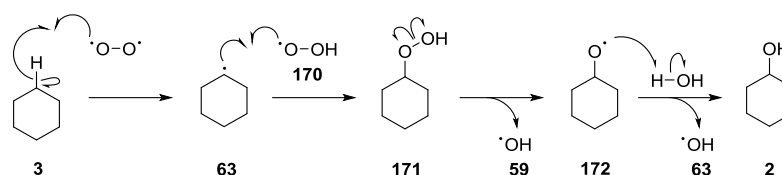
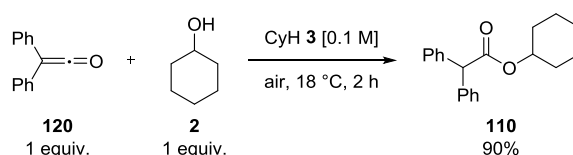


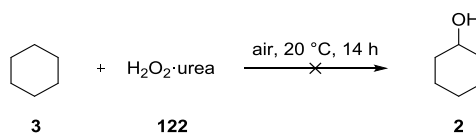
Figure 2.11. Proposed mechanism of cyclohexanol **2** formation.

To test this hypothesis, the reactivity of cyclohexanol **2** and diphenylketene **120** was investigated by adding **120** (1 equiv.) to **2** (1 equiv.) over 2 h in cyclohexane **3** [0.1 M]. The reaction proceeded smoothly and **110** was isolated in 90% yield (Scheme 2.30).



Scheme 2.30. Reaction of diphenylketene **120** and cyclohexanol **2**.

It was therefore shown that ester **110** could be readily formed if cyclohexanol **2** was indeed present during the reaction. If this was the mechanism, then formation of cyclohexanol **2** would have to occur prior to its reaction with diphenylketene **120**. This was examined by stirring a mixture of H_2O_2 ·urea **122** and cyclohexane **3** in an open flask (Scheme 2.31).



Scheme 2.31. Investigation into the formation of cyclohexanol **2** using **3**, **122** and air.

The reaction was monitored by ^1H NMR spectroscopy, however, cyclohexanol **2** was not observed even after 14 hours, which implied the reaction did not proceed through the pathway shown in Scheme 2.30.

2.8.3. Second Proposed Mechanism

Using the experimental results in combination with the literature, another reaction pathway was proposed as shown in Figure 2.11.

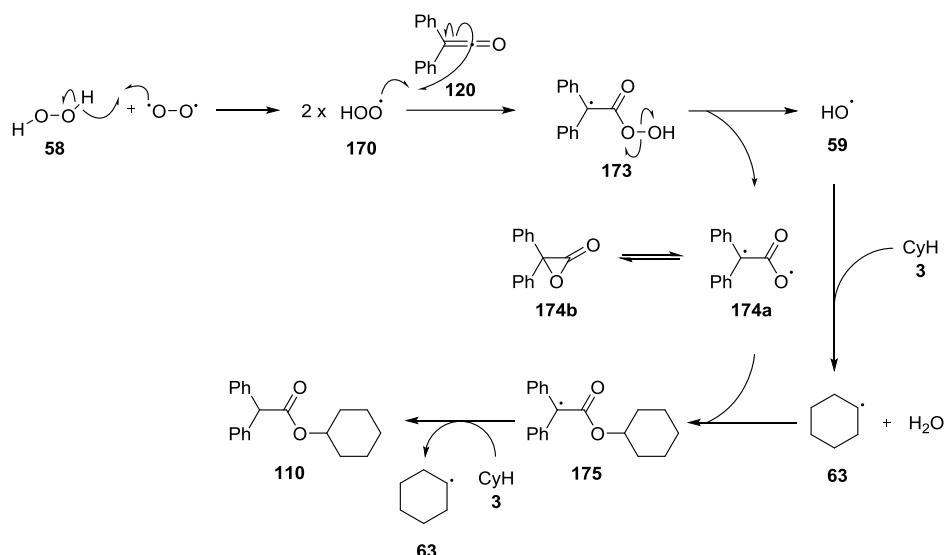


Figure 2.11. Proposed pathway for oxidation of cyclohexane **3** with H_2O_2 **58** and O_2 .

We proposed the initiation of the reaction occurred through direct hydrogen atom abstraction from hydrogen peroxide **58** by triplet molecular oxygen. If oxygen abstracted a hydrogen atom from hydrogen peroxide **58**, formation of two hydroperoxide radicals **170** would follow. The hydroperoxide radical **170** could then react with diphenylketene **120** leading to the formation of **173**. Cleavage of the weak O–O bond of **173** would generate hydroxyl radical **59** and diradical **174a**, which would be in equilibrium with its electron-paired form - the α -lactone (diphenyloxiranone **174b**). Recombination of **174a** with cyclohexyl radical **63** would give **175**. Subsequent abstraction of a hydrogen atom from cyclohexane **3** by radical **175** would give observed ester **110**.

A series of experiments were designed and conducted to give further experimental support for this proposed reaction pathway.

2.8.4. Deuterium Studies

The origin of the proton on C_α (**Figure 2.12**) was investigated first.

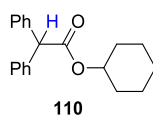
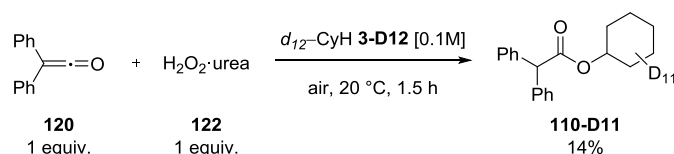


Figure 2.12. The position of proton on C_α of ester **110**.

Since cyclohexane **3** was always in excess during the reaction, it was postulated that the hydrogen atom originated from a molecule of **3**. In order to verify this hypothesis, diphenylketene **120** (1 equiv.) was added over 1.5 h at 20 °C to an open flask containing H_2O_2 •urea **122** (1 equiv.) and d_{12} -cyclohexane **3-D12** [0.1 M] (**Scheme 2.32**).



Scheme 2.32. Reaction with d_{12} -cyclohexane **3-D12**.

The product **110-D11** was partially purified by flash chromatography (14% isolated yield), although phenyl benzoate **176** and other minor impurities were not removed. Comparison of 1H NMR spectrum of the authentic sample of ester **110** (**Figure 2.13**) with that of **110-D11** (**Figure 2.14**) showed that the multiplet at 4.90–4.83 ppm and the peaks at 1.85–1.81 ppm, 1.69–1.64 ppm, and 1.54–1.23 ppm were not present. 2H NMR spectrum of **110-D11** (**Figure 2.15**) revealed peaks at 4.84 ppm (1D), 1.77 ppm (2D), 1.59 ppm (2D), 1.37 ppm (3D), 1.28 ppm (2D), and 1.17 ppm (1D) thus complementing the 1H NMR spectrum of ester **110-D11**. Mass spectrometry (LC-MS) showed ions at m/z 306.2 $[M+H]^+$ and 323.2 $[M+NH_4]^+$ (**Figure 2.17**) unequivocally confirming the correct identification of **110-D11**.

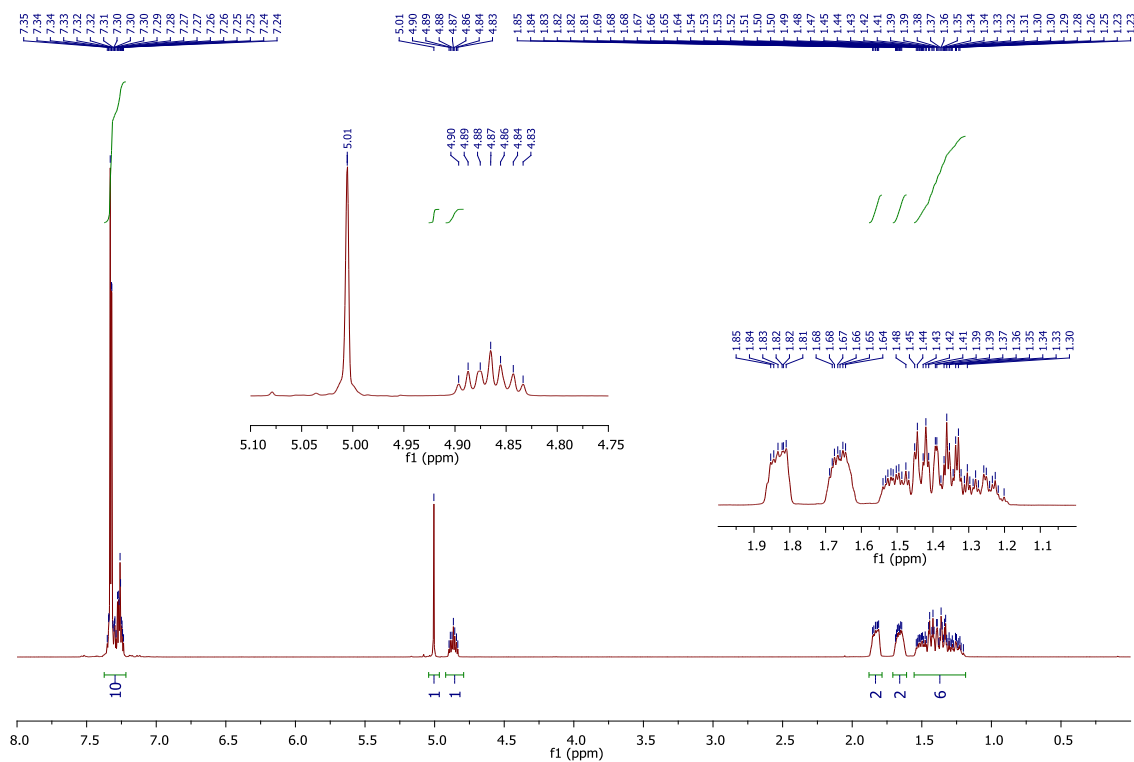


Figure 2.13. ^1H NMR spectrum of cyclohexyl 2,2-diphenylacetate **110**.

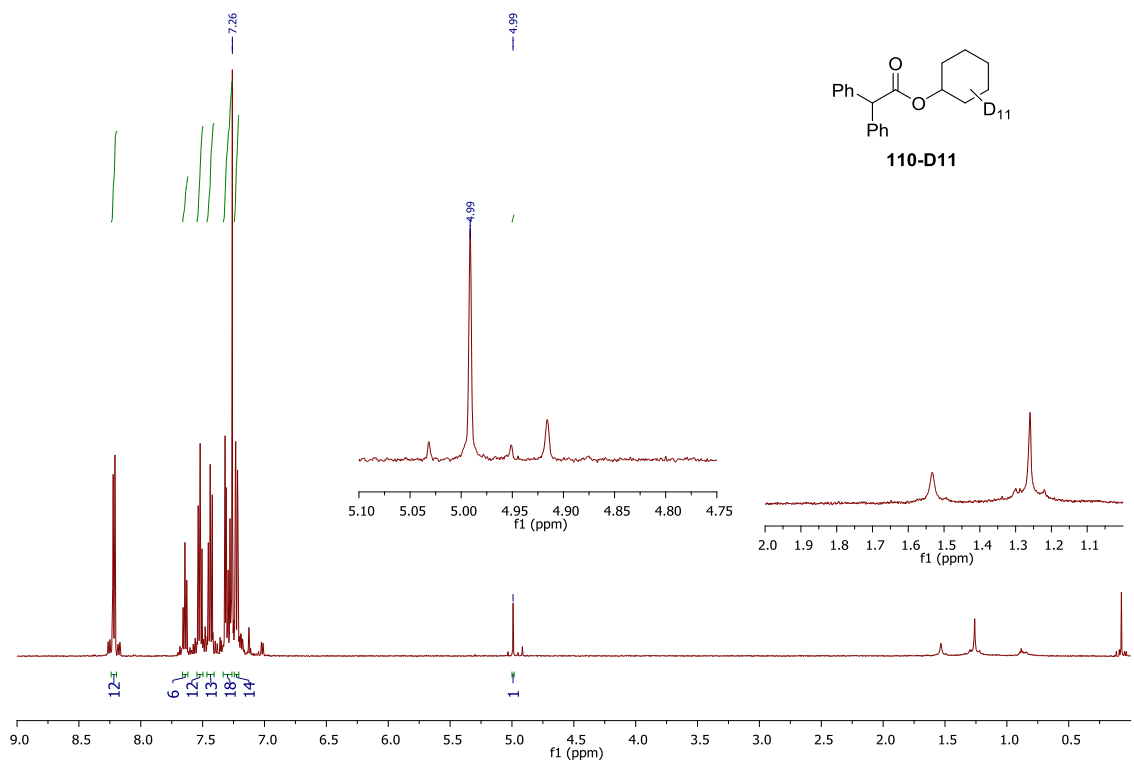


Figure 2.14. ^1H NMR spectrum of **110-D11**.

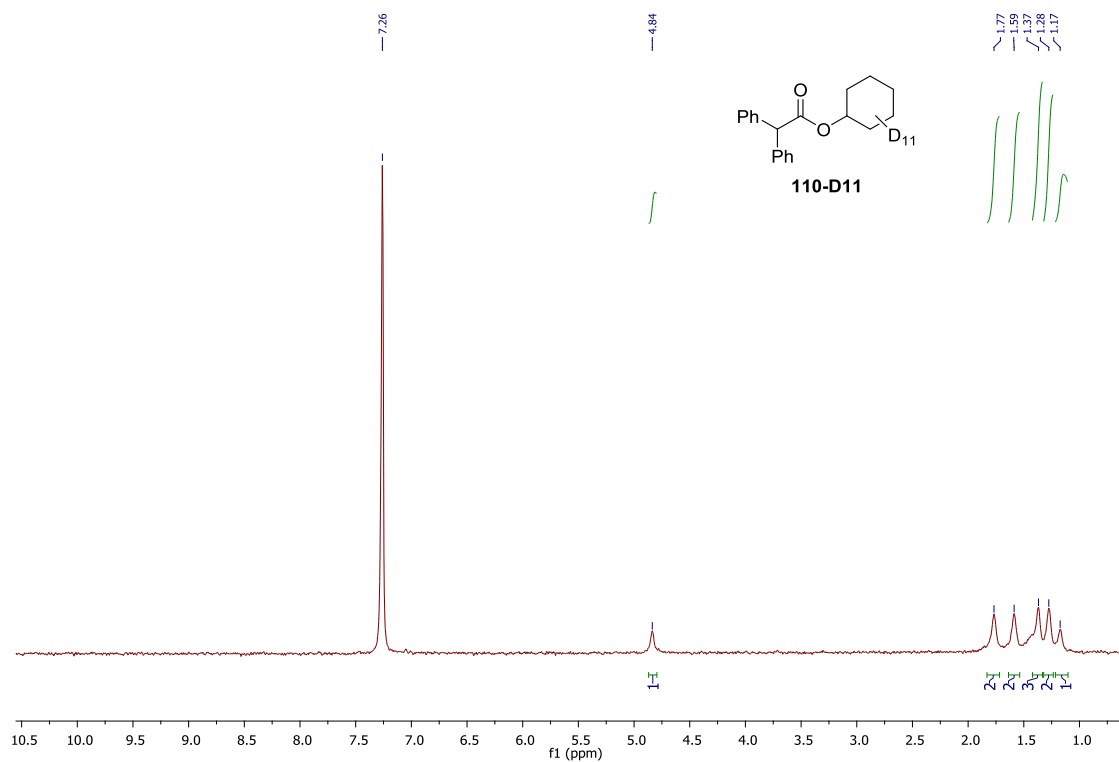


Figure 2.15. ^2H NMR spectrum of **110-D11**.

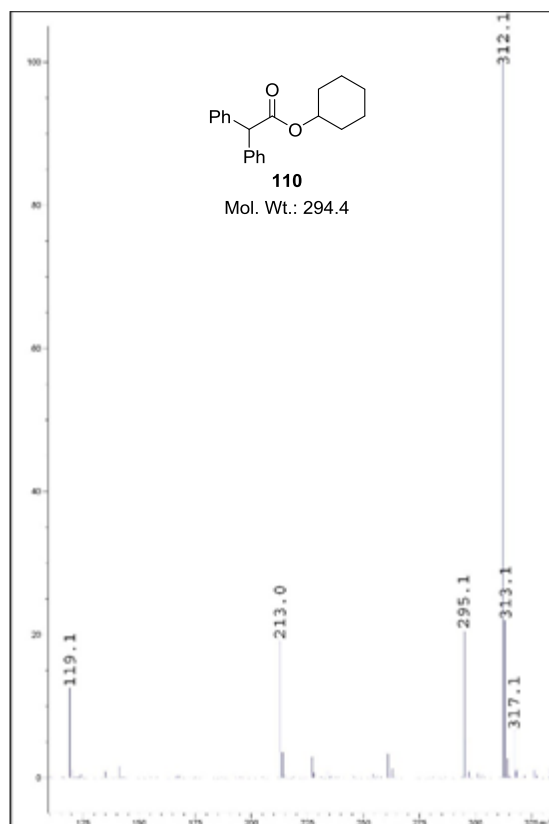


Figure 2.16. Mass spectrum of **110**.

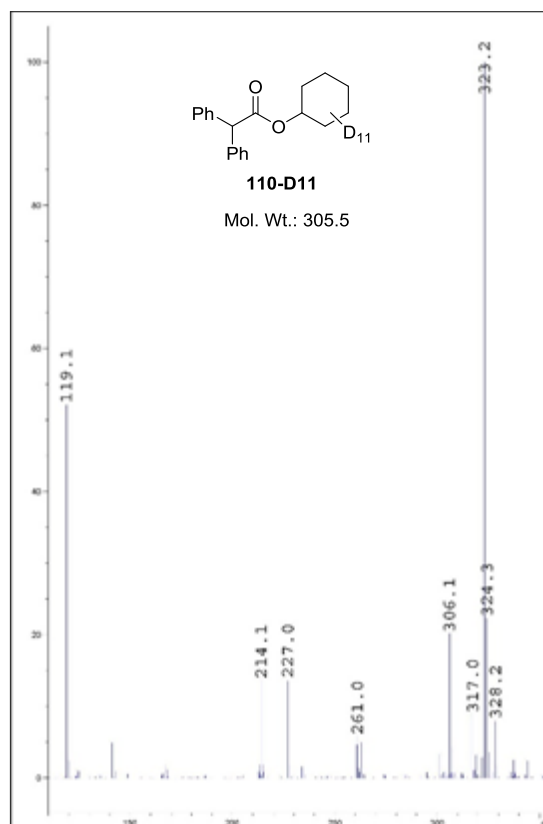
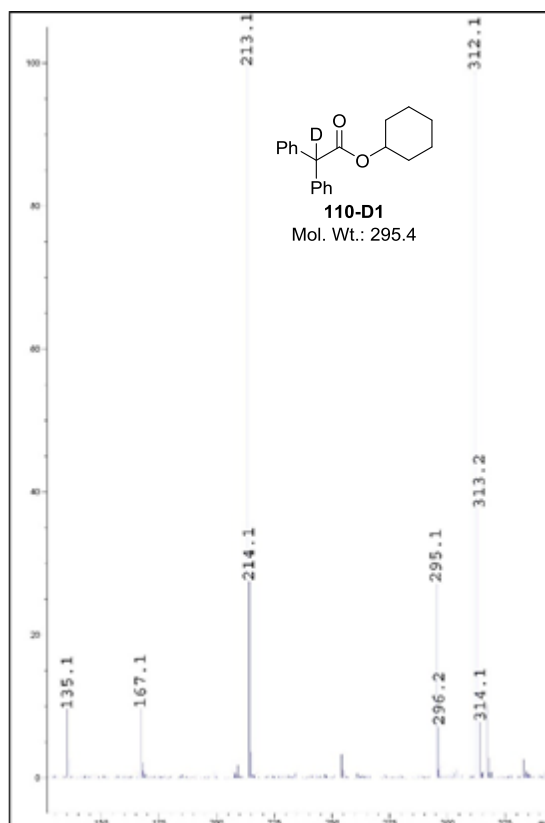
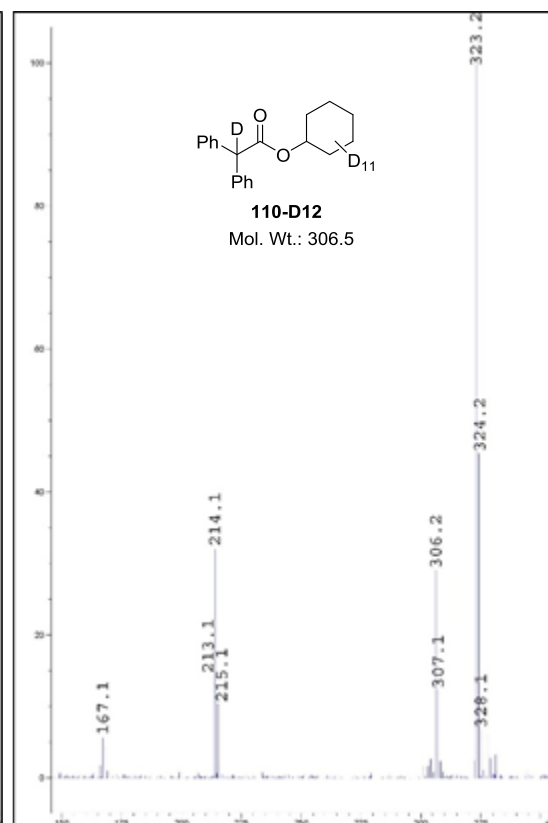
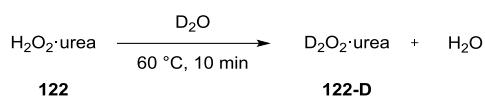


Figure 2.17. Mass spectrum of **110-D11**.

Figure 2.18. Mass spectrum of **110-D1**.Figure 2.19. Mass spectrum of **110-D12**.

Lack of evidence for the presence of a deuterium on C_α seemed to indicate that cyclohexane **3** was not the source of the proton in the final step of the proposed mechanism (Section 2.8.3., Figure 2.11), although deuterium-proton exchange during column chromatography could not be ruled out at this point. This result pointed to H_2O_2 •urea **122** being the most likely source of the proton on C_α . The only other possible sources were water and a fraction of non-deuterated **3** that is ever-present in commercial d_{12} -cyclohexane **3-D12** (0.4 atom %). However, both would only be present in small amounts and were disregarded as likely sources of protons. It was decided to probe the possible role of **122** as the proton source by synthesising its deuterated analogue, D_2O_2 •urea **122-D**. It was synthesised by dissolving **122** in D_2O and stirring the aqueous solution at 60 °C for 10 min (Scheme 2.33).⁷⁴ Careful removal of D_2O and H_2O under reduced pressure gave **122-D**.

Scheme 2.33. Preparation of $\text{D}_2\text{O}_2\cdot\text{urea}$ **122-D**.⁷⁴

The characterisation of **122-D** presented a considerable difficulty. Analysis by IR spectroscopy showed the characteristic O–D stretch as well as the O–H stretch. However, no quantitative information on the ratio of D_2O_2 to H_2O_2 or HOOD was available. Therefore, an effort was made to estimate the deuterium content by employing elemental analysis.

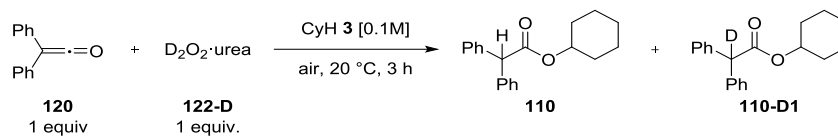
Table 2.19. Elemental analysis of $\text{H}_2\text{O}_2\cdot\text{urea}$ **122** and $\text{D}_2\text{O}_2\cdot\text{urea}$ **122-D**.

Entry	Compound	C [%]	H [%]	N [%]
1	$\text{H}_2\text{O}_2\cdot\text{urea}$	12.77	6.58	29.90
2	$\text{H}_2\text{O}_2\cdot\text{urea}$	12.61	6.52	29.88
3	$\text{D}_2\text{O}_2\cdot\text{urea}^1$	13.38	6.27	30.75
4	$\text{D}_2\text{O}_2\cdot\text{urea}^2$	12.84	6.33	29.95
5	$\text{D}_2\text{O}_2\cdot\text{urea}^3$	13.20	6.35	30.69
6	$\text{D}_2\text{O}_2\cdot\text{urea}^4$	14.45	6.17	31.78

¹reaction time 10 min; ²reaction time 1 h; ³reaction time 6 h; ⁴ $\text{D}_2\text{O}_2\cdot\text{urea}$ **122-D** prepared as shown in Scheme 2.33 but after evaporation of H_2O and D_2O the prepared sample was subjected to the same reaction conditions.

Table 2.19 shows the results of elemental analysis of a commercially available sample of $\text{H}_2\text{O}_2\cdot\text{urea}$ **122** performed in duplicate (Entries 1 and 2) and the prepared samples of $\text{D}_2\text{O}_2\cdot\text{urea}$ **122-D** (Entries 3–6). The percentage amount of hydrogen in $\text{D}_2\text{O}_2\cdot\text{urea}$ **122-D** samples (Entries 3–6) was close to those of $\text{H}_2\text{O}_2\cdot\text{urea}$ **122** samples (Entries 1 and 2), which revealed that this method was insufficiently sensitive to distinguish between H_2O and D_2O that formed upon combustion of the samples.

The sample of $\text{D}_2\text{O}_2\cdot\text{urea}$ **122-D** prepared (Scheme 2.33) was then used to obtain more information about the origin of the proton on C_α . Following our standard oxidation procedure, diphenylketene **120** (1 equiv.) was added over 3 h to an open flask containing $\text{D}_2\text{O}_2\cdot\text{urea}$ **122-D** (1 equiv.) and cyclohexane **3** [0.1 M] (Scheme 2.35).



Scheme 2.35. Oxidation reaction with D₂O₂•urea **122-D**.

Following completion of the reaction, the crude mixture was not subjected to an aqueous work up to avoid deuterium-proton exchange in the benzylic position. Instead, silica gel flash chromatography was used to isolate **110** and **110-D1** in 16% yield, but some impurities remained in the product, as was the case for ester **110**. It is possible that formation of **110** occurred during the isolation step. Nonetheless, comparison of ¹H NMR spectrum of the authentic sample of **110** (**Figure 2.13**) with that of **110-D1** (**Figure 2.20**) showed that the integration of the singlet at 5.01 ppm and the multiplet at 4.90–4.83 ppm did not match with the signal intensity being nearly 40% lower for the singlet (relative ratio 0.63:1.00) as would be expected if **110-D1** was partially deuterated in the benzylic position (37% deuterium incorporation). ²H NMR spectrum of **110-D1** revealed a single peak at 5.00 ppm (**Figure 2.21**), while mass spectrometry showed both ions at m/z 312.1 and 313.2 [M+H]⁺ (**Figure 2.18**). The abundance of the ion at m/z 313.2 was 38% relative to m/z 312.1, which was nearly twice as high as that of the authentic sample of **110** (22%). It is therefore clear that the presence of D₂O₂•urea **122-D** within the reaction mixture led to incorporation of deuterium at the C_α position of the product. It is entirely possible that this incorporation arose from exchange of the protonated product from D₂O₂•urea **122-D** although this possibility was not investigated further.

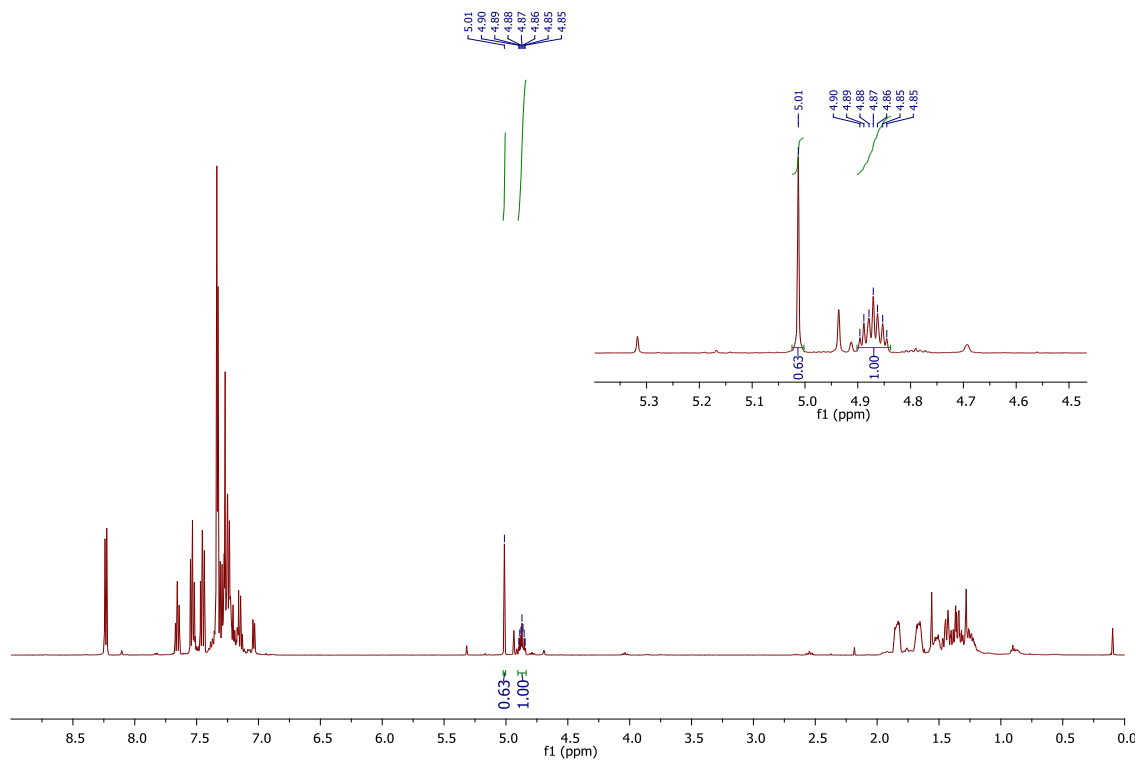


Figure 2.20. ^1H NMR spectrum of 110-D.

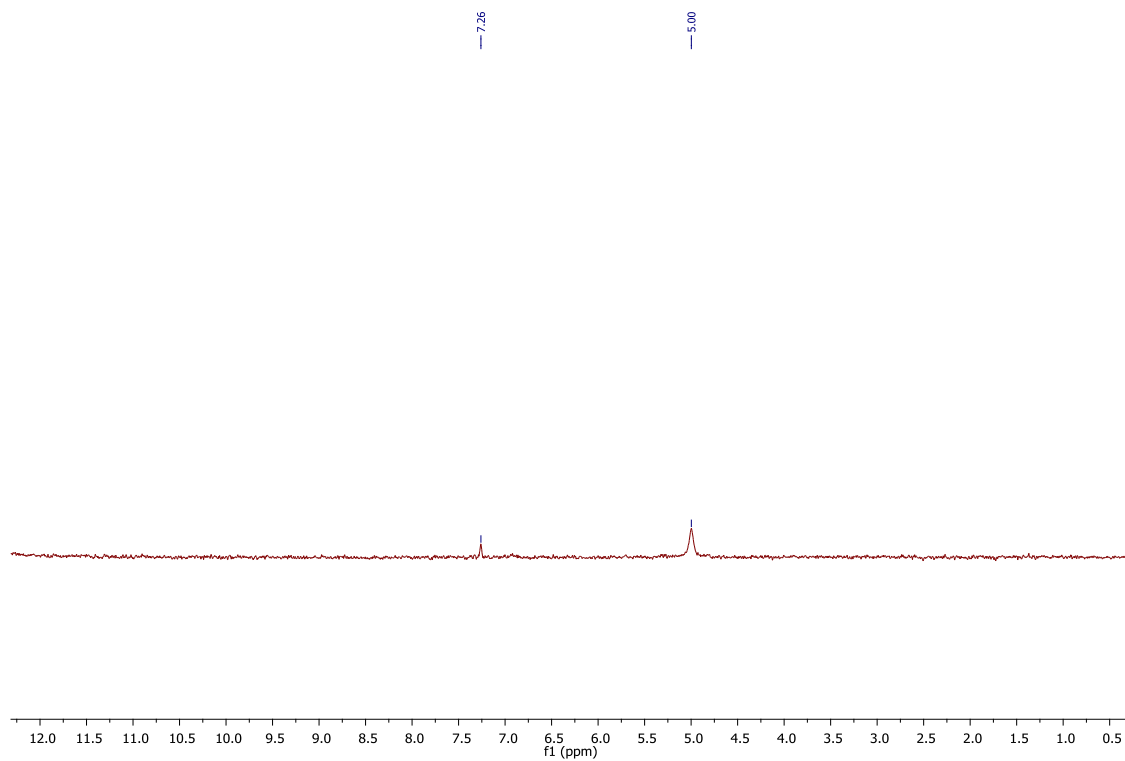
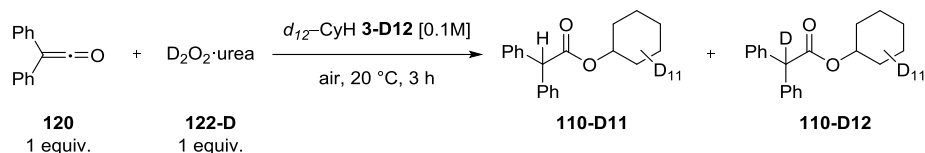


Figure 2.21. ^2H NMR spectrum of 110-D.

To gain further evidence, diphenylketene **120** (1 equiv.) was added over 3 h to a flask containing D_2O_2 •urea **122-D** (1 equiv.) and d_{12} -cyclohexane **3-D12** [0.1 M] (Scheme 2.36).



Scheme 2.36. Oxidation reaction with both D_2O_2 •urea **122-D** and d_{12} -CyH **3-D12**.

After 3 h the crude reaction mixture was not worked up to avoid proton-deuteron exchange, and a mixture of **110-D11** and **110-D12** was partially purified by silica gel flash chromatography (12% isolated yield). Comparison of the 1H NMR spectrum of the authentic sample of ester **110** (Figure 2.13) with that of the isolated products (Figure 2.22) showed two peaks in the 5.1–4.7 ppm region. Based on previous results (Figures 2.13 and 2.15), the singlet at 4.99 ppm is believed to belong to the benzylic proton of **110-D11**. 2H NMR spectrum (Figure 2.23) revealed a peak at 4.99 ppm, 4.84 ppm (1D), 1.77 ppm (2D), 1.59 ppm (2D), 1.37 ppm (3D), 1.28 (2D), and 1.17 ppm (1D). The intensity of the peak at 4.99 ppm was only 11% of that of the peak at 4.84 ppm, which means that more **110-D11** than **110-D12** was formed. This was expected due to the high concentration of **3-D12** relative to **122-D** during the reaction. Mass spectrometry showed ions at m/z 306.2 and 307.1 $[M+H]^+$ as well as m/z 323.2 and 324.3 $[M+NH_4]^+$ (Figure 2.19). The abundance of the ion at m/z 307.1 and 324.3 was 45% relative to the ion at m/z 306.2 and 323.2, which was twice as high as that of **110-D11** (22%) (Figure 2.17). By putting all this information together, it can be inferred that **110-D12** was deuterated on both the cyclohexyl ring and on C_α . This evidence supported the hypothesis that the proton on C_α originated from H_2O_2 •urea **122**.

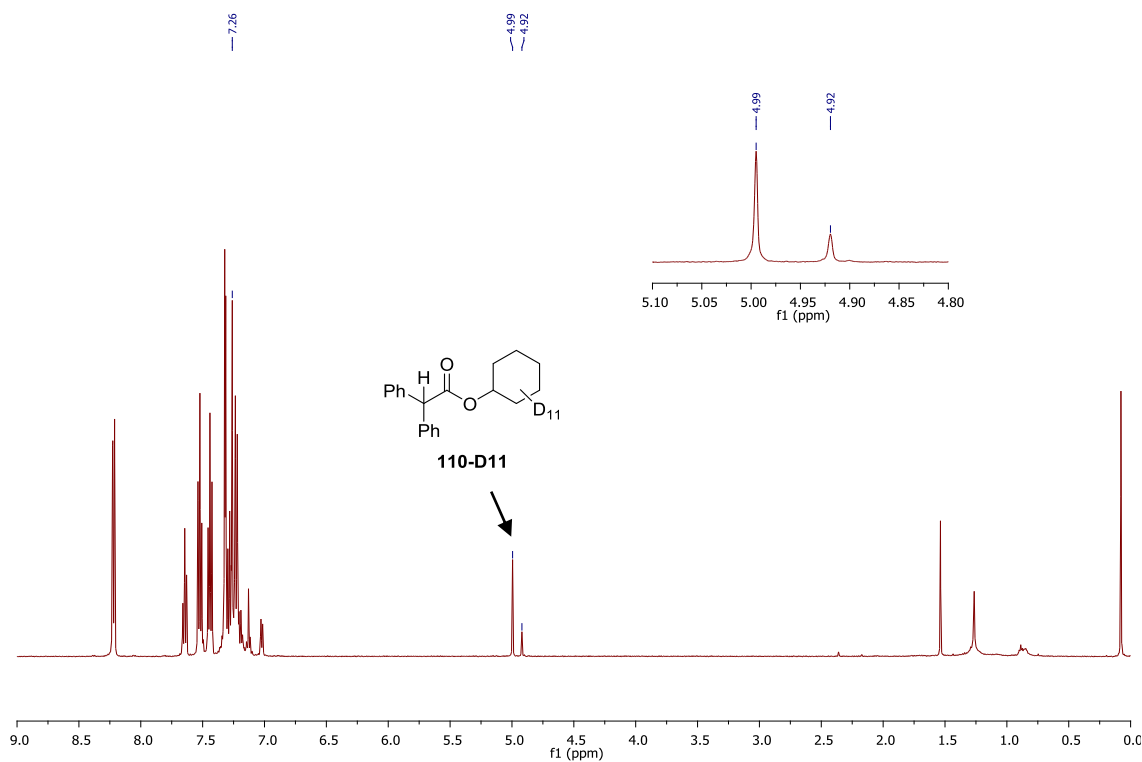


Figure 2.22. ^1H NMR spectrum of **110-D12**.

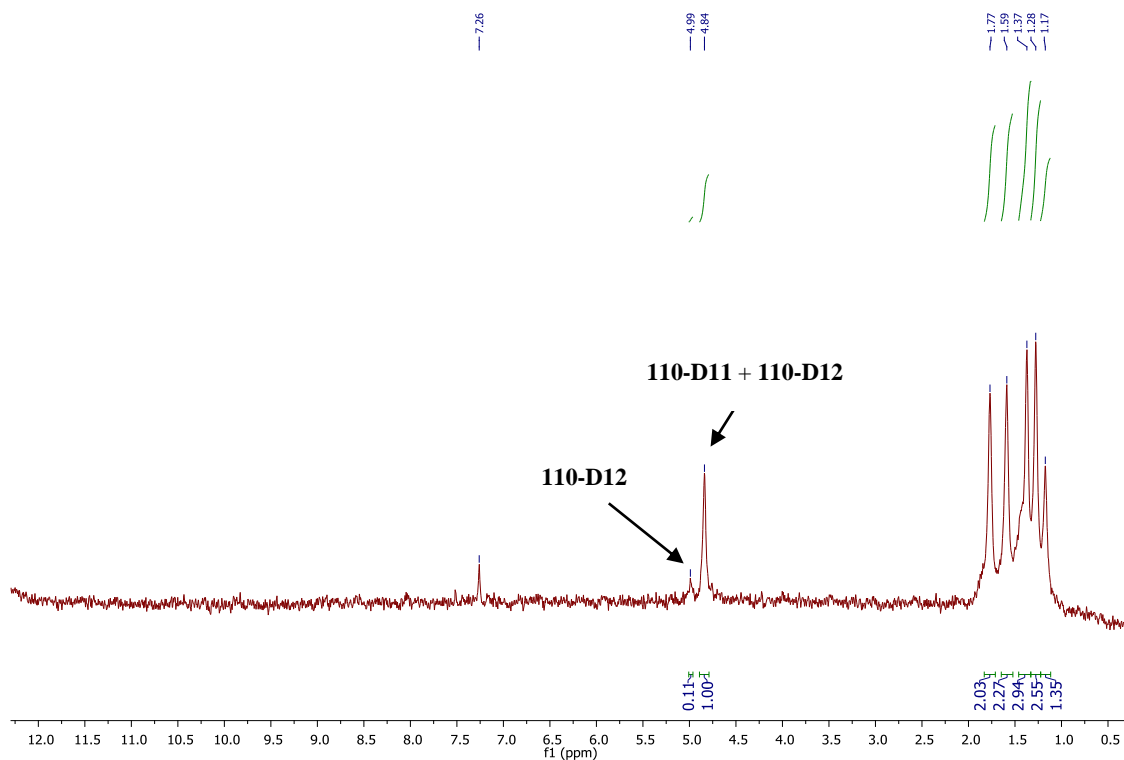


Figure 2.23. ^2H NMR spectrum of **110-D11** and **110-D12**.

Accordingly, the last step of the proposed mechanism was changed (**Figure 2.24**).

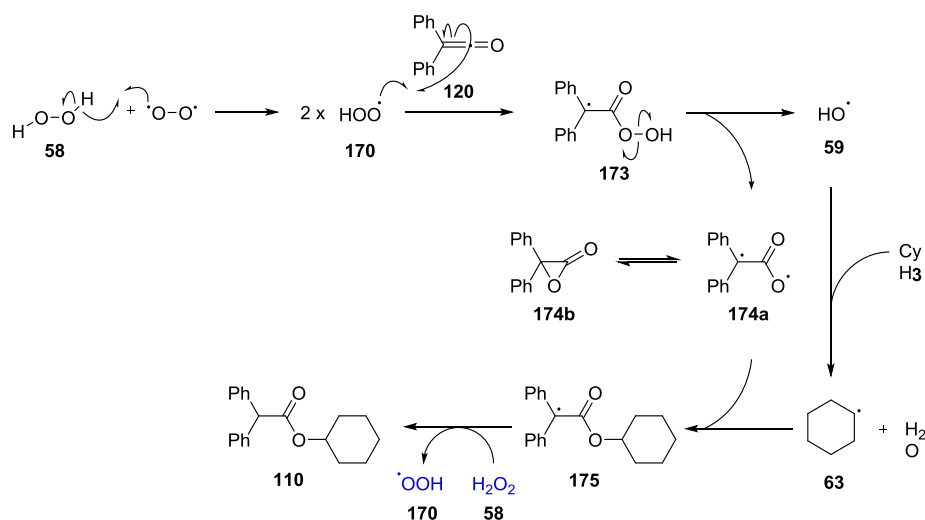
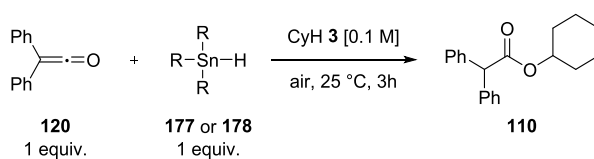


Figure 2.24. Revised proposed reaction mechanism.

Another approach to understanding this fascinating question was by using a well-known source of hydrogen atoms in radical chemistry. Organotin hydrides are the most frequently used hydrogen atom donors, and tributyltin hydride **177** and triphenyltin hydride **178** are the most commonly used reagents. Theoretically, they could have the same role as H_2O_2 •urea **122** in the reaction and so they were used as a substitute for **122** (**Table 2.20**).

Table 2.20. Investigations into organotin hydrides as a source of hydrogen atoms.



Entry	R	Conversion [%]
1	<i>n</i> -Bu	0
2	Ph	0

Disappointingly, neither reaction gave ester **110**. Perhaps elevated temperatures or irradiation with light was needed to generate free hydrogen atoms, although there are numerous literature examples where tributyltin hydride **177** was successfully used at

room temperature.⁷⁵ It also has to be taken into consideration that an increase in temperature may accelerate unwanted reactions leading to decomposition of diphenylketene **120**.

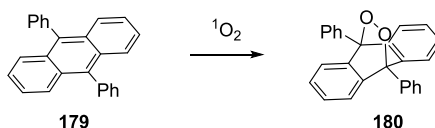
Despite this, substantial evidence was produced in support of H_2O_2 •urea **122** acting as the source of the proton on C_a . Further investigations into alternative radical initiators could greatly benefit the study if higher conversions of oxidised product were obtained.

2.8.5. Singlet vs. Triplet Oxygen

Triplet oxygen does not normally react with organic compounds that have a singlet ground state due to spin restriction. Singlet oxygen, on the other hand, is an active oxidant often used in chemical reactions. The singlet state of O_2 is experimentally⁷⁶ and theoretically⁷⁷ measured to be about 24 kcal mol⁻¹ higher in energy than the triplet state. Generation of singlet oxygen would therefore not be expected to occur under the mild conditions used in our oxidation system.

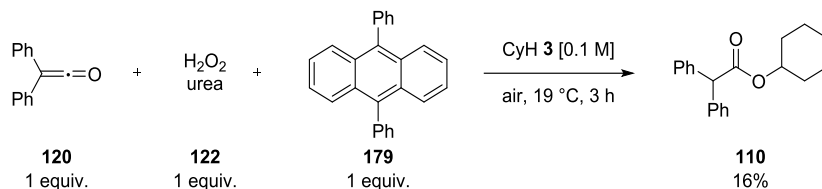
To evaluate the potential role of singlet oxygen on our reaction a series of experiments were conducted, which involved trapping singlet oxygen that may form during the reaction as well as generating singlet oxygen during the course of the reaction.

9,10-Diphenylanthracene **179** is a known chemical trap for singlet oxygen.⁷⁸ If singlet oxygen is present in the reaction, the corresponding endoperoxide **180** is formed, as shown in **Scheme 2.37**. Using **179** in our reaction should therefore result in lower conversions to ester **110**, if singlet oxygen is actively involved in the reaction.



Scheme 2.37. Trapping singlet oxygen.

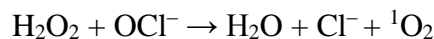
Diphenylketene **120** (1 equiv.) was added over 3 h to a mixture of H_2O_2 •urea **122** (1 equiv.), 9,10-diphenylanthracene **179** (1 equiv.), and cyclohexane **3** [0.1 M] (Scheme 2.38).



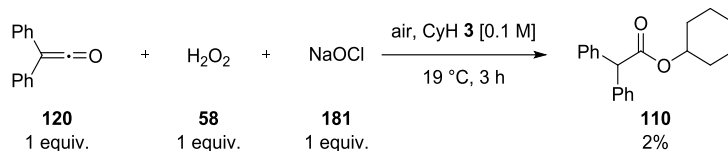
Scheme 2.38. Trapping singlet oxygen in the oxidation reaction of cyclohexane **3**.

Analysis of the reaction mixture showed no formation of 9,10-diphenylanthracene endoperoxide **180**. Furthermore, the conversion to **110** monitored by ^1H NMR spectroscopy did not seem to be greatly affected and was almost identical (16%) to those typically observed (17%).

The formation of singlet oxygen can be easily induced by adding aqueous hydrogen peroxide **58** to a hypochlorite **181** solution according to the equation:⁷⁹



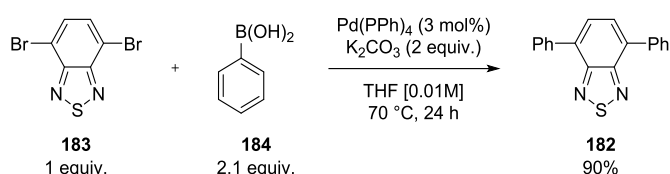
This process was used in our reaction in an attempt to generate singlet oxygen by adding aqueous hydrogen peroxide **58** (30% w/w, 1 equiv.) over 1 h to a mixture of sodium hypochlorite **181** (1 equiv.), diphenylketene **120** (1 equiv.), and cyclohexane **3** [0.1 M]. Subsequently, the biphasic system was stirred for 3 h at 19 °C (Scheme 2.39).



Scheme 2.39. Generation of singlet oxygen during the reaction.

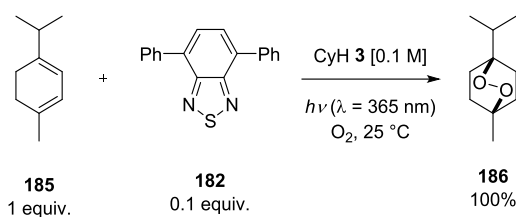
The conversion to **110** was only 2% by ^1H NMR spectroscopy. This result is in accord with our assumption that singlet oxygen does not participate in the reaction. However, since the conversion could have been lowered by the presence of water and the sodium

hypochlorite solution **181**, an alternative method of generating singlet oxygen was proposed in collaboration with Dr Filipe Vilela (Heriott-Watt University).⁸⁰ Different dyes and transition metal complexes can generate singlet oxygen upon irradiation, and they can be conveniently used in homogeneous solution or immobilised on a solid support. Polymer networks based on benzothiadiazole as a building block have been successfully used by the Vilela group to generate singlet oxygen,⁸¹ and the idea to use **182** (Scheme 2.40) in a similar manner emerged. Palladium-catalysed Suzuki-Miyaura cross-coupling of **183** and **184** gave **182** in 90% isolated yield upon purification by flash chromatography (Scheme 2.40).⁸¹



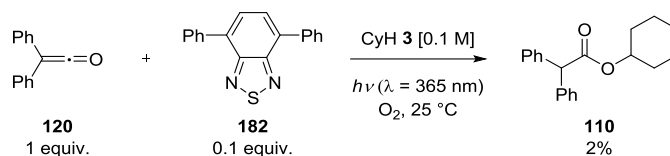
Scheme 2.40. Synthesis of **182**.

The efficiency of **182** as a photocatalyst in the production of singlet oxygen was evaluated by stirring α -terpinene **185** (1 equiv.) and **182** (0.1 equiv.) in cyclohexane **3** [0.1 M] under UV light (365 nm) while oxygen gas was bubbled through the solution (Scheme 2.41). The conversion was monitored by ¹H NMR spectroscopy.



Scheme 2.41. Conversion of α -terpinene **185** into ascaridole **186** using singlet oxygen.

Following the complete conversion of α -terpinene **185** to ascaridole **186** after only 3 h, **182** (1 equiv.) was used in place of H₂O₂•urea **122** within our oxidation procedure (Scheme 2.42). However, unlike **122** it did not induce a better conversion to ester **110** (2%) compared to the control reaction with oxygen gas (Scheme 2.41).



Scheme 2.42. Generation of singlet oxygen in the benchmark reaction using **182**.

In combination with the previous experimental results, it was concluded that no experimental evidence was found to suggest the involvement of singlet oxygen in the reaction.

2.8.6. ^{18}O -Labelling Studies

Taking into consideration the fact that oxygen promoted the reaction, experiments using $^{18}O_2$ gas were carried out to determine the origin of the oxygen atom in the ester product. To reduce the effect of fortuitous $^{16}O_2$ to a negligible level, extensive precautionary measures were undertaken. All reactions were conducted in a custom-made four-neck flask of our design (**Figure 2.25**). The flask can be easily fabricated from readily available components: a 25 mL round-bottom flask and Young taps with basic glassblowing skills. In addition, the flask was placed in a glove bag, from which air was removed and replaced with an inert gas (argon or nitrogen).

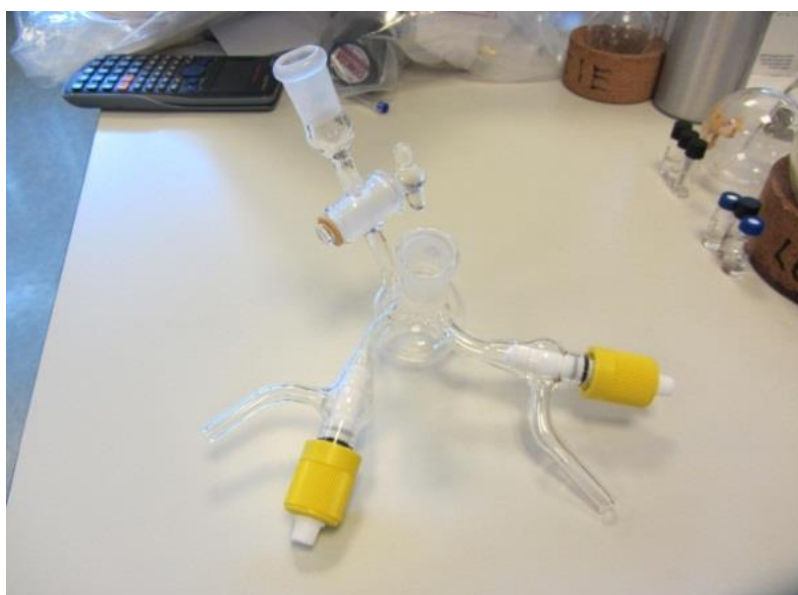
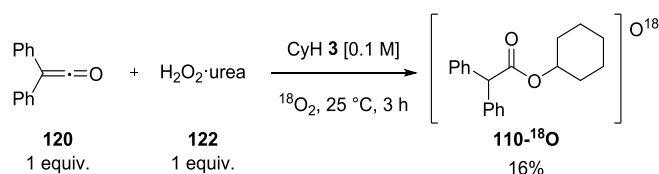


Figure 2.25. Custom-made flask for ^{18}O -labelling studies.

With these precautionary measures in place, diphenylketene **120** (1 equiv.) in a small amount of degassed, anhydrous cyclohexane **3** [0.5 M] was added over 3 h to a sealed flask containing degassed cyclohexane **3** [0.1 M] and H_2O_2 •urea **122** (1 equiv.) under a saturated $^{18}\text{O}_2$ atmosphere (**Scheme 2.43**). The reaction proceeded as expected and the product was isolated in a 16% yield following flash chromatography.



Scheme 2.43. Benchmark reaction under a saturated $^{18}\text{O}_2$ atmosphere.

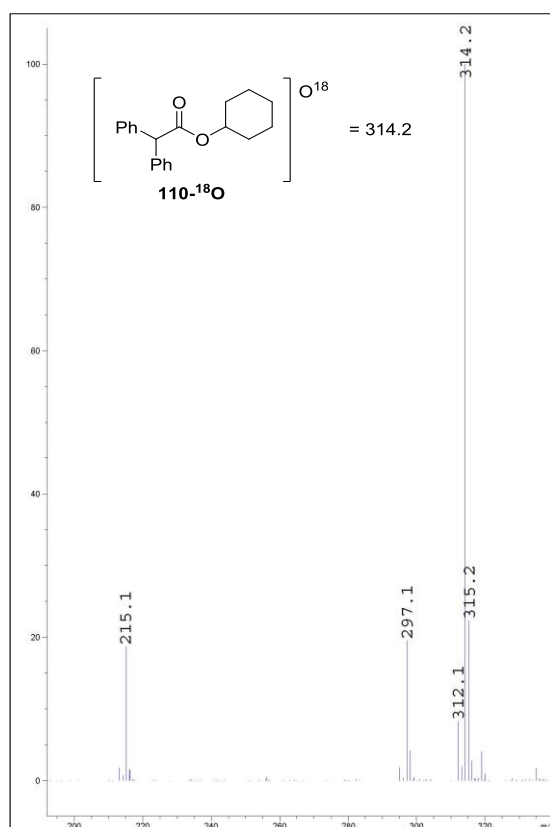
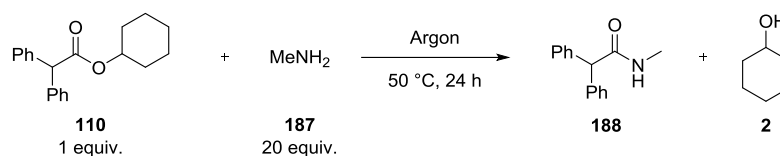


Figure 2.26. Mass spectrum of **110-¹⁸O**.

Mass spectroscopic analysis showed ions m/z 215.1, 297.1 $[\text{M}+\text{H}]^+$ and 314.2 $[\text{M}+\text{NH}_4]^+$ (**Figure 2.26**), all of which showed the difference of two mass units when compared to the corresponding ions of the non-labelled sample of **110** (**Section 2.8.4, Figure 2.10**). This result revealed that one isotopic oxygen atom was indeed incorporated into the product **110-¹⁸O** from $^{18}\text{O}_2$ gas, but the position of the ^{18}O atom could not be deduced from the fragmentation pattern obtained. This was instead established through derivatisation, which was first performed on an authentic sample of **110** (1 equiv.) that was stirred in methylamine **187** (20 equiv., 33 wt. % in

ethanol) under an argon atmosphere at 50 °C for 24 h (**Scheme 2.44**).

Scheme 2.44. Derivatisation of **110**.

Detection of both *N*-methyl-2,2-diphenylacetamide **188** and cyclohexanol **2** could be achieved by GC-MS (CI) on the crude reaction mixture. **Figure 2.28** shows the m/z 226.1 ion of **188** $[M+H]^+$ and **Figure 2.29** shows the m/z 99.0 ion of cyclohexanol **2** $[M-H]^-$ (matching the mass spectrum of commercially available cyclohexanol **2**). **110- ^{18}O** was next derivatised following the same method (**Scheme 2.44**). Mass spectrum of **188** derivatised from **110- ^{18}O** (**Figure 2.30**) showed the molecular ion m/z 226.1 $[M+H]^+$, revealing the absence of the ^{18}O atom. The m/z 228.1 ion was also present but its abundance was 3% relative to the m/z 226.1 ion, which closely matched that of the non-labelled ester **110** (2%). The mass spectrum of cyclohexanol **2** derivatised from **110- ^{18}O** (**Figure 2.31**) showed the molecular ion m/z 101.0 $[M-H]^+$ expected for a molecule of cyclohexanol **2** with an incorporated ^{18}O atom. The m/z 99.0 ion was also present but its abundance relative to the m/z 101.0 ion was only 66%. In contrast, the abundance of the m/z 100.9 ion relative to the m/z 99.0 ion was only 15% in **110**. All the available evidence suggested that ester **110- ^{18}O** had an ^{18}O atom incorporated between the carbonyl carbon atom and the cyclohexyl ring (**Figure 2.27**).

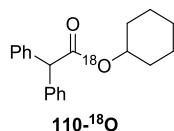


Figure 2.27.

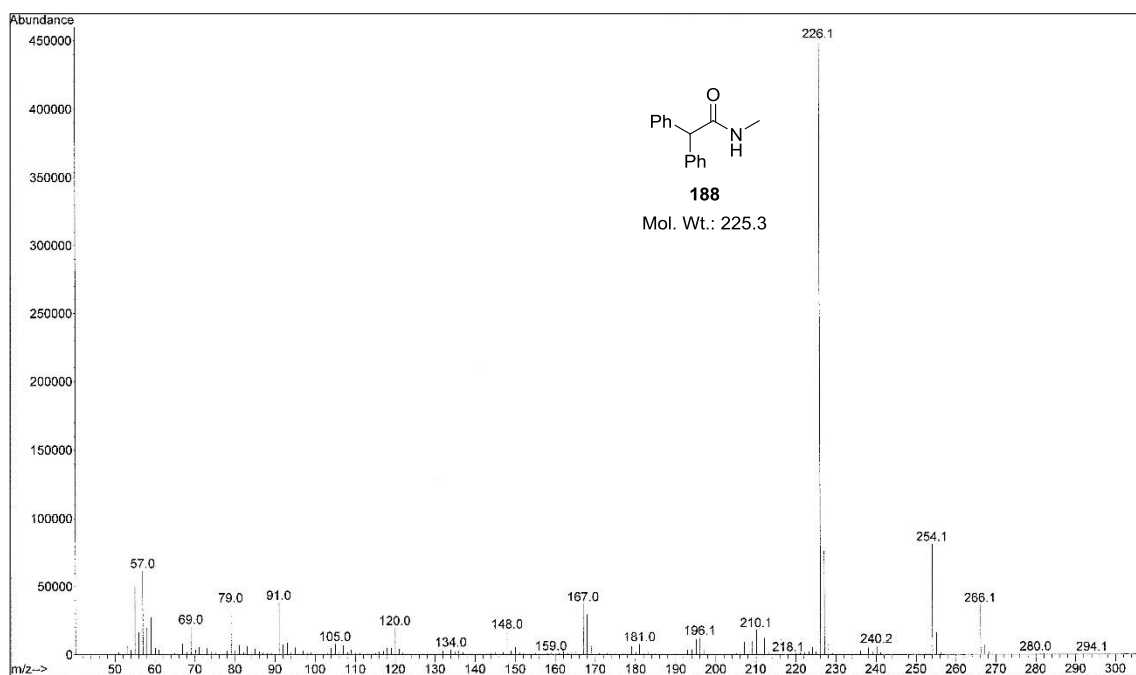


Figure 2.28. Mass spectrum of *N*-methyl-2,2-diphenylacetamide **188** after derivatisation of **110**.

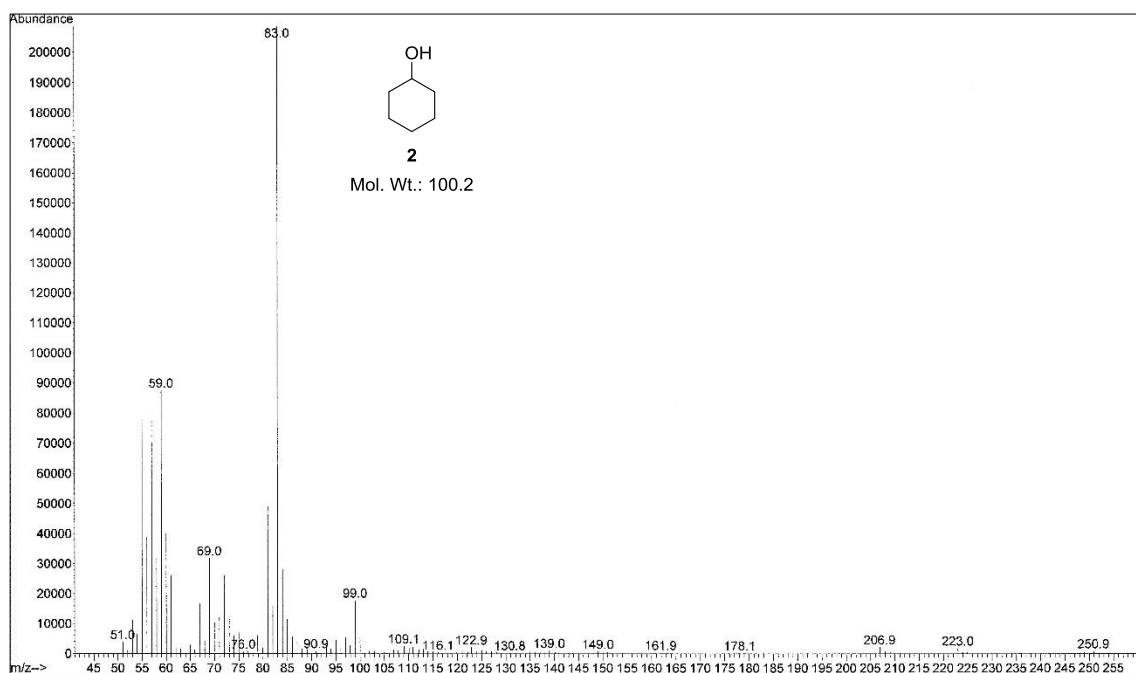


Figure 2.29. Mass spectrum of cyclohexanol **2** after derivatisation of **110**.

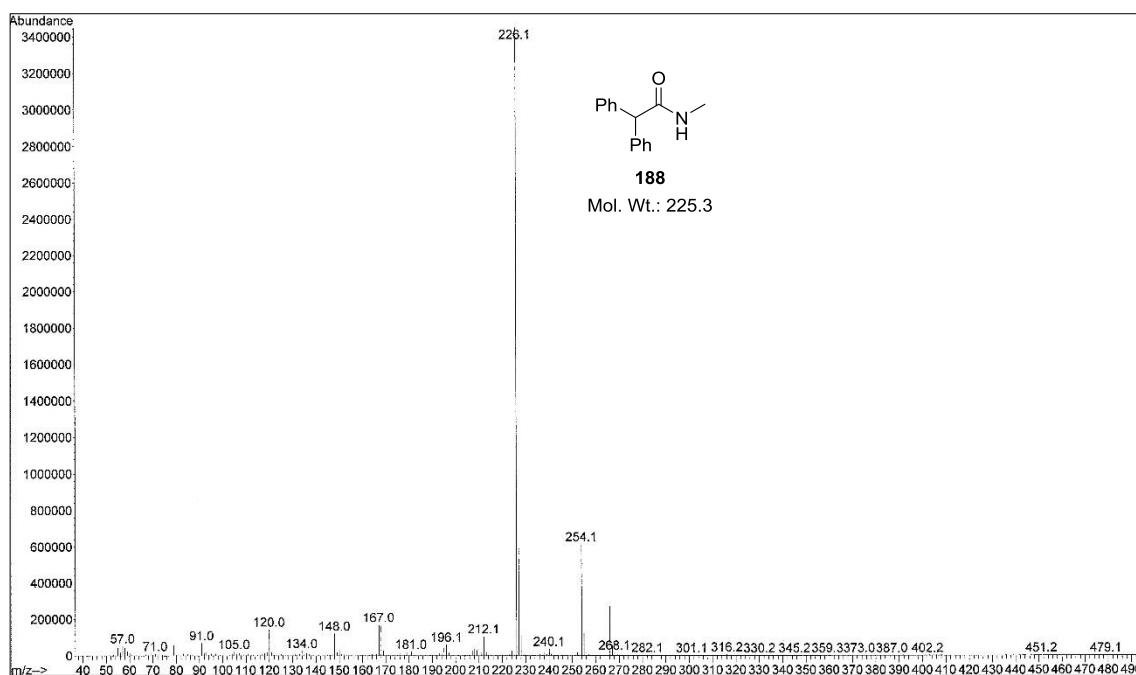


Figure 2.30. Mass spectrum of *N*-methyl-2,2-diphenylacetamide **188** after derivatisation of **110–O18**.

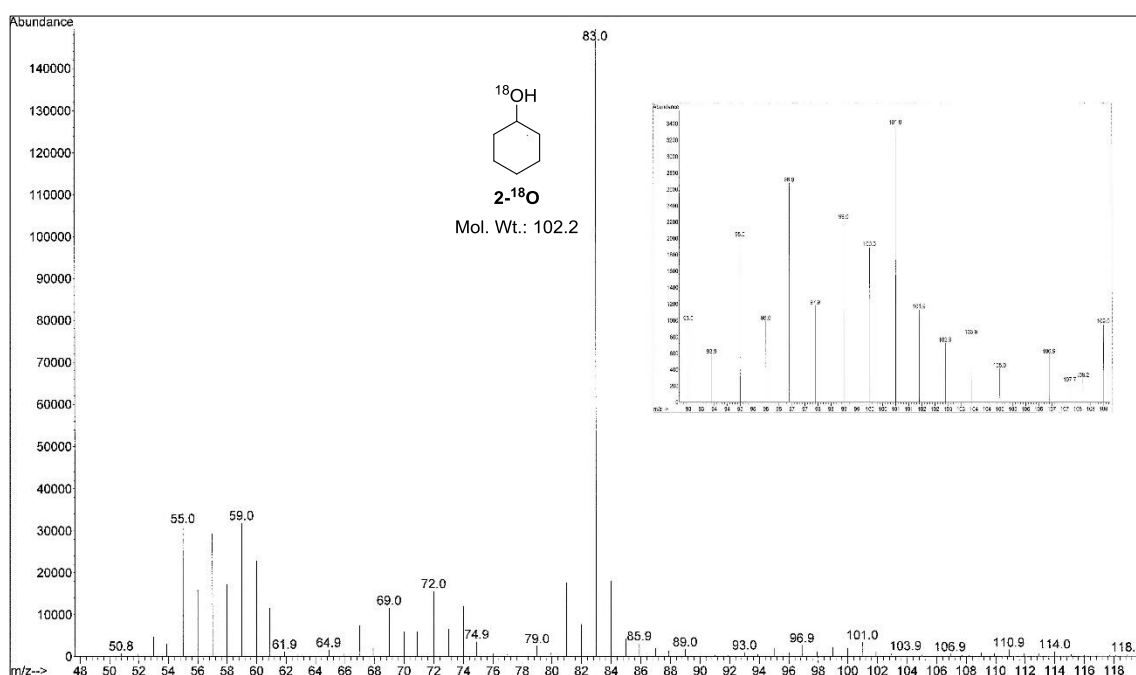
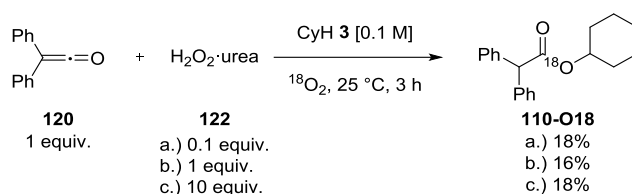


Figure 2.31. Mass spectrum of cyclohexanol **2** with an ^{18}O atom.

Having gathered this important information, we endeavoured to gain evidence for the first step of our proposed mechanism by varying the amount of hydrogen peroxide **58** in the reaction. According to our hypothesis, if oxygen gas was in equilibrium with hydrogen peroxide **58**, a smaller amount of H_2O_2 :urea **122** used in the reaction should be reflected

in more ^{18}O -incorporation in the product. Likewise, if more $\text{H}_2\text{O}_2\cdot\text{urea}$ **122** was used, less ^{18}O -labelled product should form. Substoichiometric (0.1 equiv.) and superstoichiometric (10 equiv.) amounts of $\text{H}_2\text{O}_2\cdot\text{urea}$ **122** were used in the experiments, which involved a 3 hour addition of diphenylketene **120** (1 equiv.) to the respective amount of $\text{H}_2\text{O}_2\cdot\text{urea}$ **122** in cyclohexane **3** [0.1 M] under an atmosphere saturated with $^{18}\text{O}_2$ (**Scheme 2.45**).



Scheme 2.45. Isotope labelling experiments with various amounts of $\text{H}_2\text{O}_2\cdot\text{urea}$ **122**.

The products were partially purified by flash chromatography and were isolated in similar yields (16–18%). Mass spectra of the products were acquired to determine the extent of ^{18}O incorporation. **Figure 2.32** and **2.33** show that the singly-labelled product was formed predominantly regardless of the amount of $\text{H}_2\text{O}_2\cdot\text{urea}$ **122** used in the reaction. This suggests that hydrogen peroxide does not serve as a source of the introduced oxygen atom in the reaction.

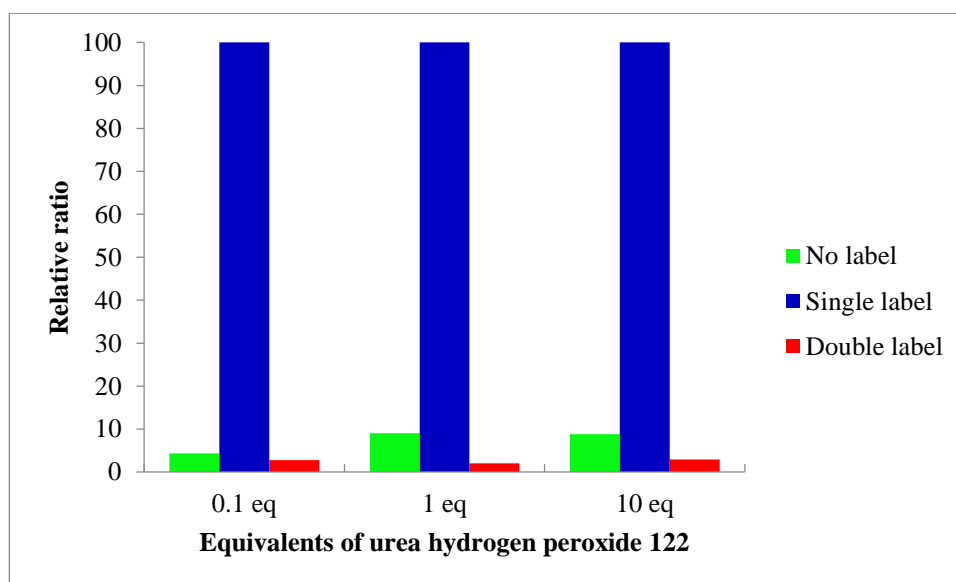


Figure 2.32. Relative ratio of ^{18}O incorporation into **110- ^{18}O** $[\text{M}+\text{H}]^+$.

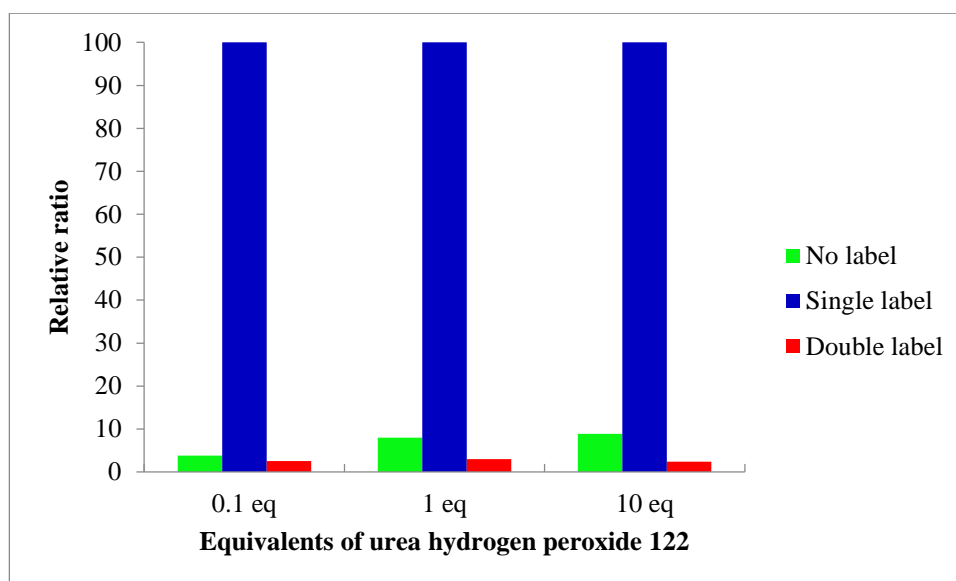


Figure 2.33. Relative ratio of ^{18}O incorporation into the ammonium adduct of $110\text{-}^{18}\text{O}$ $[\text{M}+\text{NH}_4]^+$.

2.8.7. Further ^{18}O -labelling Studies

The results of the labelling experiments were at odds with our proposed first step of the mechanism (Section 2.8.4., Scheme 2.24). This was surprising as it is commonly accepted that oxygen can abstract a hydrogen atom from organic molecules. Further support to that assertion came from the oxidation of 1,4-dihydroxynaphthalene **189** to 1,4-naphthaquinone **190** which was monitored on the NMR scale over a month (Figure 2.34).

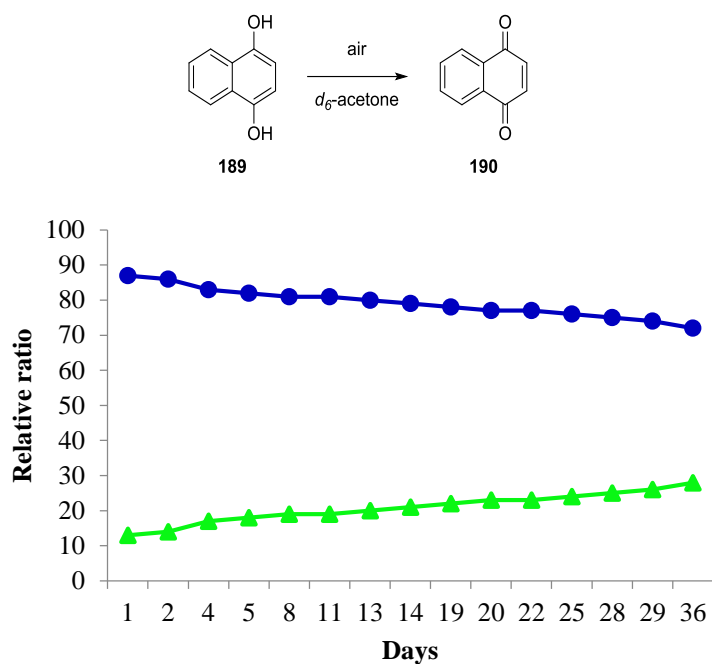
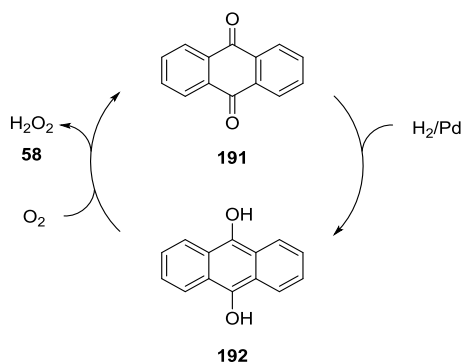


Figure 2.34. Oxidation of 1,4-dihydroxynaphthalene **189** (●) to 1,4-naphthaquinone **190** (▲) under an air atmosphere.

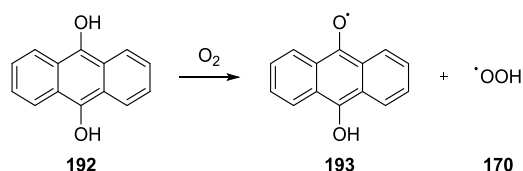
The oxidation was relatively slow although it should be noted that the sample was not mechanically stirred. A 17% conversion of 1,4-dihydroxynaphthalene **189** to 1,4-naphthaquinone **190** was observed by ^1H NMR spectroscopy after 36 days, demonstrating that atmospheric oxygen was capable of hydrogen atom abstraction.

Air and oxygen-containing gases are also used in the large-scale production of hydrogen peroxide **58**. In this process, anthraquinone **191** is reduced to anthrahydroquinone **192**, which enters a catalytic cycle to regenerate **191** and hydrogen peroxide **58** (Scheme 2.46).



Scheme 2.46. Process for the commercial production of H_2O_2 **58**.

Despite the industrial importance of this process, little is known about the precise reaction mechanism. Recently, Nishimi and co-workers proposed a mechanism for the formation of hydrogen peroxide **58** in this process.⁸² Interestingly, it was postulated that a hydrogen atom is abstracted from a hydroxyl group of anthrahydroquinone **192** to give the hydroperoxy radical **170** and the 10-hydroxy-9-anthroxyl radical **193**, which is also the rate-determining step of the process (**Scheme 2.47**).



Scheme 2.47. Abstraction of a hydrogen atom from anthrahydroquinone **192** by triplet O_2 .

Once radicals **193** and **170** are formed, anthraquinone **191** is produced in almost a barrierless fashion along **Pathways A** and/or **B** (**Figure 2.35**) according to computational studies.

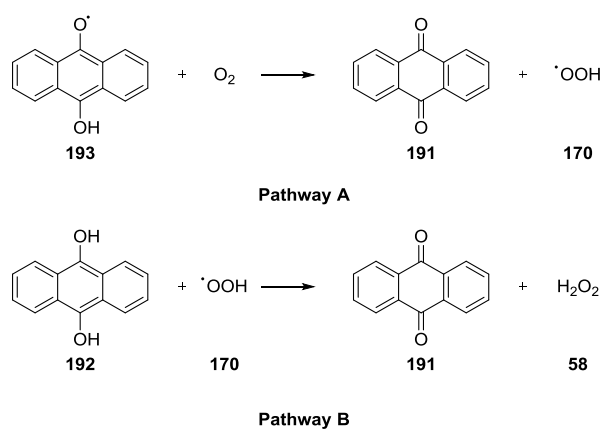
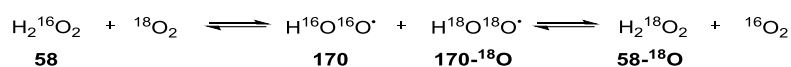


Figure 2.35. Proposed reaction pathways for the formation of H_2O_2 **58**.

The authors calculated the energy barrier for the abstraction of a hydrogen atom from anthrahydroquinone **192** to be only about $12.0 \text{ kcal mol}^{-1}$. Given the enthalpy of formation of the hydroperoxy radical **170** of $3.49 \text{ kcal mol}^{-1}$,⁷¹ direct abstraction of a hydrogen atom from hydrogen peroxide **58** seemed to be energetically viable under the reaction conditions in our system.

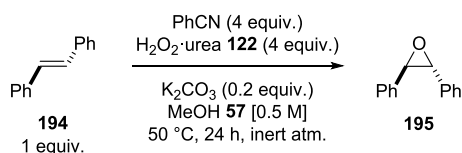
However, changing the amount of $\text{H}_2\text{O}_2\cdot\text{urea}$ **122** did not seem to have much effect on the ^{18}O -incorporation into the product, and so another experiment was designed to re-evaluate the first step of the proposed mechanism.

We hypothesised that hydrogen atom abstraction from $\text{H}_2\text{O}_2\cdot\text{urea}$ **122** must occur sufficiently fast during the 3 hour reaction to produce the target product. Furthermore, we postulated that molecular oxygen was in equilibrium with hydrogen peroxide **58**. Hence, if $\text{H}_2\text{O}_2\cdot\text{urea}$ **122** was exposed to an atmosphere of $^{18}\text{O}_2$ gas, a level of ^{18}O -incorporation into **122** should be observed as shown in **Scheme 2.48**.



Scheme 2.48. Theoretical equilibrium between oxygen gas and hydrogen peroxide **58**.

To test this theory, $\text{H}_2\text{O}_2\cdot\text{urea}$ **122** was stirred in a small amount of cyclohexane **3** under a saturated $^{18}\text{O}_2$ atmosphere for 3 h. Before the sample was exposed to $^{18}\text{O}_2$ gas, argon was removed by the freeze-pump-thaw method. As a precautionary measure the flask was placed in a glove bag. Air was evacuated from the glove bag and replaced with argon gas, which was repeated two more times. The obtained $\text{H}_2\text{O}_2\cdot\text{urea}$ **122** was then used in Payne epoxidation⁸³ of *trans*-stilbene **194**. A control reaction with **122** was run prior to the use of **122**- ^{18}O . *trans*-Stilbene oxide **195** was obtained by mixing benzonitrile (4 equiv.), $\text{H}_2\text{O}_2\cdot\text{urea}$ **122** (4 equiv.), potassium carbonate (0.2 equiv.), and *trans*-stilbene **194** (1 equiv.) in anhydrous methanol **57** [0.5 M] under an inert atmosphere at 50 °C for 24 h (**Scheme 2.49**).



Scheme 2.49. Payne epoxidation of *trans*-stilbene **194**.

The crude reaction mixture was analysed by GC-MS (CI). **Figure 2.36** shows the mass spectrum of the crude reaction mixture from the reaction with $\text{H}_2\text{O}_2\cdot\text{urea}$ **122**, while **Figure 2.37** shows the mass spectrum of the crude reaction mixture from the reaction

with H_2O_2 •urea **122- ^{18}O** (obtained after exposure to $^{18}\text{O}_2$). Comparison of the two samples showed that ^{18}O was not incorporated into *trans*-stilbene oxide **195**. This observation suggested that the first step of the reaction mechanism was different to the one proposed and we were not generating $\text{H}_2^{18}\text{O}_2$ within the reaction mixture (Section 2.8.4, Scheme 2.24).

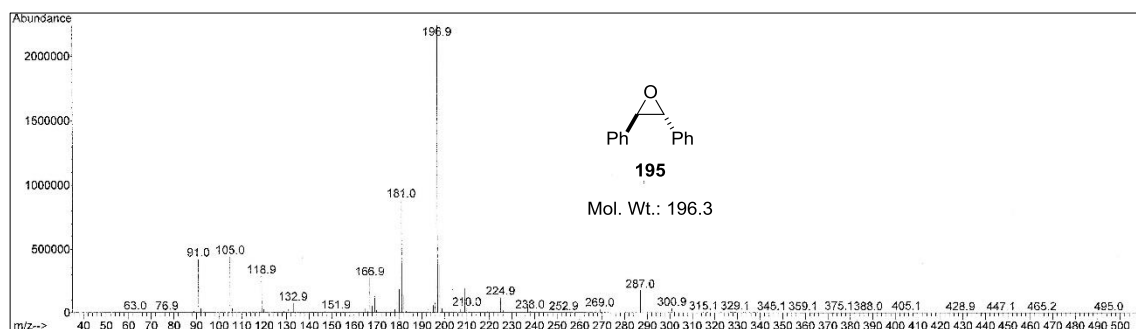


Figure 2.36. Mass spectrum of *trans*-stilbene oxide **195** from a control reaction with **122**.

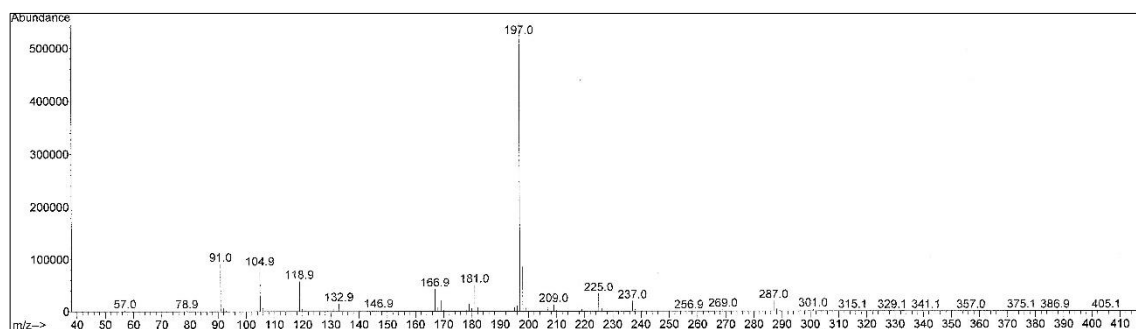
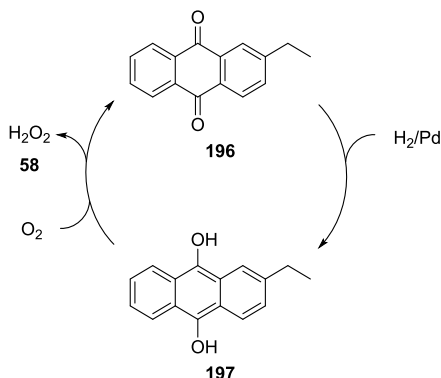


Figure 2.37. Mass spectrum of *trans*-stilbene oxide **195** from the reaction with **122- ^{18}O** .

2.8.8. Generation of ^{18}O -Labelled Hydrogen Peroxide **58- ^{18}O**

While valuable mechanistic information on the importance of oxygen was gained, the function of hydrogen peroxide **58** was still not known. Monitoring the fate of hydrogen peroxide **58** in the course of the reaction would be highly insightful and could be achieved through isotope-labelling. Unfortunately, ^{18}O -labelled hydrogen peroxide **58- ^{18}O** currently has limited commercial availability and comprises only 2–3% of the aqueous solution with 90% ^{18}O -atom incorporation. Worse yet, all efforts to obtain a commercial sample of **58- ^{18}O** were fruitless and therefore attempts were made to synthesise **58- ^{18}O** according to the method described by Jankowski and Kamiński.⁸⁴ The synthesis was

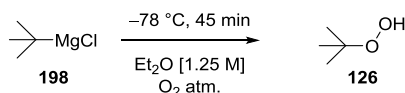
based on the commercial production process of hydrogen peroxide **58** (Section 2.8.7, Scheme 2.46) but used ethylanthraquinone **196** rather than anthraquinone **191** as the catalytic substrate (Scheme 2.50).



Scheme 2.50. Synthesis of ^{18}O -labelled hydrogen peroxide **58- ^{18}O** .⁸⁴

A series of experiments were conducted to find optimal reaction conditions under an $^{16}O_2$ atmosphere, resulting in the formation of hydrogen peroxide **58** (30–100 mg L⁻¹ quantified by Quantofix Peroxide 100[®] strips). Work is currently on-going within the group to implement this methodology in the synthesis of ^{18}O -labelled hydrogen peroxide **58- ^{18}O** to further mechanistic investigations.

An alternative approach was the use of labelled alkyl peroxides.⁸⁵ Although not as efficient as **122** in our reaction, peroxides could be used in the reaction to gain additional mechanistic knowledge. The limited range of commercially available peroxides prompted us to synthesise *t*-butyl hydroperoxide **126**. Stirring *t*-butyl magnesium chloride **198** (1 M in THF) under an $^{16}O_2$ atmosphere at low temperature (-78 °C) gave **126** in low quantities (1 mg L⁻¹ by Quantofix Peroxide[®] strips) (Scheme 2.51).



Scheme 2.51. Formation of *t*-butyl hydroperoxide **126**.⁸⁵

Further improvements of this method leading to increased yields would give a valuable tool that could help gain more mechanistic information. Currently work is in progress to optimise this methodology.

In summary, although we were unable to source any ^{18}O -labelled peroxide commercially, two methods have been established within the group which resulted in peroxide formation from $^{16}\text{O}_2$ gas. Application of these methods to the labelled gas will be of significant benefit in further delineating this fascinating mechanism.

2.8.9. Generation of Hydroperoxy Radical **170**

Assuming the first step of the proposed mechanism was correct (**Section 2.8.4, Scheme 2.24**), hydroperoxy radicals **170** were generated during the reaction. More information about the mechanism could be obtained if their formation was induced by alternative processes, which should still lead to the desired product. We attempted to generate hydroperoxy radicals **170** by using different oxidants instead of H_2O_2 •urea **122**. Hydroquinone **199**, catechol **200**, and 1,4-dihydroxynaphthalene **189** were all considered and screened. A typical procedure involved a 3 h addition of diphenylketene **120** (1 equiv.) to an open flask containing cyclohexane **3** [0.1 M] and an oxidant (1 equiv.) with vigorous stirring of the reactants (**Table 2.21**).

Table 2.21. Attempted generation of hydroperoxy radicals **170** using various oxidants.

$\text{Ph}_2\text{C}=\text{O} + \text{oxidant} \xrightarrow[\text{air, 20 }^\circ\text{C, 3 h}]{\text{CyH 3 [0.1 M]}} \text{Ph}_2\text{CH}-\text{C}(=\text{O})-\text{C}_6\text{H}_{11}$

120 (1 equiv.) + **oxidant** (1 equiv.) → **110**

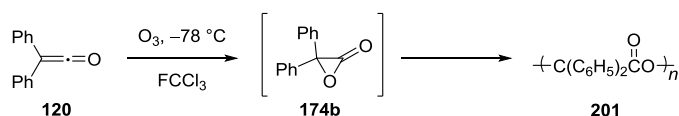
Entry	Oxidant	Conversion [%]
1	<p>199</p>	1
2	<p>200</p>	0
3	<p>189</p>	0

As is evident from **Table 2.21**, the presence of the selected oxidants did not result in formation of ester **110** to any significant extent. The slow hydrogen abstraction from **199** and **200** is the most likely explanation for the lack of **110** formation. However, it is not clear why **189** did not give the desired product. The starting material **189** was not present at the end of the reaction. Instead, a number of unidentified products were observed. Attempts to purify and analyse these products met with no success despite extensive efforts.

2.8.10. α -Lactone Intermediate

There are a few references to α -lactones in the literature, even though they have been invoked as reactive intermediates in diverse transformations such as nucleophilic substitution reactions, the thermolysis of cyclic anhydrosulfites, in displacement and free-radical reactions, photochemical reactions, and in the ozonolysis of ketenes.⁸⁶ A variety of ingenious approaches have been used in order to generate α -lactones such as photodecarboxylation of malonoyl peroxides or the epoxidation of ketenes.^{86f} These elusive species are usually generated as short-lived intermediates that react further under

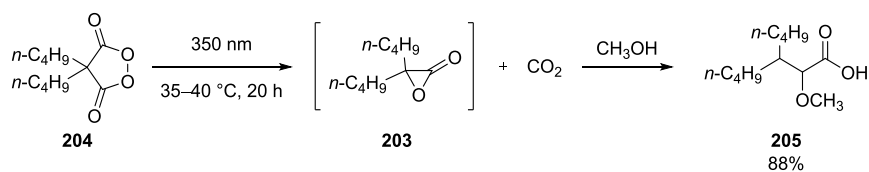
their conditions of formation and characterisation of these compounds has been limited to indirect evidence of their formation and a single NMR observation.^{86g} The synthesis of these intriguing molecules poses a challenge but a method of generating diphenyloxiranone **174b**, independent of our procedure, in an alkane solvent would help in delineating the mechanism of our reaction. The most promising method for the preparation of this class of compound was reported by Wheland and Bartlett,^{86g} who ozonised diphenylketene **120** in chlorotrifluoromethane at $-78\text{ }^\circ\text{C}$ to gain evidence for the formation of **174b** (Scheme 2.52).



Scheme 2.52. Potential ozonolysis of diphenylketene **120**.

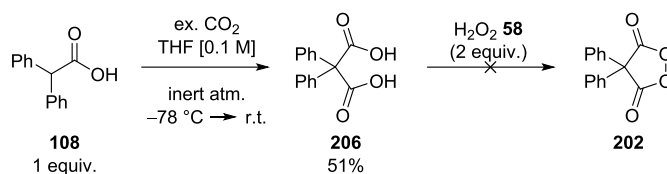
Unfortunately, the low temperature applied in this reaction renders the two cyclic alkanes that gave the highest yields - cyclohexane **3** and cycloheptane **149** - impractical due to their melting points.

However, it is possible to generate **174b** by photodecarboxylation of a suitable cyclic peroxide, such as diphenyl malonoyl peroxide **202**. It has been demonstrated by Adam and Rucktäschel^{86f} that lactone **203** can be formed from peroxide **204** and intercepted by a nucleophile such as methanol **57** when 0.1 M methanolic solutions of peroxide **204** are irradiated at 350 nm in the temperature range of 35–40 °C for 20 h (Scheme 2.53).

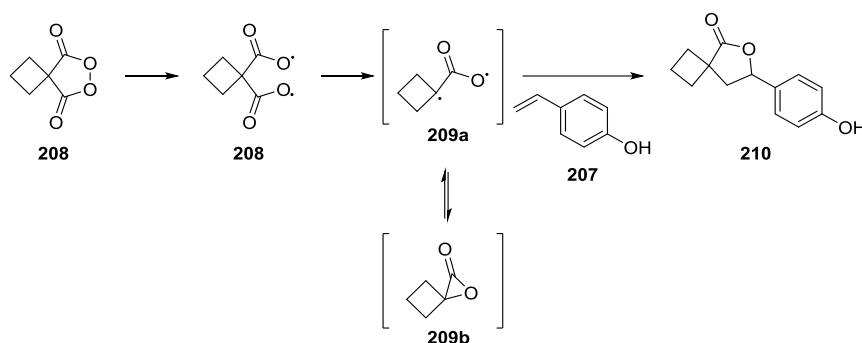


Scheme 2.53. Photolysis of peroxide **202**.

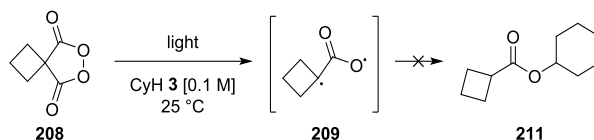
Ideally, the above reaction could be performed with diphenyl malonoyl peroxide **202**. However, although synthesis of diphenylmalonic acid **206** was achieved through a carboxylation sequence (51%), all attempts to form the corresponding peroxide **202** resulted in the formation of a gross mixture of compounds (Scheme 2.54).

Scheme 2.54. Attempted synthesis of diphenyl malonoyl peroxide **202**.

Coincidentally, Jones had noted during his studies on metal-free *syn* dihydroxylation⁸⁷ the competing formation of lactones when styrene substrates, e.g. *p*-hydroxystyrene **207**, were reacted with cyclobutyl malonoyl peroxide **208**. This transformation was proposed to proceed through decarboxylation of peroxide **208** to give cyclobutyloxiranone **209a**, followed by addition to styrene **207** to give lactone **210** (19%) (Scheme 2.55).

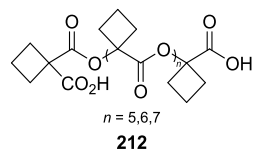
Scheme 2.55. Proposed reaction mechanism for the formation of lactone **210**.

No direct evidence existed to support the existence of **209** but the possibility of its formation offered a great opportunity to test peroxide **208** in the oxidation of alkanes. Different sources of light were used to induce decarboxylation of peroxide **208** to give **209** in cyclohexane **3** [0.1 M] at 25 °C (Table 2.22). An authentic sample of ester **211** was prepared and the reactions were monitored by ^1H NMR spectroscopy.

Table 2.22. Attempted formation of **211** through generation of **209** using different sources of light.

Entry	Source of light	Conversion [%]
1	Sunlight	0
2	Fumehood light	0
3	UV light ($\lambda = 365$ nm)	0
4	Visible light	0

The desired ester **211** was not formed in any of the reactions undertaken but a polymeric product **212** (Figure 2.38) was observed when the reaction mixture was exposed to UV light over two days (Table 2.22, Entry 3). This important experiment demonstrated that the O–O bond of peroxide **208** could be cleaved by shining UV light on the reaction mixture. More importantly, it showed that **208**

**Figure 2.38.**

reacted preferably with itself despite a much higher concentration of cyclohexane **3** (1:10). Despite obvious differences between cyclobutyloxiranone **209** and diphenyloxiranone **174** this result does not support the intermediacy of α -lactones in the oxidation reaction.

2.8.11. Co-product Identification

The reaction between molecular oxygen, diphenylketene **120**, H_2O_2 •urea **122**, and cyclohexane **3** did not give exclusively the desired product. A number of co-products were produced during the reaction. In an effort to identify the other compounds, different analytical techniques were employed (^1H NMR and ^{13}C NMR spectroscopy, mass spectrometry, infrared spectroscopy). To date, four co-products have been successfully identified. Purification of a standard reaction by flash chromatography resulted in the isolation of benzophenone **213** (8%), and phenyl benzoate **176** (3%) along with the desired ester product **110** (17%) (Figure 2.39). Diphenylacetic acid **108** and

diphenylacetic anhydride **214** were also identified as co-products by mass spectrometry and ^1H NMR spectroscopy although accurate quantification was not possible with the techniques used. Instead, crude reaction mixture was spiked with authentic samples of **108** and **214**.

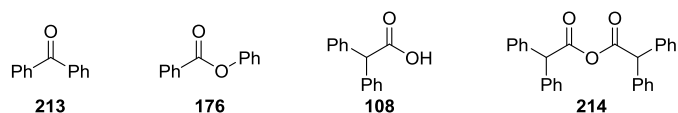


Figure 2.39. Identified co-products.

Benzophenone **213** is believed to be produced in the direct reaction of molecular oxygen and diphenylketene **120** through the formation of peroxy lactone **215b** and its subsequent decarboxylation (**Figure 2.40**).⁸⁸

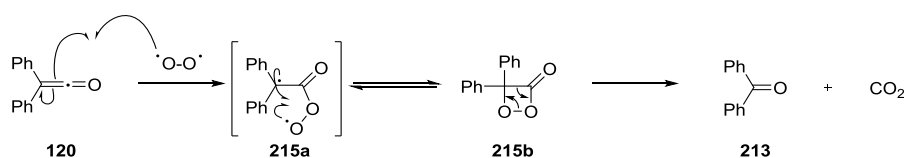


Figure 2.40. Proposed reaction mechanism for the formation of benzophenone **213**.⁸⁸

More evidence towards this proposed pathway was obtained during the ^{18}O -labelling studies. Mass spectrometric data revealed ^{18}O -incorporation into the molecule of **213- ^{18}O**

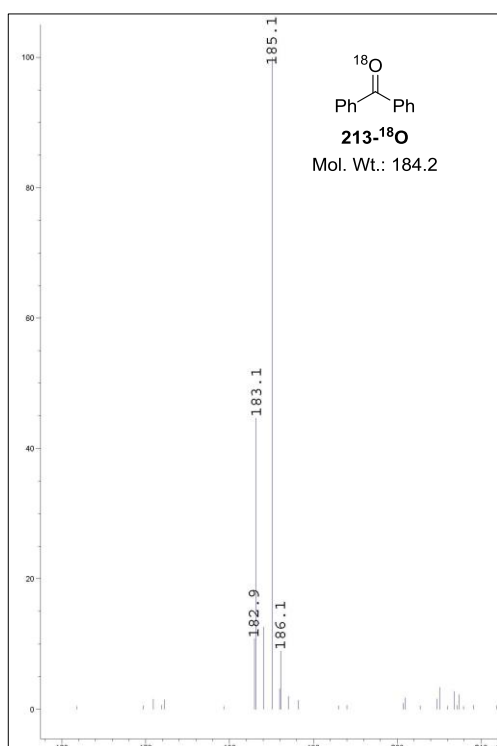


Figure 2.41. Mass spectrum of benzophenone **213- ^{18}O** .

(m/z 185.1) (Figure 2.41). Figure 2.42 shows the relative ^{16}O and ^{18}O isotope ratio in benzophenone **213** obtained from the reactions with 0.1, 1, and 10 equivalents of $\text{H}_2\text{O}_2\cdot\text{urea}$ **122** with diphenylketene **120** (Section 2.8.6, Scheme 2.45). The ratio of **213** to **213- ^{18}O** obtained from each reaction was different. The presence of **213** in the starting diphenylketene **120** (typically less than 3%) could be a possible cause of a higher amount of unlabelled **213**. Although measures were taken during the synthesis, storage, and handling of diphenylketene **120**, contact with air was unavoidable. The total yield of benzophenone **213** after 3 hours was in the range of 7–8% (1 equiv. of $\text{H}_2\text{O}_2\cdot\text{urea}$

122) which may explain why the ratio of the ^{16}O to ^{18}O isotope in benzophenone **213** was about 1:1.5, given that **213** (3%) was present in the starting material. It is not certain why reactions with 0.1 and 10 equivalents of **122** resulted in different ratios of **213** to **213- ^{18}O** .

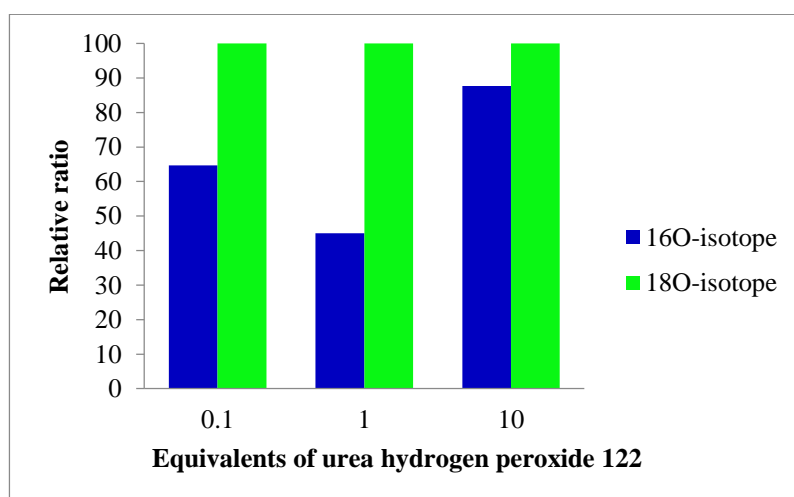


Figure 2.42. Relative ratio of **213** and **213- ^{18}O** .

The reactions were not carried out in duplicate and more data is needed before definitive conclusions can be drawn. It could also be that a pathway exists for formation of benzophenone **213** that is independent of our reaction.

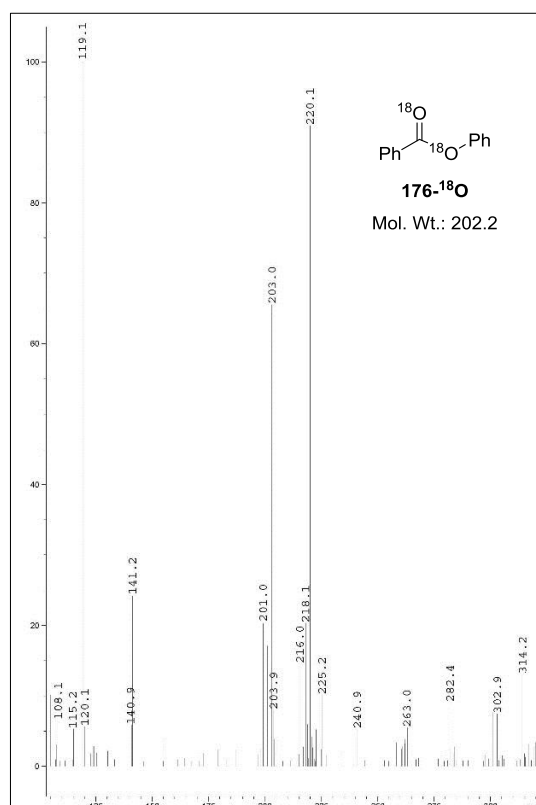


Figure 2.43. Mass spectrum of phenyl benzoate **176- ^{18}O** .

Identification of phenyl benzoate **176** was not straightforward as it could not be separated from ester **110** by flash chromatography, *i.e.* cyclohexyl 2,2-diphenylacetate **110** and phenyl benzoate **176** have identical R_f values. The co-product **176** was identified after comparison of ^1H , ^{13}C NMR, and mass spectra of a commercially available sample of phenyl benzoate **176** with the mixture obtained from the reaction. When mass spectra of the $^{18}\text{O}_2$ -labelling studies were analysed it was found that the doubly-labelled phenyl benzoate **176** was primarily formed, as shown in **Figure 2.43** and **2.44**.

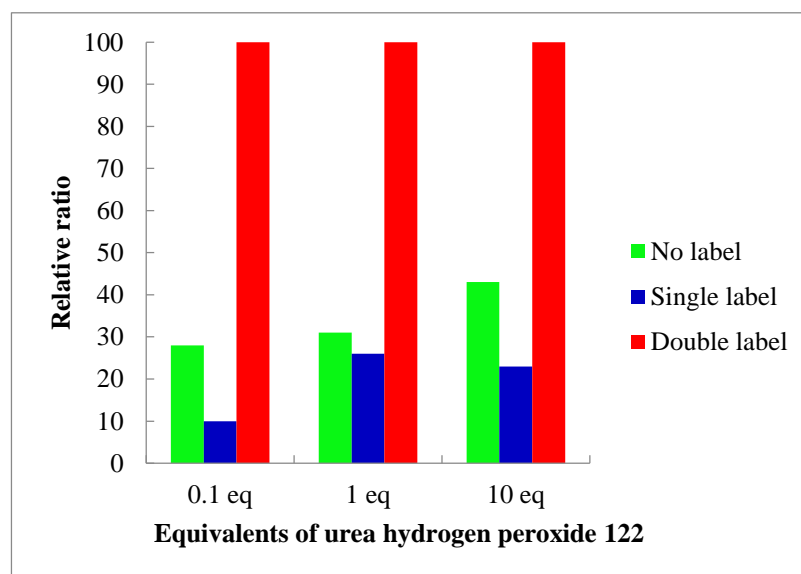


Figure 2.44. Relative ratio of ^{16}O to ^{18}O incorporation into phenyl benzoate **176**.

Uncertainty exists as to how the formation of phenyl benzoate **176** came about but a Bayer-Villiger type of reaction is a potential route. The ^{18}O -labelling ratio in the final product **176- ^{18}O** (**Figure 2.44**) shows that formation of diphenylacetic peracid **107k** must

arise from the reaction of diphenylketene **120** with molecular oxygen because reaction with hydrogen peroxide **58** would yield non-labelled phenyl benzoate **176**. Deprotonation of peracid **107k** and subsequent attack on benzophenone **213** gives rise to intermediate **216**, which rearranges to form products **176- ^{18}O** and **108k** (**Figure 2.45**).

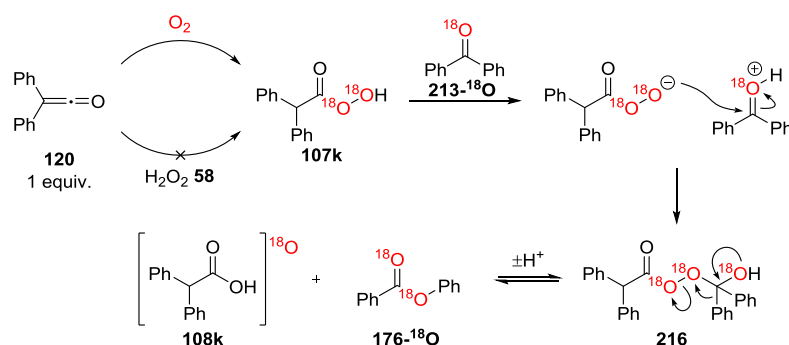


Figure 2.45. Proposed reaction mechanism for the formation of phenyl benzoate **176**.

Bartlett postulated⁸⁸ that phenyl benzoate **176** could be produced in a series of steps as shown in **Figure 2.46** (Pathway B). First, diphenylketene **120** reacts with oxygen to give **215**, which then combines with another molecule of **120** and forms dimeric product **217**. Further reaction with oxygen leads to intermediate **218**, which subsequently collapses to α -lactone **174**, carbon dioxide **38** and diphenyldioxirane **219**. Criegee proposed⁸⁹ that formation of phenyl benzoate **176** could be explained by the rearrangement of dioxirane **219** along Pathway A. Bartlett further hypothesised that this process could be facilitated by diphenylketene **120** (Pathway B) but this route would give products inconsistent with the ^{18}O -labelling studies since more singly labelled phenyl benzoate **176** would be produced. However, formation of **176** during the auto-oxidation of diphenylketene **120** means that neither mechanistic pathway can be completely ruled out.

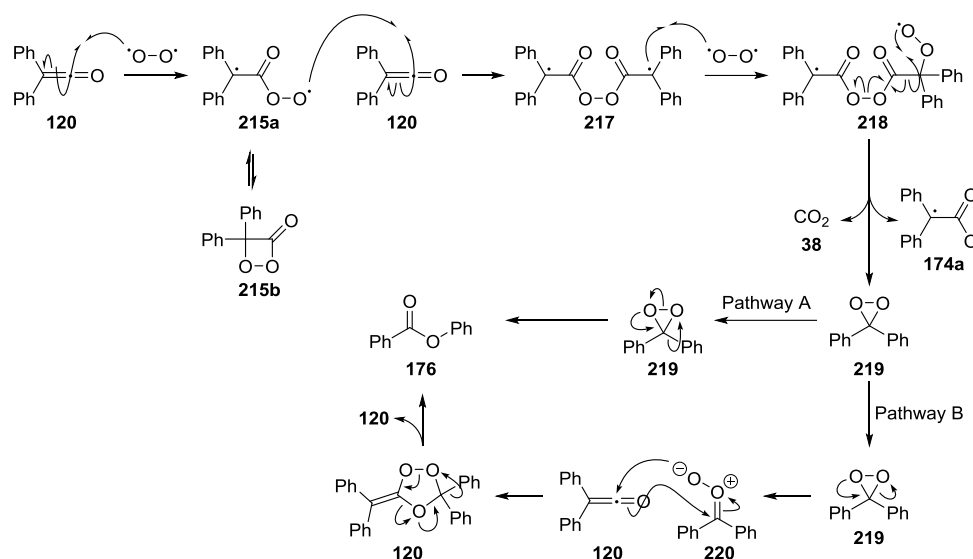


Figure 2.46. Alternative routes leading to phenyl benzoate **176**.

Phenyl benzoate **176** typically made up to 5% of the isolated yield of ester **110**. Presumably, low conversions were a direct consequence of small amounts of benzophenone **213** (the limiting reagent) in the reaction.

Diphenylacetic acid **108** and diphenylacetic acid anhydride **214** were also identified as co-products in the reaction by spiking the crude reaction mixture with authentic samples of **108** and **214** and comparison of ^1H NMR data. It is believed that the majority of both co-products formed either during the reaction or the aqueous work-up (Figure 2.47 and 2.48).

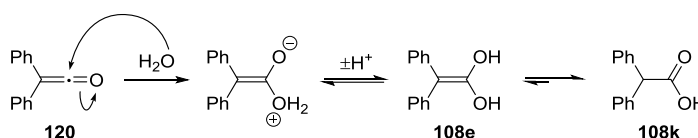


Figure 2.47. A plausible mechanism for the formation of diphenylacetic acid **108k**.

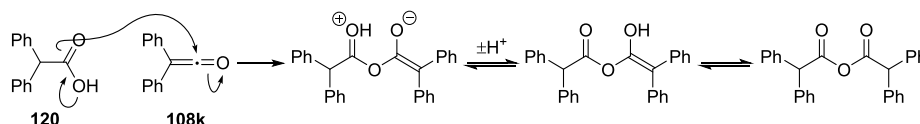


Figure 2.48. A plausible mechanism for the formation of diphenylacetic anhydride **214**.

Attempts to isolate and characterise other co-products were unsuccessful. Among other products that could be expected to form were bicyclohexyl **221**, diphenylmethanol **222**, 1,1,2,2-tetraphenylethane **223**, cyclohexyl hydroperoxide **171**, 2-hydroxy-2,2-diphenylacetic acid **224**, diphenylmethane **225**, 3-phenylisocoumarone **226**, 1-phenylethyl 2,2-diphenylacetate **227**, and cyclohexanol **2** (**Figure 2.49**). To date, no evidence for the formation of any of these compounds has been obtained.

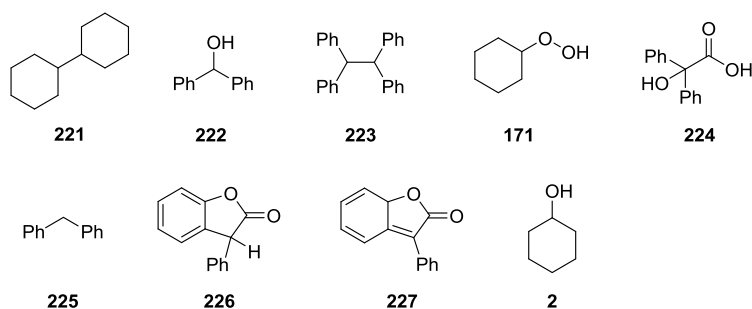


Figure 2.49. Possible co-products.

2.8.12. Over-oxidation

Authentic samples of the different diesters **228–233** (**Figure 2.50**) that could form in the course of the reaction as a result of over-oxidation were prepared and fully characterised.

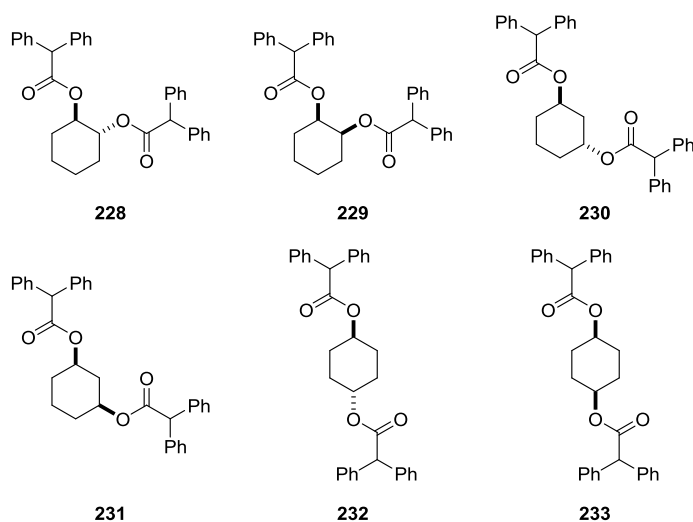
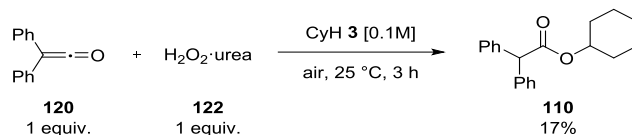


Figure 2.50. Possible over-oxidation products.

^1H NMR, ^{13}C NMR, and mass spectra of **228–233** were compared with those of the crude reaction mixture obtained after the 3 h addition of diphenylketene **120** (1 equiv.) to an open flask containing $\text{H}_2\text{O}_2\cdot\text{urea}$ **122** (1 equiv.) and cyclohexane **3** [0.1 M] at 25 °C (**Scheme 2.56**).



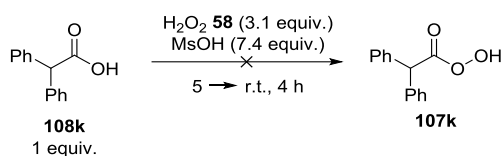
Scheme 2.56. The benchmark reaction.

No evidence for the presence of any of the diesters **228–233** in the reaction mixture was obtained, which led to the conclusion that over-oxidation did not take place during the reaction. This important result suggests that high selectivity should be possible within this transformation if methods to optimise the formation of **110** can be realised.

2.8.13. Reactions with Peracids

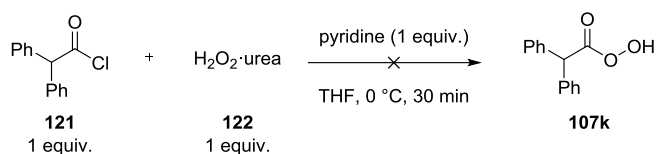
Our initial goal, based on Carpenter's calculations,⁵⁰ was to find conditions favouring the formation of the enol tautomer of diphenylacetic peracid **107e** because less energy would be required to cleave the O–O bond (**Section 2.1, Scheme 2.1**). We have since found a different route to generate the desired esters. However, cleavage of the O–O bond of the keto tautomer **107k** under the reaction conditions was not investigated. Although we do not advocate isolating and handling peracids due to the associated safety issues, we considered it crucial to synthesise diphenylacetic peracid **107k** for mechanistic purposes. Prior to experimental work, necessary safety measures were implemented. The reaction flask was wrapped in Nescofilm[®], and addition and mixing of reactants was carried out behind a blast shield.

Several attempts have been made to generate and isolate diphenylacetic peracid **107k**. As a starting point, a slightly modified synthesis reported by Crandall and others⁵⁶ was followed. Diphenylacetic acid **108k** (1 equiv.), hydrogen peroxide **58** (aq 30% w/w, 3.1 equiv.) and methanesulfonic acid (7.4 equiv.) were reacted and worked-up as described but the peracid **107k** (reported as a yellow solid) was not obtained (**Scheme 2.57**).



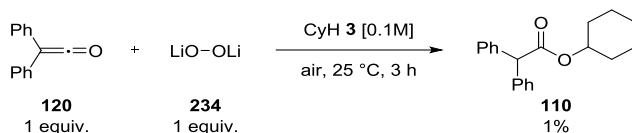
Scheme 2.57. Attempted synthesis of diphenylacetic peracid **107k** by Crandall and others.⁵⁶

For our second attempt, a more reactive electrophile, diphenylacetyl chloride **121**, and H_2O_2 •urea **122** were stirred in tetrahydrofuran [0.1 M] at 0 °C in the presence of a nucleophilic catalyst - pyridine (**Scheme 2.58**).



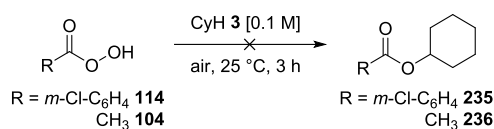
Scheme 2.58. Reacting diphenylacetyl chloride **121** with H_2O_2 •urea **122** in cyclohexane **3**.

Only one product, identified as diphenylacetic acid anhydride **214**, was isolated and recrystallised. Varying the quantities of H_2O_2 •urea **122** (0.5–3.1) and pyridine was equally ineffective in the formation of peracid **107k**. The level of reactivity was then further increased by switching to more potent reactants – diphenylketene **120** and lithium peroxide **234**, which were stirred in cyclohexane **3** [0.1 M] to facilitate the formation of ester **110** should the cleavage of the O–O bond of peracid **107k** occur (**Scheme 2.59**).



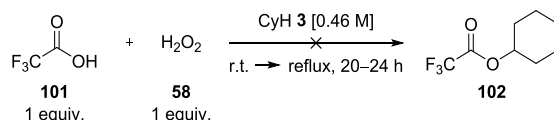
Scheme 2.59. Reacting diphenylketene **120** and lithium peroxide **230** in cyclohexane **3**.

None of the attempts to generate peracid **107k** provided the desired results orientating the investigation towards commercially available peracids. Acetic peracid **104** and *m*-chlorobenzoic peracid **114** were purchased and their potential ability to oxidise cyclohexane **3** was investigated (**Scheme 2.60**).



Scheme 2.60. Investigation into the potential oxidation ability of peracid **114** and **104**.

^1H NMR spectra were screened against those of the authentic samples of the respective esters **235** and **236**.⁹⁰ Starting materials were observed demonstrating that the O–O bond of peracid **114** and **104** could not be cleaved under the reaction conditions. However, caution must be exercised when interpreting these results and drawing general conclusions regarding cleavage of peracidic O–O bond. It has been demonstrated by Deno and Messer that such process is possible (**Section 1.4.7.4, Scheme 1.26**).⁴⁸ However, our efforts to change the stoichiometry of the reaction were unsuccessful (**Scheme 2.61**), which may suggest that hydroxyl radicals **59** are formed in small quantities under the reaction conditions shown in **Scheme 2.61**.



Scheme 2.61. An attempt to use trifluoroacetic acid **101** in C–H functionalisation of cyclohexane **3**.

2.8.14. Revision of Reaction Mechanism 2

By piecing all this information gathered together we obtain the following picture. Hydrogen peroxide **58** does not perform a nucleophilic attack on diphenylketene **120** or, if it does so, the equilibrium towards the enol tautomer of diphenylacetic peracid **107e** is not favoured. Frey and Rappoport^{58b} have shown the hydration of ditipylketene **116** to be reversible, which should also be applicable to **107e**. Moreover, the conditions for successful formation of enediols (and therefore peracidic enols) listed by them were not met under our reaction conditions (lack of hydrogen-bond acceptor and water-miscible solvent). Further evidence came from the observation that ester formation did not take place under an inert atmosphere (**Section 2.6.1**). Another nucleophile therefore must be in operation. Isotope labelling studies have shown that molecular oxygen can react with diphenylketene **120**, as evidenced by the formation of ^{18}O -labelled benzophenone **213- ^{18}O** (**Section 2.8.11**). Such a reaction is, in fact, documented in the literature.⁹¹ The

position of the isotopic ^{18}O -atom was found to be exclusively between the carbonyl carbon atom and the cyclohexyl ring (**Section 2.8.6**), which means that peroxy lactone **215** must form in the first step of the reaction (**Figure 2.51**).

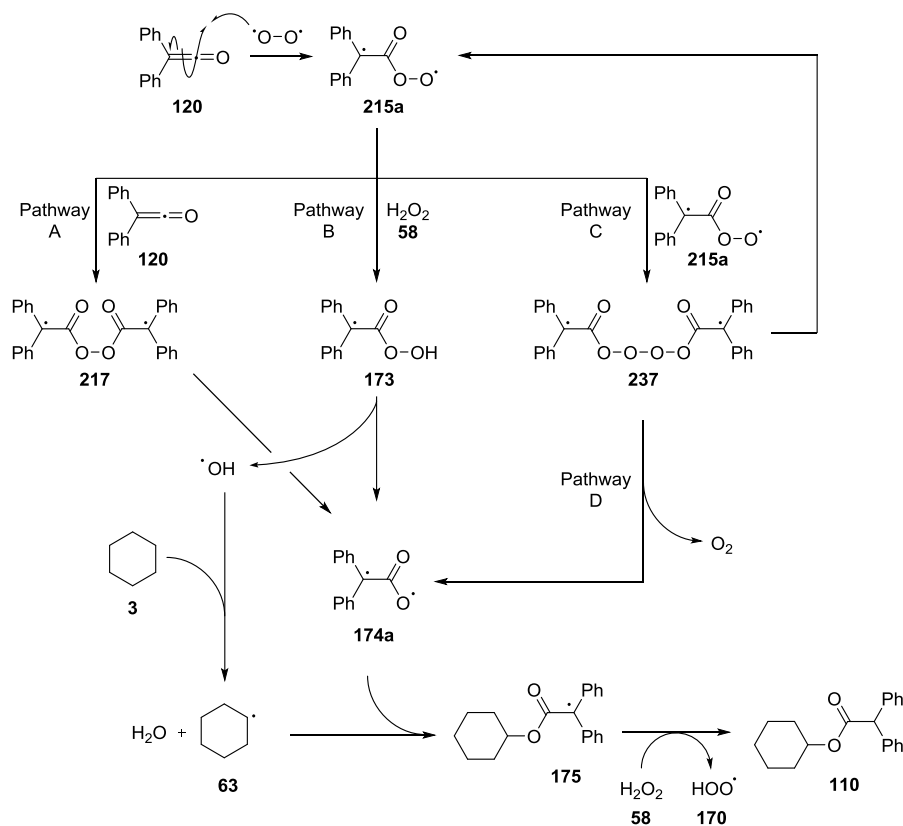


Figure 2.51. New proposed mechanism.

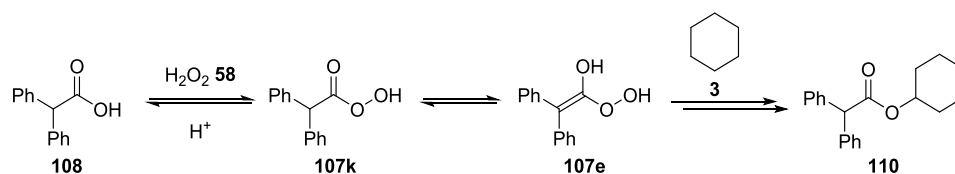
Upon formation, intermediate **215a** may (1) react with another molecule of diphenylketene **120** (Pathway A), (2) abstract a hydrogen atom (Pathway B), or (3) react with itself (Pathway C). At the end of the reaction a new C–O bond and, as a result, a new ester molecule is formed. Therefore, the O–O bond must be broken in all instances. If we followed Pathway A, homolytic cleavage of intermediate **217** would generate two molecules of **174a**. Pathway C shows intermediate **237**, a tetroxide belonging to a class of compounds which have been postulated to decay along Pathway D.⁹² Low concentrations of both diphenylketene **120** and **215a** make Pathway B more likely than either Pathway A or C. What is important is that all pathways share a common intermediate – α -lactone **174**. Although studies with cyclobutyl malonyl peroxide **208** did not lend any support to the intermediacy of α -lactones, diphenyl malonyl peroxide

202 could exhibit a completely different behaviour due to steric and electronic effects. Independent preparation of intermediate **217** or **237** and their use in the oxidation reaction would be another way to gain evidence for, or against, the mechanistic role of the elusive intermediate **174a** (even if it may be necessary to use UV light to ensure homolytic O–O bond cleavage).

In the overall process shown in **Figure 2.50** (Pathway B) the attack of oxygen on diphenylketene **120** could be expected to be the rate-determining step. Performing the reaction under high pressure in an oxygen-saturated atmosphere could result in higher conversion to ester **110**, and would provide further support for the reaction mechanism proposed in **Figure 2.37**.

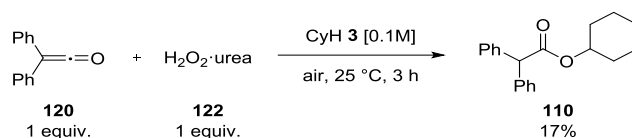
2.9. Concluding Remarks and Future Directions

The aim of this project was to develop a novel C–H functionalisation method based on *in situ* formation of peracids, finding conditions favouring formation of peracidic enols, spontaneous homolytic O–O bond cleavage, and reaction with hydrocarbons to give the corresponding esters (**Scheme 2.62**).



Scheme 2.62. Unsuccessful oxidation of hydrocarbons.

Following unsuccessful attempts at this methodology, an alternative approach was adopted leading to the development of a novel, metal-free C–H functionalisation method. Development of a practical method for alkane oxidation requires that the reaction be coupled to consumption of an inexpensive stoichiometric oxidant, preferably O_2 or H_2O_2 **58**. Functionalisation of various hydrocarbons to the corresponding esters was achieved using stoichiometric amounts of diphenylketene **120** and H_2O_2 •urea **122** in hydrocarbon solvents under an air atmosphere, an example of which is shown in **Scheme 2.63**.



Scheme 2.63. The benchmark reaction.

This method makes use of readily accessible oxidants, H₂O₂ and O₂, and permits the direct oxidation of C–H bonds without recourse to pre-functionalisation. It further benefits from relative simplicity of the experimental procedure, mild reaction conditions (25 °C, atm. pressure), and does not require a metal catalyst.

Investigations into the reactivity of various hydrocarbons revealed interesting selectivity patterns. A number of hydrocarbons (cyclic, linear, saturated heterocycles, and aryl substrates) were subjected to the oxidation process with varying outcomes. In general, secondary C–H bonds appeared to be oxidised preferentially to primary and tertiary C–H bonds. Cyclic hydrocarbons also reacted better than linear alkanes in most cases, unless the latter had electron-donating substituents. However, the key factors affecting the selectivity are yet to be firmly established.

Another area to explore is the reaction mechanism, which will be the key to unlocking the potential of the reaction. Our understanding of the mechanistic principles governing this process is increasing but is not yet complete. A more detailed experimental design is required to investigate the intimate nature of interactions between the reactants. One of the most crucial experiments will be performing the reaction under high pressure in an oxygen-saturated atmosphere. The use of ¹⁸O-labelled hydroperoxides should also provide additional mechanistic insights if their successful synthesis can be achieved. Equally interesting may be employing cyclohexyl hydroperoxide **171** in the reaction as different hydroperoxides have shown the ability to facilitate the reaction and cyclohexyl radical **63** is believed to be involved in the process of ester formation. Identification of other co-products may also provide important mechanistic clues.

One interesting area for future work on this project would be the development of an alternative ketene backbone. Although synthetically challenging, it presents the opportunity to improve the yield as well as the atom efficiency of the overall process.

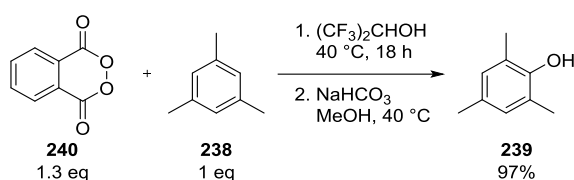
Finally, development of a one-pot process, without the additional synthetic step required to make diphenylketene **120**, would be a great advance and would improve the chances of this method being adopted by the wider scientific community.

Chapter 3: Functionalisation of sp^3 C–H Bonds

3. Functionalisation of sp^2 C–H Bonds

3.1. Introduction

Metal-free C–H functionalisation is at the heart of our research interests. It was, therefore, with great curiosity that we read the article by Yuan *et al.*⁹³ describing metal-free oxidation of aromatic C–H bonds. The authors reported a phenomenal transformation of various arenes into the corresponding phenols. For example, mesitylene **238** was reacted with phthaloyl peroxide **240** (1.3 equiv.) at 40 °C to give, after hydrolysis, 2,4,6-trimethylphenol **239** (97% yield) (**Scheme 3.1**).



Scheme 3.1. Oxidation of mesitylene **238** using peroxide **240**.

Following the publication, we identified an opportunity to improve operational safety of the reaction through the use of an alternative peroxide, with which we had some experience within the laboratory, cyclopropyl malonyl peroxide **241**. A second aspect of the article that caught our attention was the theoretical study of the reaction mechanism. Interestingly, a radical mechanism was proposed, but, disappointingly, this proposal was based solely on molecular modelling (**Section 3.5.1, Figure 3.3**). These two aspects of the work spurred us to explore the possibility of using a peroxide that would be safer and easier to handle, and to enhance the mechanistic knowledge and understanding of the reaction.

3.2. Attribution

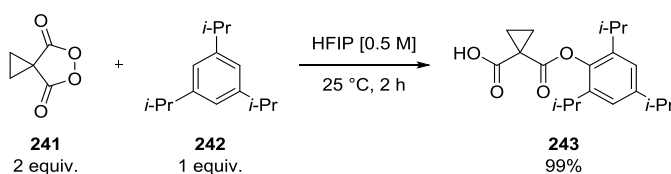
This project was carried out in conjunction with Andrei Dragan of the Tomkinson group. His scientific contributions and work, particularly on the labelling studies, the acid catalysis, and the reaction kinetics, enabled better understanding of the new metal-free

method for the oxidation of arenes described herein, and are noted where appropriate within this report.

3.3. Initial Investigations

Peroxides are potentially dangerous compounds because they can detonate upon exposure to heat, light, friction or shock. Phthaloyl peroxide **240** belongs to that group of compounds, and is both heat- and shock-sensitive. Decomposition of **240** can occur at temperatures as low as room temperature (solvent-dependent) and is accelerated by the presence of acids.⁹⁴ Reports of violent explosions are common in the literature,⁹⁴⁻⁹⁵ and are supported by similar observations made by our group. The risk associated with the use of phthaloyl peroxide **240** makes it less attractive as a synthetic reagent, and should be avoided wherever and whenever possible.

In light of the hazards associated with the formation and handling of phthaloyl peroxide **240**, cyclopropyl malonoyl peroxide **241** was investigated as an alternative peroxide reagent. The benefits offered by **241** are significant when compared to **240**.⁹⁶ Moreover, the structural similarity to **240** and improved reactivity exhibited in the *syn*-dihydroxylation of alkenes⁹⁷ made peroxide **241** a promising candidate for the oxidation of arenes. In an exploratory reaction, peroxide **241** (2 equiv.) was stirred with 1,3,5-triisopropylbenzene **242** (1 equiv.) in HFIP [0.5 M] (**Scheme 3.2**).



Scheme 3.2. Exploratory oxidation reaction using peroxide **241**.

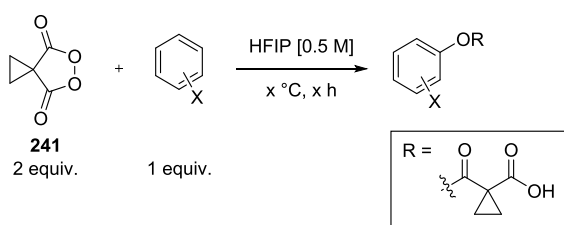
Under mild conditions (25 °C) and after only 2 h, the corresponding ester product **243** was isolated in a quantitative yield. In contrast, the analogous reaction with phthaloyl peroxide **240** required a temperature of 40 °C and 12 hours to achieve a similar yield (97%).⁹³

Cyclopropyl malonoyl peroxide **241** therefore proved to be a very efficient reagent in the oxidation of arenes. A lower temperature and a shorter reaction time also indicated that **241** was capable of higher levels of reactivity compared to **240**. Encouraged by this result, we decided to extend this procedure to other aromatic compounds.

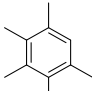
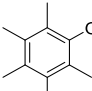
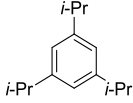
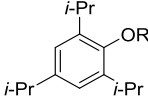
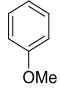
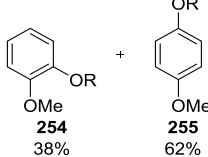
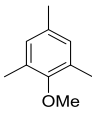
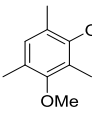
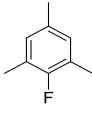
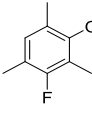
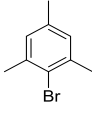
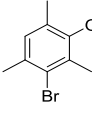
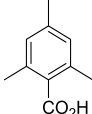
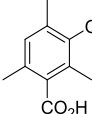
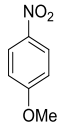
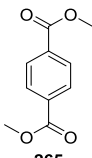
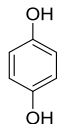
3.4. Substrate Scope

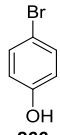
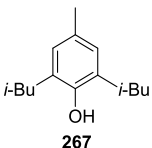
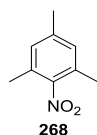
Reactivity of cyclopropyl malonoyl peroxide **241** was further examined with a series of aromatic compounds (**Table 3.1**).

Table 3.1. Substrate scope investigation.



Entry	Aromatic compound	Product(s)	Temperature of reaction (°C)	Time of reaction (h)	Yield (%)
1	 154	—	80	168	0
2	 5	 244 50% + 245 50%	50	72	63
3	 246	 247	25	96	97
4	 238	 248	25	4.5	99
5	 249	 250	25	0.3	99

6	 251	 252	25	24	70
7	 242	 243	25	2	99
8	 253	 254 38% 255 62%	50	72	63
9	 256	 257	25	6	98
10	 258	 259	25	8	96
11	 260	 261	25	120	91
12	 262	 263	50	42	86
13	 264	—	50	18	0
14	 265	—	50	40	0
15	 199	—	25→50	20	0

16		–	25→50	96	0
17		–	25	20	0
18		–	50	72	0

The following picture emerged from the results in **Table 3.1**. First, the substrate scope was limited to electron-rich arenes. The reactivity was directly proportional to the number and properties of substituents, and was greatly enhanced with substrates that had electron-donating groups (EDG's). Arenes with fewer electron-donating groups typically required longer reaction times or/and elevated temperatures to achieve good to excellent yields (**Table 3.1, Entries 2–4, 8**). Conversely, arenes with a larger number or/and stronger EDG's reacted rapidly under mild conditions (**Table 3.1, Entries 5 and 9**). The requirement for EDG's was further manifested in the reactions of benzene **154** (**Table 3.1, Entry 1**), and arenes with strong electron-withdrawing groups (EWG's) (**Table 3.1, Entries 11-14**). Second, aromatic compounds with hydroxyl groups were inert to the oxidation. Alcoholic solvents (methanol, isopropanol) have been previously shown to react with malonoyl peroxides.⁹⁶ However, the reaction proceeded in HFIP ($pK_a = 9.3$) without similar problems and ^1H NMR analysis (**Figure 3.1**) of the unsuccessful reaction of hydroquinone **199** (**Table 3.1, Entry 15**) provided further evidence that phenolic compounds did not induce decomposition of peroxide **241** as well as showing no reaction occurred between these substrates. It was unclear why this particular group of arenes was resistant to oxidation, but it may open opportunities for selective oxidations in the future.

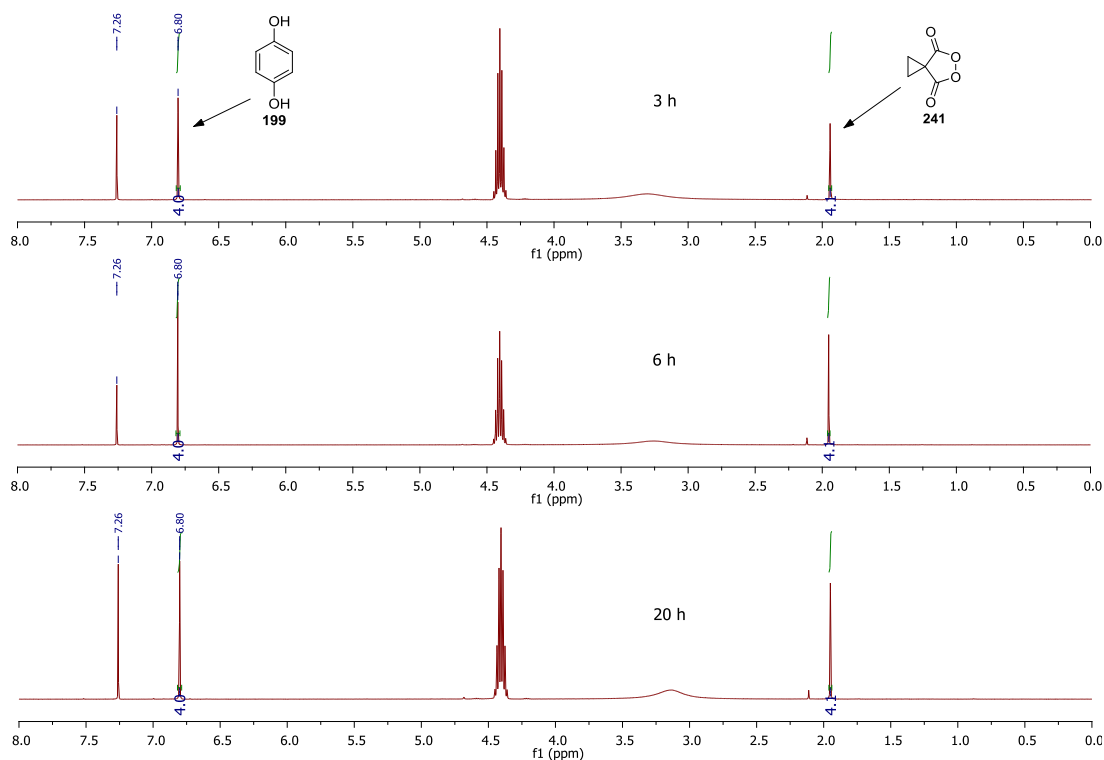
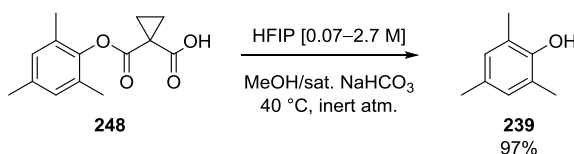


Figure 3.1. Unsuccessful oxidation of hydroquinone **199**.

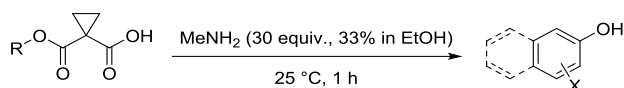
Finally, the selectivity of the reaction was governed by electronic and, to a lesser extent, steric properties of the arene substrates (**Table 3.1, Entries 2, 8**). Mixtures of *ortho* and *para* products were obtained, while *meta* products were not observed, giving concordant results with those reported.⁹³

The half acid-ester products proved to be problematic and time-consuming in terms of isolation and purification. One way to circumvent this problem was to react them further to obtain the corresponding phenols, which were considerably easier to purify, as exemplified in **Scheme 3.3**. The reported hydrolysis method was initially used but was found to give inconsistent and irreproducible results.⁹³ The necessity to degas methanol and keep the reaction under an inert atmosphere made it even less desirable.



Scheme 3.3. An example of hydrolysis reported by Yuan.⁹³

An operationally simple, quick, and reliable method was developed instead. Stirring half acid-esters with methylamine (30 equiv., 33 wt. % in ethanol) for 1 h at 25 °C gave moderate to excellent yields of the desired phenol product (**Table 3.2**).

Table 3.2. Hydrolysis of half-acid esters.

Entry	R	Product	Yield (%)
1			92%
2			93%
3		 66% 33%	60%

In summary, successful oxidations were exclusive to electron-rich arenes, and where positional selectivity was possible *ortho* and *para* products were formed showing a Friedel-Crafts reactivity pattern. The oxidation was unsuccessful when applied to phenolic aromatics and substrates with electron-withdrawing groups. Some oxidation products were reacted with methylamine to give the corresponding phenols for ease of purification.

3.5. Mechanistic Considerations

Three potential mechanisms could account for the formation of the observed products and are discussed separately.

3.5.1. The Radical Mechanism

Subjection of any organic molecule to a sufficiently high temperature in the gas phase results in the formation of free radicals. When the bond strength is between 20 and 40 kcal mol⁻¹, cleavage can be triggered in the liquid phase.⁹⁸ The energy required to induce the homolytic fission of phthaloyl peroxide **240** was calculated to be about 31.9 (±0.9) kcal mol⁻¹ by Oae *et al.*⁹⁹ and about 21.1 kcal mol⁻¹ by Yuan *et al.*⁹³ Although there is significant discrepancy between the two results, they both fall within an acceptable range for homolytic fission to occur. Experimental studies have shown that phthaloyl peroxide **240a** can undergo homolytic O–O bond cleavage at elevated temperatures, thereby generating a diradical species **240b** (Figure 3.2).⁹⁹

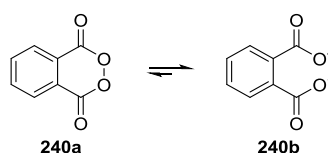


Figure 3.2. Homolytic O–O bond cleavage of phthaloyl peroxide **240a**.

On the basis of quantum mechanical calculations, it has been proposed that the oxidation of arenes mediated by peroxide **240** (Section 3.1, Scheme 3.1) proceeds through an addition-abstraction pathway called a ‘reverse-rebound mechanism’ (Figure 3.3).⁹³

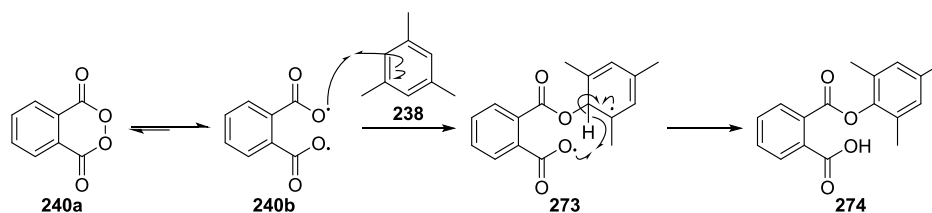


Figure 3.3. The reverse-rebound mechanism.

In this mechanism, the reaction is initiated by a homolytic O–O bond cleavage of **240a** to give **240b**, which then reacts with arene **238** to form intermediate **273**. Subsequent intramolecular abstraction of a hydrogen atom to restore aromaticity gives the half acid-ester product **274**. Although strong theoretical basis for this pathway exists, no experimental verification was presented.⁹³

Since the energy barrier for the homolytic cleavage of the O–O bond of cyclopropyl malonyl peroxide **241a** had been calculated to be $28.9 \text{ kcal mol}^{-1}$,¹⁰⁰ the reaction pathway illustrated in **Figure 3.4** deserved careful consideration.

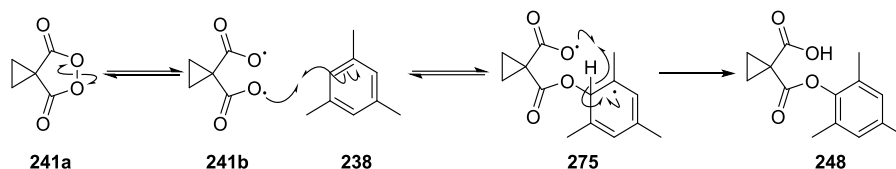


Figure 3.4. Plausible radical mechanism.

Upon homolytic fission of the O–O bond of peroxide **241a**, the diradical **241b** could react with arene **238** to give intermediate **275**. Following hydrogen atom abstraction, product **248** could be formed.

3.5.2. Single Electron Transfer (SET) Mechanism

Cyclic peroxides, including malonyl peroxides, have been shown to produce light in a process known as chemically initiated electron-exchange luminescence (CIEEL).¹⁰¹ CIEEL can operate in systems where there are electron-acceptor (peroxide) and electron-donor (activator) groups, which can be part of one or different molecules. A mechanistic investigation of this process was recently investigated by Khalid and others (**Figure 3.5**).¹⁰²

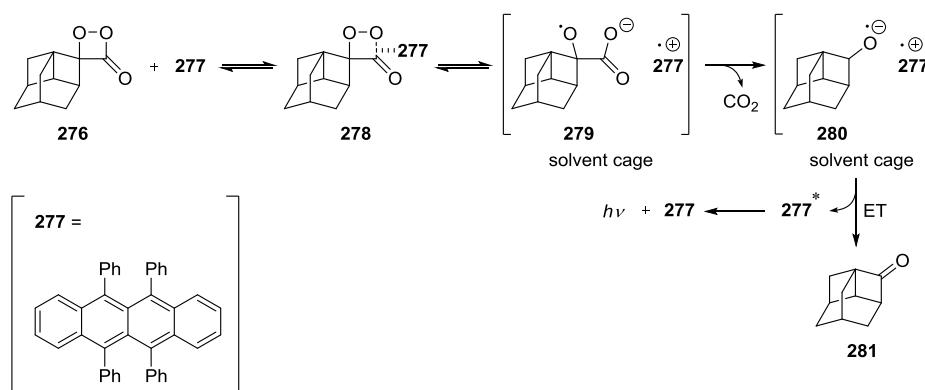


Figure 3.5. Intermolecular CIEEL decomposition mechanism of **276** catalysed by rubrene **277**.¹⁰²

When peroxide **276** and rubrene **277** form complex **278**, the stretching of the O–O bond results in electron transfer from the activator to the peroxide group, cleavage of the O–O bond and biradical formation: an anion radical on the peroxide **279** and a cation radical on the activator group **280**. The electron transfer, occurring after the C–C bond cleavage, leads to the formation of **281** and activator's excited state **277*** and subsequent light emission.

Light emission in this process is most efficient when certain conditions are met. The first requirement is that peroxide should be easily reduced, which can be achieved if the peroxide is substituted with electron-accepting groups such as carbonyl groups. A second requirement for the operation of CIEEL is that an irreversible reaction must occur upon the reduction of the peroxide. Typically, it is the cleavage of the O–O bond and decarboxylation. If the electron transfer were reversible, the electron would just go back to the activator. The third requirement is that there be a chemical route available for the release of energy, e.g. by loss of a molecule of CO_2 . The fourth requirement is that sufficient energy must be released in the ion radical annihilation to form an electronically excited state.¹⁰³

Since the key element of the CIEEL process is a single electron transfer (SET), typically from an aromatic compound to a peroxide, a reaction between mesitylene **238** and peroxide **241a** could occur as shown in **Figure 3.6**. Upon formation of radical anion **282** and radical cation **283** and their combination, intermediate **284** could form. Subsequent irreversible aromatisation would give product **248**.

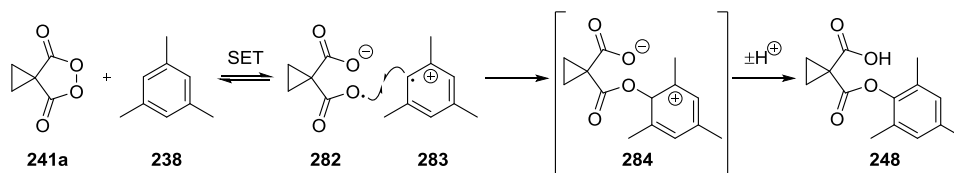


Figure 3.6. Plausible SET mechanism.

3.5.3. The Ionic Mechanism

A third mechanistic possibility to account for the observed transformation involves nucleophilic attack of arene **238** on the O–O bond of peroxide **241** to give the charged intermediate **284**. After protonation and de-protonation steps, formation of product **248** would follow (**Figure 3.7**).

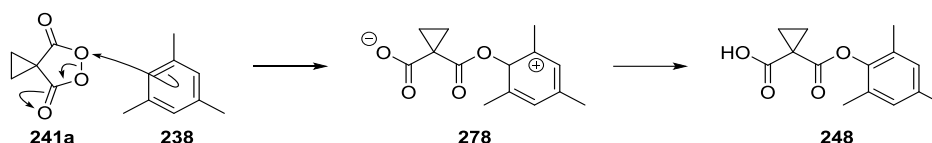


Figure 3.7. Plausible ionic mechanism.

Previous work within our group had shown that malonoyl peroxides can react with nucleophilic species, *i.e.* alkenes, through an ionic mechanism.¹⁰⁰ Thus, this reaction pathway was also plausible.

3.5.4. Initial Observations

Although none of the mechanisms could be definitely disqualified before more detailed studies were carried out, the mild reaction conditions, the Friedel-Crafts reactivity patterns, and substrate scope were suggestive of an ionic mechanism.

3.5.5. Preliminary Experiments

Exposure to light, heat, or oxygen are common methods used to initiate the formation of free-radicals. The mechanistic investigations therefore began by performing a set of experiments in the absence of light, at a low temperature, under an inert atmosphere, and at low temperature in the absence of light and atmospheric oxygen (**Figure 3.8**).

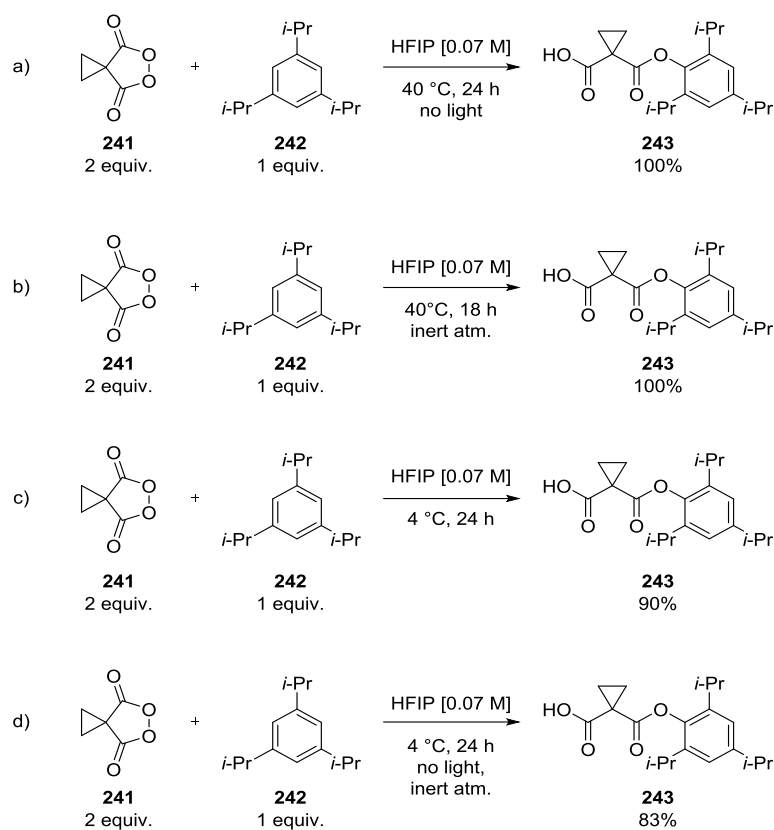


Figure 3.8. Oxidation of triisopropylbenzene **242** under various conditions.

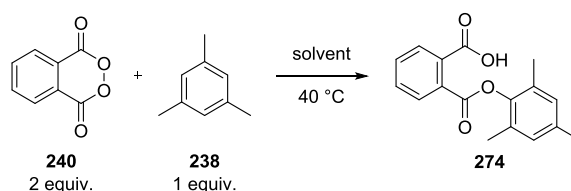
No difference in conversion (100%) was observed when the reaction was performed in the absence of light (**Figure 3.8a**) or under an inert atmosphere (**Figure 3.8b**). As a result, light and oxygen could be excluded as reaction initiators. A slight decrease in conversion (**Figure 3.8c** and **Figure 3.8d**) was observed when the reaction was carried out at lower temperatures (4 °C). Homolytic fission of the O–O bond should not be expected at low temperatures given the energy barrier (**Section 3.5.1**). Although the rate of reaction was slower, it occurred nonetheless giving an 83% yield of **243** and indicating that the process was not radical.

3.5.6. Mechanistic Studies

The above results provided further evidence that a radical reaction mechanism was not likely but were far from conclusive. Consequently, further mechanistic studies were undertaken and are discussed in the following sections.

3.5.6.1. Acid Catalysis

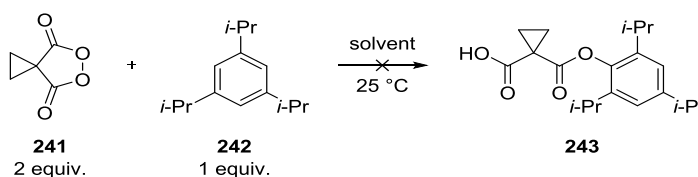
An intriguing aspect of the reported oxidation of arenes with phthaloyl peroxide **240** was the medium in which the reactions were carried out. The authors investigated a range of solvents and found that good yields in the oxidation of mesitylene **238** (Scheme 3.4) were only achieved in fluorinated alcohols (TFE 85% and HFIP 97%).



Scheme 3.4. Oxidation of mesitylene **238**.

Disappointingly, no explanation was provided as to why these particular solvents facilitated the reaction to such an extent.

HFIP also proved to be a good solvent for the oxidations with malonoyl peroxide **241**. However, the irritant and harmful properties associated with this alcohol as well as the high cost of this material made HFIP undesirable as a solvent. In the search for an alternative solvent, attempts to oxidise **238** in common organic solvents (CHCl_2 , EtOAc, THF, CHCl_3 , CH_3CN , DME) were made (Scheme 3.5) but without success with reactions only returning starting material. It was thought that the hydrogen-bonding properties of HFIP were activating the peroxide to addition of the arene.



Scheme 3.5. Oxidation of 1,3,5-triisopropylbenzene **242**.

Performing the reaction in 2-chloroethanol (CETOH) gave a 39% conversion to **243** after 24 h. Furthermore, switching to 2,2,2-trichloroethanol (TCE) gave a 96% conversion to **243** after 24 h. Even better conversion was observed when pefluoro-*tert*-butanol was used

(99%, 0.5 h). The reaction was also carried out in HFIP for comparison, which gave a 95% conversion in just 2 h (**Figure 3.9**).

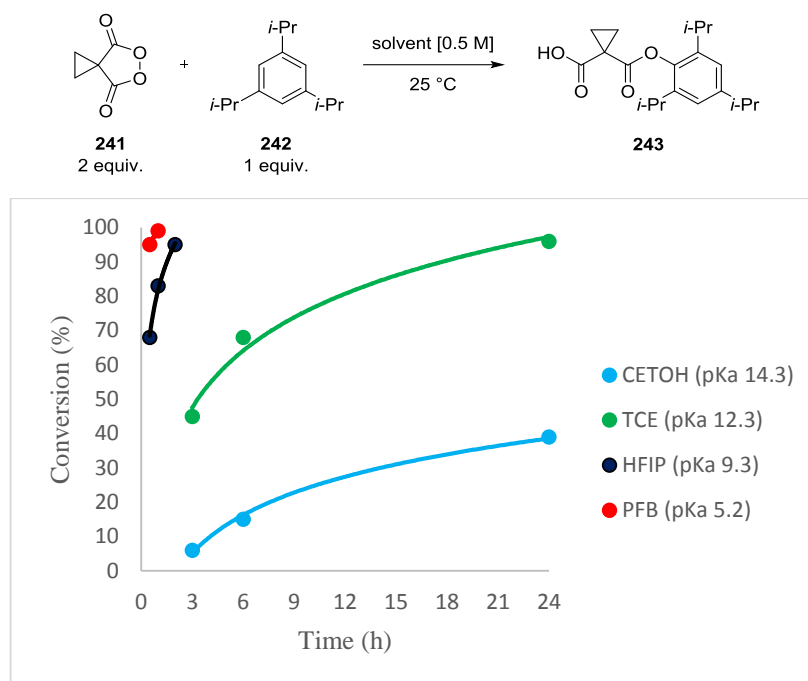


Figure 3.9. Plot of conversion to **243** against time in halogenated solvents.

Although these results were clearly qualitative, there was a clear correlation between the excellent and rapid conversions observed and the pK_a values of the solvents (CETOH - $pK_a = 14.3$; TCE - $pK_a = 12.3$; HFIP - $pK_a = 9.3$; PFB - $pK_a = 5.2$)¹⁰⁴ as shown in **Figure 3.9**. Therefore, we postulated that these results could, in fact, be indicative of an acid catalysed process (**Figure 3.10**). Presence of a catalytic amount of acid could activate peroxide **241** and subsequent reaction with **238** could give intermediate **279**, which would form product **248** upon aromatisation.

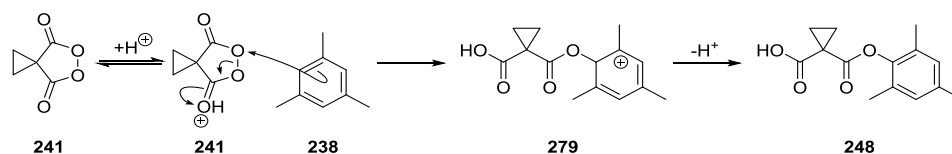


Figure 3.10. Plausible ionic mechanism.

To further test this hypothesis and to improve the stoichiometry of the reaction, a series of additives of varying acidity were investigated as potential catalysts by Dragan (**Table**

3.3). In this study, 1,3,5-triisopropylbenzene **242** was reacted with cyclopropyl malonoyl peroxide **241** (2 equiv.) and additive (2 equiv.) in dichloromethane [0.5 M] at 25 °C (**Figure 3.11**).

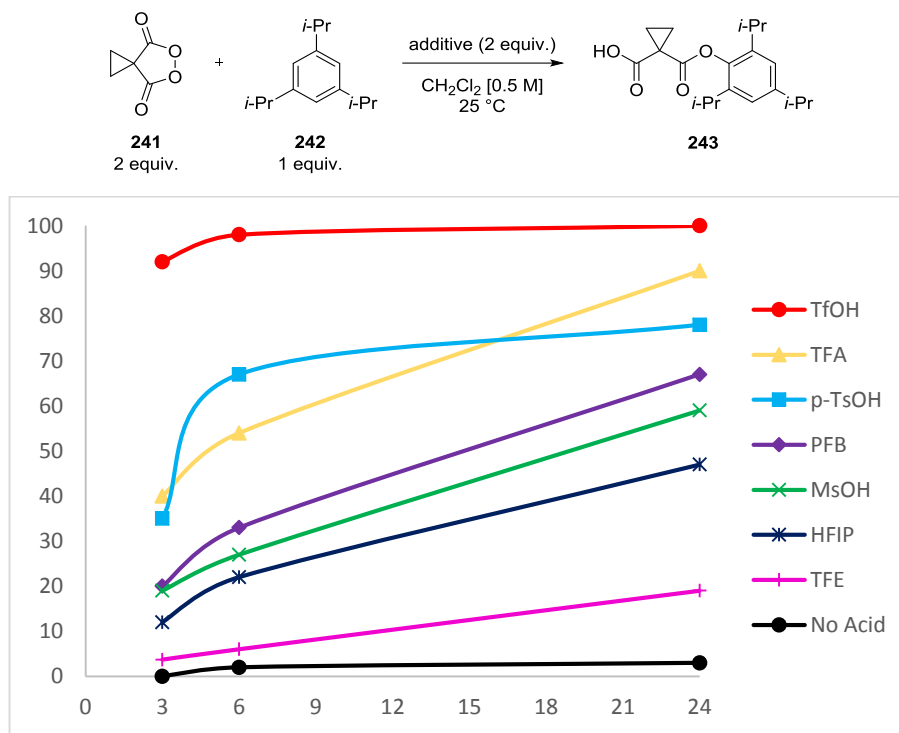


Figure 3.11. Plot of conversion to **239** against time in halogenated solvents.

Table 3.3. Various additives in the oxidation reaction.

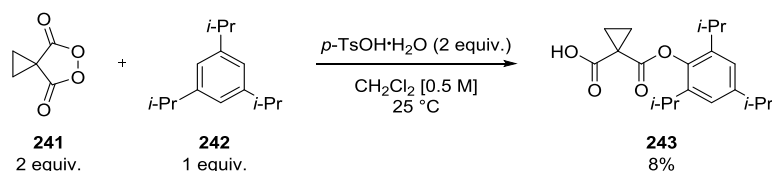
Entry	Additive	$\text{p}K_{\text{a}}^{95, 104\text{a}, 105}$	Conversion after 24 h (%)
1	None	–	3
<i>alcohols</i>			
2	TFE	12.4	19
3	HFIP	9.30	47
4	PFB	5.20	67
<i>acids</i>			
5	MsOH	-1.90	59
6	<i>p</i> -TsOH	-4.50	78
7	TFA	0.50	90
8	TfOH	-14.0	100

Both fluorinated alcohols and acids were investigated as potential catalysts and both groups of additives were found to accelerate the reaction as shown above. In accordance with previous observations, alcoholic additives with lower pK_a 's, such as PFB ($pK_a = 5.20$) catalysed the reaction better (67% conversion, **Table 3.3, Entry 4**) than those with higher pK_a 's - HFIP ($pK_a = 9.30$; 47% conversion; **Table 3.3, Entry 3**) and TFE ($pK_a = 12.4$; 19% conversion; **Table 3.3, Entry 2**). Similar trend was observed for acidic additives (**Table 3.3, Entries 5–8**). An interesting difference in the catalytic activity was observed between trifluoroacetic acid and the other acids. Despite having a higher pK_a , trifluoroacetic acid attained a conversion ($pK_a = 0.50$, 90% conversion, **Table 3.3, Entry 7**) higher than either methanesulfonic or *p*-toluenesulfonic acid and almost as good as triflic acid. The reason of this observation is not clear. Triflic acid ($pK_a = -14.0$) was the most efficient catalyst with a conversion of 92% in under 30 min (**Figure 3.11**).

These results indicated a general acid catalysis and showed that the reaction could be effectively catalysed by most additives with low pK_a values but was generally most effective with very strong acids ($pK_a < -5$). Hence, the necessity of using fluorinated solvents could be avoided with further optimisation as these solvents are prohibitively expensive for large-scale applications.

3.5.6.2. Effect of Water

The low conversion (8%) in the oxidation of 1,3,5-triisopropylbenzene **242** with 4-toluenesulfonic acid monohydrate (**Scheme 3.6**) alerted us to the possibility of an adverse effect of water on the reaction.



Scheme 3.6. Oxidation of **242** with peroxide **241** in the presence of *p*-toluenesulfonic acid monohydrate.

Although no problems were encountered when solvents were used without prior drying, a set of experiments was performed to assess the impact of water on the reaction.

Conversions of mesitylene **238** to **248** in HFIP [0.5 M] in the presence of peroxide **241** (2 equiv.) and water were observed at different time intervals (**Figure 3.12**).

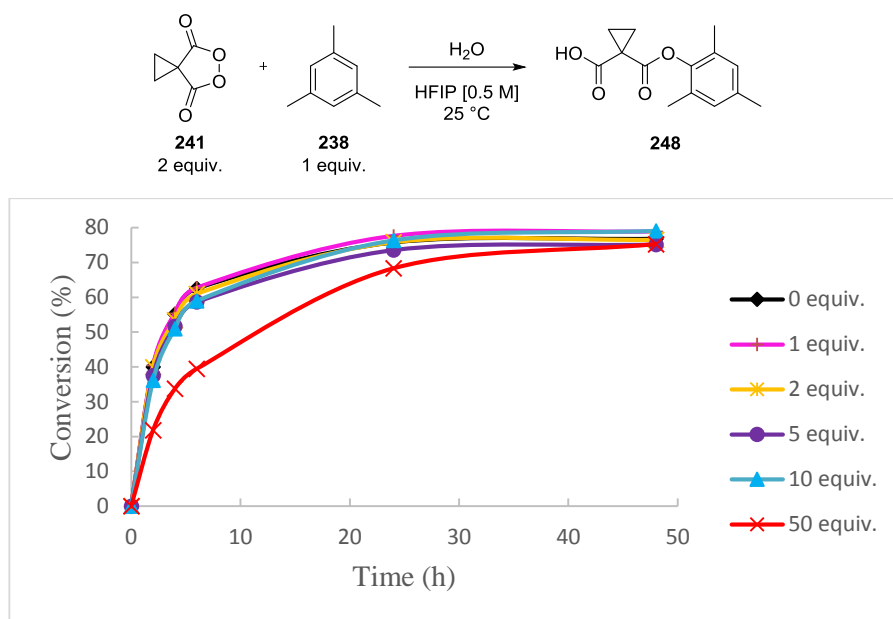


Figure 3.12. Plot of conversion to **248** against time in the presence of water.

Addition of up to 10 equivalents of water did not negatively affect the conversion. A substantial amount of water (50 equiv.) was needed to slow down the initial rate of reaction but a high conversion (75%) comparable to the test reaction (77%) was achieved after 48 h as shown in **Figure 3.12**. These results confirmed that the use of solvents as supplied from commercial sources was acceptable for this transformation.

This detrimental effect of water on the oxidation can be reasonably explained by the competition between HFIP and water in hydrogen bonding to peroxide **241** (**Figure 3.13**).

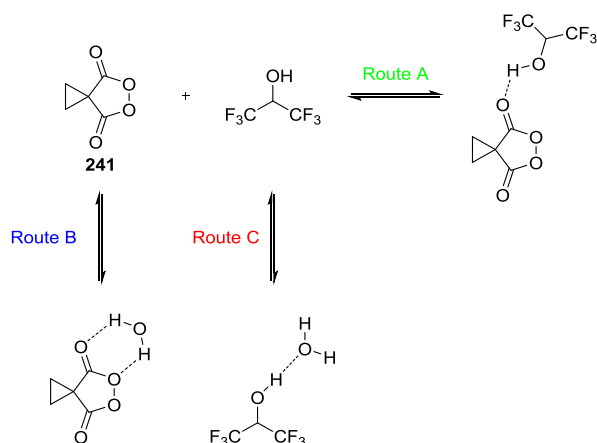


Figure 3.13. Hydrogen bonding between various components of the oxidation.

Hydrogen bonding between peroxide **241** and HFIP (Route A) activates **241**, but is disrupted when water is present. The interactions between water and peroxide **241** (Route B) decrease the availability of **241** for the reaction, effectively slowing it down. Water can also form hydrogen bonds to the solvent (Route C) but the high concentration of HFIP makes the interactions less likely to affect the reaction rate to any great extent. Increasing the amount of water to 50 equivalents may make this interaction significant and the result is a slower reaction process.

These conclusions were further supported by the considerable decrease in conversion observed when 1,3,5-triisopropylbenzene **242** (1 equiv.) was reacted with peroxide **241** (2 equiv.) in the presence of acid additive (2 equiv.) and water (2 equiv.) (**Figure 3.14**). Each reaction was run in duplicate and the points shown are the average of these two runs.

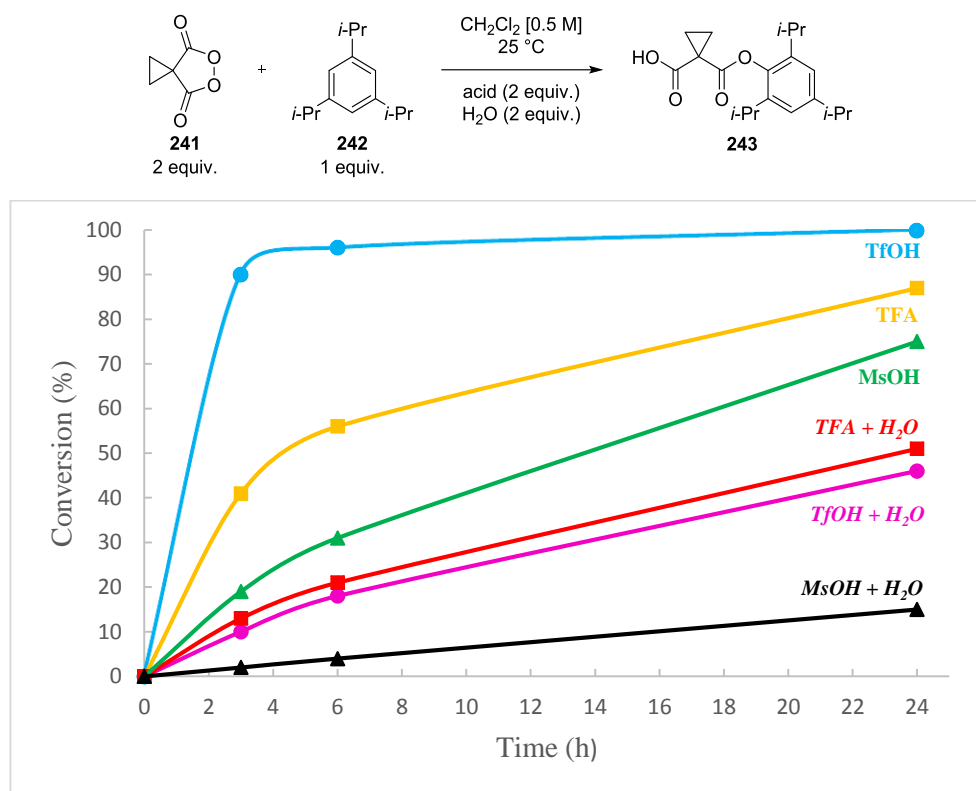


Figure 3.14. Effect of water on acid catalysis.

The conversion was lower by 71% for triflic acid, 33% for trifluoroacetic acid, and 35% for methanesulfonic acid (on average), highlighting the detrimental effect of water and the activating properties of acids on the reaction.

In summary, water was found to slow down the reaction but residual amounts of water present in commercially available solvents did not inhibit the process to a significant extent.

3.5.6.3. Reaction Kinetics

Measurement of the order of a chemical reaction is of major importance as it often provides evidence in support of, or against, a reaction mechanism. The rate of a chemical reaction at a given temperature may depend on the concentration of one or more reactants and products. A series of kinetic experiments were performed to study the dependence of the rate of reaction on the concentration of cyclopropyl malonyl peroxide **241** and mesitylene **238**.

The study of reaction kinetics began by monitoring the reaction between equimolar amounts of mesitylene **238** and peroxide **241**. Consumption of both reagents as well as product **248** was monitored by ^1H NMR spectroscopy (relative to an internal standard – 1,4-dinitrobenzene) under the reaction conditions shown in **Figure 3.15**.

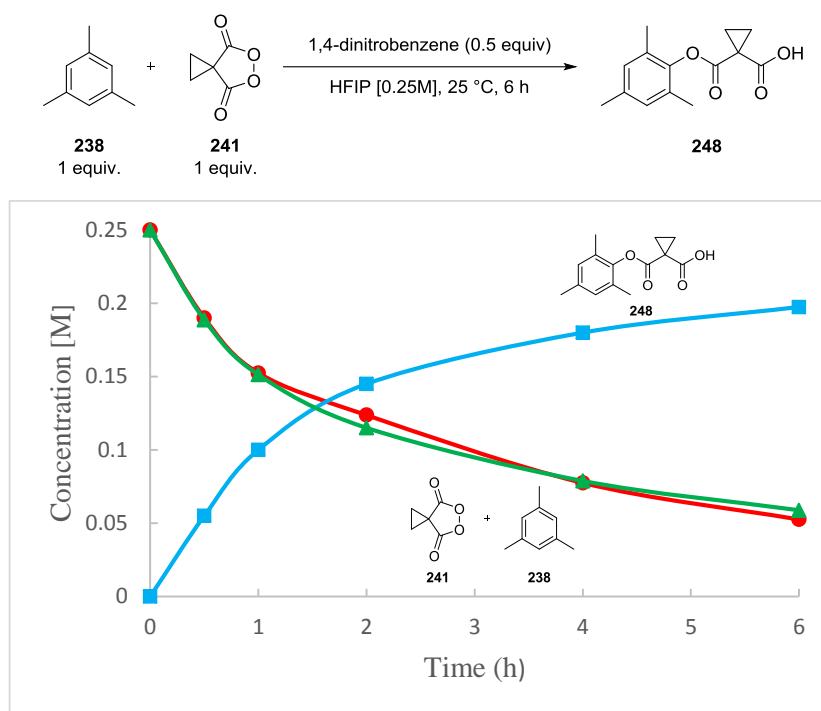


Figure 3.15. Reaction profile of peroxide **241** (●) mediated oxidation of mesitylene **238** (▲) to product **248** (■).

Both mesitylene **238** and peroxide **241** were consumed at the same rate, which was directly proportional to the formation of product **248**.

The kinetic order in **241** was then determined using an excess of mesitylene **238** (10 equiv.) under identical conditions (**Figure 3.16**). The reaction was subsequently repeated with a reversed molar ratio (10 equiv. of peroxide **241**) to establish the kinetic order in mesitylene **238** (**Figure 3.17**).

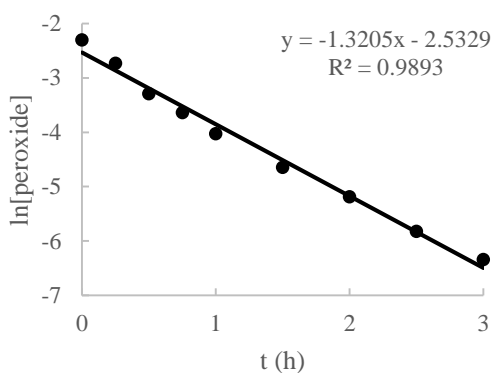


Figure 3.16. Logarithmic plot of peroxide **241** concentration against time showing first-order dependence in peroxide **241**.

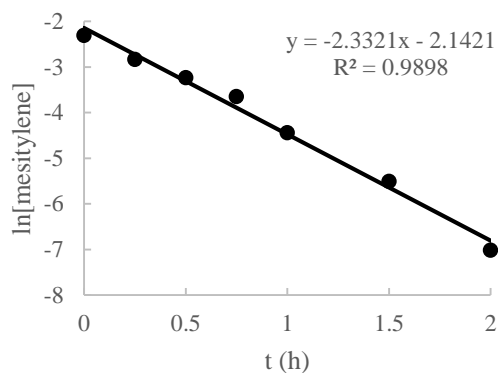


Figure 3.17. Logarithmic plot of mesitylene **238** concentration against time showing first-order dependence in mesitylene **238**.

The concentration of product **248** was followed over time (relative to 1,4-dinitrobenzene) using ^1H NMR spectroscopy. A linear correlation was observed in the logarithmic plot of the concentration of the limiting reagent against time, showing a first-order dependence in both peroxide **241** (**Figure 3.16**) and mesitylene **238** (**Figure 3.17**).

The kinetic study of peroxide **241**-mediated oxidation of mesitylene **238** by ^1H NMR analysis revealed that the reaction was second order overall (first order in both cyclopropyl malonyl peroxide **241** and mesitylene **238**), indicating that the rate-determining step involved one molecule of **241** and one molecule of **238** in the transition state.

3.5.6.4. Hammett Study

The mechanism shown in **Figure 3.7** (**Section 3.5.3**) is a two-step process. The first step requires nucleophilic attack by the substrate onto peroxide **241** to form Wheland intermediate **284**. The intermediate **284** is then deprotonated to restore aromaticity, which results in the formation of the final compound **248**. In order to ascertain whether a positive charge was developed in the course of the reaction a Hammett analysis was performed, where the influence of the electronic effects of the substituents was studied. The oxidation of a series of X-substituted mesitylene derivatives, where X was H, Me, Br, OMe, or F was investigated in the reaction with peroxide **241** (1 equiv.) in HFIP [0.1 M] (**Figure 3.18**).

Nitromesitylene **268** and 2,4,6-trimethylbenzoic acid **262** were excluded from the investigation due to their low reactivity (**268**: 72 h, 50 °C, 0%; **262**: 42 h, 50 °C, 86%). The conversions were determined using ^1H NMR spectroscopy by monitoring the consumption of peroxide **241** relative to the internal standard (1,4-dinitrobenzene, 0.2 equiv.). The conversions to **250** were obtained by monitoring the consumption of isodurene **249** (aromatic protons, 6.84 ppm) due to the overlapping signals of **250** (2.13 ppm) and cyclopropyl malonoyl peroxide **241** (2.12 ppm). Reaction times between 10 minutes to 4 hours were chosen to ensure only modest conversions (<10%).

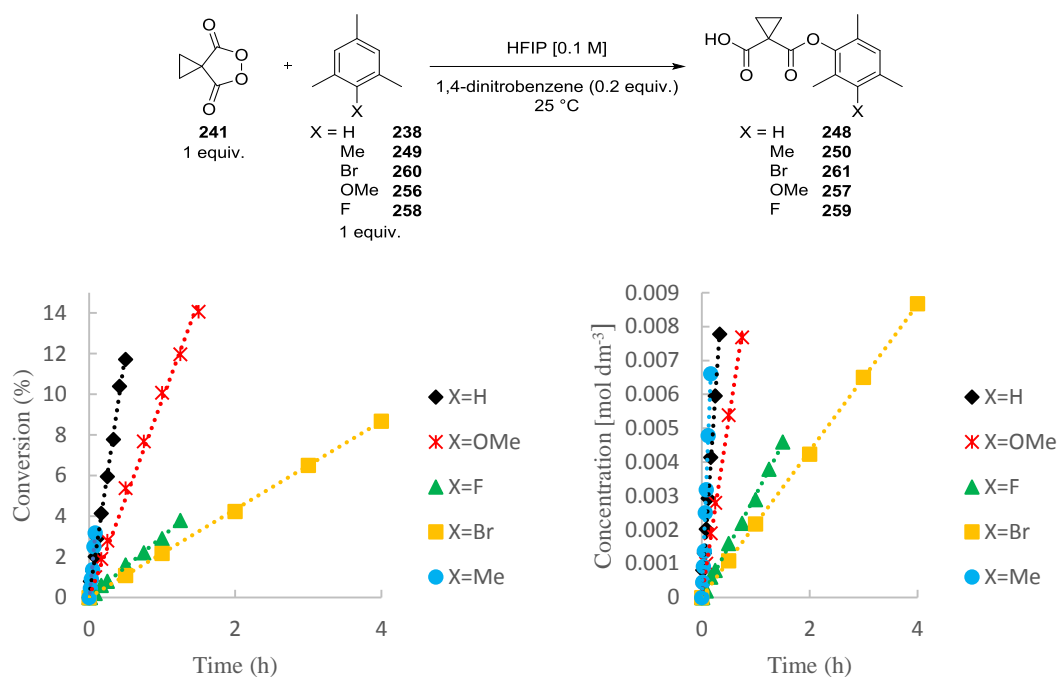


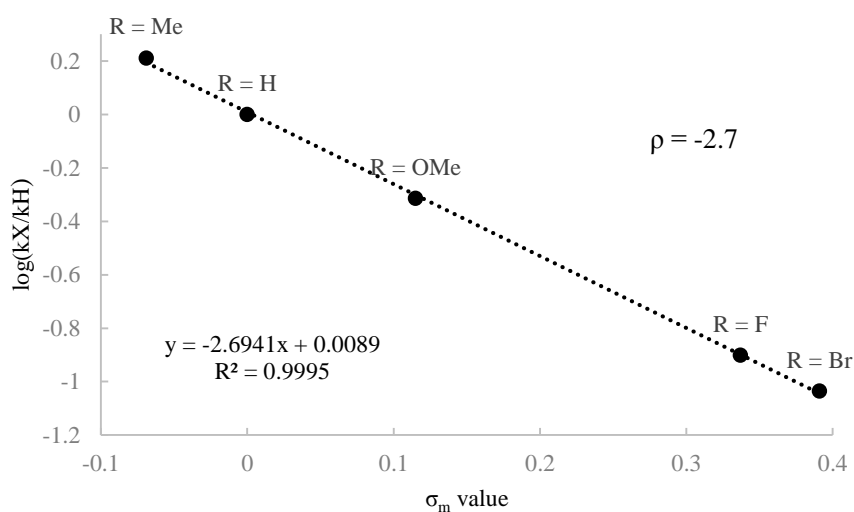
Figure 3.18. Plot of conversion against time for the reaction of peroxide **241** with mesitylene derivatives.

Figure 3.19. Plot of product concentration against time.

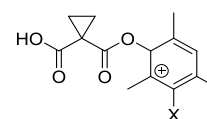
The conversions were then used to calculate the concentration of products over time (**Figure 3.19**). The initial rates of reactions were obtained graphically (**Table 3.4**) since the initial rate of reaction is equal to the positive of the slope of product concentration *versus* time. The initial rate of reaction for each arene was used to construct a Hammett plot based on literature σ_m values¹⁰⁶ (**Figure 3.20**).

Table 3.4. Initial rates and literature σ_m values of selected arenes.

X	Initial rate (mol dm ⁻³ s ⁻¹)	log(k _X /k _H)	σ_m^{106}
3-Me	1.08×10^{-5}	0.21	-0.069
3-H	6.64×10^{-6}	0	0
3-OMe	3.22×10^{-6}	-0.31	0.115
3-F	8.33×10^{-7}	-0.90	0.337
3-Br	6.11×10^{-7}	-1.04	0.391

**Figure 3.20.** Hammett plot of arene oxidation with peroxide **241**.

Generally, the inductive effect is transmitted about equally to the *meta* and *para* positions. Since mesitylene derivatives were studied, σ_p values could not be considered for the Hammett plot. Similarly, σ_m^+ and σ_m^- values were not taken into consideration as there were no electron-withdrawing or electron-donating groups in the *meta* position that could stabilise the positive charge through resonance (**Figure 3.21**). An excellent linear correlation ($R^2 = 0.9995$) was observed when $\log(k_X/k_H)$ values were plotted against σ_m parameters, demonstrating the importance of inductive effects and providing important mechanistic implications. The good linear fit illustrated in **Figure 3.20** corroborated that there was a single mechanism in operation when both electron-donating and electron-withdrawing groups were present. What is more, the ρ value obtained (-2.7)

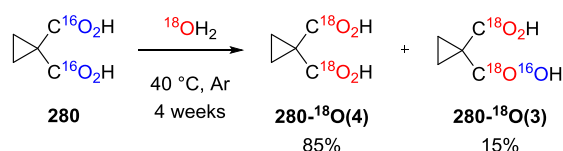
**Figure 3.21.**

was consistent with significant development of positive charge on the ring in the transition state during the reaction (diagnostic of electrophilic aromatic substitution),¹⁰⁷ providing strong evidence against the radical mechanism while not dismissing the SET mechanism. The σ ρ relationship also applies to free-radical reactions as they can have some polar character, but ρ values are usually smaller than 1.5 whether positive or negative.¹⁰⁸

3.5.6.5. Isotopic Labelling Studies

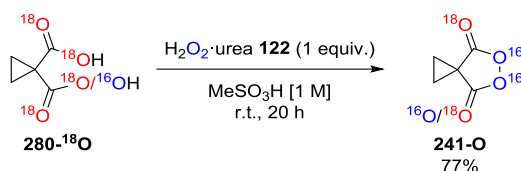
Further evidence in support of an ionic mechanism (Section 3.5.3, Figure 3.7) arose from the use of isotopically labelled peroxide **241-¹⁸O** in the oxidation of mesitylene **238** by Dragan (Scheme 3.7).

Peroxide **241-¹⁸O** was synthesised by stirring diacid **280** in ¹⁸OH₂ (97% ¹⁸O incorporation, 26.5 equiv., 1 mL) under an argon atmosphere at 40 °C for 2 weeks. Care was taken when setting up and carrying out the reaction to ensure that moisture from the atmosphere was not present in the reaction flask. The ¹⁸O incorporation into **241-¹⁸O** was monitored by mass spectrometry (ESI–) during this time. After 2 weeks and careful removal of ¹⁸OH₂ under reduced pressure, the procedure was repeated. After a total of 4 weeks, **241-¹⁸O** was obtained as a mixture of quadruply labelled diacid **280-¹⁸O(4)** (85%) and triply labelled diacid **280-¹⁸O(3)** (15%) in a quantitative yield (Scheme 3.7).



Scheme 3.7. Preparation of ¹⁸O enriched cyclopropane-1,1-dicarboxylic acid **280-¹⁸O**.

Isotopically labelled cyclopropane-1,1-dicarboxylic acid **280-¹⁸O** was then treated with H₂O₂•urea **122** (3 equiv.) in methanesulfonic acid [1 M] to afford the ¹⁸O enriched peroxide **241-¹⁸O** in a 77% yield (Scheme 3.8).



Scheme 3.8. Preparation of ^{18}O enriched cyclopropyl malonyl peroxide **241- ^{18}O** .

The extent to which **241- ^{18}O** was enriched with ^{18}O could not be established by mass spectrometry as peroxide **237** readily undergoes fragmentation during the process of acquiring mass spectra. Therefore, it was assumed that a maximum of 85% of **241- ^{18}O** was doubly labelled in the carbonyl positions.

If the peroxide **241- ^{18}O** was in equilibrium with its diradical form, scrambling of the labels across the molecule could be expected as shown in **Figure 3.22**. Whilst it was possible that the rate of radical-radical recombination of **241- ^{18}O** was faster than bond rotation which would prevent scrambling of the label, it is expected that reaction of the diradical with the aromatic ring would result in scrambling of the label, the reaction occurring through each of the two stages.

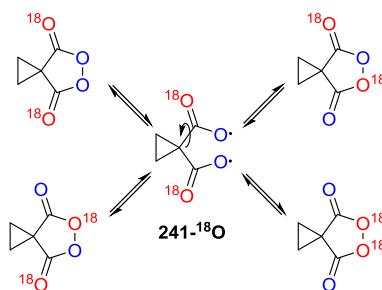


Figure 3.22. Scrambling of label on peroxide **241- ^{18}O** .

It could be expected that a radical reaction between peroxide **241- ^{18}O** and mesitylene **238** would give a mixture of products, for example **248-1** and **248-2** with ^{18}O in different positions (**Figure 3.23**).

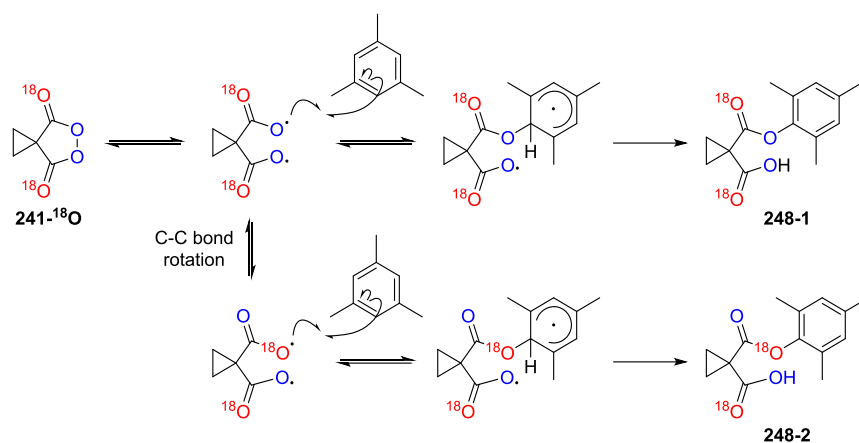


Figure 3.23. Plausible scrambling of labels in the oxidation reaction reaction.

As a result a new C– ^{18}O and C– ^{16}O bond would be formed. Lower incorporation of ^{18}O into 241- ^{18}O would consequently mean a lower level of isotopic label in the product 248.

In the case of an ionic mechanism, a nucleophilic attack of mesitylene 238 on the peroxide 241- ^{18}O would result in the formation of a new C– ^{16}O bond (Figure 3.24). Therefore, the label would remain on the carbonyl oxygen atom.

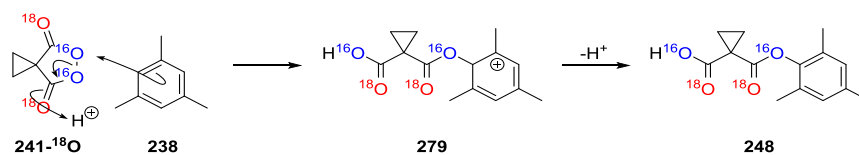
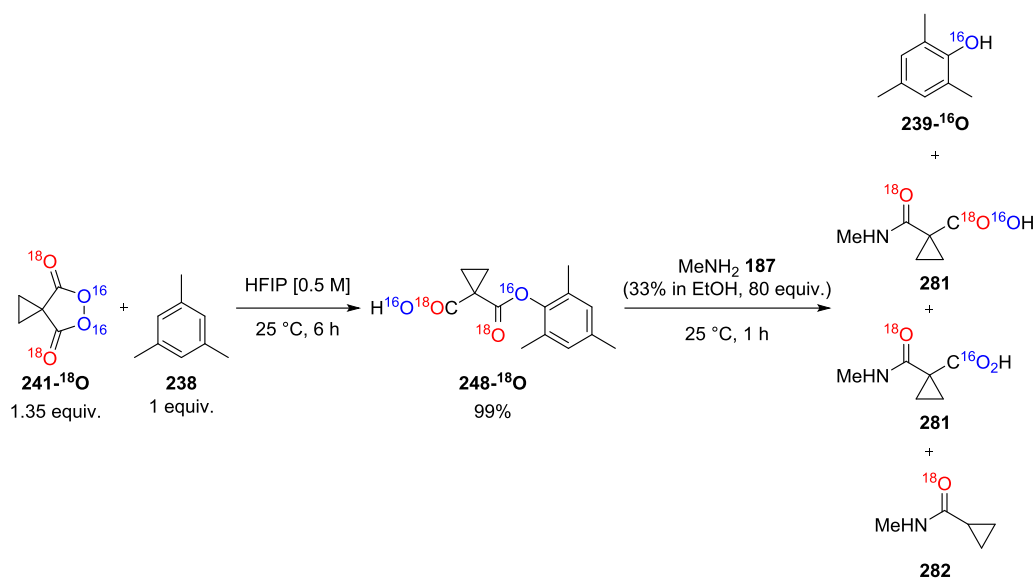


Figure 3.24. Plausible ionic mechanism.

Mesitylene 238 was treated with peroxide 241- ^{18}O in HFIP [0.5 M] for 6 h at 25 °C (Scheme 3.9).



Scheme 3.9. Oxidation of **238** with peroxide **241-¹⁸O** and subsequent derivatisation with methylamine **187**.

Mass spectrometric analysis (GC-MS/CI) revealed incorporation of two ^{18}O atoms into **248**. The fragmentation pattern indicated the position of ^{18}O to be on the ester carbonyl oxygen atom. This was unequivocally established through derivatisation, which was first performed on an unlabelled sample of **248**. Product **248-¹⁸O** was then subjected to aminolysis by stirring in methylamine (80 equiv., 33 wt. % in ethanol) at 25 °C for 1 h (**Scheme 3.8**). Analysis of GC-MS data revealed unlabelled 2,4,6-trimethylphenol **239-¹⁶O** along with product **281** and **282** providing decisive evidence that the ^{18}O atom was exclusively located on the ester carbonyl position in compound **248** and that no scrambling occurred during the reaction.

These compelling results are consistent with the ionic mechanism (**Section 3.5.3, Figure 3.7**), where the electrophilic oxygen atom of peroxide **241** is attacked by a nucleophilic arene molecule.

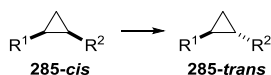
3.5.6.6. Mechanistic Probes

Phenylcyclopropylcarbinyl radicals **283** have previously been used as mechanistic probes for fast radical reactions by Newcomb's¹⁰⁹ and Ingold's¹¹⁰ groups through diagnostic ring-opening to phenylbutenyl radicals **284** (**Figure 3.25**).



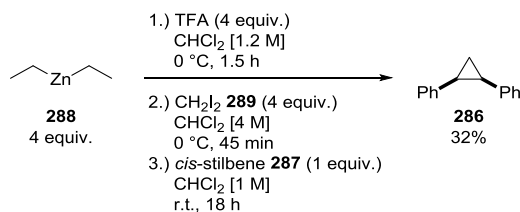
Figure 3.25. Radical rearrangement used to provide mechanistic information.

Precursors to these reactive radical intermediates, such as **285-cis**, undergo essentially irreversible rearrangements as shown in **Scheme 3.10**. Conversely, ionic intermediates adjacent to a three-membered ring have not been reported to induce ring-opening and rearrangement. By establishing the relative stereochemistry of the reaction product, it has been shown that the interconversion of substrates such as **285-cis** to **285-trans** during a reaction (**Scheme 3.10**) provides evidence for a phenylcyclopropylcarbinyl radical intermediate within the transformation.



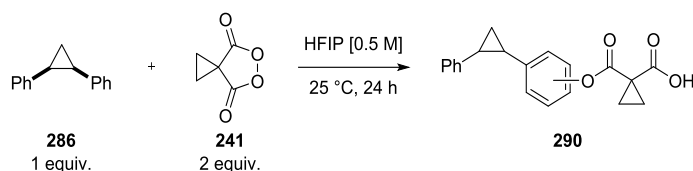
Scheme 3.10. Rearrangement of **285**.

To test this hypothesis, *cis*-1,2-diphenylcyclopropane **286** was prepared by reacting commercially available *cis*-stilbene **287** (1 equiv.) with trifluoroacetic acid (4 equiv.), diethylzinc **288** (4 equiv.), and diiodomethane **289** (4 equiv.) in anhydrous dichloromethane [0.5 M] at 0 °C under an inert atmosphere (**Scheme 3.11**). After 24 h and upon purification, **286** was obtained as a white solid in a 32% yield.



Scheme 3.11. Preparation of *cis*-1,2-diphenylcyclopropane **286**.

cis-1,2-Diphenylcyclopropane **286** (1 equiv.) was then reacted with cyclopropyl malonoyl peroxide **241** (2 equiv.) in HFIP [0.5 M] at 25 °C for 24 h (**Scheme 3.12**).

Scheme 3.12. Probing the mechanistic clock **286**.

This reaction could proceed *via* a radical pathway (**Figure 3.26**) through a reverse-rebound mechanism,⁹³ where the O–O bond of **241** is homolytically cleaved, and a reaction with *cis*-1,2-diphenylcyclopropane **286** follows to give the diradical intermediate **291**. The radical on the phenyl ring in that case could be delocalised across the ring. It could also be further delocalised by ring-opening of the three-membered ring. Rotation around the σ -bond followed by reformation of the three-membered ring would give the thermodynamically favoured isomer **292-trans**.

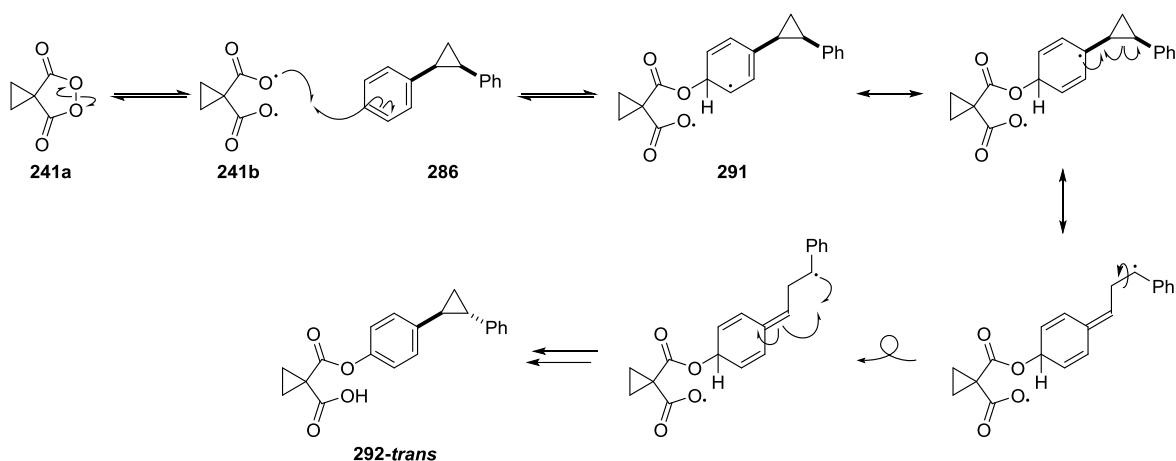


Figure 3.26. Plausible radical mechanism.

Alternatively, the reaction could proceed by an ionic mechanism (**Figure 3.27**), where the electron-rich arene **286** reacts with the electrophilic peroxide **241** to give the positively charged intermediate **293**. Subsequent proton abstraction to restore aromaticity could result in the formation of **292-cis**.

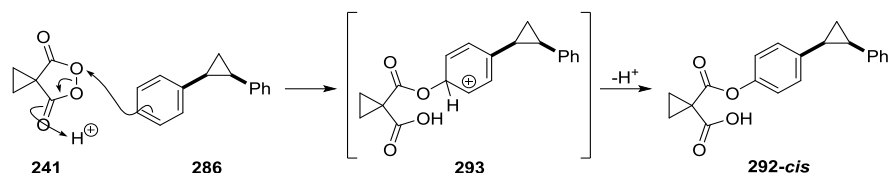
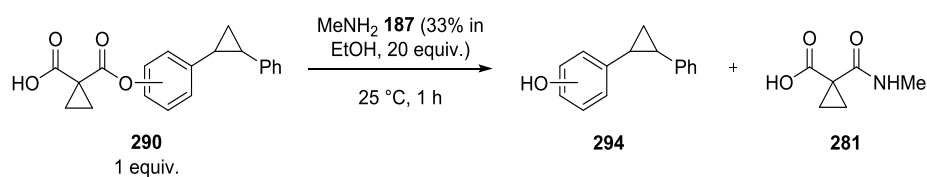


Figure 3.27. Plausible ionic mechanism.

It was hoped that this reaction could lead to a specific stereoisomer of the product providing strong evidence on which mechanism was in operation during the arene oxidation process.

Analysis of the reaction shown in **Scheme 3.12** posed considerable challenges. ^1H NMR spectroscopy of the crude reaction mixture did not provide definite answers due to a number of products being present in the crude reaction mixture. Further purification by silica gel column chromatography did not lead to isolation of any pure compounds. It could be that the reaction resulted in a larger number of products than anticipated due to the fact that both aromatic rings of the substrate could be functionalised in one of the two positions.

To provide more easily separable products the reaction was repeated and subjected to aminolysis (**Scheme 3.13**). The crude reaction mixture (1 equiv.) was dissolved in the minimum amount of ethanol and stirred with methylamine **187** (33% MeNH_2 in EtOH *w/v*, 20 equiv.) at $25\text{ }^\circ\text{C}$ for 1 h to give the phenols **294** and 1-(methylcarbamoyl)cyclopropane-1-carboxylic acid **281** as a co-product.



Scheme 3.13. Aminolysis of half acid-ester products.

Purification by flash chromatography did not result in isolation of any of the expected phenols as single isomers. This presented a serious problem, presumably caused by the high reactivity of *cis*-1,2-diphenylcyclopropane **286**. To reduce the number of potential products, it was decided that compound **286** could be made less reactive by introducing an electron-withdrawing group on one of the phenyl rings. From the substrate scope screening we knew that strong electron-withdrawing groups rendered substrates unreactive, even when exposed to harsh conditions (50 °C) and longer reaction times (Section 3.4). Therefore, the nitro group was chosen as the electron-withdrawing group and *cis*-1-(4-nitrophenyl)-2-phenylcyclopropane **295** as the new target mechanistic probe (Figure 3.28). The precursor *cis*-alkene **296** (Figure 3.29) was not

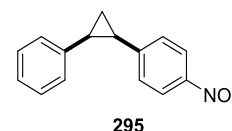


Figure 3.28.

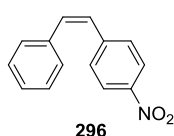
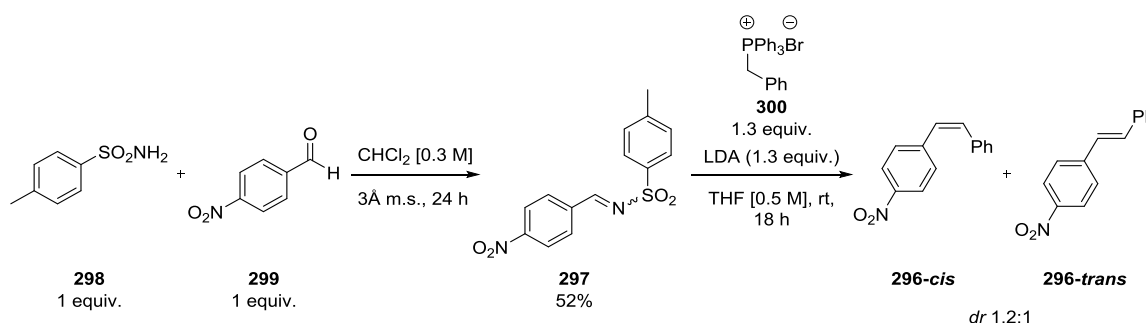


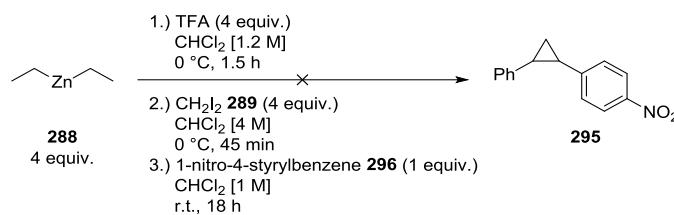
Figure 3.29.

commercially available. However, it had been reported that the target compound **295** could be prepared in a 77% yield with excellent stereoselectivity (99>1 *Z/E*).¹¹¹ The precursor to *cis*-alkene **296** was prepared in 52% yield by reaction of 4-nitrobenzaldehyde **299** with 4-toulenesulfonamide **298** in the presence of 3Å molecular sieves (Scheme 3.14).

Scheme 3.14. Preparation of alkene **297**.

The crystalline product **297** was then reacted with triphenylphosphonium ylide **300** as reported. The reaction resulted in the formation of two alkenes, **296-cis** and **296-trans**, in a 1.2:1 ratio. Upon purification by flash chromatography, the isomeric ratio improved significantly (4:1 *Z/E*). However, further purification attempts were abandoned owing to the reported isomerisation of the *Z*-alkenes under the influence of light and air at room

temperature and the difficulty of separating both isomers. The mixture was carried through and subjected to cyclopropanation conditions shown in **Scheme 3.15**.



Scheme 3.15. Attempted synthesis of 1-nitro-(4-phenylcyclopropyl)benzene **295**.

Purification of the crude reaction mixture did not lead to isolation of either of the isomers of **295**. Since the synthesis of **295** proved to be of considerable difficulty, an alternative approach was taken. Rather than make one of the phenyl rings less reactive, it was decided to examine the effect of increasing the reactivity of one of the rings through introduction of an electron-donating group. Substrates with one or two EDG's, such as toluene **5** or xylene **246**, required higher temperatures and/or longer reaction times to give decent yields (**Section 3.4**). In contrast, mesitylene **238** was rapidly oxidised (4.5 h) at 25 °C in a near quantitative yield (**Section 3.4**). Therefore, *cis*-1-phenyl-2-(3,5-

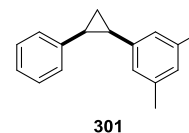
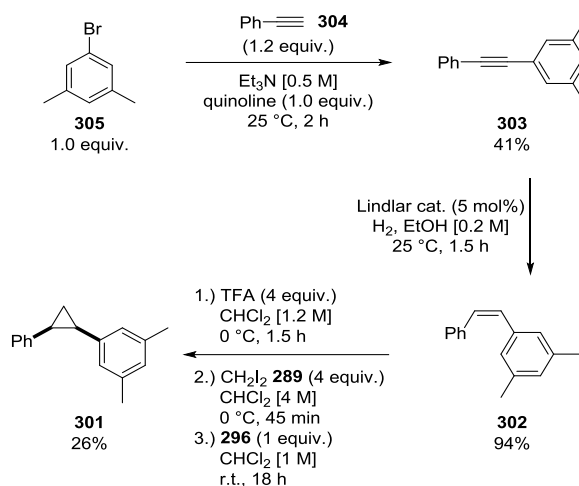
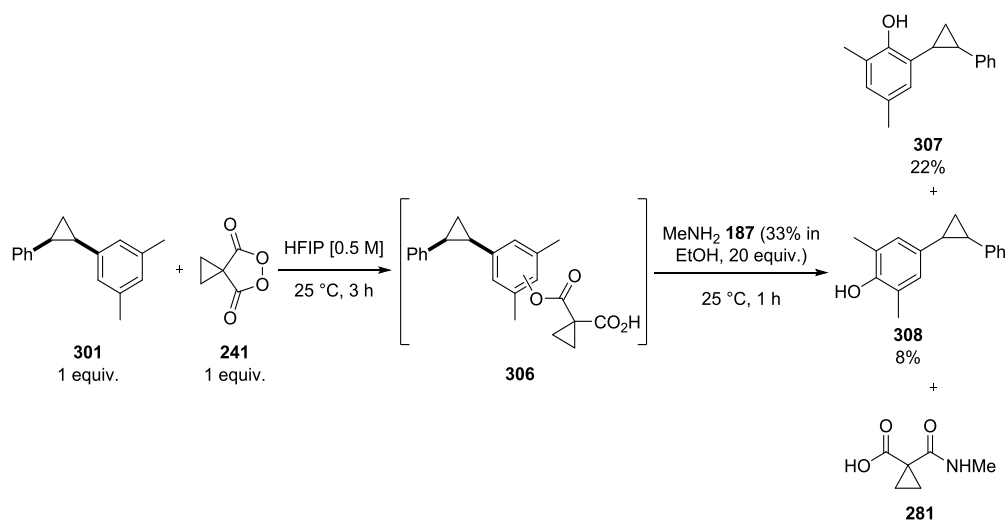


Figure 3.30.

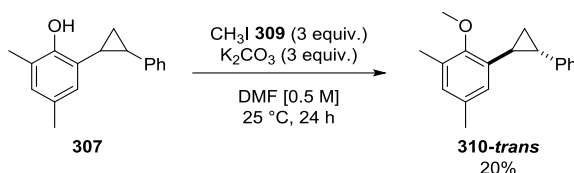
dimethylphenyl)cyclopropane **301** (**Figure 3.30**) appeared attractive as a potential mechanistic probe as the tri-substituted phenyl ring should react in preference to the mono-substituted phenyl ring. The precursor alkene **302** had to be prepared prior to cyclopropanation, which was achieved in two stages. First, alkyne **303** was prepared through a Sonogashira coupling of phenylacetylene **304** (1.2 equiv.) and 1-bromo-3,5-dimethylbenzene **305** (1 equiv.) in a 41% yield. Alkyne **303** was then reduced using Lindlar catalyst to give alkene **302** (94%) as a single isomer. Finally, the mechanistic probe **301** was synthesised in 26% yield under standard conditions (**Scheme 3.16**).

Scheme 3.16. Preparation of *cis*-1-phenyl-2-(3,5-dimethylphenyl)cyclopropane **301**.

Compound **301** was reacted with 1 equivalent of cyclopropyl malonoyl peroxide **241** at 25 °C. After 3 h, the reaction mixture was immediately subjected to aminolysis without prior purification (Scheme 3.17).

Scheme 3.17. Probing the mechanistic clock **301**.

Upon purification by flash chromatography phenols **307** and **308** were isolated in 22% and 8% yield, respectively, but the relative stereochemistry of each product could not be unequivocally established from ^1H NMR spectroscopic data. Compound **307** was then methylated with iodomethane **309** (Scheme 3.18) and compared against the *trans* and *cis* isomers of **307**, which were prepared independently by Dragan.

Scheme 3.18. Methylation of phenol **307**.

It was found that compound **310** had a *trans* stereochemistry. This may imply a radical mechanism but previous results and the EPR studies discussed in the next section indicate that the rearrangement was most likely a result of an ionic intermediate-induced ring opening which is outlined in **Figure 3.31**.

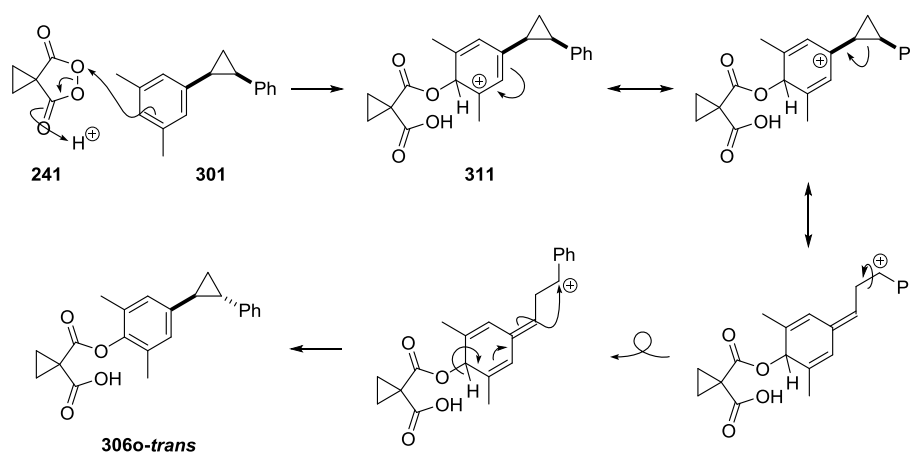


Figure 3.31. Testing isomerisation before and after the oxidation.

Reaction of peroxide **241** with the mechanistic probe **311** could give the positively charged intermediate **311**. The charge could be delocalised across the ring and further by ring-opening of the three-membered ring. Rotation around the σ -bond followed by reformation of the three-membered ring could give the thermodynamically favoured isomer **306o-trans**.

Obviously, isomerisation could occur before or after the oxidation. To eliminate that possibility, the *cis* isomer of the mechanistic probe **310-cis** and the methylated product **310-cis** were simultaneously stirred under the same reaction conditions under which the oxidation reaction was performed (**Figure 3.32**).

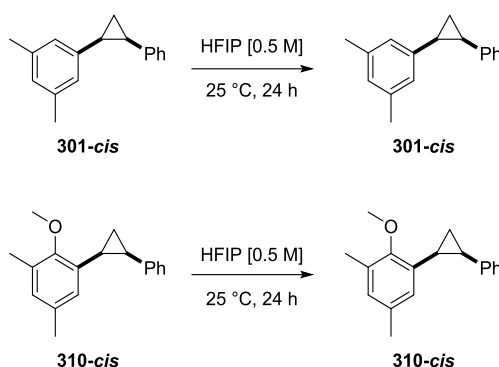


Figure 3.32. Testing isomerisation before and after the oxidation.

In each case isomerisation was not observed suggesting it was occurring during the oxidation process.

3.5.6.7. Electron Paramagnetic Resonance Studies

Further mechanistic investigations were carried out in collaboration with Dr Stephen Sproules of the University of Glasgow using Electron Paramagnetic Resonance (EPR) spectroscopy.

The most direct experiment to invoke the existence of **241b** would be to use EPR spectroscopy to detect the diradical form of peroxide **241a** in solution (**Figure 3.33**).

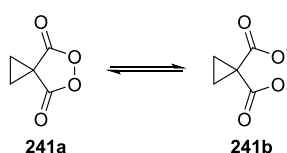


Figure 3.33. Peroxide **241** in equilibrium with its diradical form.

Unfortunately, it is not always possible to directly observe radicals as their concentration may be below the detection limit of the spectrometer. In addition, some radicals, even if present at higher concentrations, are not observable at room temperature as their spin relaxation times are very short, making their line width too broad to be observed by EPR. However, the technique of spin trapping can be used to overcome these problems. Spin traps are molecules that react rapidly with radicals, converting them into stable radicals that accumulate and can be

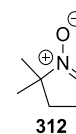


Figure 3.34.

readily detected. The best results are usually obtained using nitron precursors due to the high stability of the resulting nitroxide adducts. 5,5-Dimethyl-1-pyrroline-*N*-oxide **312** (DMPO) (**Figure 3.34**), a spin trap commonly used in EPR spectroscopy for the detection of oxygen-based radicals,¹¹² was chosen to be used in our EPR studies.

Before any experiments were performed, the EPR spectrometer was calibrated using a solution of 2,2,6,6-tetramethylpiperidine 1-oxyl (TEMPO, **313**) (**Figure 3.35**) in TFE [0.05 M]. In addition, it was necessary to distil the commercial sample of DMPO **312**

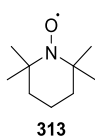


Figure 3.35.

prior to use. The solution of **312** in TFE [0.5 M] was checked for the presence of radical impurities by EPR (**Figure 3.36a**). The solution of peroxide **241** in TFE [0.5 M] was then examined (**Figure 3.36b**), followed by the solution of **312** and peroxide **241** in TFE [1 M] (**Figure 3.36c**).

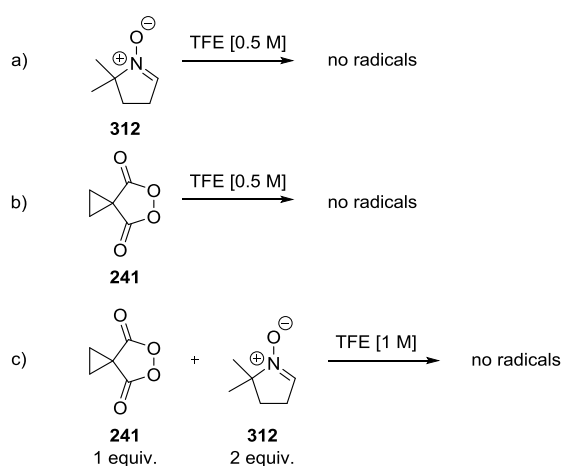
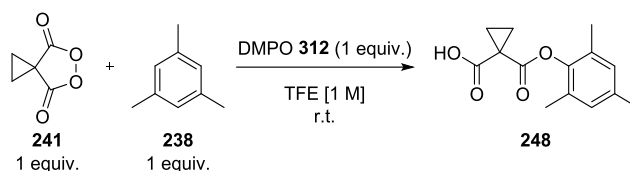


Figure 3.36. EPR studies of peroxide **241**, DMPO **312**, and a mixture of **241** and **312**.

No radicals were detected in any of the above experiments, which is consistent with previous studies conducted by Mike Rawling of the Tomkinson group.¹⁰⁰ He showed, through the use of isotopically labelled peroxide **241-¹⁸O**, that the O–O bond of peroxide **241** was stable to homolytic fission at room temperature in both the solid-state and solution (CHCl_3).

A solution of peroxide **241** (1 equiv.), mesitylene **238** (1 equiv.) and DMPO **312** (1 equiv.) was then analysed by EPR spectroscopy for the presence of radical species (**Scheme 3.19**).



Scheme 3.19. EPR study of the oxidation reaction of mesitylene **238**.

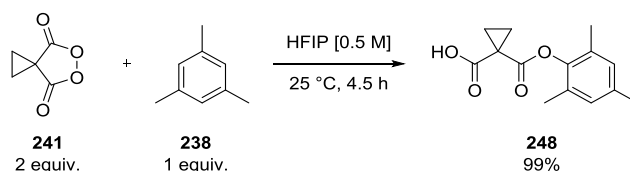
Radicals were not detected during the course of the reaction over 6 h. All experiments were carried out in duplicate. Furthermore, another set of experiments, using HFIP as solvent, was conducted. In each experiment, no evidence for the presence of radicals was obtained.

On the basis of these results, a mechanism involving the formation of oxygen-based radicals, *i.e.* the diradical form of peroxide **241** (**Figure 3.24**), can be ruled out, since these would rapidly react with DMPO **312**.

The EPR results are in accordance with previous observations and validate our conclusions that the reaction mechanism is most likely ionic in nature.

3.6. Conclusions

In summary, cyclopropyl malonoyl peroxide **241** has been shown to be a more reactive and safer alternative to phthaloyl peroxide **240** in the oxidation of aromatic compounds.¹¹³ This innovative C–H functionalisation method uses peroxide **241** and arene under mild reaction conditions (25–40 °C) in HFIP to give the corresponding half acid-esters, as exemplified in **Scheme 3.20**.



Scheme 3.20. An example of arene oxidation.

The reaction was found to be sensitive to electronic and, to a lesser extent, steric properties of aromatic substrates. Yields were highly dependent on the electron-donating

ability of substituents. The protocol was most effective with electron-rich arenes due to the electrophilic nature of the malonoyl peroxide **241**. Substrates with weak electron-donating, and electron-withdrawing groups either required higher temperatures or/and reaction times or were completely inert to oxidation. Likewise, phenols were unreactive regardless of the reaction conditions employed. Where positional selectivity was possible, mixtures of *ortho* and *para* products were formed.

An extensive mechanistic investigation involving acid catalysis, addition of hydrogen-bonding additives, reaction kinetics, Hammett analysis, isotopic labelling experiments, introduction of mechanistic probes, and EPR studies allowed substantial evidence to be gained for the ionic mechanism of this fascinating reaction.

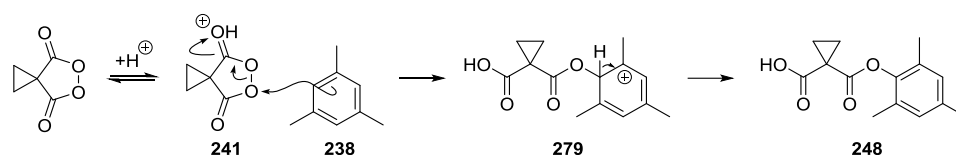


Figure 3.37. Aromatic oxidation mechanism.

A nucleophilic attack of arene **238** on the weak O–O bond of cyclopropyl malonoyl peroxide **241** produces Wheland intermediate **279**, which upon deprotonation yields the half acid-ester product **248** (**Figure 3.37**).

The efficiency of the reaction was improved through the use of a hydrogen-bond donor as additive rather than solvent. Effective catalysis was achieved with most compounds that have low pK_a values but was generally most successful with very strong acids ($pK_a < -5$).

The study on the effect of water demonstrated that although water hinders the reaction to a small extent the use of solvents as supplied from commercial sources is permissible.

Chapter 4: Experimental

4. Experimental

4.1. General Experimental Details

Reagents were purchased from Sigma Aldrich, Alfa Aesar, or Fluorochem and used without further purification. Anhydrous toluene, dichloromethane, tetrahydrofuran and diethyl ether were obtained from an SPS system at the University of Strathclyde. Other anhydrous reagents were bought from Sigma Aldrich. ^{18}O -labelled oxygen gas (1 L, 89%, approx. 16 Bar) was obtained from CK Gas Products Ltd.

Nuclear magnetic resonance (NMR) spectra were recorded on a Bruker Avance III 400 (^1H 400 MHz and ^{13}C 101 MHz), Bruker Avance 400 (^1H 400 MHz and ^{13}C 101 MHz) or Bruker Avance DRX 500 (^1H 500 MHz and ^{13}C 125 MHz) spectrometer. NMR spectra were recorded at 25 °C. Chemical shifts are given in parts per million (ppm) referenced to residual protium or carbon of the solvents. Data for ^1H NMR spectra are reported as follows: chemical shift, multiplicity, coupling constant, and integration. Coupling constants (J values) are reported in Hertz (Hz) and multiplicities are expressed according to the usual conventions.

Low-resolution mass spectra (LRMS) were determined on an Agilent 6130 single quadrupole with an APCI/electrospray dual source or ThermoQuest Finnigan LCQ DUO electrospray. High resolution mass spectra were obtained courtesy of the EPSRC Mass Spectrometry Service at University of Wales, Swansea, U.K., using the ionisation methods specified. GC-MS was performed using an Agilent 7890A GC system, equipped with a 30 m DB5MS column connected to a 5975C inert XL CI MSD with Triple-Axis Detector.

Infrared spectra were determined on neat samples and were recorded in the range 4000–600 cm^{-1} on a Shimadzu IRAffinity-1 equipped with an ATR (Attenuated Total Reflectance) accessory. Measured relative intensities are abbreviated as follows: s = strong, med = medium, wk = weak, br = broad.

Melting points were determined on a Stuart SMP11 and are uncorrected.

Flash chromatography was carried out using head pressure by means of compressed air and Merck Kieselgel 60 H silica. The solvents used for chromatography were not purified. When required organic solvents were removed under reduced pressure. Evaporation was affected at about 20 mmHg using Büchi rotary evaporators and water bath, followed to evaporation to dryness under high vacuum (4 mbar).

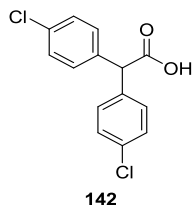
Analytical thin-layer chromatography (TLC) was carried out using 0.2 mm commercial silica gel plates (silica gel 60, F254, EMD chemical), and visualised under UV light (at 254 nm) or by staining with a solution of 2% aqueous potassium permanganate followed by gentle heating.

Single-crystal X-ray diffraction data were measured on Oxford Diffraction Xcalibur E and Gemini S instruments. The structures were refined to convergence on F^2 and against all independent reflections by full-matrix least-squares, using the SHELXL-97 program. Selected parameters are given in Appendix (Chapter 5).

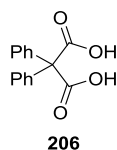
All glassware used in anhydrous reactions was either oven-dried (100 °C) or flame-dried under vacuum and cooled under a stream of nitrogen or argon prior to use.

4.2. Synthesis of Carboxylic Acids

Bis(*p*-chlorophenyl)acetic acid **142**¹¹⁴



1,1-Di(*p*-chlorophenyl)-2,2,2-trichloroethane **143** (10.0 g, 28.2 mmol, 1.0 equiv.) and diethylene glycol **313** (81 mL) were added to a three-neck round bottom flask fitted with a magnetic stirrer, a glass stopper, a thermometer, and a reflux condenser. To this was added a solution of potassium hydroxide (12.7 g, 226 mmol, 8.0 equiv.) in de-ionised water (7.0 mL). The mixture was stirred at reflux for 6 h. The mixture was allowed to cool and, with vigorous stirring, was poured into a beaker with cold water (200 mL). The insoluble material was filtered and washed with warm water (50 mL). The filtrate was then boiled gently for 5 minutes with activated charcoal (400 mg). The charcoal was removed by filtration through Celite, and the filtrate was boiled again with activated charcoal (400 mg) until the solution was no longer brown. The filtrate was acidified with 20% sulfuric acid. The flask was placed in an ice bath. The precipitate was collected by filtration under suction to give **142** as an off-white solid (3.72 g, 13.2 mmol, 47%). Further purification was achieved by dissolving **142** in the minimum amount of ethanol, which was heated to its boiling point. Water was then added drop-wise until the solution turned cloudy, at which point a drop of ethanol was added. The clear solution was left to recrystallise to give **142** as a white solid (3.20 g, 11.4 mmol, 40%); m.p. 162–165 °C (lit. 163–164 °C, recryst. from ethanol)¹¹⁴; IR (neat)/cm⁻¹: 2872–2525 (wk, br), 1703 (str), 1090 (str); ¹H NMR (400 MHz, *d*₆-acetone): δ (ppm) 7.44–7.35 (m, 8H), 5.18 (s, 1H); ¹³C NMR (101 MHz, *d*₆-acetone): δ (ppm) 173.0, 139.0, 133.5, 131.3, 129.5, 55.9; LRMS (ESI+) *m/z* 281.0 [M(³⁵Cl)+H]⁺, 283.0 [M(³⁷Cl)+H]⁺.

Diphenylmalonic acid 206¹¹⁵

A dry three-neck round bottom flask connected to a vacuum line with a stopcock was charged with diphenylacetic acid **108** (1.00 g, 4.71 mmol, 1.0 equiv.). Air was evacuated and the flask was filled with argon gas. This was repeated two more times. Anhydrous THF (47 mL) was added and the solution was cooled to 0 °C before *t*-BuLi (8.3 mL, 1.7 M in hexanes) was added dropwise over 15 min using a syringe pump. After the addition, the solution was stirred at -78 °C for 1 h. A 500 mL flask was then charged with solid CO₂. A CaCl₂ drying tube was placed on top of the flask and sealed with a Suba™ seal. A cannula was immediately inserted into both flasks and CO₂ was bubbled through the solution of THF until there was no more CO₂ left. The solution was then transferred to a separatory funnel, acidified with concentrated HCl, and the organics were extracted with diethyl ether (4 × 70 mL). The combined organic phase were then dried over MgSO₄, filtered, and concentrated under reduced pressure. The residue (2.88 g) was washed with dichloromethane to remove the remaining diphenylacetic acid **108**. The title compound **206** was obtained as a white solid (0.62 g, 2.42 mmol, 51%); m.p. 148–149 °C (decomp. onset at 144 °C; lit.¹¹⁵ 143 °C); IR (neat)/cm⁻¹: 3028 (med, br), 2876 (wk), 1694 (str), 1261 (str); ¹H NMR (400 MHz, *d*₆-acetone): δ (ppm) 7.49–7.44 (m, 4H), 7.37–7.30 (m, 6H); ¹³C NMR (100 MHz, *d*₆-acetone): δ (ppm) 171.7, 140.4, 130.6, 128.6, 128.2, 57.4; LRMS (ESI+) *m/z* 257.0 [M+H]⁺, 274.0 [M+NH₄]⁺, 279.0 [M+K]⁺; HRMS (APCI, *m/z*, assignment): calculated for 257.0808 [M+H]⁺, 274.1079 [M+NH₄]⁺, 279.0628 [M+K]⁺, found 257.0555, 274.1079, 279.0632.

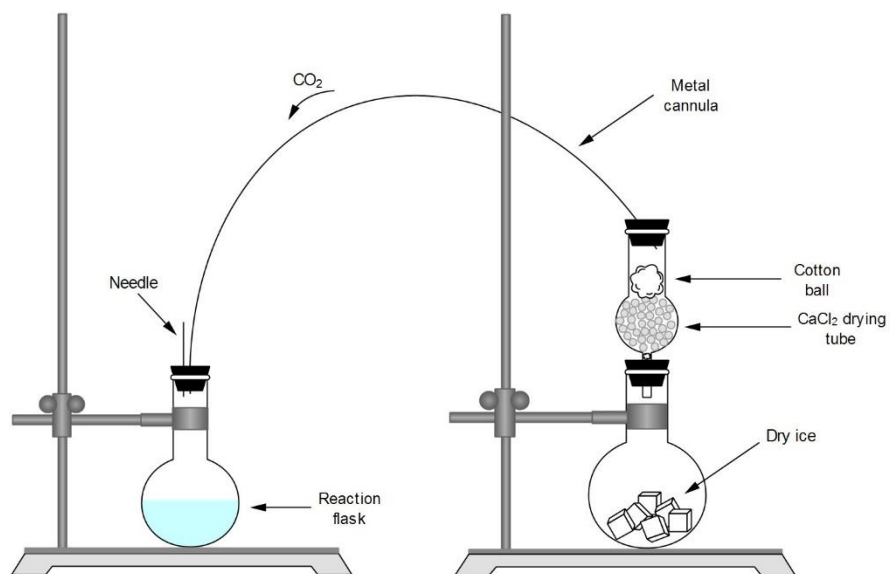
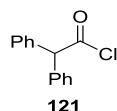


Figure 4.1. Experimental setup for the formation of diphenylmalonic acid **206**.

4.3. General Procedure 1: Acid Chloride Synthesis

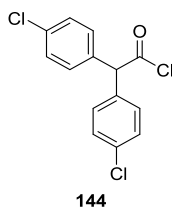
Carboxylic acid (1.0 equiv.) was placed in a round-bottom flask fitted with a reflux condenser (with a CaCl₂ drying tube on top). Oxalyl chloride (1.5 equiv.) was added and the resulting solution was stirred at reflux for 2 h. The excess oxalyl chloride was removed under reduced pressure to leave a residual oil which solidified upon standing. The crude product was dissolved in warm petroleum ether 30–40 °C and activated charcoal was added (0.2 g). The suspension was filtered and the product was allowed to crystallise.

Diphenylacetyl chloride **121**¹¹⁶



Prepared following General Procedure 1 using diphenylacetic acid **108** (10.0 g, 47.3 mmol). Following the described work-up procedure, the title compound **121** was isolated as colourless crystals (10.3 g, 44.6 mmol, 94%); m.p. 48–51 °C (lit. 52–53 °C, recryst. from anhydrous hexane)¹¹⁷; IR (neat)/cm⁻¹: 3029, 1773, 1495, 1452; ¹H NMR (400 MHz, CDCl₃): δ (ppm) 7.42–7.27 (m, 10H) 5.46 (s, 1H); ¹³C NMR (100 MHz, CDCl₃): δ (ppm) 173.7, 136.3, 129.2, 128.9, 128.3, 68.8.

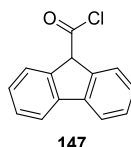
Bis(*p*-chlorophenyl)acetyl chloride **144**



Prepared following General Procedure 1 using di-(*p*-chlorophenyl)acetic acid **142** (1.00 g, 3.56 mmol). Conversion to **144** was monitored by ¹NMR spectroscopy and, if incomplete, the crude reaction mixture was subjected to the same reaction conditions and refluxed until acid **142** was fully consumed. After 4 h, following the described work-up

procedure, the title compound **144** was obtained as a dark green oil (1.00 g, 3.34 mmol, 94%); IR (neat)/cm⁻¹: 3051 (wk), 1788 (str), 1092 (str); ¹H NMR (400 MHz, CDCl₃): δ (ppm) 7.38–7.34 (m, 4H), 7.23–7.18 (m, 4H), 5.38 (s, 1H); ¹³C NMR (101 MHz, CDCl₃): δ (ppm) 159.2, 134.7, 134.4, 130.1, 129.5, 67.3.

9-Fluorenylcarboxylic acid chloride **147**¹¹⁸

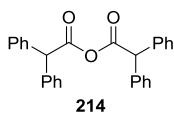


Prepared following General Procedure 1 using fluorene-9-carboxylic acid **146** (1.0 g, 4.8 mmol). Following the described work-up procedure, the title compound **147** was isolated as a dark yellow solid (0.7 g, 3.1 mmol, 64%). Colourless crystals (in the form of needles) were obtained upon recrystallisation of **147** from petroleum ether 30–40 and diethyl ether (minimum amount to dissolve **147**), and storing at –24 °C overnight; m.p. 71–73 °C (lit. 73–74 °C)¹¹⁸; IR (neat)/cm⁻¹: 3059 (wk), 1767 (str), 1449 (med), 1047 (str); ¹H NMR (400 MHz, CDCl₃): δ (ppm) 7.83–7.78 (m, 2H), 7.69–7.64 (m, 2H), 7.54–7.47 (m, 2H), 7.43–7.36 (m, 2H), 5.18 (s, 1H); ¹³C NMR (101 MHz, CDCl₃): δ (ppm) 173.1, 142.0, 138.9, 129.4, 128.1, 125.7, 120.7, 63.3.

4.4. Synthesis of diphenylketene **120¹¹⁹**

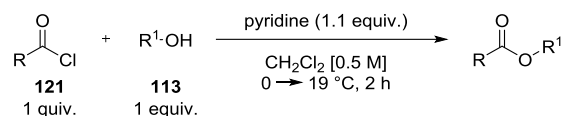
A 100 mL round-bottom flask was charged with diphenylacetyl chloride **121** (8.0 g, 35 mmol, 1.0 equiv.) and placed under an inert atmosphere. Dry ether (70 mL) was added and the mixture was stirred at 19 °C until all diphenylacetyl chloride **121** dissolved. The solution was cooled to 0 °C before dry triethylamine (4.8 mL, 35 mmol, 1.0 equiv.) was added over 20 minutes using a syringe pump. The flask was tightly sealed and stored at 0 °C overnight. Next, triethylamine hydrochloride was filtered off on a sintered funnel under a N₂ gas flow and washed with dry ether until white. Excess ether was removed under reduced pressure and the crude product was transferred from a 250 mL flask to a 25 mL flask under positive nitrogen pressure (N₂) using a cannula. The crude product was then distilled *via* a K \ddot{u} gelrohr distillation (92 °C, 6 × 10⁻² mbar; lit.¹¹⁹ 118 °C, 1 Torr) to afford product **120** as an orange oil (3.9 g, 20 mmol, 57%); IR (neat)/cm⁻¹: 3059 (wk), 2087 (med), 1595 (med), 1491 (med); ¹H NMR (400 MHz, CDCl₃): δ (ppm) 7.47–7.39 (m, 2H), 7.33–7.25 (m, 3H); ¹³C NMR (101 MHz, CDCl₃): δ (ppm) 201.2, 130.9, 129.4, 127.8, 126.3, 47.0.

4.5. Synthesis of diphenylacetic anhydride **214**¹²⁰

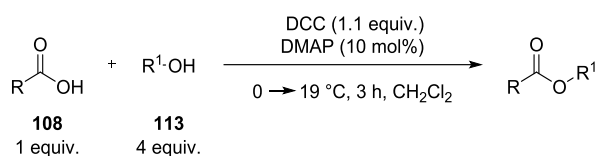


A round-bottom flask was charged with diphenylacetic acid **108** (10.0 g, 47.1 mmol, 1.0 equiv.). Acetic anhydride **314** (9.26 mL, 98.0 mmol, 2.1 equiv.) was added in one portion and the solution was refluxed for 3 h. Excess acetic anhydride **314** and other impurities were removed under reduced pressure using a Kügelrohr (0.15 mbar, 180 °C) to give the title compound **214** as a pale pink solid (13.8 g, 33.9 mmol, 72%); m.p. 97–98 °C (lit. 97–99)¹²⁰; IR (neat)/cm⁻¹: 1800 (med), 1734 (med), 1061 (str); ¹H NMR (400 MHz, CDCl₃): δ (ppm) 7.35–7.27 (m, 12H), 7.21–7.15 (m, 8H), 5.04 (s, 2H); ¹³C NMR (101 MHz, CDCl₃): δ (ppm) 167.7, 137.0, 128.9, 128.8, 127.8, 57.9. LRMS (ESI+, *m/z*): 424.1 [M+NH₄]⁺.

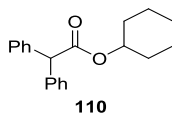
4.6. General Procedure 2: Ester Synthesis



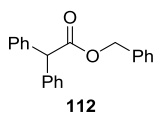
Diphenylacetyl chloride **121** (1.0 equiv.) was dissolved in anhydrous dichloromethane [0.5 M]. The solution was cooled and stirred at 0 °C while pyridine (1.1 equiv.) was added drop-wise. Then alcohol (1.0 equiv.) was added and the resulting solution was stirred for 2 h. The solution was allowed to warm up to room temperature by letting ice melt. The reaction mixture was filtered and the filtrate was washed with 1 M HCl (3 × 50 mL), brine (3 × 50 mL), dried over MgSO₄, and filtered. Excess solvent was removed under reduced pressure and the product was purified and isolated by silica gel flash chromatography using toluene as the eluent.

4.7. General Procedure 3: Ester Synthesis 2⁵³

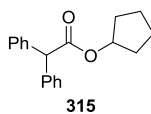
To a stirred solution of carboxylic acid (1.0 equiv.) in anhydrous dichloromethane [0.5 M] was added 4-dimethylaminopyridine (10 mol%) and alcohol (4.0 equiv.). The reaction mixture was cooled to 0 °C and *N,N'*-dicyclohexylcarbodiimide (1.1 equiv.) was added slowly in portions. The flask was stoppered and the reaction mixture was stirred at 19 °C for an additional 3 h. The reaction mixture was filtered and the filtrate was washed with 0.5 N HCl (2 × 50 mL), aqueous saturated NaHCO₃ (2 × 50 mL), dried over MgSO₄, and filtered. Excess solvent was removed under reduced pressure and the product was purified and isolated by silica gel flash chromatography using toluene as the eluent.

Cyclohexyl 2,2-diphenylacetate 110

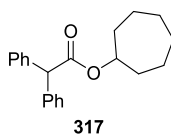
Prepared following General Procedure 2 using diphenylacetyl chloride **121** (5.0 g, 22 mmol) and cyclohexanol **2** (2.3 mL, 22 mmol) and isolated as a white solid (4.0 g, 14 mmol, 62%); m.p. 31–32 °C; IR (neat)/cm⁻¹: 3020 (wk), 2940 (wk), 1724 (str), 1146 (str); ¹H NMR (400 MHz, CDCl₃): δ (ppm) 7.36–7.23 (m, 10H), 5.01 (s, 1H), 4.90–4.82 (m, 1H), 1.88–1.79 (m, 2H), 1.71–1.61 (m, 2H), 1.56–1.18 (m, 6H); ¹³C NMR (101 MHz, CDCl₃): δ (ppm) 172.0, 139.1, 128.8, 128.6, 127.2, 73.5, 57.6, 31.5, 25.5, 23.7; HRMS (NSI+, *m/z*, assignment): calculated for 295.1698 [M+H]⁺, 312.1958 [M+NH₄]⁺, found 295.1697, 312.1961.

Benzyl 2,2-diphenylacetate 112¹²¹

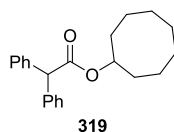
Prepared following General Procedure 3 using diphenylacetic acid **108** (2.13 g, 10.0 mmol) and benzyl alcohol **15** (4.13 mL, 39.9 mmol), and isolated as colourless oil (1.63 g, 5.39 mmol, 54%); IR (neat)/cm⁻¹: 3030 (wk), 1732 (s), 1140 (s); ¹H NMR (400 MHz, CDCl₃): δ (ppm) 7.33–7.24 (m, 15H), 5.20 (s, 2H), 5.09 (s, 1H); ¹³C NMR (101 MHz, CDCl₃): δ (ppm) 172.5, 138.7, 135.8, 128.8, 128.7, 128.6, 128.4, 128.3, 127.4, 67.0, 57.2; HRMS (NSI+, *m/z*, assignment): calculated for 303.1385 [M+H]⁺, 320.1645 [M+NH₄]⁺, found 303.1382, 320.1644.

Cyclopentyl 2,2-diphenylacetate 315

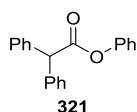
Prepared following General Procedure 3 using diphenylacetic acid **108** (2.13 g, 10.0 mmol) and cyclopentanol **316** (3.63 mL, 40.0 mmol), and isolated as a white solid (1.76 g, 6.28 mmol, 63%); m.p. 34 °C; IR (neat)/cm⁻¹: 2932 (med), 2116 (med), 1713 (str), 1148 (str); ¹H NMR (400 MHz, CDCl₃): δ (ppm) 7.34–7.23 (m, 10H), 5.28–5.22 (m, 1H), 4.98 (s, 1H), 1.90–1.79 (m, 2H), 1.73–1.51 (m, 6H); ¹³C NMR (101 MHz, CDCl₃): δ (ppm) 172.3, 139.0, 128.7, 128.6, 127.3, 78.1, 57.4, 32.7, 23.8; HRMS (NSI+, *m/z*, assignment): calculated for 281.1542 [M+H]⁺, 298.1802 [M+NH₄]⁺, found 281.1541, 298.1807.

Cycloheptyl 2,2-diphenylacetate 317

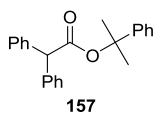
Prepared following General Procedure 3 using diphenylacetic acid **108** (2.13 g, 10.0 mmol) and cycloheptanol **318** (4.82 mL, 40.0 mmol), and isolated as a colourless oil (1.31 g, 4.25 mmol, 42%); IR (neat)/cm⁻¹: 3018 (wk), 2926 (med), 1728 (str), 1148 (str); ¹H NMR (400 MHz, CDCl₃): δ (ppm) 7.35–7.23 (m, 10H), 5.07–5.01 (m, 1H), 5.00 (s, 1H), 1.95–1.84 (m, 2H), 1.72–1.36 (m, 10H); ¹³C NMR (101 MHz, CDCl₃): δ (ppm) 171.9, 139.1, 128.8, 128.6, 127.2, 76.1, 57.6, 33.7, 28.3, 23.0; HRMS (NSI+, *m/z*, assignment): calculated for 309.1855 [M+H]⁺, 326.2115 [M+NH₄]⁺, found 309.1855, 326.2120.

Cyclooctyl 2,2-diphenylacetate 319

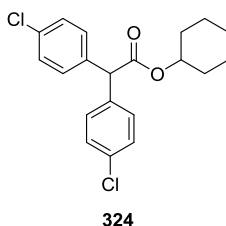
Prepared following General Procedure 3 using diphenylacetic acid **108** (2.13 g, 10.0 mmol) and cyclooctanol **320** (5.30 mL, 40.1 mmol), and isolated as a colourless oil (2.09 g, 6.48 mmol, 65%); IR (neat)/cm⁻¹: 2920 (med), 1726 (str), 1150 (str); ¹H NMR (400 MHz, CDCl₃): δ (ppm) 7.34–7.22 (m, 10H), 5.06–4.99 (tt, *J* = 8.3, 4.0 Hz, 1H), 4.98 (s, 1H), 1.83–1.56 (m, 7H), 1.55–1.41 (m, 7H); ¹³C NMR (100 MHz, CDCl₃): δ (ppm) 171.9, 139.1, 128.8, 128.6, 127.2, 76.1, 57.6, 31.5, 27.2, 25.5, 23.0; HRMS (NSI+, *m/z*, assignment): calculated for 340.2271 [M+NH₄]⁺, found 340.2273.

Phenyl 2,2-diphenylacetate 321¹²¹

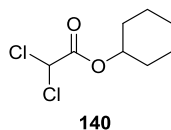
Prepared following General Procedure 3 using diphenylacetic acid **108** (2.13 g, 10.0 mmol) and phenol **322** (3.76 g, 39.9 mmol), and isolated as a white solid (1.51 g, 5.24 mmol, 52%); m.p. 58 °C; IR (neat)/cm⁻¹: 3061 (wk), 1742 (str), 1142 (str); ¹H NMR (400 MHz, CDCl₃): δ (ppm) 7.51–7.45 (m, 4H), 7.44–7.32 (m, 8H), 7.28–7.23 (m, 1H), 7.14–7.09 (m, 2H), 5.32 (s, 1H); ¹³C NMR (101 MHz, CDCl₃): δ (ppm) 171.1, 150.9, 138.3, 129.5, 128.9, 128.8, 127.6, 126.0, 121.5, 57.2; HRMS (NSI+, *m/z*, assignment): calculated for 289.1223 [M+H]⁺, 306.1489 [M+NH₄]⁺, 311.1043 [M+Na]⁺, found 289.1227, 306.1492, 311.1044.

α,α -Dimethylbenzyl 2,2-diphenylacetate 157

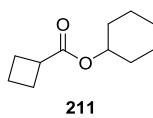
Prepared following General Procedure 3 using diphenylacetic acid **108** (2.13 g, 10.0 mmol) and 2-phenyl-2-propanol **323** (5.6 mL, 40.0 mmol), and isolated as a white solid (2.16 g, 6.55 mmol, 66%); m.p. 52 °C; IR (neat)/cm⁻¹: 3061 (wk), 2978 (wk), 1726 (str), 1123 (str); ¹H NMR (400 MHz, CDCl₃): δ (ppm) 7.37–7.21 (m, 15H), 5.07 (s, 1H), 1.82 (s, 6H); ¹³C NMR (101 MHz, CDCl₃): δ (ppm) 170.8, 145.6, 138.9, 128.8, 128.6, 128.2, 127.2, 127.1, 124.4, 82.6, 58.0, 28.5; HRMS (NSI+, *m/z*, assignment): calculated for 348.1958 [M+NH₄]⁺, 369.1251 [M+K]⁺, found 348.1960, 369.1251.

Cyclohexyl 2,2-bis(4-chlorophenyl)acetate 324

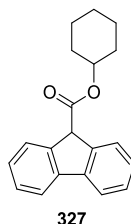
Prepared following General Procedure 3 using di-(*p*-chlorophenyl)acetic acid **142** (100 mg, 0.36 mmol), cyclohexanol **2** (0.15 mL, 1.42 mmol), DCC (82.0 mg, 0.40 mmol), and DMAP (5.00 mg). After 6 h, following the described work-up procedure, the title compound **324** was isolated as a yellow solid (99.0 mg, 0.27 mmol, 76%); m.p. 60 °C; IR (neat)/cm⁻¹: 2932 (med), 1730 (str), 1489 (str), 1092 (str); ¹H NMR (400 MHz, CDCl₃): δ (ppm) 7.31–7.27 (m, 4H), 7.24–7.20 (m, 4H), 4.91 (s, 1H), 4.88–4.80 (m, 1H), 1.85–1.78 (m, 2H), 1.69–1.61 (m, 2H), 1.52–1.18 (m, 6H); ¹³C NMR (101 MHz, CDCl₃): δ (ppm) 171.3, 137.2, 133.5, 130.0, 128.9, 74.0, 56.2, 31.5, 25.4, 23.7; LRMS (ESI+) *m/z* 380.0 [M+NH₄]⁺; HRMS (NSI+, *m/z*, assignment): calculated for 363.0913 [M+H]⁺, 380.1184 [M+NH₄]⁺, found 363.0907, 380.1173.

Cyclohexyl dichloroacetate 140

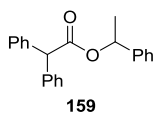
Prepared following General Procedure 3 using dichloroacetic acid **325** (0.83 mL, 10.0 mmol) and cyclohexanol **2** (4.20 mL, 39.8 mmol), and isolated as an off-white oil (1.67 g, 7.91 mmol, 79%); IR (neat)/cm⁻¹: 2926 (med), 1728 (str), 1148 (str); ¹H NMR (400 MHz, CDCl₃): δ (ppm) 5.91 (s, 1H), 4.92–4.84 (m, 1H), 1.92–1.83 (m, 2H), 1.79–1.70 (m, 2H), 1.59–1.48 (m, 3H), 1.45–1.24 (m, 3H); ¹³C NMR (101 MHz, CDCl₃): δ (ppm) 164.1, 76.5, 64.8, 31.0, 25.2, 23.4.

Cyclohexyl cyclobutanecarboxylate 211

Prepared following General Procedure 3 using cyclobutanecarboxylic acid **326** (1.01 g, 10.0 mmol) and cyclohexanol **2** (4.20 mL, 39.8 mmol). After 6 h, following the described work-up procedure, the title compound **211** was isolated as a yellow oil (343 mg, 1.88 mmol, 19%); IR (neat)/cm⁻¹: 2936 (med), 1724 (str), 1175 (str); ¹H NMR (400 MHz, CDCl₃): δ (ppm) 4.81–4.69 (m, 1H), 3.10 (dp, *J* = 8.6, 1.0 Hz, 1H), 2.33–2.12 (m, 4H), 2.04–1.78 (m, 4H), 1.78–1.66 (m, 2H), 1.60–1.48 (m, 1H), 1.47–1.17 (m, 5H); ¹³C NMR (101 MHz, CDCl₃): δ (ppm) 175.2, 72.3, 38.6, 31.7, 25.6, 25.4, 23.9, 18.5; LRMS (CI) *m/z* 183.1 [M+H]⁺; HRMS (NSI+, *m/z*, assignment): calculated for 183.1380 [M+H]⁺, found 183.1375.

Cyclohexyl 9-fluorene-9-carboxylate 327

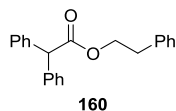
Prepared following General Procedure 3 using fluorene-9-carboxylic acid **146** (2.10 g, 10.0 mmol) and cyclohexanol **2** (4.20 mL, 39.8 mmol). After 6 h, following the described work-up procedure, the title compound **327** was isolated as a pale yellow oil (1.18 g, 4.05 mmol, 40%); IR (neat)/ cm^{-1} : 3065 (wk), 2934 (med), 1722 (str), 1192 (str); ^1H NMR (400 MHz, CDCl_3): δ (ppm) 7.76 (d, $J = 7.5$ Hz, 2H), 7.68 (d, $J = 7.6$ Hz, 2H), 7.42 (t, $J = 7.4$ Hz, 2H), 7.34 (td, $J = 7.5, 1.1$ Hz, 2H), 4.91–4.81 (m, 2H), 1.91–1.80 (m, 2H), 1.76–1.64 (m, 2H), 1.58–1.43 (m, 3H), 1.43–1.22 (m, 3H); ^{13}C NMR (101 MHz, CDCl_3): δ (ppm) 170.4, 141.6, 141.1, 128.1, 127.4, 125.8, 120.1, 73.8, 53.8, 31.6, 25.5, 23.7; LRMS (ESI+) m/z 293.1 $[\text{M}+\text{H}]^+$, 310.1 $[\text{M}+\text{NH}_4]^+$; HRMS (NSI+, m/z , assignment): calculated for 293.1536, 310.1802, found 293.1539, 310.1804.

1-Phenylethyl 2,2-diphenylacetate 159¹²²

Prepared following General Procedure 3 using diphenylacetic acid **108** (2.13 g, 10.0 mmol) and 1-phenylethanol **328** (4.80 mL, 40.0 mmol). After 6 h, following the described work-up procedure, the title compound **159** was isolated as a pale yellow oil (1.63 g, 5.15 mmol, 52%); IR (neat)/ cm^{-1} : 3030 (wk), 2980 (wk), 1732 (med), 1148 (str); ^1H NMR (400 MHz, CDCl_3): δ (ppm) 7.37–7.22 (m, 15H), 5.98 (q, $J = 6.6$ Hz, 1H), 5.09 (s, 1H), 1.55 (d, $J = 6.6$ Hz, 3H); ^{13}C NMR (101 MHz, CDCl_3): δ (ppm) 171.8, 141.5, 138.9, 138.7, 128.8, 128.5, 127.9, 127.3, 126.2, 73.3, 57.4, 22.2; LRMS (ESI+) m/z 334.2

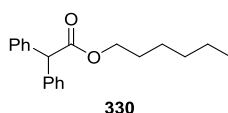
[M+NH₄]⁺; HRMS (NSI+, *m/z*, assignment): calculated for 317.1536 [M+H]⁺, 334.1802 [M+NH₄]⁺, found 317.1537, 334.1802.

Phenylethyl 2,2-diphenylacetate **160**¹²¹



Prepared following General Procedure 3 using diphenylacetic acid **108** (2.13 g, 10.0 mmol) and 2-phenylethanol **329** (4.80 mL, 40.0 mmol). After 17 h, following the described work-up procedure, the title compound **160** was isolated as a white solid (994 mg, 3.14 mmol, 31%); m.p. 77–78 °C; IR (neat)/cm⁻¹: 3030 (wk), 2953 (wk), 1730 (med), 1142 (str); ¹H NMR (400 MHz, CDCl₃): δ (ppm) 7.36–7.20 (m, 13 H), 7.15–7.10 (m, 2H), 5.02 (s, 1H), 4.40 (t, *J* = 6.9 Hz, 2H), 2.94 (t, *J* = 6.9 Hz, 2H); ¹³C NMR (101 MHz, CDCl₃): δ (ppm) 172.5, 138.7, 137.8, 129.1, 128.8, 128.7, 128.6, 127.4, 126.7, 65.8, 57.4, 35.1; LRMS (ESI+) *m/z* 317.1 [M+H]⁺, 334.1 [M+NH₄]⁺; HRMS (NSI+, *m/z*, assignment): calculated for 317.1536 [M+H]⁺, 334.1802 [M+NH₄]⁺, found 317.1538, 334.1800.

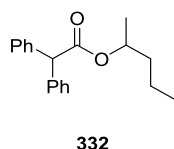
1-Hexyl 2,2-diphenylacetate **330**



Prepared following General Procedure 3 using diphenylacetic acid **108** (2.13 g, 10.0 mmol) and 1-hexanol **331** (5.0 mL, 39.8 mmol). After 24 h, following the described work-up procedure, the title compound **330** was isolated as a colourless oil (1.99 g, 6.71 mmol, 67%); IR (neat)/cm⁻¹: 3028 (wk), 2928 (wk), 1734 (str), 1148 (str); ¹H NMR (400 MHz, CDCl₃): δ (ppm) 8.00–7.90 (m, 10H), 5.69 (s, 1H), 4.81 (t, *J* = 6.7 Hz, 2H), 2.32–2.23 (m, 2H), 1.99–1.87 (m, 6H), 1.52 (t, *J* = 6.8 Hz, 3H); ¹³C NMR (101 MHz, CDCl₃): δ (ppm) 172.7, 138.9, 128.8, 128.7, 127.3, 65.5, 57.4, 31.5, 28.6, 25.6, 22.6, 14.1; LRMS

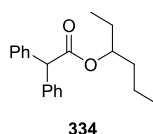
(ESI+) m/z 297.1 $[M+H]^+$, 314.2 $[M+NH_4]^+$; HRMS (NSI+, m/z , assignment): calculated for 297.1849 $[M+H]^+$, 314.2115 $[M+NH_4]^+$, found 297.1849, 314.2112.

2-Hexyl 2,2-diphenylacetate **332**



Prepared following General Procedure 3 using diphenylacetic acid **108** (2.13 g, 10.0 mmol) and 2-hexanol **333** (5.0 mL, 40.0 mmol). After 17 h, following the described work-up procedure, the title compound **332** was isolated as a colourless oil (455 mg, 1.54 mmol, 15%); IR (neat)/ cm^{-1} : 3028 (wk), 2932 (wk), 1730 (str), 1153 (str); ^1H NMR (400 MHz, CDCl_3): δ (ppm) 7.35–7.23 (m, 10H), 5.02–4.93 (m, 2H), 1.63–1.41 (m, 2H), 1.30–1.12 (m, 7H), 0.83 (t, $J = 7.0$ Hz, 3H); ^{13}C NMR (101 MHz, CDCl_3): δ (ppm) 172.2, 139.1, 128.8, 128.6, 127.3, 72.1, 57.6, 35.6, 27.5, 22.6, 20.0, 14.1; LRMS (ESI+) m/z 297.2 $[M+H]^+$, 314.2 $[M+NH_4]^+$; HRMS (NSI+, m/z , assignment): calculated for 297.1849 $[M+H]^+$, 314.2115 $[M+NH_4]^+$, found 297.1848, 314.2111.

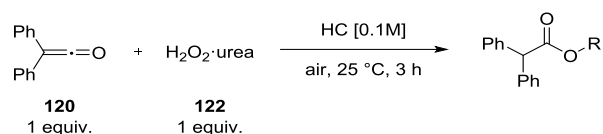
3-Hexyl 2,2-diphenylacetate **334**



Prepared following General Procedure 3 using diphenylacetic acid **108** (2.13 g, 10.0 mmol) and 3-hexanol **335** (5.0 mL, 40.1 mmol). After 17 h, following the described work-up procedure, the title compound **334** was isolated as a colourless oil (1.1 g, 3.71 mmol, 37%); IR (neat)/ cm^{-1} : 3028 (wk), 2961 (wk), 1730 (str), 1153 (str); ^1H NMR (400 MHz, CDCl_3): δ (ppm) 7.36–7.22 (m, 10H), 5.01 (s, 1H), 4.94–4.86 (m, 1H), 1.60–1.41 (m, 4H), 1.30–1.14 (m, 2H), 0.84 (t, $J = 7.4$ Hz, 3H), 0.79 (t, $J = 7.4$ Hz, 3H); ^{13}C NMR (101 MHz, CDCl_3): δ (ppm) 172.5, 139.1, 128.8, 128.6, 127.3, 76.4, 57.7, 35.8, 27.0,

18.6, 14.0, 9.6; LRMS (ESI+) m/z 297.0 $[M+H]^+$, 314.1 $[M+NH_4]^+$; HRMS (NSI+, m/z , assignment): calculated for 297.1849 $[M+H]^+$, 314.2115 $[M+NH_4]^+$, found 297.1850, 314.2113.

4.8. General Procedure 4: sp³ C–H Bond Oxidation



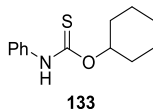
A round-bottom flask was charged with H₂O₂·urea **122** (1 equiv.) and a hydrocarbon solvent (15 mL) was added. Diphenylketene **120** (1 equiv.) was weighed out under an inert atmosphere into a vial, to which an anhydrous hydrocarbon solvent (3 mL) was added. The mixture was stirred at 25 °C while the solution of diphenylketene **120** was added over 3 h using a syringe pump. After the addition, the reaction was quenched by adding ice and aqueous saturated Na₂S₂O₅ (20 mL). The contents of the flask were poured into a separatory funnel and 1,4-dinitrobenzene (0.25 equiv.) dissolved in ethyl acetate (5 mL) was added. The flask, the magnetic stirrer and the vial (which contained 1,4-dinitrobenzene) were carefully washed with ethyl acetate (5 mL) and the washings were also added, followed by more ethyl acetate (20 mL) and aqueous saturated Na₂S₂O₅ (30 mL). The organic layer (15 mL cyclohexane and 25 mL ethyl acetate) was washed with aqueous saturated Na₂S₂O₅ (3 × 50 mL), brine (3 × 50 mL), dried over MgSO₄, and filtered. Excess solvent and volatiles were removed under reduced pressure. The resulting residue was dissolved in deuterated chloroform and was analysed by NMR spectroscopy.

4.9. General Procedure 5: Internal Standard Checks

Various amounts of cyclohexyl 2,2-diphenylacetate **110** were weighed out, i.e. as a certain percentage of the theoretical yield obtained from a reaction with 300 mg (1.54 mmol) of **120**. For example, for 8% conversion 36 mg of **110** was weighed out. All samples were then dissolved in ethyl acetate (5 mL). The internal standard (1,4-dinitrobenzene) was weighed out (0.25 equiv.) and also dissolved in ethyl acetate (5 mL). Both solutions were subsequently combined, dissolved in ethyl acetate (50 mL), washed with aqueous saturated Na₂S₂O₅ (3 × 50 mL), brine (3 × 50 mL), dried over MgSO₄, and filtered. Excess solvent was removed under reduced pressure and the resulting residue was dissolved in deuterated chloroform to allow examination by ¹H NMR spectroscopy.

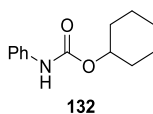
4.10. Synthesis of Carbamates and Thiocarbamates

O-Cyclohexyl *N*-phenylthiocarbamate **133**



A solution of cyclohexanol **2** (2.30 mL, 21.8 mmol, 2.9 equiv.) and phenyl isothiocyanate **131** (0.90 mL, 7.52 mmol, 1.0 equiv.) was stirred at reflux for 24 h. The solution was concentrated under reduced pressure and the crude was purified by silica gel flash chromatography (pet ether 40–60 °C/EtOAc = 1:1 *v/v* elution) to give the title compound **133** as colourless bricks (240 mg, 1.02 mmol, 14%), which formed upon removal of the solvent mixture under reduced pressure; m.p. 75–77 °C; IR (neat)/cm⁻¹: 3233 (wk), 2938 (wk), 2857 (wk), 1595 (med), 1547 (str); ¹H NMR (400 MHz, CDCl₃): δ (ppm) 8.55 (s, 1H), 7.33 (t, *J* = 7.7 Hz, 4H), 7.19–7.13 (m, 1H), 5.51–5.40 (m, 1H), 2.09–1.97 (m, 2H), 1.78–1.67 (m, 2H), 1.66–1.51 (m, 3H), 1.50–1.38 (m, 2H), 1.37–1.26 (m, 1H); ¹³C NMR (101 MHz, CDCl₃): δ (ppm) 188.0, 137.4, 129.1, 125.4, 121.7, 81.9, 31.4, 25.4, 23.7; HRMS (NSI+, *m/z*, assignment): calculated for 236.1104 [M+H]⁺, 274.0662 [M+K]⁺, found 236.1104, 274.0665.

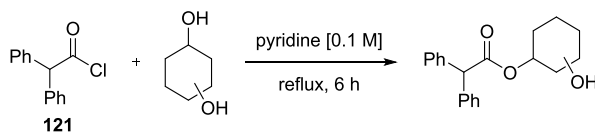
O-Cyclohexyl *N*-phenylcarbamate **132**



A solution of cyclohexanol **2** (0.29 mL, 2.74 mmol, 3.0 equiv.) and phenyl isocyanate **130** (0.10 mL, 0.92 mmol, 1.0 equiv.) in dichloromethane (1.85 mL) was stirred at reflux for 5 h 45 min. The solution was concentrated under reduced pressure and the crude was chromatographed by silica gel flash chromatography (pet ether 40–60 °C/EtOAc = 7:3 *v/v* elution) to give the title compound **132** as colourless bricks (138 mg, 0.63 mmol, 68%), which formed upon standing in solvent at room temperature over 16 h; m.p.

77-79 °C; IR (neat)/cm⁻¹: 3356 (med), 3059 (wk), 2928 (med), 2859 (med), 1703 (str), 1519 (str); ¹H NMR (400 MHz, CDCl₃): δ (ppm) 7.38 (d, *J* = 7.9 Hz, 2H), 7.33–7.27 (m, 2H), 7.08–7.02 (m, 1H), 6.60 (brs, 1H), 4.80–4.72 (m, 1H), 1.99–1.90 (m, 2H), 1.79–1.70 (m, 2H), 1.60–1.21 (m, 6H); ¹³C NMR (101 MHz, CDCl₃): δ (ppm) 153.3, 138.3, 129.1, 123.3, 118.7, 73.8, 32.1, 25.5, 23.9; HRMS (NSI+, *m/z*, assignment): calculated for 220.1332 [M+H]⁺, 242.1151 [M+Na]⁺, found 220.1332, 242.1151.

4.11. General Procedure 6: Diester Synthesis



Cyclohexanediol (1 equiv.) was added to a solution of diphenylacetyl chloride **121** (4 equiv.) in pyridine [0.1 M]. The solution was heated to reflux and stirred for 6 h. Pyridine was removed under reduced pressure and the reaction mixture was purified by silica gel column chromatography using toluene as the eluent. Single crystals for X-ray analysis were obtained by vapour diffusion of petroleum ether 30–40 °C into a saturated toluene solution of the product as shown in **Figure 4.2**.

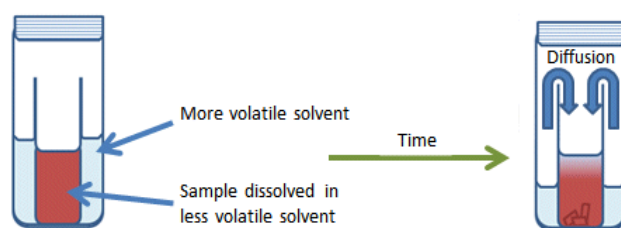
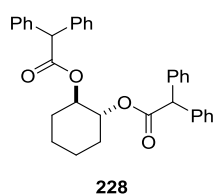


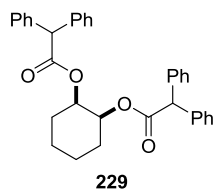
Figure 4.2. Recrystallisation by vapour diffusion.

(1*R*, 2*R*)-2-(diphenylacetyloxy)cyclohexyl diphenylacetate **228**

Prepared following General Procedure 6 using *trans*-1,2-cyclohexanediol **336** (117 mg, 1.00 mmol) and isolated as a white solid (486 mg, 0.96 mmol, 96%); m.p. 98–99 °C; IR (neat)/cm⁻¹: 3030 (wk), 2936 (wk), 1723 (med), 1185 (med), 1141 (med); ¹H NMR (400 MHz, CDCl₃): δ (ppm) 7.37–7.27 (m, 20H), 4.99–4.95 (m, 2H), 4.95 (s, 2H), 2.13–2.02 (m, 2H), 1.72–1.61 (m, 2H), 1.44–1.28 (m, 4H); ¹³C NMR (101 MHz, CDCl₃): δ (ppm) 171.7, 138.7, 128.6, 128.5, 127.2, 74.0, 57.0, 29.6, 23.1; HRMS (NSI+, *m/z*, assignment):

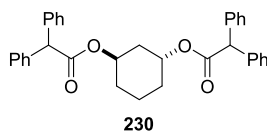
calculated for 522.2639 $[M+NH_4]^+$, 527.2193 $[M+Na]^+$, found 522.2631, 527.2182.

(1R, 2S)-2-(diphenylacetyloxy)cyclohexyl diphenylacetate 229



Prepared following General Procedure 6 using *cis*-1,2-cyclohexanediol **337** (117 mg, 1.00 mmol) and isolated as a white solid (315 mg, 0.62 mmol, 62%); m.p. 102–104 °C; IR (neat)/ cm^{-1} : 3029 (wk), 2949 (wk), 1724 (med), 1152 (med), 1187 (med); 1H NMR (400 MHz, $CDCl_3$): δ (ppm) 7.34–7.23 (m, 20H), 5.13 (dd, $J = 5.9, 2.6$ Hz, 2H), 4.93 (s, 2H), 1.80–1.70 (m, 2H), 1.64–1.56 (m, 2H), 1.50–1.39 (m, 2H), 1.39–1.29 (m, 2H); ^{13}C NMR (101 MHz, $CDCl_3$): δ (ppm) 171.7, 138.8, 128.8, 128.6, 127.3, 72.0, 57.4, 27.6, 21.6; HRMS (NSI+, m/z , assignment): calculated for 505.2379 $[M+H]^+$, 522.2639 $[M+NH_4]^+$, 527.2193 $[M+Na]^+$, 543.1938 $[M+K]^+$, found, 505.2368, 522.2630, 527.2178, 543.1920.

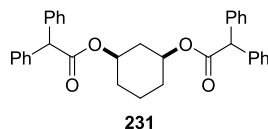
(1R, 3R)-3-(diphenylacetyloxy)cyclohexyl diphenylacetate 230



Prepared following General Procedure 6 using *rac*-1,3-cyclohexandiol **338** (465 mg, 4.0 mmol) and isolated as an off-white oil (510 mg, 1.0 mmol, 25%); IR (neat)/ cm^{-1} : 3027 (wk), 2946 (wk), 1733 (str), 1185 (med), 1142 (str); 1H NMR (400 MHz, $CDCl_3$): δ (ppm) 7.37–7.26 (m, 20H), 4.98 (s, 2H), 4.87 (td, $J = 10.1, 4.6$ Hz, 2H), 2.32–2.23 (m, 1H), 2.02–1.91 (m, 2H), 1.84–1.75 (m, 1H), 1.49 (q, $J = 11.2$ Hz, 1H), 1.41–1.19 (m, 3H); ^{13}C NMR (101 MHz, $CDCl_3$): δ (ppm) 171.7, 138.8, 138.8, 128.7, 127.3, 71.3, 57.3, 36.8, 30.6, 20.0; HRMS (NSI+, m/z , assignment): calculated for 522.2639 $[M+NH_4]^+$,

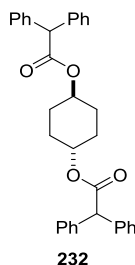
527.2193 [M+Na]⁺, found 522.2631, 527.2182.

(1R, 3S)-3-(diphenylacetyloxy)cyclohexyl diphenylacetate 231



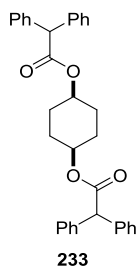
Prepared following General Procedure 6 using *rac*-1,3-cyclohexandiol **338** (465 mg, 4.00 mmol) and isolated as a white solid (389 mg, 0.77 mmol, 19%); m.p. 74.5–76.5 °C; IR (neat)/cm⁻¹: 3029 (wk), 2943 (wk), 1723 (str), 1150 (str), 1121 (str); ¹H NMR (400 MHz, CDCl₃): δ (ppm) 7.36–7.22 (m, 20H), 5.13–5.06 (m, 2H), 5.00 (s, 2H), 1.84 (t, *J* = 5.6 Hz, 2H), 1.71–1.63 (m, 2H), 1.57–1.43 (m, 4H); ¹³C NMR (101 MHz, CDCl₃): δ (ppm) 171.8, 138.9, 128.8, 128.7, 127.3, 70.8, 57.4, 35.4, 30.1, 19.1; HRMS (NSI+, *m/z*, assignment): calculated for 522.2639 [M+NH₄]⁺, 527.2193 [M+Na]⁺, 543.1938 [M+K]⁺, found 522.2632, 527.2184, 543.1923.

***E*-4-(diphenylacetyloxy)cyclohexyl diphenylacetate 232**



Prepared following General Procedure 6 using *rac*-1,4-cyclohexandiol **339** (465 mg, 4.00 mmol) and isolated as a white solid (480 mg, 0.95 mmol, 24%); m.p. 157–159 °C; IR (neat)/cm⁻¹: 3025 (wk), 2938 (wk), 1729 (med), 1149 (str), 1029 (med); ¹H NMR (400 MHz, CDCl₃): δ (ppm) 7.40–7.27 (m, 20H), 5.06 (s, 2 H), 4.98–4.91 (m, 2H), 1.91–1.79 (m, 4H), 1.64–1.52 (m, 4H); ¹³C NMR (101 MHz, CDCl₃): δ (ppm) 171.9, 138.8, 128.6, 127.3, 71.3, 57.4, 27.0; HRMS (NSI+, *m/z*, assignment): calculated for 522.2639 [M+NH₄]⁺, 527.2193 [M+Na]⁺, 543.1932 [M+K]⁺, found 522.2632, 527.2182, 543.1921.

Z-4-(diphenylacetyloxy)cyclohexyl diphenylacetate 233



Prepared following General Procedure 6 *rac*-1,4-cyclohexandiol **339** (465 mg, 4.00 mmol) and isolated as a white solid (292 mg, 058 mmol, 14%); m.p. 112–114 °C; IR (neat)/cm⁻¹: 3028 (wk), 2952 (wk), 1723 (str), 1192 (str), 1166 (str); ¹H NMR (400 MHz, CDCl₃): δ (ppm) 7.36–7.23 (m, 20H), 5.00 (s, 2H), 4.95–4.86 (m, 2H), 1.72–1.61 (m, 8H); ¹³C NMR (101 MHz, CDCl₃): δ (ppm) 171.9, 138.9, 128.7, 128.7, 127.3, 70.9, 57.5, 27.2; HRMS (NSI+, *m/z*, assignment): calculated for 505.2379 [M+H]⁺, 522.2639 [M+NH₄]⁺, 527.2193 [M+K]⁺, 543.1932 [M+Na]⁺, found 505.2369, 522.2632, 527.2179, 543.1921.

4.12. General Procedure 7: Keto-enol Studies

A pre-dried NMR tube was filled with a deuterated solvent (d_{12} -cyclohexane or d_8 -toluene) and placed in an ice bath. Diphenylketene **120** (1 equiv.) was added and the tube was sealed. The nucleophile (1 equiv.) was added prior to NMR analysis, which was carried out at 0 °C.

4.13. General Procedure 8: Isotopic Labelling Studies Using $^{18}\text{O}_2$ Gas

All reactions were conducted in a custom-made four-neck flask of our design, which was made from readily available components: a 25 mL round-bottom flask, a high vacuum stopcock, and Young taps.

The flask was placed in a glove bag with inlet holes for tubing and power cables. Tubing from the $^{18}\text{O}_2$ gas cylinder was attached to neck 1, vacuum tubing was attached to neck 2, and neck 3 was sealed with a SubaTM seal and parafilm (**Figure 4.3**).

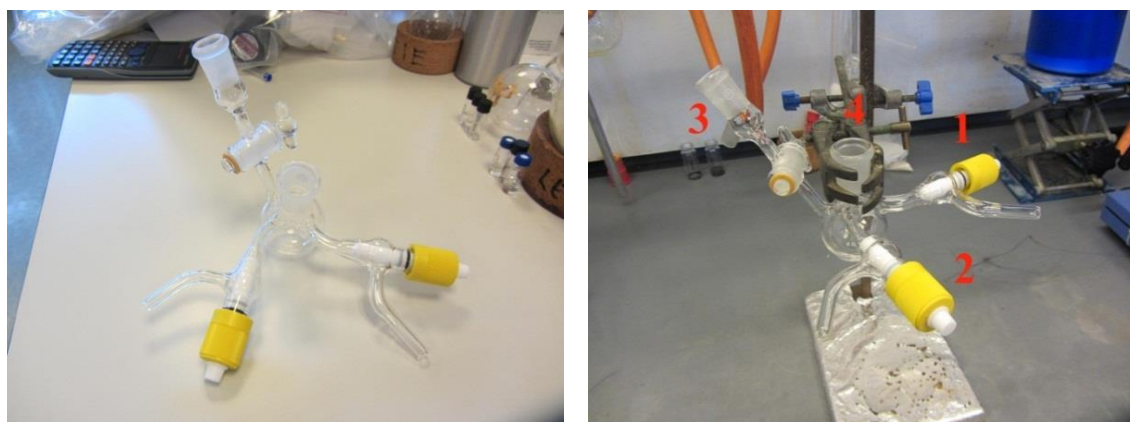


Figure 4.3. Photographs of the custom-made flask.

A syringe pump, a temperature probe, an IKA hotplate, an oil bath, and a 20 mL syringe with aqueous saturated $\text{Na}_2\text{S}_2\text{O}_5$ were placed in the glove bag.

The flask was charged with urea hydrogen peroxide **122** through neck 4, tightly sealed with a SubaTM seal and parafilm. Air was removed and the flask was backfilled with argon gas three times.

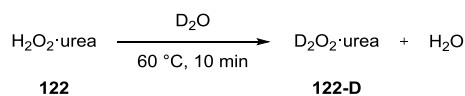
Anhydrous cyclohexane **3** was degassed by sparging with argon gas in a sealed flask for 1 h 30 min prior to use. Degassed cyclohexane **3** [0.1 M] was then added to the custom-made flask equipped with a nitrogen balloon. Diphenylketene **120** (79 mg, 0.4 mmol) was weighed out into a pre-dried sealed vial (7.0 mL) filled with argon gas and equipped with a nitrogen gas balloon. Anhydrous degassed cyclohexane **3** [0.5 M] was injected to the vial and the solution of diphenylketene **120** was taken up in a syringe. The custom-made flask and the syringe with a solution of diphenylketene **120** were placed in the glove bag. The glove bag was closed and air was removed (using a vacuum pump) until no further volume change could occur without piercing the bag. The glove bag was then backfilled with argon gas. This last step was repeated three times.

Finally, the flask was filled with $^{18}\text{O}_2$ gas and the solution of diphenylketene **120** was added over 3 h through neck 3 using syringe pump while the mixture was stirred at 25 °C. The complete set-up is shown in **Figure 4.4**.



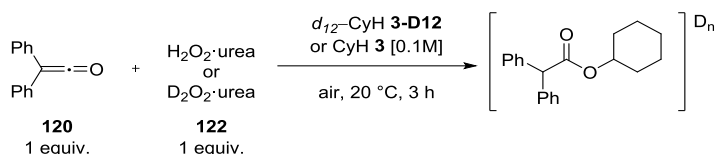
Figure 4.4. Photographs of the complete set-up.

After the addition, the reaction was quenched with saturated $\text{Na}_2\text{S}_2\text{O}_2$ and worked up as described in General Procedure 2.

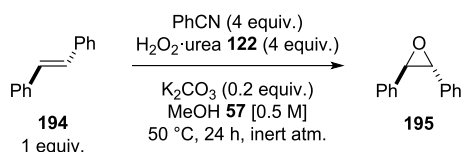
4.14. Synthesis of D₂O₂•urea **122-D**

A 10 mL round-bottom flask was charged with urea hydrogen peroxide **122** (300 mg, 3.2 mmol) and D₂O (5.8 mL, 311.2 mmol). The aqueous solution was heated to 60 °C and stirred for 10 min. Careful removal of D₂O and H₂O under reduced pressure gave D₂O₂•urea **122-D** (299 mg, 99%).

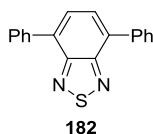
4.15. General Procedure 9: Deuterium Studies



Diphenylketene **120** (78 mg, 0.4 mmol) was weighed out into a pre-dried sealed vial (7.0 mL) filled with argon gas and equipped with a nitrogen gas balloon. Deuterated or non-deuterated cyclohexane **3** [0.5 M] was added to the vial and the solution of diphenylketene **120** was taken up in a syringe. A round-bottom flask was charged with either H₂O₂•urea **122** or D₂O₂•urea **122-D** (58 mg, 0.6 mmol) and deuterated **3-D12** or non-deuterated cyclohexane **3** (4.8 mL). The mixture was stirred at 25 °C while the solution of diphenylketene **120** was added over 3 h using a syringe pump. After the addition, the reaction was quenched by adding ice and aqueous saturated Na₂S₂O₅ (20 mL). The flask's contents were poured into a separatory funnel, and ethyl acetate (25 mL) and aqueous saturated Na₂S₂O₅ (30 mL) were added. The organic layer (17 mL cyclohexane and 23 mL ethyl acetate) was washed with aqueous saturated Na₂S₂O₅ (3 × 50 mL), brine (3 × 50 mL), dried over MgSO₄, and filtered. Excess solvent was removed under reduced pressure to give a mixture of products. The product was isolated by silica gel flash chromatography using toluene as eluent.

4.16. General Procedure 10: Payne Epoxidation⁸³

A pre-dried 7 mL vial was charged with H₂O₂·urea **122** (4.0 equiv.) and potassium carbonate (0.2 equiv.). The vial was sealed with a Suba™ seal, filled with argon gas, and fitted with a nitrogen gas balloon. Methanol **57** [0.5 M], benzonitrile (4.0 equiv.), and *trans*-stilbene **194** (1.0 equiv.) were added. The mixture was stirred at 50 °C for 24 h. The crude reaction mixture was analysed by GC-MS (CI) without purification.

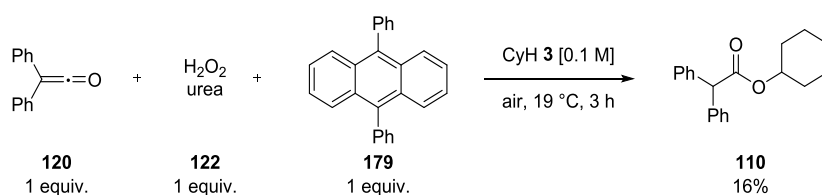
4.17. Preparation of 4,7-diphenylbenzo[*c*]-1,2,5-thiadiazole **182**¹²³

A pre-dried 2-neck 500 mL flask filled with argon gas was charged with 4,7-dibromobenzo[*c*]-1,2,5-thiadiazole **183** (816 mg, 2.78 mmol, 1.0 equiv.), phenyl boronic acid **184** (712 mg, 5.84 mmol, 2.1 equiv.), and tetrakis(triphenylphosphine)palladium (0) (94.0 mg, 3 mol%). The flask was sealed, placed under vacuum and backfilled with argon gas. Anhydrous tetrahydrofuran was degassed by sparging with argon gas for 2 hours and was added to the flask (277 mL). Potassium carbonate (767 mg, 5.55 mmol, 2.0 equiv.) was dissolved in de-ionised water (30 mL) and the aqueous solution was degassed (by sparging with argon gas for 2 h) and also added to the flask. The reaction flask was heated to 70 °C and stirred for 24 h. Excess solvent was evaporated under reduced pressure. The resulting solid was purified by silica-gel flash chromatography using petroleum ether 40-60 °C/ethyl acetate solvent system (9:1 v/v) to give the title compound **182** as yellow needles (718 mg, 2.49 mmol, 90%); m.p. 141–142 °C (lit. 127 °C, eluent - diethyl ether)¹²⁴; IR (neat)/cm⁻¹: 3034 (wk), 1549 (wk), 1476 (med), 1449 (med), 750 (str); ¹H NMR (400 MHz, CDCl₃): δ (ppm) 8.00-7.94

(m, 4H), 7.80 (s, 2H), 7.60–7.53 (m, 4H), 7.50–7.43 (m, 2H); ^{13}C NMR (101 MHz, CDCl_3): δ (ppm) 154.3, 137.6, 133.6, 129.4, 128.8, 128.5, 128.3; LRMS (ESI+) m/z 289.0 $[\text{M}+\text{H}]^+$.

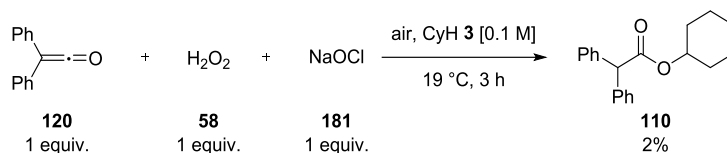
4.18. Singlet Oxygen Experiments

4.18.1. Trapping Singlet Oxygen⁷⁸

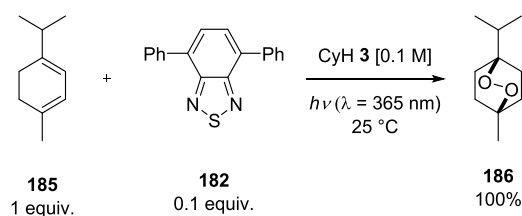


A round-bottom flask was charged with $\text{H}_2\text{O}_2\cdot\text{urea}$ **122** (144 mg, 1.53 mmol, 1.00 equiv.), cyclohexane **3** (15 mL), and 9,10-diphenylanthracene **179** (506 mg, 1.53 mmol, 1.00 equiv.). Diphenylketene **120** (297 mg, 1.53 mmol, 1.00 equiv.) was weighed out under an inert atmosphere into a vial, to which anhydrous cyclohexane **3** (3 mL) was added. The mixture was stirred at 25 °C while the solution of diphenylketene **120** was added over 3 h using a syringe pump. After the addition, the reaction was quenched by adding ice and aqueous saturated $\text{Na}_2\text{S}_2\text{O}_5$ (20 mL). The contents of the flask were poured into a separatory funnel and 1,4-dinitrobenzene (64.2 mg, 0.25 equiv.) dissolved in ethyl acetate (5 mL) was added. The flask, the magnetic stirrer and the vial (which contained 1,4-dinitrobenzene) were carefully washed with ethyl acetate (5 mL) and the washings were also added, followed by more ethyl acetate (20 mL) and aqueous saturated $\text{Na}_2\text{S}_2\text{O}_5$ (30 mL). The organic layer (15 mL cyclohexane and 25 mL ethyl acetate) was washed with aqueous saturated $\text{Na}_2\text{S}_2\text{O}_5$ (3×50 mL), brine (3×50 mL), dried over MgSO_4 , and filtered. Excess solvent was removed under reduced pressure. The resulting residue was dissolved in deuterated chloroform and was analysed by NMR spectroscopy.

4.18.2. Generation of Singlet Oxygen

4.18.2.1. Method 1⁷⁹

A round-bottom flask was charged with diphenylketene **120** (305 mg, 1.57 mmol, 1.00 equiv.), sodium hypochlorite **181** (0.67 mL, 1.57 mmol, 1.00 equiv., available chlorine 10–15%), and cyclohexane **3** (15 mL). The biphasic system was vigorously stirred while hydrogen peroxide **58** (aq. 30% *w/w*) was added over 3 h using a syringe pump. After the addition, the reaction was quenched by adding ice and aqueous saturated $\text{Na}_2\text{S}_2\text{O}_5$ (20 mL). The contents of the flask were poured into a separatory funnel and 1,4-dinitrobenzene (66.0 mg, 0.25 equiv.) dissolved in ethyl acetate (5 mL) was added. The flask, the magnetic stirrer and the vial (which contained 1,4-dinitrobenzene) were carefully washed with ethyl acetate (5 mL) and the washings were also added, followed by more ethyl acetate (20 mL) and aqueous saturated $\text{Na}_2\text{S}_2\text{O}_5$ (30 mL). The organic layer (15 mL cyclohexane and 25 mL ethyl acetate) was washed with aqueous saturated $\text{Na}_2\text{S}_2\text{O}_5$ (3×50 mL), brine (3×50 mL), dried over MgSO_4 , and filtered. Excess solvent was removed under reduced pressure. The resulting residue was dissolved in deuterated chloroform and analysed by NMR spectroscopy.

4.18.2.2. Method 2⁸¹

A 50 mL flask was charged with 4,7-diphenylbenzo[*c*]-1,2,5-thiadiazole **182** (44.0 mg, 0.15 mmol, 0.10 equiv.) and cyclohexane **3** (15 mL). A fritted glass bubbler was placed

inside the flask (below the solvent level) and oxygen gas was bubbled through. α -Terpinene **185** (250 μ L, 1.54 mmol, 1.00 equiv.) was added and the flask was exposed to UV light ($\lambda = 365$ nm). Small aliquots were taken out at various time intervals, placed under high vacuum, dissolved in deuterated chloroform and analysed by ^1H NMR spectroscopy.

4.19. Generation of hydrogen peroxide **58**⁸⁴

Palladium on alumina (5%, 10.0 mg, 2.4 mol%) and 2-ethylanthraquinone **196** (418 mg, 1.77 mmol) were placed in a Parr Hydrogenator reaction vessel and dissolved in a mixture (9 mL) of toluene and 1-decanol (2:7 v/v). The solution was hydrogenated over 19 h under a hydrogen pressure of 3.5 atm. When the hydrogenation was complete, the reaction vessel was stoppered with a Suba™ seal and filled with argon gas. The bright yellow-green solution was filtered through a dropping funnel filled with a Celite plug into the custom-made flask (**Figure 4.3, Section 4.13**) using a cannula and positive argon gas pressure as shown in **Figure 4.5**. The oxidation flask was connected to a vacuum line and an oxygen gas cylinder, and placed in a glove bag. The glove bag was sealed, air was removed and the glove bag was filled with argon gas (step 2 and 3 was repeated twice). The flask was then placed under vacuum and backfilled with oxygen gas (line open for a few seconds). The solution was subsequently vigorously stirred at 25 °C for 4 h. The solution was extracted with cold de-ionised water (4×10 mL). Semi-quantitative analysis using Quantofix Peroxide 100 test strips showed a peroxide concentration of 30–100 mg L⁻¹ in 40 mL of water.

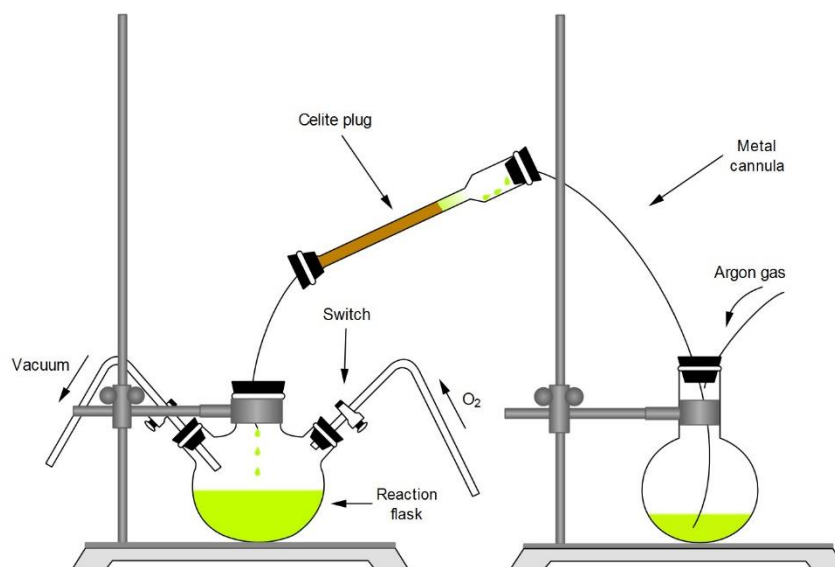
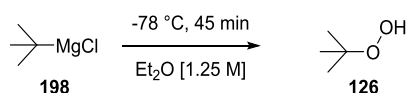
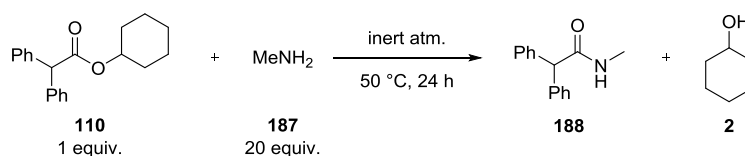


Figure 4.5. Hydrogen peroxide **58** reaction setup.

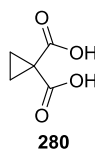
4.20. Generation of *t*-butyl hydroperoxide **126**⁸⁵



The method was based on that of Reile *et al.*⁸⁵ The custom-made flask shown in **Figure 4.3 (Section 4.13)** was flame-dried, placed under vacuum and backfilled with oxygen gas (step 2 and 3 was repeated twice). The flask was then charged with anhydrous diethyl ether (4 mL) and cooled to $-78\text{ }^\circ\text{C}$. *t*-Butyl magnesium chloride **198** (5 mL, 5 mmol) was added over 45 min using a syringe pump. After 45 min the flask was allowed to slowly warm up by letting dry ice/acetone evaporate. The solution was transferred into a separatory funnel containing ice, acidified, and extracted with diethyl ether ($4 \times 40\text{ mL}$). Semi-quantitative analysis using Quantofix Peroxide 100 test strips showed a peroxide concentration of 1 mg L^{-1} .

4.21. General Procedure 11: Derivatisation of cyclohexyl 2,2-diphenylacetate **110**

A 7 mL vial was charged with cyclohexyl 2,2-diphenylacetate **110** (20.0 mg, 67.9 μmol), sealed with a Suba™ seal, filled with argon gas, and fitted with a nitrogen gas balloon. Methylamine **187** (0.5 mL, 33 wt. % in ethanol) was added and the solution was stirred at 50 °C for 24 hours. The crude reaction mixture was analysed by GC-MS (CI) without purification.

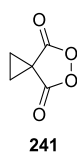
4.22. Synthesis of cyclopropane-1,1-dicarboxylic acid **280¹²⁵**

Benzyltriethyl ammonium chloride **340** (56.5 g, 248 mmol, 1.0 equiv.) was added to a 50% (by weight) aqueous solution of sodium hydroxide (500 mL) and stirred vigorously using a mechanical stirrer. A mixture of diethyl malonate **341** (37.6 mL, 248 mmol, 1.0 equiv.) and 1,2-dibromoethane **342** (31.9 mL, 370 mmol, 1.5 equiv.) was added and the resulting mixture was stirred for 2 h at room temperature. The contents of the flask were transferred to a 2 L conical flask, diluted with water (150 mL), and cooled down by submerging the flask in an ice bath. The aqueous phase was acidified with 500 mL HCl (37%, [12 M]) over 1.5 h (to ensure the temperature was below 25 °C) until pH 1 was reached. The aqueous layer was extracted with diethyl ether (3 \times 300 mL), the organics were combined, washed with brine (500 mL), dried over MgSO₄, and filtered. The solvent was removed under reduced pressure and the resulting white-yellow solids were triturated with petroleum ether 40–60 to give the title compound **280** as a white solid (21.9 g, 168 mmol, 68%); m.p. 133 °C (lit. 134–136 °C)¹²⁵; IR (neat)/cm⁻¹: 2515 (br, med), 1705 (str),

1161 (str); ^1H NMR (400 MHz, d_6 -DMSO) δ 12.41 (s, 2H), 1.31 (s, 4H); ^{13}C NMR (101 MHz, d_6 -DMSO) δ 171.8, 27.3, 16.2; LRMS (APCI/ESI) m/z 129.1 $[\text{M}-\text{H}]^-$.

4.23. Synthesis of cyclopropyl malonyl peroxide **241**⁹⁷

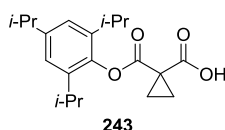
WARNING: Many peroxides are classified as dangerous or hazardous materials. Their preparation and use should be carried out with due caution. Differential Scanning Calorimetry (DSC) data for cyclopropyl malonyl peroxide **241** is available and shows an onset temperature of 114.5 °C.⁹⁷



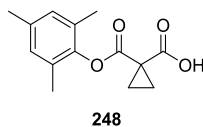
A 100 mL round-bottom flask was wrapped in parafilm, placed behind a blast shield, and charged with cyclopropane-1,1-dicarboxylic acid **280** (4.00 g, 30.7 mmol, 1.0 equiv.) and methanesulfonic acid (31 mL). Urea hydrogen peroxide **122** (8.7 g, 93 mmol, 3.0 equiv.) was added in three portions over one minute. The flask was loosely capped and the mixture was stirred at room temperature for 20 h. The contents of the reaction flask were poured into separatory funnel containing a mixture of ice (40 mL) and ethyl acetate (40 mL). The phases were separated and the aqueous phase was extracted using ethyl acetate (3 \times 40 mL). The combined organics were washed with a saturated aqueous NaHCO_3 solution (3 \times 40 mL), brine (40 mL), dried over MgSO_4 and filtered. Excess solvent was removed under reduced pressure (caution!) to give the title compound **241** as colourless crystals (3.07g, 24.0 mmol, 78%); m.p. 77–78 °C (lit. 90 °C)⁹⁷; IR (neat)/ cm^{-1} : 3121 (wk), 1790 (str), 1148 (str); ^1H NMR (400 MHz, CDCl_3) δ 2.10 (s, 4H); ^{13}C NMR (101 MHz, CDCl_3) δ 172.3, 23.8, 19.9.

4.24. General Procedure 12: Oxidation of Arenes

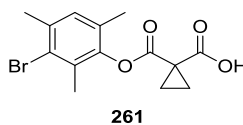
A 7 mL vial with magnetic stir bar was charged with cyclopropyl malonoyl peroxide **241** (76.9 mg, 0.60 mmol). HFIP (0.6 mL), followed by arene (0.30 mmol), was then added. The vial was placed in a heating block set to 25 °C unless noted otherwise and the reaction was allowed to stir for the specified time. Upon completion, the mixture was diluted with EtOAc (20 mL) and stirred with a saturated solution of Na₂S₂O₅ in water (20 mL) for 2 h. The layers were then separated and the aqueous solution was extracted again with EtOAc (2 × 20 mL). The organic extracts were combined and washed with brine (20 mL) and dried (MgSO₄). The solution was concentrated under reduced pressure and, if needed, the crude was chromatographed on silica gel (EtOAc) to afford the target compound.

1,3,5-Triisopropylbenzene half acid-ester 243

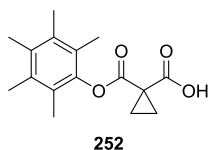
Prepared following General Procedure 12 using 1,3,5-triisopropylbenzene **242** (73 μL, 0.3 mmol). After 2 h, following the described work-up procedure, the title compound **243** was isolated as a white solid (99 mg, 0.3 mmol, 99%); m.p. 121–122 °C; IR (neat)/cm⁻¹: 2961 (med), 1746 (med), 1690 (str), 1165 (str); ¹H NMR (400 MHz, CDCl₃): δ (ppm) 7.01 (s, 2H), 2.90 (hept, *J* = 13.8, 6.9 Hz, 1H), 2.69 (hept, *J* = 13.7, 6.9 Hz, 2H), 2.07 (s, 4H), 1.25 (d, *J* = 6.9 Hz, 6H), 1.22 (d, *J* = 6.8 Hz, 6H), 1.18 (d, *J* = 6.8 Hz, 6H); ¹³C NMR (101 MHz, CDCl₃): δ (ppm) 175.6, 170.5, 148.0, 142.4, 139.4, 122.3, 34.2, 27.9, 25.3, 24.2, 24.1, 22.8, 22.6; LRMS (ESI+) *m/z* 333.2 [M+H]⁺; HRMS (NSI+, *m/z*, assignment): calculated for 333.2060 [M+H]⁺, 350.2326 [M+NH₄]⁺, found 333.2063, 350.2328.

Mesitylene half acid-ester 248

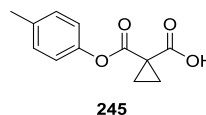
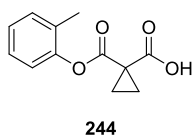
Prepared following General Procedure 12 using mesitylene **238** (42 μL , 0.3 mmol). After 4.5 h, following the described work-up procedure, the title compound **248** was isolated as a white solid (74 mg, 0.3 mmol, 99%); m.p. 74–75 $^{\circ}\text{C}$; IR (neat)/ cm^{-1} : 3019 (wk), 2922 (wk), 1751 (str), 1682 (str), 1130 (str); ^1H NMR (400 MHz, CDCl_3): δ (ppm) 6.89 (s, 2H), 2.28 (s, 3H), 2.09 (s, 6H), 2.05 (dt, $J = 5.9, 3.8$ Hz, 4H); ^{13}C NMR (101 MHz, CDCl_3): δ (ppm) 174.2, 170.5, 144.8, 136.5, 129.7, 129.3, 25.4, 22.5, 20.8, 16.2; LRMS (ESI+) m/z 249.1 $[\text{M}+\text{H}]^+$, 266.1 $[\text{M}+\text{NH}_4]^+$; HRMS (NSI+, m/z , assignment): calculated for 249.1121 $[\text{M}+\text{H}]^+$, 271.0941 $[\text{M}+\text{Na}]^+$, found 249.1124, 271.0944.

Bromomesitylene half acid-ester 261

Prepared following General Procedure 12 using 2-bromomesitylene **330** (55.0 μL , 0.36 mmol, 1 equiv.), cyclopropyl malonyl peroxide **241** (92.0 mg, 0.72 mmol, 2 equiv.), and HFIP (0.72 mL). After 5 days, following the described work-up procedure, the title compound **261** was isolated as a white solid (107 mg, 0.33 mmol, 91%); m.p. 157–160 $^{\circ}\text{C}$; IR (neat)/ cm^{-1} : 2930 (br, wk), 1743 (med), 1684 (str), 1130 (str); ^1H NMR (400 MHz, CDCl_3): δ (ppm) 7.01 (s, 1H), 2.38 (s, 3H), 2.20 (s, 3H), 2.09–2.03 (m, 7H); ^{13}C NMR (101 MHz, CDCl_3): δ (ppm) 173.8, 170.3, 144.9, 137.1, 130.3, 129.7, 128.4, 125.4, 25.5, 23.7, 22.5, 17.3, 16.2; LRMS (ESI+) m/z 326.9 $[\text{M}(^{79}\text{Br})+\text{H}]^+$, 329.0 $[\text{M}(^{81}\text{Br})+\text{H}]^+$; HRMS (NSI+, m/z , assignment): calculated for 327.0226 $[\text{M}(^{79}\text{Br})+\text{H}]^+$, 329.0206 $[\text{M}(^{81}\text{Br})+\text{H}]^+$, found 327.0225, 329.0203.

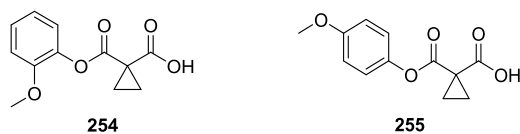
Pentamethylbenzene half acid-ester 252

Prepared following General Procedure 12 using pentamethylbenzene **251** (100 mg, 0.67 mmol, 1.0 equiv.), cyclopropyl malonoyl peroxide **241** (95.0 mg, 0.74 mmol, 1.1 equiv.), and HFIP (1.34 mL). After 24 h, following the described work-up procedure, the title compound **252** was isolated as a dark yellow solid (128 mg, 0.46 mmol, 69%); m.p. 144-147 °C; IR (neat)/cm⁻¹: 3022 (wk), 2930 (wk), 1732 (str), 1705 (str), 1144 (str); ¹H NMR (400 MHz, CDCl₃): δ (ppm) 2.22 (s, 9H), 2.09 (m, 4H), 2.04 (s, 6H); ¹³C NMR (101 MHz, CDCl₃): δ (ppm) 174.5, 170.6, 144.8, 134.0, 133.8, 124.8, 25.4, 22.4, 16.7, 16.5, 13.4; HRMS (NSI+, *m/z*, assignment): calculated for 277.1434 [M+H]⁺, 299.1254 [M+Na]⁺, found 277.1433, 299.1251.

Toluene half acid-esters 244 and 245

Prepared following General Procedure 12 using toluene **5** (107 μL, 1.0 mmol, 1 equiv.), cyclopropyl malonoyl peroxide **241** (256 mg, 2.0 mmol, 2 equiv.), and HFIP (2 mL) at 50 °C. After 72 h, following the described work-up procedure, the title compounds **244** and **245** were isolated as a colourless oil (138 mg, 0.63 mmol, 63%, **244**:**245** = 1:1); IR (neat)/cm⁻¹: 3030 (wk), 2926 (wk), 1748 (str), 1751 (str), 1693 (str), 1128 (str); ¹H NMR (400 MHz, CDCl₃): δ (ppm) 11.67 (br s, 2H), 7.29–7.18 (m, 5H), 7.01–6.97 (m, 1H), 6.94 (d, *J* = 8.5 Hz, 2H), 2.36 (s, 3H), 2.17 (s, 3H), 2.07–1.98 (m, 8H); ¹³C NMR (101 MHz, CDCl₃): δ (ppm) 174.9, 174.3, 170.7, 170.6, 148.2, 147.3, 136.8, 131.6, 130.3, 129.7, 127.4, 127.1, 121.4, 120.8, 25.6, 22.7, 22.6, 21.0, 16.2; LRMS (ESI-) *m/z* 219.1 [M-H]⁻

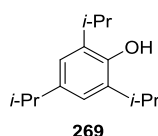
Anisole half acid-ester **254** and **255**



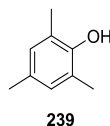
Prepared following General Procedure 12 using anisole **253** (100 μ L, 0.92 mmol, 1 equiv.), cyclopropyl malonoyl peroxide **241** (256 mg, 2.0 mmol, 2 equiv.), and HFIP (2 mL) at 50 $^{\circ}$ C. After 72 h, following the described work-up procedure, the title compounds **254** and **255** were isolated as a yellow oil (191 mg, 0.81 mmol, 81%, **254**:**255** = 1:1.6); IR (neat)/ cm^{-1} : 3119 (wk), 2839 (wk), 1757 (str), 1693 (str), 1190 (str), 1128 (str); ^1H NMR (400 MHz, CDCl_3): δ (ppm) 7.29–7.23 (m, 1H), 7.04–6.88 (m, 7H), 3.83 (s, 2H), 3.80 (s, 3H), 2.12–2.08 (m, 2H), 2.02–1.98 (m, 6H); ^{13}C NMR (101 MHz, CDCl_3): δ (ppm) 175.0, 174.7, 170.5, 170.4, 158.1, 150.7, 143.0, 138.5, 128.0, 122.4, 121.9, 120.9, 114.8, 112.6, 56.0, 55.7, 25.6, 25.5, 22.9, 22.6; LRMS (ESI $^-$) m/z 235.1 $[\text{M}-\text{H}]^-$.

4.25. General Procedure 13: Aminolysis of Esters

Crude ester (1 equiv) was dissolved in the minimum amount of ethanol. MeNH₂ in EtOH (33% MeNH₂ w/v, 20 equiv. EtNH₂) was added and the mixture was stirred for 1 h at 25 °C. Excess solvent was removed under reduced pressure. The crude product was purified and isolated by silica gel column chromatography using the specified solvent mixture.

2,4,6-Triisopropylphenol 269¹²⁶

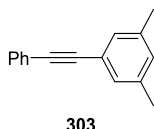
Prepared following General Procedure 13 using half acid-ester **243** (66.0 mg, 0.20 mmol). Following the described work-up procedure, the reaction mixture was purified by silica gel flash chromatography (petroleum ether 40–60/EtOAc = 1:1 v/v elution) to give **269** as a brown oil (41 mg, 0.19 mmol, 93%); IR (neat)/cm⁻¹: 3700 (wk, br), 2959 (str), 1470 (str); ¹H NMR (400 MHz, CDCl₃): δ (ppm) 6.93 (s, 2H), 4.63 (s, 1H), 3.16 (hept, *J* = 6.7 Hz, 2H), 2.86 (hept, *J* = 6.9 Hz, 1H), 1.29 (d, *J* = 6.9 Hz, 12H), 1.25 (d, *J* = 6.9 Hz, 6H); ¹³C NMR (101 MHz, CDCl₃): δ (ppm) 148.1, 140.9, 133.5, 121.5, 34.0, 27.5, 24.5, 22.9; LRMS (ESI+) *m/z* 333.2 [M]^{•+}; HRMS (NSI+, *m/z*, assignment): calculated for 221.1900 [M+H]⁺, found 221.1898.

2,4,6-Trimethylphenol 239¹²⁷

Prepared following General Procedure 13 using half acid-ester **248** (50 mg, 0.20 mmol). Following the described work-up procedure, the reaction mixture was purified by silica gel flash chromatography (pet ether 40–60/EtOAc 1:1 v/v elution) to give **239** as a beige

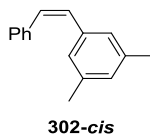
solid (25 mg, 0.18 mmol, 92%); m.p. 67–70 °C (lit. 67–69 °C, SiO₂, hexane/EtOAc 4:1 v/v elution)¹²⁷; IR (neat)/cm⁻¹: 3389 (med, br), 2914 (wk), 1481 (str); ¹H NMR (400 MHz, CDCl₃): δ (ppm) 6.79 (s, 2H), 2.24–2.21 (m, 9H); ¹³C NMR (101 MHz, CDCl₃): δ (ppm) 150.0, 129.4, 129.3, 122.9, 29.8, 20.5, 15.9; GC-MS (EI) *m/z* 136.08 [M]^{•+}.

4.26. Synthesis of 1-(3,5-dimethylphenyl)-2-phenylacetylene **303**¹²⁸

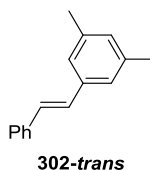


A 50 mL round-bottom flask was charged with TBAF H₂O (3.92 g, 15 mmol, 3.0 equiv.), bis(triphenylphosphine)palladium (II) chloride (351 mg, 10 mol%), magnetic stirrer, sealed with a Suba™ seal, and filled with argon gas. A N₂ gas balloon was fitted. Phenylacetylene **304** (0.66 mL, 6.0 mmol, 1.2 equiv.) and 1-bromo-3,5-dimethylbenzene **305** (0.68 mL, 5.0 mmol, 1.0 equiv.) were added. The reaction mixture was stirred at 80 °C. After 3 h, the catalyst was removed on a Celite plug. The plug was washed with ethanol into a round-bottom flask until no more product remained. Excess solvent was removed under reduced pressure and the residue was purified by silica gel flash chromatography (pet ether 40–60) to give **303** as a white solid (420 mg, 2.0 mmol, 41%); m.p. 39–40 °C (lit. 45 °C, SiO₂, hexane elution)¹²⁸; IR (neat)/cm⁻¹: 3032 (wk), 2916 (wk), 1599 (med), 1491 (med); ¹H NMR (400 MHz, CDCl₃): δ (ppm) 7.56–7.50 (m, 2H), 7.38–7.31 (m, 3H), 7.21–7.17 (m, 2H), 7.00–6.97 (m, 1H), 2.33 (d, *J* = 0.6 Hz, 6H); ¹³C NMR (101 MHz, CDCl₃): δ (ppm) 138.0, 131.7, 130.4, 129.5, 128.5, 128.2, 123.7, 123.0, 89.9, 88.9, 21.3; GC-MS (EI) *m/z* 207.1 [M+H]⁺.

4.27. Synthesis of Alkenes

(Z)-3,5-Dimethylstilbene 302

A 3-neck round-bottom flask was connected to a vacuum line, a glass stopcock with a H₂ balloon, and sealed with a Suba™ seal. The flask was flame-dried, filled with argon gas, charged with Lindlar catalyst (17.0 mg, 5 % w/w), and sealed. The flask was put under vacuum and backfilled with H₂ gas (repeated three times). 1-(3,5-dimethylphenyl)-2-Phenylacetylene **303** (326 mg, 1.58 mmol, 1.0 equiv.) in EtOAc (15 mL) was added followed by quinoline (30 μL). The reaction mixture was stirred vigorously under an H₂ atmosphere at 25 °C for 2 h. The catalyst was removed on a Celite plug, which was washed with acetone multiple times into a 500 mL round-bottom flask. The filtrate was concentrated under reduced pressure. The residue was purified by silica gel flash chromatography (pet ether 40–60) to give **302-cis** as a yellow oil (251 mg, 1.20 mmol, 76%); IR (neat)/cm⁻¹: 3009 (wk), 2916 (wk), 1599 (med); ¹H NMR (500 MHz, CDCl₃): δ (ppm) 7.28–7.25 (m, 2H), 7.24–7.16 (m, 3H), 6.88 (s, 2H), 6.84 (s, 1H), 6.55 (s, 2H), 2.22 (m, 6H); ¹³C NMR (125 MHz, CDCl₃): δ (ppm) 137.8, 137.5, 137.3, 130.6, 130.0, 129.0, 128.9, 128.2, 127.2, 126.7, 21.3; GC-MS (CI) *m/z* 209.2 [M+H]⁺; HRMS (APCI+, *m/z*, assignment): calculated for 209.1325 [M+H]⁺, found 209.1325 [M+H]⁺.

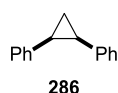
(E)-3,5-Dimethylstilbene 302¹²⁹

A dry 50 mL flask was fitted with a water condenser and was put under an argon atmosphere. Triethyl phosphite **343** (1.56 mL, 9.10 mmol, 1.2 equiv.) and benzyl bromide **344** (0.89 mL, 7.48 mmol, 1.0 equiv.) were added and stirred at 150 °C for 3 h. The condenser was removed, the flask was sealed with a Suba™ seal, and fitted with a nitrogen gas balloon. Anhydrous DMF (15.0 mL) was added and the reaction was cooled to 0 °C for 15 min. NaH (60% in mineral oil, 456 mg, 11.4 mmol, 1.5 equiv.) was added and the reaction was stirred for an additional 30 min. 3,5-Dimethylbenzaldehyde **345** (1.0 mL, 7.51 mmol, 1.0 equiv.) was added (changing the colour of the solution to yellow) and the reaction was stirred at 25 °C. After 18 h, the contents of the flask were transferred into a separatory funnel. The organics were extracted into ethyl acetate (100 mL), washed with de-ionised water (2 × 25 mL), brine (25 mL), dried over Na₂SO₄, filtered, and concentrated under reduced pressure. The crude product was purified by flash column chromatography (pet ether 40–60 elution) to give **302-trans** as colourless oil (1.42 g, 6.84 mmol, 91%). The oil can be solidified by placing the sample in a low temperature environment (4–8 °C) to give a white solid; m.p. 22 °C (lit. 30 °C)¹³⁰; IR (neat)/cm⁻¹: 3024 (wk), 2916 (wk), 1599 (med); ¹H NMR (400 MHz, CDCl₃): δ (ppm) 7.51 (d, *J* = 7.9 Hz, 2H), 7.36 (t, *J* = 7.5 Hz, 2H), 7.29–7.23 (m, 1H), 7.15 (s, 2H), 7.08 (s, 1H), 7.07 (s, 1H), 6.92 (s, 1H), 2.35 (s, 6H); ¹³C NMR (101 MHz, CDCl₃): δ (ppm) 138.3, 137.7, 137.4, 129.6, 129.1, 128.8, 128.5, 127.6, 126.6, 124.6, 21.4; LRMS (ESI+) *m/z* 209.1 [M+H]⁺.

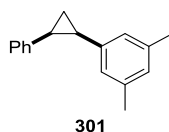
4.28. General Procedure 14: Cyclopropanation

WARNING: Extreme caution should be used when working with diethylzinc. Neat diethylzinc spontaneously combusts upon exposure to atmospheric moisture.

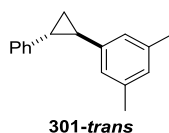
A solution of trifluoroacetic acid (2.15 mL, 28.0 mmol, 4.0 equiv.) in anhydrous dichloromethane (7 mL) was added at 0 °C over 60 min using a syringe pump to a solution of diethylzinc (2.87 mL, 28 mmol, 4.0 equiv.) in anhydrous dichloromethane (15 mL) and the mixture was stirred at 0 °C for 30 min – formation of a solid on the side of the flask. A solution of diiodomethane (2.25 mL, 28.0 mmol, 4.0 equiv.) in anhydrous dichloromethane (7 mL) was added to the previous mixture at 0 °C. The resulting mixture was stirred for 40 min at 0 °C. A solution of alkene (7 mmol, 1 equiv.) in anhydrous dichloromethane (7 mL) was then added to the mixture at 0 °C. The resulting mixture was stirred for 18 h (unless stated otherwise) at room temperature. The reaction was quenched by carefully adding a saturated solution of NH₄Cl in water (50 mL). The aqueous layer was extracted with dichloromethane (4 × 70 mL). The combined organic layers were washed with sat. NaHCO₃ (2 × 50 mL), de-ionised water (50 mL), brine (2 × 50 mL), dried over Na₂SO₄, and concentrated under reduced pressure. The residue was then purified by silica gel column chromatography (petroleum ether 40–60 °C elution).

***cis*-1,2-Diphenylcyclopropane 286¹³¹**

Prepared following General Procedure 14 using *cis*-stilbene **287** (1.2 mL, 6.93 mmol, 1 equiv.) in anhydrous dichloromethane (7.0 mL) to give **286** as a white solid (430 mg, 2.21 mmol, 32%); m.p. 33–35 °C (lit. 34–35 °C)¹³¹; IR (neat)/cm⁻¹: 3082 (wk), 2997 (wk), 1601 (med), 1495 (med); ¹H NMR (400 MHz, CDCl₃): δ (ppm) 7.12–7.01 (m, 6H), 6.96–6.92 (m, 4H), 2.49 (dd, *J* = 8.6, 6.3 Hz, 2H), 1.47 (dt, *J* = 8.6, 5.4 Hz, 1H), 1.40–1.35 (dt, *J* = 6.3 Hz, 5.9 Hz, 1H); ¹³C NMR (101 MHz, CDCl₃): δ (ppm) 138.5, 129.1, 127.8, 125.7, 24.5, 11.5; GC-MS (CI) *m/z* 195.1 [M+H]⁺.

***cis*-1-Phenyl-2-(3,5-dimethylphenyl)cyclopropane 301**

Prepared following General Procedure 14 using *cis*-3,5-dimethylstilbene **302-*cis*** (693 mg, 3.33 mmol) in anhydrous dichloromethane (7 mL) to give **301-*cis*** as a colourless oil (189 mg, 0.85 mmol, 26%); IR (neat)/cm⁻¹: 3024 (wk), 2916 (wk), 1603 (med), 1497 (med); ¹H NMR (400 MHz, CDCl₃): δ (ppm) 7.14–7.01 (m, 3H), 7.01–6.93 (m, 2H), 6.68 (s, 1H), 6.55 (s, 2H), 2.43 (ddd, *J* = 11.8, 8.8, 6.4 Hz, 2H), 2.14 (s, 6H), 1.44 (dt, *J* = 8.7, 5.3 Hz, 1H), 1.33 (dt, *J* = 11.7, 6.3 Hz, 1H); ¹³C NMR (101 MHz, CDCl₃): δ (ppm) 138.8, 138.4, 137.0, 129.2, 127.7, 127.4, 127.0, 125.6, 24.4, 24.3, 21.3, 11.7; GC-MS (CI) *m/z* 223.2 [M+H]⁺; HRMS (APCI+, *m/z*, assignment): calculated for 223.1481 [M+H]⁺, found 223.1480.

***trans*-1-Phenyl-2-(3,5-dimethylphenyl)cyclopropane 301**

Prepared following General Procedure 14 using *trans*-3,5-dimethylstilbene **302-*trans*** (985 mg, 4.73 mmol) in anhydrous dichloromethane (2 mL). The procedure was repeated using the mixture of alkene **302-*trans*** and **302-*cis*** due to identical R_f values (0.20) to give solely **301-*trans*** as a colourless oil (272 mg, 1.22 mmol, 26%); IR (neat)/cm⁻¹: 3024 (wk), 2916 (wk), 2359 (wk), 2342 (wk), 1603 (med), 1497 (wk); ¹H NMR (400 MHz, CDCl₃): δ (ppm) 7.35–7.30 (m, 2H), 7.24–7.15 (m, 3H), 6.88–6.86 (m, 1H), 6.81 (s, 2H), 2.34 (s, 6H), 2.22–2.11 (m, 2H), 1.50–1.42 (m, 2H); ¹³C NMR (101 MHz, CDCl₃): δ (ppm) 142.8, 142.6, 138.0, 128.5, 127.6, 125.9, 125.8, 123.8, 28.1, 28.0, 21.4, 18.2; GC-MS (CI) *m/z* 223.1 [M+H]⁺, 251.1 [M+C₂H₅]⁺; HRMS (APCI+, *m/z*, assignment): calculated for 223.1482 [M+H]⁺, found 223.1479.

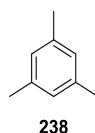
4.29. General Procedure 15: Hammett Analysis

A 7 mL vial was charged with cyclopropyl malonoyl peroxide **241** (38.4 mg, 0.3 mmol, 1.0 equiv.), followed by a standard solution of 1,4-dinitrobenzene in HFIP [0.01 M] (3.0 mL, 0.2 equiv. of 1,4-dinitrobenzene). 100 μ L of the solution was taken and added to an NMR tube containing CDCl_3 (500 μ L) to determine the initial ratio of **241** to the internal standard by ^1H NMR spectroscopy. Arene (0.3 mmol, 1.0 equiv.) was added and timing commenced immediately. The reaction was stirred at 25 $^\circ\text{C}$. Aliquots were taken for ^1H NMR analysis (as described above) at the specified time intervals. All reactions were performed in duplicate.

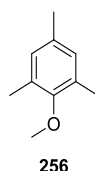
The rate of reaction was monitored by consumption of cyclopropyl malonoyl peroxide **241** relative to the internal standard (1,4-dinitrobenzene) by integration of the corresponding ^1H NMR signals:

Cyclopropyl malonoyl peroxide **241**: ^1H NMR (400 MHz, CDCl_3) δ 2.11 (s, 4H, CH_2)

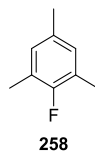
1,4-Dinitrobenzene: ^1H NMR (400 MHz, CDCl_3) δ 8.43 (s, 4H, ArH)



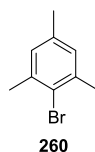
Hammett analysis was performed on mesitylene **238** (42 μ L, 0.3 mmol, 1.0 equiv.) following General Procedure 15. The consumption of peroxide **241** was monitored against the internal standard at the following time intervals (min): 1, 3, 5, 7, 10, 15, 20, 25, 30.



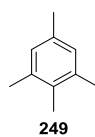
Hammett analysis was performed on 2,4,6-trimethylanisole **256** (47 μL , 0.3 mmol, 1.0 equiv.) following General Procedure 15. The consumption of peroxide **241** was monitored against the internal standard at the following time intervals (min): 1, 5, 10, 15, 30, 45, 60, 75, 90.



Hammett analysis was performed on 2-fluoromesitylene **258** (42.5 μL , 0.3 mmol, 1.0 equiv.) following General Procedure 15. The consumption of peroxide **241** was monitored against the internal standard at the following time intervals (min): 1, 5, 10, 15, 30, 45, 60, 75, 90.



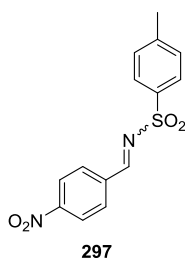
Hammett analysis was performed on 2-bromomesitylene **260** (45 μL , 0.3 mmol, 1.0 equiv) following General Procedure 15. The consumption of peroxide **241** was monitored against the internal standard at the following time intervals (h): 0.5, 1, 2, 3, 4.



A 7 mL vial was charged with a standard solution of 1,4-dinitrobenzene in HFIP [0.01 M] (2.0 mL, 0.2 equiv 1,4-dinitrobenzene), followed by isodurene **249** (30 μL , 0.2 mmol, 1.0 equiv). 100 μL of the solution was taken and added to an NMR tube containing CDCl_3 (500 μL) to determine the initial ratio of **249** to the internal standard by ^1H NMR spectroscopy. Cyclopropyl malonyl peroxide **241** (25.6 mg, 0.2 mmol, 1.0 equiv) was then added. 100 μL aliquots were taken at the specified time intervals and quenched in

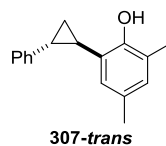
vials containing CDCl_3 (0.6 mL) and a saturated solution of $\text{Na}_2\text{S}_2\text{O}_5$ in water (0.8 mL). The organic layers were pipetted out and filtered through a short plug of MgSO_4 directly into the NMR tube. The consumption of isodurene **249** relative to the internal standard was monitored at the following time intervals (min): 1, 2, 3, 4, 5, 7, 10.

4.30. Synthesis of *N*-sulfonyl imine **297**¹³²



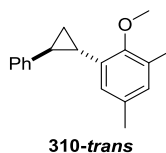
A dry 50 mL round-bottom flask was charged with 4-toluenesulfonamide **346** (1.00 g, 5.84 mmol, 1.0 equiv.), 4-nitrobenzaldehyde **347** (0.91 g, 6.02 mmol, 1.0 equiv.), 3 Å molecular sieves, and anhydrous dichloromethane (20 mL). The flask was sealed and the solution was stirred at 25 °C under an N_2 atmosphere. After 18 h, the crude reaction mixture was filtered, washed with DCM (2×10 mL), and concentrated under reduced pressure to give a white crystalline solid (0.96 g, 3.1 mmol, 54%); m.p. 207–209 °C (m.p. 205–207 °C)¹³²; IR (neat)/ cm^{-1} : 3123 (wk), 1593 (str), 1522 (str), 1346 (str), 1319 (str), 1184 (str); ^1H NMR (400 MHz, CDCl_3): δ (ppm) 9.10 (s, 1H), 8.35–8.30 (m, 2H), 8.13–8.08 (m, 2H), 7.93–7.88 (m, 2H), 7.38 (d, $J = 8.1$ Hz, 2H), 2.46 (s, 3H); ^{13}C NMR (101 MHz, CDCl_3): δ (ppm) 167.4, 151.4, 145.5, 137.6, 134.3, 132.0, 130.2, 128.6, 124.3, 21.9; GC-MS (CI) m/z 305.1 $[\text{M}+\text{H}]^+$.

4.31. Synthesis of **307-trans**



Cyclopropyl malonoyl peroxide **241** (202 mg, 1.58 mmol, 1.0 equiv.) was stirred with *trans*-1-phenyl-2-(3,5-dimethylphenyl)cyclopropane **301-trans** (350 mg, 1.57 mmol, 1.0 equiv.) in HFIP (7.85 mL) at 25 °C. After 3 h, the reaction was quenched by adding a mixture of EtOAc (8 mL) and a saturated solution of Na₂S₂O₅ (aq, 16 mL) and stirring it at 25 °C for 2 h. The contents of the flask were transferred into a separatory funnel. The aqueous was extracted with EtOAc (4 × 20 mL). The combined organic extracts were washed with de-ionised water (20 mL), brine (20 mL), dried over MgSO₄, filtered, and concentrated under reduced pressure. The crude product was purified by silica gel flash chromatography (pet ether 40–60/Et₂O = 9.5:0.5 *v/v* elution) to give **307-trans** as a brown solid (31 mg, 0.13 mmol, 8%); m.p. 72–74 °C; IR (neat)/cm⁻¹: 3399 (br, wk), 3028 (wk), 2916 (wk), 1605 (med), 1487 (med), 1209 (str); ¹H NMR (400 MHz, CDCl₃): δ (ppm) 7.35–7.29 (m, 2H), 7.24–7.18 (m, 3H), 6.85 (s, 1H), 6.81 (s, 1H), 5.07 (s, 1H), 2.25 (s, 3H), 2.23 (s, 3H), 2.13–2.05 (m, 2H), 1.45–1.39 (m, 2H); ¹³C NMR (101 MHz, CDCl₃): δ (ppm) 151.4, 142.0, 130.1, 129.2, 128.8, 126.4, 126.2, 126.0, 125.9, 123.5, 24.7, 22.2, 20.7, 15.9, 15.7; GC-MS (CI) *m/z* 239.1 [M+H]⁺.

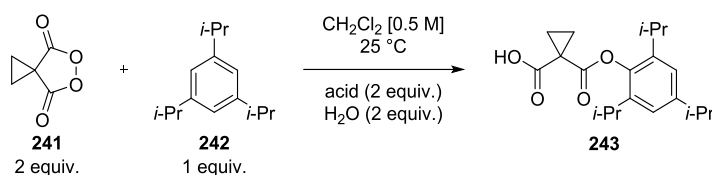
4.32. Synthesis of **310-trans**



trans-1-Phenyl-2-(3,5-dimethyl-2-hydroxyphenyl)cyclopropane **307-trans** (34 mg, 0.14 mmol, 1 equiv.), iodomethane **311** (26 μm, 0.42 mmol, 3 equiv.), and potassium carbonate (58 mg, 0.42 mmol, 3 equiv.) were stirred in DMF (0.3 mL) at 25 °C. After 17 h, the reaction was quenched with 10% NH₄OH (10 mL) and extracted with Et₂O

(2 × 10 mL). The organic extracts were combined, washed with water (3 × 10 mL), dried (MgSO₄) and the solvent was evaporated to give the title compound **310-trans** as a yellow oil (7 mg, 0.03 mmol, 20%); IR (neat)/cm⁻¹ 3024 (wk), 2924 (wk), 1605 (wk), 1456 (med), 1481 (med); ¹H NMR (400 MHz, CDCl₃) δ 7.34–7.28 (m, 2H), 7.23–7.17 (m, 3H), 6.88–6.85 (m, 1H), 6.63–6.60 (m, 1H), 3.67 (s, 3H), 2.52–2.44 (m, 1H), 2.30, (s, 3H), 2.29 (s, 3H), 2.16–2.09 (m, 1H), 1.50–1.40 (m, 2H); ¹³C NMR (101 MHz, CDCl₃) δ 155.4, 142.8, 134.8, 133.4, 130.7, 129.3, 128.5, 126.0, 125.8, 122.9, 60.6, 27.7, 22.0, 21.1, 17.5, 16.1; LRMS (CI) *m/z* 253.2 [M+H]⁺; HRMS (APCI+) calculated for [M+H]⁺ 253.1587, found 253.1588.

4.33. General Procedure 16: Effect of Water

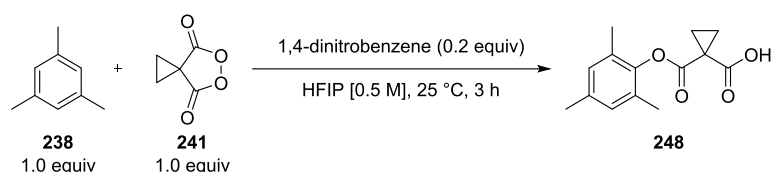


Cyclopropyl malonoyl peroxide **241** (25 mg, 0.20 mmol, 2.0 equiv.) was dissolved in dichloromethane (0.2 mL) and the acid (0.20 mmol, 2.0 equiv.), 1,3,5-triisopropylbenzene **242** (24 μL, 0.10 mmol, 1.0 equiv.) and water (3.5 μL, 0.20 mmol, 2.0 equiv.) were added. Aliquots (20 μL) were taken out at the specified times. Excess solvent was evaporated carefully under a stream of compressed air. The aliquots were diluted in 0.6 mL CDCl₃ and the conversion of the 1,3,5-triisopropylbenzene **242** to product **243** was monitored by ¹H NMR spectroscopy.

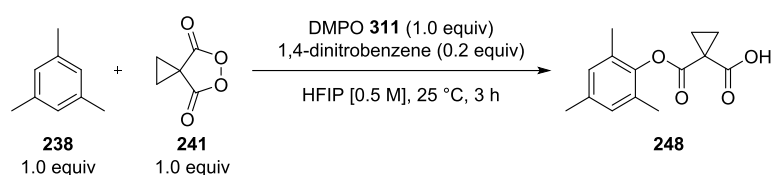
4.34. General Procedure 17: EPR Experiments

4.34.1. Control Reactions

Two control reactions were carried out to ensure sufficient conversion to product **248** with and without DMPO **312** on the given timescale and to monitor for competing reactions.



Cyclopropyl malonoyl peroxide **241** (26 mg, 0.20 mmol, 1.0 equiv.) was weighed into a 1.5 mL vial equipped with a stir bar, and a standard solution of 1,4-dinitrobenzene in HFIP (0.4 mL, 0.20 equiv., 1,4-dinitrobenzene) was added. An aliquot 20 (μL) was taken out and diluted in CDCl_3 to record the initial ratio between the internal standard and cyclopropyl malonoyl peroxide **241** using ^1H NMR spectroscopy. Mesitylene **238** (28 μL , 0.20 mmol, 1.0 equiv.) was then added and the reaction was monitored over 3 h. The reaction showed a 52% conversion after 1 h and 73% after 3 h with no other products present.



The above procedure was repeated with the exception that DMPO **312** (23 mg, 0.20 mmol) was added along with mesitylene **238** (28 μL , 0.20 mmol, 1.0 equiv.). The reaction showed a 48% conversion after 1 h and 68% after 3 h with no other products present.

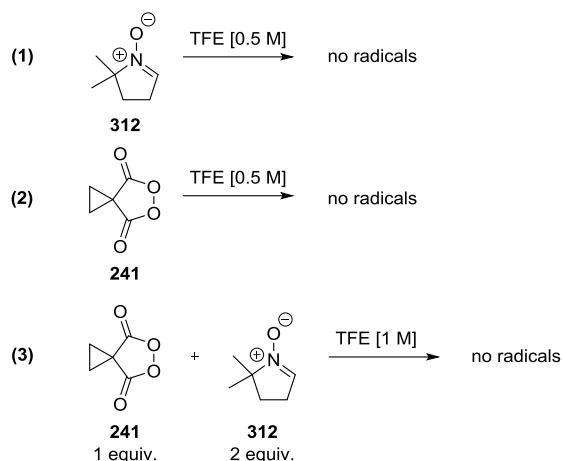
4.34.2. Purification of DMPO **312**

A distillation setup consisting of a 10 mL round bottom flask equipped with a Vigreux column and a short-path condenser with three 10 mL round bottom collection flasks was charged with a commercially available (Fluorochem, 5 g, brown solid with a low melting point) sample of 5,5-dimethyl-1-pyrroline-*N*-oxide **312** (DMPO, 1.6 g). The distillation setup was placed under vacuum (4.1 mbar) and the Vigreux column and the upper part of the short-path condenser were covered in glass wool and aluminium foil to better retain heat. The oil bath was heated to 140 °C. A heat gun was used occasionally to warm up the upper part of the condenser to prevent DMPO **312** (b.p. 88 °C at 4.1 mbar) from condensing at the top of the condenser. DMPO **312** (1.2 g, colourless oil) was distilled into a 10 mL round bottom flask and stored under argon. The collected DMPO **312** crystallised as a white solid upon standing at –24 °C.

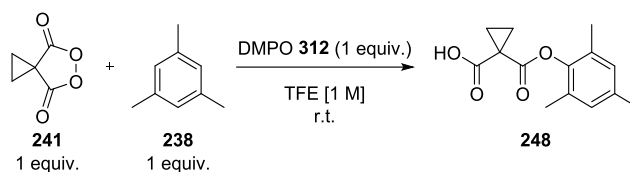
4.34.3. Sample Preparation for EPR Studies

The EPR spectrometer was calibrated using a solution of TEMPO **313** in 2,2,2-trifluoroethanol [0.05 M]. Standard solutions of DMPO **312**, cyclopropyl malonoyl peroxide **241** and mesitylene **238** in TFE [0.5 M] were prepared under a nitrogen atmosphere.

First, a series of control reactions were carried out. These included monitoring for the presence of radical species when (1) DMPO **312** (0.2 mL, 0.5 M), (2) cyclopropyl malonoyl peroxide **241** (0.1 mL, 0.5 M), and (3) both **241** and **312** (0.1 mL and 0.2 mL, respectively, 1 M) were present in the solution (TFE).



Next, a reaction between cyclopropyl malonoyl peroxide **241**, DMPO **312** and mesitylene **238** was monitored for the presence of radical species. Mesitylene **238** (5.6 μ L, 0.04 mmol) was added to a solution of cyclopropyl malonoyl peroxide **241** (0.1 mL, 0.5 M), followed by DMPO **312** (0.2 mL, 0.5 M) and the resulting mixture was analysed by EPR spectroscopy.



All the experiments were repeated using HFIP as a solvent and all the experiments were carried out in duplicate. No radicals were observed by EPR spectroscopy in any of the experiments performed.

Chapter 5: Appendix

5. Appendix

5.1. X-Ray Crystallographic Data

Single crystal diffraction data for diesters **230**, **232**, and **233** were recorded at 123 K on a diffractometer using Cu ($\lambda = 1.5418 \text{ \AA}$) radiation. All structures were determined using SHELX-97 (Sheldrick, G. M. *Acta Crystallogr. A*, 2008, 64, 112) and selected crystallographic and refinement parameters are attached.

E-4-(diphenylacetyloxy)cyclohexyl diphenylacetate **232**

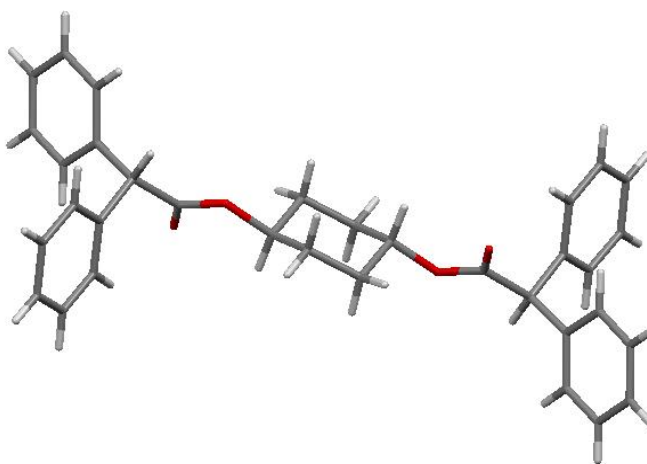


Table 1. Crystal data and structure refinement for tomk_tamasz2.

Identification code	tomk_tamasz2	
Empirical formula	C ₃₄ H ₃₂ O ₄	
Formula weight	504.60	
Temperature	123(2) K	
Wavelength	1.54180 \AA	
Crystal system	Monoclinic	
Space group	P2 ₁ /n	
Unit cell dimensions	a = 6.0330(18) \AA	$\alpha = 90^\circ$.
	b = 16.4817(5) \AA	$\beta = 97.478(3)^\circ$.
	c = 13.6747(4) \AA	$\gamma = 90^\circ$.
Volume	1348.2(4) \AA^3	
Z	2	

Density (calculated)	1.243 Mg/m ³
Absorption coefficient	0.637 mm ⁻¹
F(000)	536
Crystal size	0.35 x 0.20 x 0.10 mm ³
Theta range for data collection	4.22 to 73.16°.
Index ranges	-7<=h<=7, -20<=k<=19, -16<=l<=11
Reflections collected	5427
Independent reflections	2644 [R(int) = 0.0288]
Completeness to theta = 70.00°	99.5 %
Absorption correction	Semi-empirical from equivalents
Max. and min. transmission	1.00000 and 0.82982
Refinement method	Full-matrix least-squares on F ²
Data / restraints / parameters	2644 / 32 / 200
Goodness-of-fit on F ²	1.037
Final R indices [I>2sigma(I)]	R1 = 0.0407, wR2 = 0.1029
R indices (all data)	R1 = 0.0511, wR2 = 0.1115
Largest diff. peak and hole	0.242 and -0.193 e.Å ⁻³

Table 2. Atomic coordinates (x 10⁴) and equivalent isotropic displacement parameters (Å²x 10³) for tomk_tamasz2. U(eq) is defined as one third of the trace of the orthogonalized U^{ij} tensor.

	x	y	z	U(eq)
O(1)	5940(2)	1222(1)	3691(1)	38(1)
O(2)	8989(2)	1852(1)	4449(1)	34(1)
C(1)	4978(4)	179(1)	6050(1)	33(1)
C(2)	5041(4)	860(1)	5291(2)	32(1)
C(3)	6161(5)	568(2)	4428(2)	26(1)
C(4)	7525(2)	1795(1)	3770(1)	26(1)
C(5)	7228(2)	2334(1)	2854(1)	25(1)
C(6)	7559(2)	3228(1)	3114(1)	26(1)
C(7)	5750(3)	3752(1)	2946(1)	35(1)
C(8)	5996(3)	4569(1)	3197(1)	45(1)
C(9)	8034(3)	4862(1)	3614(1)	45(1)
C(10)	9859(3)	4347(1)	3773(1)	40(1)
C(11)	9623(3)	3532(1)	3514(1)	31(1)
C(12)	8748(2)	2051(1)	2113(1)	25(1)

C(13)	8076(2)	2201(1)	1117(1)	31(1)
C(14)	9426(3)	1969(1)	419(1)	38(1)
C(15)	11440(3)	1577(1)	699(1)	36(1)
C(16)	12109(2)	1425(1)	1686(1)	31(1)
C(17)	10784(2)	1666(1)	2393(1)	28(1)
C(3A)	5674(11)	776(5)	4655(6)	26(2)
C(2A)	3244(8)	616(3)	4740(4)	30(1)
C(1A)	6927(9)	2(3)	4428(4)	29(1)

Table 3. Bond lengths [\AA] and angles [$^\circ$] for tomk_tamasz2.

O(1)-C(4)	1.3378(16)
O(1)-C(3)	1.471(3)
O(1)-C(3A)	1.536(9)
O(2)-C(4)	1.1986(17)
C(1)-C(3)#1	1.515(3)
C(1)-C(2)	1.533(2)
C(1)-H(1A)	0.9900
C(1)-H(1B)	0.9900
C(2)-C(3)	1.512(3)
C(2)-H(2A)	0.9900
C(2)-H(2B)	0.9900
C(3)-C(1)#1	1.515(3)
C(3)-H(3)	1.0000
C(4)-C(5)	1.5274(17)
C(5)-C(6)	1.5227(18)
C(5)-C(12)	1.5259(18)
C(5)-H(5)	1.0000
C(6)-C(11)	1.387(2)
C(6)-C(7)	1.387(2)
C(7)-C(8)	1.392(2)
C(7)-H(7)	0.9500
C(8)-C(9)	1.374(3)
C(8)-H(8)	0.9500
C(9)-C(10)	1.384(2)
C(9)-H(9)	0.9500
C(10)-C(11)	1.393(2)

C(10)-H(10)	0.9500
C(11)-H(11)	0.9500
C(12)-C(17)	1.391(2)
C(12)-C(13)	1.3918(19)
C(13)-C(14)	1.386(2)
C(13)-H(13)	0.9500
C(14)-C(15)	1.386(2)
C(14)-H(14)	0.9500
C(15)-C(16)	1.381(2)
C(15)-H(15)	0.9500
C(16)-C(17)	1.391(2)
C(16)-H(16)	0.9500
C(17)-H(17)	0.9500
C(3A)-C(2A)	1.509(7)
C(3A)-C(1A)	1.534(6)
C(3A)-H(3A)	1.0000
C(2A)-C(1A)#1	1.541(7)
C(2A)-H(2A1)	0.9900
C(2A)-H(2A2)	0.9900
C(1A)-C(2A)#1	1.541(7)
C(1A)-H(1A1)	0.9900
C(1A)-H(1A2)	0.9900
C(4)-O(1)-C(3)	117.50(14)
C(4)-O(1)-C(3A)	114.9(3)
C(3)-O(1)-C(3A)	21.7(2)
C(3)#1-C(1)-C(2)	110.63(17)
C(3)#1-C(1)-H(1A)	109.5
C(2)-C(1)-H(1A)	109.5
C(3)#1-C(1)-H(1B)	109.5
C(2)-C(1)-H(1B)	109.5
H(1A)-C(1)-H(1B)	108.1
C(3)-C(2)-C(1)	110.31(19)
C(3)-C(2)-H(2A)	109.6
C(1)-C(2)-H(2A)	109.6
C(3)-C(2)-H(2B)	109.6
C(1)-C(2)-H(2B)	109.6

H(2A)-C(2)-H(2B)	108.1
O(1)-C(3)-C(2)	106.92(19)
O(1)-C(3)-C(1)#1	107.69(19)
C(2)-C(3)-C(1)#1	111.8(2)
O(1)-C(3)-H(3)	110.1
C(2)-C(3)-H(3)	110.1
C(1)#1-C(3)-H(3)	110.1
O(2)-C(4)-O(1)	124.40(12)
O(2)-C(4)-C(5)	125.83(12)
O(1)-C(4)-C(5)	109.73(11)
C(6)-C(5)-C(12)	112.29(10)
C(6)-C(5)-C(4)	111.96(11)
C(12)-C(5)-C(4)	110.51(11)
C(6)-C(5)-H(5)	107.3
C(12)-C(5)-H(5)	107.3
C(4)-C(5)-H(5)	107.3
C(11)-C(6)-C(7)	119.12(13)
C(11)-C(6)-C(5)	121.67(12)
C(7)-C(6)-C(5)	119.21(13)
C(6)-C(7)-C(8)	120.37(16)
C(6)-C(7)-H(7)	119.8
C(8)-C(7)-H(7)	119.8
C(9)-C(8)-C(7)	120.19(16)
C(9)-C(8)-H(8)	119.9
C(7)-C(8)-H(8)	119.9
C(8)-C(9)-C(10)	120.03(14)
C(8)-C(9)-H(9)	120.0
C(10)-C(9)-H(9)	120.0
C(9)-C(10)-C(11)	119.89(16)
C(9)-C(10)-H(10)	120.1
C(11)-C(10)-H(10)	120.1
C(6)-C(11)-C(10)	120.38(15)
C(6)-C(11)-H(11)	119.8
C(10)-C(11)-H(11)	119.8
C(17)-C(12)-C(13)	119.02(12)
C(17)-C(12)-C(5)	122.80(11)
C(13)-C(12)-C(5)	118.17(13)

C(14)-C(13)-C(12)	120.14(14)
C(14)-C(13)-H(13)	119.9
C(12)-C(13)-H(13)	119.9
C(15)-C(14)-C(13)	120.75(13)
C(15)-C(14)-H(14)	119.6
C(13)-C(14)-H(14)	119.6
C(16)-C(15)-C(14)	119.26(13)
C(16)-C(15)-H(15)	120.4
C(14)-C(15)-H(15)	120.4
C(15)-C(16)-C(17)	120.45(14)
C(15)-C(16)-H(16)	119.8
C(17)-C(16)-H(16)	119.8
C(16)-C(17)-C(12)	120.37(13)
C(16)-C(17)-H(17)	119.8
C(12)-C(17)-H(17)	119.8
C(2A)-C(3A)-C(1A)	112.3(6)
C(2A)-C(3A)-O(1)	111.1(6)
C(1A)-C(3A)-O(1)	96.6(4)
C(2A)-C(3A)-H(3A)	112.0
C(1A)-C(3A)-H(3A)	112.0
O(1)-C(3A)-H(3A)	112.0
C(3A)-C(2A)-C(1A)#1	109.4(5)
C(3A)-C(2A)-H(2A1)	109.8
C(1A)#1-C(2A)-H(2A1)	109.8
C(3A)-C(2A)-H(2A2)	109.8
C(1A)#1-C(2A)-H(2A2)	109.8
H(2A1)-C(2A)-H(2A2)	108.2
C(3A)-C(1A)-C(2A)#1	108.5(5)
C(3A)-C(1A)-H(1A1)	110.0
C(2A)#1-C(1A)-H(1A1)	110.0
C(3A)-C(1A)-H(1A2)	110.0
C(2A)#1-C(1A)-H(1A2)	110.0
H(1A1)-C(1A)-H(1A2)	108.4

Symmetry transformations used to generate equivalent atoms: #1 -x+1,-y,-z+1

Table 4. Anisotropic displacement parameters ($\text{\AA}^2 \times 10^3$) for tomk_tamasz2. The anisotropic displacement factor exponent takes the form: $-2\pi^2 [h^2 a^{*2} U^{11} + \dots + 2 h k a^* b^* U^{12}]$

	U ¹¹	U ²²	U ³³	U ²³	U ¹³	U ¹²
O(1)	43(1)	36(1)	32(1)	14(1)	-3(1)	-15(1)
O(2)	41(1)	34(1)	26(1)	5(1)	-1(1)	-9(1)
C(1)	50(1)	27(1)	23(1)	0(1)	12(1)	-8(1)
C(2)	47(1)	21(1)	28(1)	0(1)	10(1)	-4(1)
C(3)	35(1)	24(2)	19(1)	5(1)	7(1)	-3(1)
C(4)	30(1)	24(1)	25(1)	0(1)	7(1)	-2(1)
C(5)	28(1)	24(1)	24(1)	3(1)	3(1)	-3(1)
C(6)	34(1)	24(1)	23(1)	3(1)	11(1)	-1(1)
C(7)	37(1)	33(1)	38(1)	7(1)	13(1)	4(1)
C(8)	58(1)	30(1)	54(1)	7(1)	26(1)	13(1)
C(9)	75(1)	22(1)	45(1)	-2(1)	31(1)	-3(1)
C(10)	55(1)	32(1)	36(1)	-5(1)	16(1)	-13(1)
C(11)	37(1)	27(1)	32(1)	-1(1)	9(1)	-2(1)
C(12)	31(1)	20(1)	24(1)	0(1)	5(1)	-7(1)
C(13)	35(1)	32(1)	26(1)	3(1)	2(1)	-5(1)
C(14)	47(1)	43(1)	22(1)	0(1)	4(1)	-9(1)
C(15)	44(1)	35(1)	31(1)	-8(1)	14(1)	-10(1)
C(16)	33(1)	25(1)	36(1)	-5(1)	6(1)	-4(1)
C(17)	34(1)	24(1)	24(1)	0(1)	2(1)	-4(1)
C(3A)	29(3)	24(4)	25(5)	-3(3)	10(3)	0(2)
C(2A)	29(3)	26(2)	36(3)	12(2)	12(2)	2(2)
C(1A)	33(3)	25(3)	30(3)	7(2)	14(2)	4(2)

Table 5. Hydrogen coordinates ($\times 10^4$) and isotropic displacement parameters ($\text{\AA}^2 \times 10^3$) for tomk_tamasz2.

	x	y	z	U(eq)
H(1A)	6522	40	6338	39
H(1B)	4160	367	6590	39
H(2A)	3498	1039	5053	38
H(2B)	5872	1330	5605	38
H(3)	7776	452	4648	31

H(5)	5650	2267	2536	30
H(7)	4337	3553	2658	42
H(8)	4750	4925	3080	55
H(9)	8191	5418	3793	54
H(10)	11270	4550	4059	48
H(11)	10883	3181	3611	38
H(13)	6690	2464	915	38
H(14)	8965	2081	-259	45
H(15)	12351	1414	216	43
H(16)	13483	1153	1883	37
H(17)	11273	1568	3072	33
H(3A)	6442	1067	5245	31
H(2A1)	2486	400	4108	36
H(2A2)	2498	1129	4886	36
H(1A1)	8515	129	4386	34
H(1A2)	6259	-227	3788	34

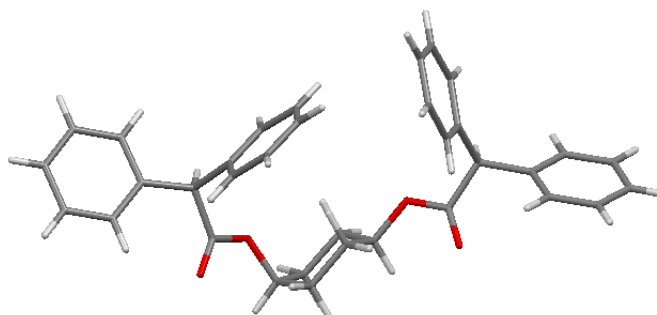
Table 6. Torsion angles [°] for tomk_tamasz2.

C(3)#1-C(1)-C(2)-C(3)	-55.7(3)
C(4)-O(1)-C(3)-C(2)	87.6(2)
C(3A)-O(1)-C(3)-C(2)	-1.1(8)
C(4)-O(1)-C(3)-C(1)#1	-152.07(16)
C(3A)-O(1)-C(3)-C(1)#1	119.3(10)
C(1)-C(2)-C(3)-O(1)	174.08(17)
C(1)-C(2)-C(3)-C(1)#1	56.4(3)
C(3)-O(1)-C(4)-O(2)	-7.2(2)
C(3A)-O(1)-C(4)-O(2)	16.8(3)
C(3)-O(1)-C(4)-C(5)	170.61(16)
C(3A)-O(1)-C(4)-C(5)	-165.4(3)
O(2)-C(4)-C(5)-C(6)	-44.48(19)
O(1)-C(4)-C(5)-C(6)	137.72(12)
O(2)-C(4)-C(5)-C(12)	81.50(17)
O(1)-C(4)-C(5)-C(12)	-96.30(13)
C(12)-C(5)-C(6)-C(11)	-58.37(16)
C(4)-C(5)-C(6)-C(11)	66.63(16)
C(12)-C(5)-C(6)-C(7)	121.59(13)

C(4)-C(5)-C(6)-C(7)	-113.41(14)
C(11)-C(6)-C(7)-C(8)	-1.5(2)
C(5)-C(6)-C(7)-C(8)	178.59(13)
C(6)-C(7)-C(8)-C(9)	0.0(2)
C(7)-C(8)-C(9)-C(10)	0.9(2)
C(8)-C(9)-C(10)-C(11)	-0.2(2)
C(7)-C(6)-C(11)-C(10)	2.1(2)
C(5)-C(6)-C(11)-C(10)	-177.95(12)
C(9)-C(10)-C(11)-C(6)	-1.3(2)
C(6)-C(5)-C(12)-C(17)	96.39(14)
C(4)-C(5)-C(12)-C(17)	-29.40(16)
C(6)-C(5)-C(12)-C(13)	-82.19(15)
C(4)-C(5)-C(12)-C(13)	152.02(12)
C(17)-C(12)-C(13)-C(14)	0.0(2)
C(5)-C(12)-C(13)-C(14)	178.68(13)
C(12)-C(13)-C(14)-C(15)	0.8(2)
C(13)-C(14)-C(15)-C(16)	-0.7(2)
C(14)-C(15)-C(16)-C(17)	-0.4(2)
C(15)-C(16)-C(17)-C(12)	1.3(2)
C(13)-C(12)-C(17)-C(16)	-1.08(19)
C(5)-C(12)-C(17)-C(16)	-179.64(12)
C(4)-O(1)-C(3A)-C(2A)	140.9(4)
C(3)-O(1)-C(3A)-C(2A)	-117.0(12)
C(4)-O(1)-C(3A)-C(1A)	-102.1(4)
C(3)-O(1)-C(3A)-C(1A)	0.0(6)
C(1A)-C(3A)-C(2A)-C(1A)#1	59.4(8)
O(1)-C(3A)-C(2A)-C(1A)#1	166.4(5)
C(2A)-C(3A)-C(1A)-C(2A)#1	-59.0(8)
O(1)-C(3A)-C(1A)-C(2A)#1	-175.1(4)

Symmetry transformations used to generate equivalent atoms:

#1 -x+1,-y,-z+1

Z-4-(diphenylacetyloxy)cyclohexyl diphenylacetate 233**Table 1.** Crystal data and structure refinement for tmk209_3.

Identification code	tmk209_3	
Empirical formula	C ₃₄ H ₃₂ O ₄	
Formula weight	504.60	
Temperature	123(2) K	
Wavelength	1.54180 Å	
Crystal system	Monoclinic	
Space group	P2 ₁ /c	
Unit cell dimensions	a = 25.0132(10) Å	α = 90°.
	b = 6.1475(2) Å	β = 93.702(4)°.
	c = 17.1534(9) Å	γ = 90°.
Volume	2632.15(19) Å ³	
Z	4	
Density (calculated)	1.273 Mg/m ³	
Absorption coefficient	0.652 mm ⁻¹	
F(000)	1072	
Crystal size	0.30 x 0.15 x 0.05 mm ³	
Theta range for data collection	5.17 to 73.07°.	
Index ranges	-31 ≤ h ≤ 29, -7 ≤ k ≤ 7, -21 ≤ l ≤ 14	
Reflections collected	10952	
Independent reflections	5178 [R(int) = 0.0201]	
Completeness to theta = 70.00°	99.7 %	
Absorption correction	Semi-empirical from equivalents	
Max. and min. transmission	1.00000 and 0.76311	

Refinement method	Full-matrix least-squares on F ²
Data / restraints / parameters	5178 / 0 / 343
Goodness-of-fit on F ²	1.048
Final R indices [I>2sigma(I)]	R1 = 0.0429, wR2 = 0.1095
R indices (all data)	R1 = 0.0530, wR2 = 0.1178
Largest diff. peak and hole	0.267 and -0.230 e.Å ⁻³

Table 2. Atomic coordinates ($\times 10^4$) and equivalent isotropic displacement parameters ($\text{\AA}^2 \times 10^3$) for tmk209_3. U(eq) is defined as one third of the trace of the orthogonalized U^{ij} tensor.

	x	y	z	U(eq)
O(1)	1663(1)	374(2)	3010(1)	36(1)
O(2)	2306(1)	2577(2)	2595(1)	28(1)
O(3)	3774(1)	-466(2)	1587(1)	27(1)
O(4)	3934(1)	-3605(2)	970(1)	35(1)
C(1)	1800(1)	2103(2)	2761(1)	27(1)
C(2)	1438(1)	4056(2)	2579(1)	27(1)
C(3)	928(1)	4010(2)	3019(1)	27(1)
C(4)	808(1)	5808(3)	3470(1)	31(1)
C(5)	346(1)	5833(3)	3882(1)	36(1)
C(6)	7(1)	4064(3)	3853(1)	36(1)
C(7)	116(1)	2284(3)	3396(1)	36(1)
C(8)	575(1)	2256(3)	2978(1)	32(1)
C(9)	1326(1)	4258(2)	1695(1)	26(1)
C(10)	1160(1)	2505(3)	1232(1)	34(1)
C(11)	1055(1)	2755(3)	432(1)	37(1)
C(12)	1126(1)	4741(3)	81(1)	36(1)
C(13)	1292(1)	6498(3)	535(1)	39(1)
C(14)	1385(1)	6258(3)	1339(1)	33(1)
C(15)	2695(1)	822(2)	2717(1)	29(1)
C(16)	2654(1)	-739(3)	2035(1)	33(1)
C(17)	3070(1)	-2543(3)	2162(1)	36(1)
C(18)	3633(1)	-1628(3)	2289(1)	31(1)
C(19)	3671(1)	69(3)	2930(1)	33(1)
C(20)	3246(1)	1851(3)	2812(1)	29(1)
C(21)	3888(1)	-1655(2)	964(1)	26(1)

C(22)	3912(1)	-141(2)	267(1)	26(1)
C(23)	3328(1)	229(2)	-35(1)	26(1)
C(24)	3084(1)	2215(3)	92(1)	33(1)
C(25)	2544(1)	2524(3)	-136(1)	36(1)
C(26)	2250(1)	861(3)	-491(1)	34(1)
C(27)	2491(1)	-1115(3)	-624(1)	34(1)
C(28)	3029(1)	-1438(3)	-393(1)	30(1)
C(29)	4281(1)	-805(3)	-365(1)	27(1)
C(30)	4420(1)	814(3)	-878(1)	38(1)
C(31)	4773(1)	413(3)	-1454(1)	46(1)
C(32)	4993(1)	-1623(3)	-1525(1)	39(1)
C(33)	4857(1)	-3251(3)	-1027(1)	39(1)
C(34)	4501(1)	-2853(3)	-451(1)	36(1)

Table 3. Bond lengths [\AA] and angles [$^\circ$] for tmk209_3.

O(1)-C(1)	1.2030(18)
O(2)-C(1)	1.3454(17)
O(2)-C(15)	1.4588(17)
O(3)-C(21)	1.3401(17)
O(3)-C(18)	1.4631(17)
O(4)-C(21)	1.2046(18)
C(1)-C(2)	1.524(2)
C(2)-C(3)	1.525(2)
C(2)-C(9)	1.529(2)
C(2)-H(2)	1.0000
C(3)-C(4)	1.393(2)
C(3)-C(8)	1.393(2)
C(4)-C(5)	1.395(2)
C(4)-H(4)	0.9500
C(5)-C(6)	1.379(2)
C(5)-H(5)	0.9500
C(6)-C(7)	1.384(2)
C(6)-H(6)	0.9500
C(7)-C(8)	1.392(2)
C(7)-H(7)	0.9500
C(8)-H(8)	0.9500

C(9)-C(14)	1.385(2)
C(9)-C(10)	1.386(2)
C(10)-C(11)	1.390(2)
C(10)-H(10)	0.9500
C(11)-C(12)	1.377(2)
C(11)-H(11)	0.9500
C(12)-C(13)	1.379(2)
C(12)-H(12)	0.9500
C(13)-C(14)	1.391(2)
C(13)-H(13)	0.9500
C(14)-H(14)	0.9500
C(15)-C(16)	1.512(2)
C(15)-C(20)	1.516(2)
C(15)-H(15)	1.0000
C(16)-C(17)	1.528(2)
C(16)-H(16A)	0.9900
C(16)-H(16B)	0.9900
C(17)-C(18)	1.518(2)
C(17)-H(17A)	0.9900
C(17)-H(17B)	0.9900
C(18)-C(19)	1.515(2)
C(18)-H(18)	1.0000
C(19)-C(20)	1.532(2)
C(19)-H(19A)	0.9900
C(19)-H(19B)	0.9900
C(20)-H(20A)	0.9900
C(20)-H(20B)	0.9900
C(21)-C(22)	1.519(2)
C(22)-C(29)	1.525(2)
C(22)-C(23)	1.5354(19)
C(22)-H(22)	1.0000
C(23)-C(28)	1.388(2)
C(23)-C(24)	1.388(2)
C(24)-C(25)	1.395(2)
C(24)-H(24)	0.9500
C(25)-C(26)	1.378(2)
C(25)-H(25)	0.9500

C(26)-C(27)	1.382(2)
C(26)-H(26)	0.9500
C(27)-C(28)	1.391(2)
C(27)-H(27)	0.9500
C(28)-H(28)	0.9500
C(29)-C(34)	1.385(2)
C(29)-C(30)	1.387(2)
C(30)-C(31)	1.390(2)
C(30)-H(30)	0.9500
C(31)-C(32)	1.375(3)
C(31)-H(31)	0.9500
C(32)-C(33)	1.373(3)
C(32)-H(32)	0.9500
C(33)-C(34)	1.395(2)
C(33)-H(33)	0.9500
C(34)-H(34)	0.9500
C(1)-O(2)-C(15)	115.88(11)
C(21)-O(3)-C(18)	117.69(12)
O(1)-C(1)-O(2)	124.02(13)
O(1)-C(1)-C(2)	126.11(13)
O(2)-C(1)-C(2)	109.87(12)
C(1)-C(2)-C(3)	112.89(12)
C(1)-C(2)-C(9)	109.70(12)
C(3)-C(2)-C(9)	112.71(11)
C(1)-C(2)-H(2)	107.1
C(3)-C(2)-H(2)	107.1
C(9)-C(2)-H(2)	107.1
C(4)-C(3)-C(8)	118.98(14)
C(4)-C(3)-C(2)	118.47(13)
C(8)-C(3)-C(2)	122.54(13)
C(3)-C(4)-C(5)	120.36(15)
C(3)-C(4)-H(4)	119.8
C(5)-C(4)-H(4)	119.8
C(6)-C(5)-C(4)	120.08(15)
C(6)-C(5)-H(5)	120.0
C(4)-C(5)-H(5)	120.0

C(5)-C(6)-C(7)	120.08(15)
C(5)-C(6)-H(6)	120.0
C(7)-C(6)-H(6)	120.0
C(6)-C(7)-C(8)	120.08(16)
C(6)-C(7)-H(7)	120.0
C(8)-C(7)-H(7)	120.0
C(7)-C(8)-C(3)	120.39(15)
C(7)-C(8)-H(8)	119.8
C(3)-C(8)-H(8)	119.8
C(14)-C(9)-C(10)	118.31(14)
C(14)-C(9)-C(2)	119.44(13)
C(10)-C(9)-C(2)	122.25(13)
C(9)-C(10)-C(11)	120.67(15)
C(9)-C(10)-H(10)	119.7
C(11)-C(10)-H(10)	119.7
C(12)-C(11)-C(10)	120.52(15)
C(12)-C(11)-H(11)	119.7
C(10)-C(11)-H(11)	119.7
C(11)-C(12)-C(13)	119.36(15)
C(11)-C(12)-H(12)	120.3
C(13)-C(12)-H(12)	120.3
C(12)-C(13)-C(14)	120.11(15)
C(12)-C(13)-H(13)	119.9
C(14)-C(13)-H(13)	119.9
C(9)-C(14)-C(13)	121.00(15)
C(9)-C(14)-H(14)	119.5
C(13)-C(14)-H(14)	119.5
O(2)-C(15)-C(16)	110.30(12)
O(2)-C(15)-C(20)	107.46(12)
C(16)-C(15)-C(20)	111.34(12)
O(2)-C(15)-H(15)	109.2
C(16)-C(15)-H(15)	109.2
C(20)-C(15)-H(15)	109.2
C(15)-C(16)-C(17)	109.77(13)
C(15)-C(16)-H(16A)	109.7
C(17)-C(16)-H(16A)	109.7
C(15)-C(16)-H(16B)	109.7

C(17)-C(16)-H(16B)	109.7
H(16A)-C(16)-H(16B)	108.2
C(18)-C(17)-C(16)	111.70(13)
C(18)-C(17)-H(17A)	109.3
C(16)-C(17)-H(17A)	109.3
C(18)-C(17)-H(17B)	109.3
C(16)-C(17)-H(17B)	109.3
H(17A)-C(17)-H(17B)	107.9
O(3)-C(18)-C(19)	104.71(12)
O(3)-C(18)-C(17)	109.47(12)
C(19)-C(18)-C(17)	111.96(13)
O(3)-C(18)-H(18)	110.2
C(19)-C(18)-H(18)	110.2
C(17)-C(18)-H(18)	110.2
C(18)-C(19)-C(20)	112.70(12)
C(18)-C(19)-H(19A)	109.1
C(20)-C(19)-H(19A)	109.1
C(18)-C(19)-H(19B)	109.1
C(20)-C(19)-H(19B)	109.1
H(19A)-C(19)-H(19B)	107.8
C(15)-C(20)-C(19)	109.56(13)
C(15)-C(20)-H(20A)	109.8
C(19)-C(20)-H(20A)	109.8
C(15)-C(20)-H(20B)	109.8
C(19)-C(20)-H(20B)	109.8
H(20A)-C(20)-H(20B)	108.2
O(4)-C(21)-O(3)	124.17(14)
O(4)-C(21)-C(22)	127.40(14)
O(3)-C(21)-C(22)	108.33(12)
C(21)-C(22)-C(29)	116.91(12)
C(21)-C(22)-C(23)	105.71(11)
C(29)-C(22)-C(23)	113.98(12)
C(21)-C(22)-H(22)	106.5
C(29)-C(22)-H(22)	106.5
C(23)-C(22)-H(22)	106.5
C(28)-C(23)-C(24)	119.25(14)
C(28)-C(23)-C(22)	120.93(13)

C(24)-C(23)-C(22)	119.70(13)
C(23)-C(24)-C(25)	120.20(15)
C(23)-C(24)-H(24)	119.9
C(25)-C(24)-H(24)	119.9
C(26)-C(25)-C(24)	120.14(15)
C(26)-C(25)-H(25)	119.9
C(24)-C(25)-H(25)	119.9
C(25)-C(26)-C(27)	119.96(14)
C(25)-C(26)-H(26)	120.0
C(27)-C(26)-H(26)	120.0
C(26)-C(27)-C(28)	120.15(15)
C(26)-C(27)-H(27)	119.9
C(28)-C(27)-H(27)	119.9
C(23)-C(28)-C(27)	120.29(14)
C(23)-C(28)-H(28)	119.9
C(27)-C(28)-H(28)	119.9
C(34)-C(29)-C(30)	117.89(15)
C(34)-C(29)-C(22)	125.53(14)
C(30)-C(29)-C(22)	116.55(14)
C(29)-C(30)-C(31)	121.36(17)
C(29)-C(30)-H(30)	119.3
C(31)-C(30)-H(30)	119.3
C(32)-C(31)-C(30)	120.04(17)
C(32)-C(31)-H(31)	120.0
C(30)-C(31)-H(31)	120.0
C(33)-C(32)-C(31)	119.45(15)
C(33)-C(32)-H(32)	120.3
C(31)-C(32)-H(32)	120.3
C(32)-C(33)-C(34)	120.56(17)
C(32)-C(33)-H(33)	119.7
C(34)-C(33)-H(33)	119.7
C(29)-C(34)-C(33)	120.68(16)
C(29)-C(34)-H(34)	119.7
C(33)-C(34)-H(34)	119.7

Symmetry transformations used to generate equivalent atoms:

Table 4. Anisotropic displacement parameters ($\text{\AA}^2 \times 10^3$) for tmk209_3. The anisotropic displacement factor exponent takes the form: $-2\pi^2 [h^2 a^{*2} U^{11} + \dots + 2 h k a^* b^* U^{12}]$

	U ¹¹	U ²²	U ³³	U ²³	U ¹³	U ¹²
O(1)	29(1)	30(1)	50(1)	7(1)	8(1)	1(1)
O(2)	23(1)	29(1)	33(1)	4(1)	3(1)	3(1)
O(3)	27(1)	30(1)	24(1)	2(1)	3(1)	1(1)
O(4)	41(1)	30(1)	35(1)	2(1)	8(1)	6(1)
C(1)	24(1)	30(1)	27(1)	-2(1)	1(1)	-1(1)
C(2)	24(1)	25(1)	30(1)	-3(1)	-1(1)	-1(1)
C(3)	24(1)	31(1)	25(1)	1(1)	-3(1)	4(1)
C(4)	31(1)	32(1)	29(1)	0(1)	-2(1)	2(1)
C(5)	37(1)	41(1)	30(1)	-2(1)	2(1)	10(1)
C(6)	27(1)	50(1)	32(1)	5(1)	4(1)	7(1)
C(7)	25(1)	43(1)	38(1)	4(1)	-1(1)	-1(1)
C(8)	28(1)	35(1)	33(1)	-3(1)	-1(1)	2(1)
C(9)	20(1)	28(1)	31(1)	-1(1)	2(1)	2(1)
C(10)	40(1)	28(1)	33(1)	-1(1)	3(1)	-3(1)
C(11)	41(1)	36(1)	34(1)	-6(1)	0(1)	-3(1)
C(12)	33(1)	45(1)	29(1)	4(1)	1(1)	5(1)
C(13)	38(1)	36(1)	42(1)	11(1)	0(1)	-2(1)
C(14)	30(1)	29(1)	39(1)	1(1)	-3(1)	-3(1)
C(15)	25(1)	31(1)	31(1)	6(1)	4(1)	6(1)
C(16)	25(1)	31(1)	45(1)	-5(1)	5(1)	-4(1)
C(17)	38(1)	27(1)	45(1)	1(1)	16(1)	-1(1)
C(18)	32(1)	34(1)	29(1)	10(1)	7(1)	8(1)
C(19)	27(1)	48(1)	24(1)	5(1)	1(1)	8(1)
C(20)	27(1)	36(1)	25(1)	-2(1)	1(1)	2(1)
C(21)	20(1)	31(1)	27(1)	-2(1)	1(1)	2(1)
C(22)	25(1)	28(1)	26(1)	0(1)	0(1)	0(1)
C(23)	26(1)	32(1)	21(1)	2(1)	3(1)	2(1)
C(24)	34(1)	29(1)	34(1)	0(1)	0(1)	1(1)
C(25)	35(1)	34(1)	40(1)	3(1)	2(1)	9(1)
C(26)	26(1)	46(1)	31(1)	5(1)	1(1)	6(1)
C(27)	29(1)	41(1)	30(1)	-4(1)	0(1)	-2(1)
C(28)	30(1)	31(1)	29(1)	-2(1)	3(1)	2(1)

C(29)	21(1)	38(1)	23(1)	-3(1)	-2(1)	-2(1)
C(30)	39(1)	43(1)	34(1)	5(1)	7(1)	4(1)
C(31)	46(1)	58(1)	34(1)	6(1)	12(1)	-2(1)
C(32)	26(1)	64(1)	28(1)	-12(1)	4(1)	-6(1)
C(33)	32(1)	48(1)	37(1)	-9(1)	3(1)	2(1)
C(34)	35(1)	39(1)	34(1)	-2(1)	5(1)	0(1)

Table 5. Hydrogen coordinates ($\times 10^4$) and isotropic displacement parameters ($\text{\AA}^2 \times 10^3$) for tmk209_3.

	x	y	z	U(eq)
H(2)	1643	5382	2756	32
H(4)	1043	7024	3496	37
H(5)	265	7071	4185	43
H(6)	-303	4067	4146	43
H(7)	-123	1079	3367	43
H(8)	647	1034	2662	38
H(10)	1117	1119	1465	40
H(11)	933	1547	124	44
H(12)	1061	4899	-468	43
H(13)	1342	7873	298	47
H(14)	1491	7485	1648	40
H(15)	2622	19	3206	34
H(16A)	2714	53	1546	40
H(16B)	2290	-1382	1984	40
H(17A)	2986	-3419	2622	44
H(17B)	3053	-3515	1701	44
H(18)	3894	-2829	2412	38
H(19A)	4031	745	2948	39
H(19B)	3630	-652	3439	39
H(20A)	3264	2841	3268	35
H(20B)	3313	2715	2342	35
H(22)	4047	1288	477	31
H(24)	3286	3368	334	39
H(25)	2378	3884	-46	43

H(26)	1882	1073	-645	41
H(27)	2289	-2255	-874	40
H(28)	3192	-2805	-480	36
H(30)	4270	2226	-834	46
H(31)	4863	1545	-1799	55
H(32)	5237	-1900	-1916	47
H(33)	5007	-4660	-1076	47
H(34)	4407	-3999	-114	43

Table 6. Torsion angles [°] for tmk209_3.

C(15)-O(2)-C(1)-O(1)	1.3(2)
C(15)-O(2)-C(1)-C(2)	-177.97(11)
O(1)-C(1)-C(2)-C(3)	22.5(2)
O(2)-C(1)-C(2)-C(3)	-158.23(12)
O(1)-C(1)-C(2)-C(9)	-104.11(17)
O(2)-C(1)-C(2)-C(9)	75.16(15)
C(1)-C(2)-C(3)-C(4)	125.60(14)
C(9)-C(2)-C(3)-C(4)	-109.42(15)
C(1)-C(2)-C(3)-C(8)	-55.35(18)
C(9)-C(2)-C(3)-C(8)	69.64(18)
C(8)-C(3)-C(4)-C(5)	1.0(2)
C(2)-C(3)-C(4)-C(5)	-179.95(13)
C(3)-C(4)-C(5)-C(6)	0.7(2)
C(4)-C(5)-C(6)-C(7)	-1.8(2)
C(5)-C(6)-C(7)-C(8)	1.3(2)
C(6)-C(7)-C(8)-C(3)	0.3(2)
C(4)-C(3)-C(8)-C(7)	-1.5(2)
C(2)-C(3)-C(8)-C(7)	179.49(14)
C(1)-C(2)-C(9)-C(14)	-131.65(14)
C(3)-C(2)-C(9)-C(14)	101.64(16)
C(1)-C(2)-C(9)-C(10)	49.01(18)
C(3)-C(2)-C(9)-C(10)	-77.69(18)
C(14)-C(9)-C(10)-C(11)	-0.1(2)
C(2)-C(9)-C(10)-C(11)	179.24(15)
C(9)-C(10)-C(11)-C(12)	1.5(3)
C(10)-C(11)-C(12)-C(13)	-1.4(3)

C(11)-C(12)-C(13)-C(14)	-0.1(3)
C(10)-C(9)-C(14)-C(13)	-1.4(2)
C(2)-C(9)-C(14)-C(13)	179.29(14)
C(12)-C(13)-C(14)-C(9)	1.5(3)
C(1)-O(2)-C(15)-C(16)	80.26(15)
C(1)-O(2)-C(15)-C(20)	-158.19(12)
O(2)-C(15)-C(16)-C(17)	178.85(12)
C(20)-C(15)-C(16)-C(17)	59.64(17)
C(15)-C(16)-C(17)-C(18)	-56.12(18)
C(21)-O(3)-C(18)-C(19)	165.72(11)
C(21)-O(3)-C(18)-C(17)	-74.09(15)
C(16)-C(17)-C(18)-O(3)	-63.09(17)
C(16)-C(17)-C(18)-C(19)	52.56(18)
O(3)-C(18)-C(19)-C(20)	66.64(15)
C(17)-C(18)-C(19)-C(20)	-51.87(18)
O(2)-C(15)-C(20)-C(19)	-179.17(11)
C(16)-C(15)-C(20)-C(19)	-58.28(16)
C(18)-C(19)-C(20)-C(15)	54.14(17)
C(18)-O(3)-C(21)-O(4)	-7.8(2)
C(18)-O(3)-C(21)-C(22)	168.86(11)
O(4)-C(21)-C(22)-C(29)	-32.5(2)
O(3)-C(21)-C(22)-C(29)	150.99(12)
O(4)-C(21)-C(22)-C(23)	95.55(17)
O(3)-C(21)-C(22)-C(23)	-80.97(13)
C(21)-C(22)-C(23)-C(28)	-69.38(16)
C(29)-C(22)-C(23)-C(28)	60.39(18)
C(21)-C(22)-C(23)-C(24)	106.79(15)
C(29)-C(22)-C(23)-C(24)	-123.44(15)
C(28)-C(23)-C(24)-C(25)	0.3(2)
C(22)-C(23)-C(24)-C(25)	-175.97(14)
C(23)-C(24)-C(25)-C(26)	-0.3(2)
C(24)-C(25)-C(26)-C(27)	-0.2(2)
C(25)-C(26)-C(27)-C(28)	0.7(2)
C(24)-C(23)-C(28)-C(27)	0.2(2)
C(22)-C(23)-C(28)-C(27)	176.43(14)
C(26)-C(27)-C(28)-C(23)	-0.7(2)
C(21)-C(22)-C(29)-C(34)	15.3(2)

C(23)-C(22)-C(29)-C(34)	-108.62(17)
C(21)-C(22)-C(29)-C(30)	-162.42(13)
C(23)-C(22)-C(29)-C(30)	73.66(17)
C(34)-C(29)-C(30)-C(31)	-0.8(2)
C(22)-C(29)-C(30)-C(31)	177.06(15)
C(29)-C(30)-C(31)-C(32)	0.0(3)
C(30)-C(31)-C(32)-C(33)	0.5(3)
C(31)-C(32)-C(33)-C(34)	-0.2(3)
C(30)-C(29)-C(34)-C(33)	1.2(2)
C(22)-C(29)-C(34)-C(33)	-176.54(14)
C(32)-C(33)-C(34)-C(29)	-0.7(3)

Symmetry transformations used to generate equivalent atoms:

(1*R*, 3*R*)-3-(diphenylacetyloxy)cyclohexyl diphenylacetate 230

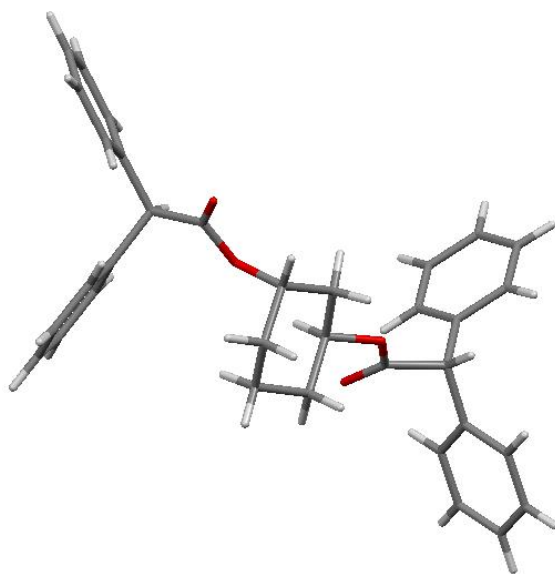


Table 1. Crystal data and structure refinement for tomk_tomaz.

Identification code	tomk_tomaz
Empirical formula	C _{37.50} H ₃₆ O ₄

Formula weight	550.66	
Temperature	123(2) K	
Wavelength	0.71073 Å	
Crystal system	Triclinic	
Space group	P-1	
Unit cell dimensions	a = 5.9715(4) Å	$\alpha = 92.539(5)^\circ$.
	b = 15.3386(11) Å	$\beta = 92.595(5)^\circ$.
	c = 16.0597(9) Å	$\gamma = 94.046(6)^\circ$.
Volume	1464.14(17) Å ³	
Z	2	
Density (calculated)	1.249 Mg/m ³	
Absorption coefficient	0.080 mm ⁻¹	
F(000)	586	
Crystal size	0.3 x 0.08 x 0.02 mm ³	
Theta range for data collection	3.01 to 27.50°.	
Index ranges	-7<=h<=7, -19<=k<=19, -20<=l<=20	
Reflections collected	13033	
Independent reflections	6477 [R(int) = 0.0333]	
Completeness to theta = 26.00°	99.7 %	
Absorption correction	Semi-empirical from equivalents	
Max. and min. transmission	1.00000 and 0.93882	
Refinement method	Full-matrix least-squares on F ²	
Data / restraints / parameters	6477 / 57 / 407	
Goodness-of-fit on F ²	1.014	
Final R indices [I>2sigma(I)]	R1 = 0.0517, wR2 = 0.0947	
R indices (all data)	R1 = 0.0890, wR2 = 0.1091	
Largest diff. peak and hole	0.223 and -0.180 e.Å ⁻³	

Table 2. Atomic coordinates ($\times 10^4$) and equivalent isotropic displacement parameters ($\text{\AA}^2 \times 10^3$) for tomk_tomaz. $U(\text{eq})$ is defined as one third of the trace of the orthogonalized U^{ij} tensor.

	x	y	z	U(eq)
O(1)	3042(2)	-1227(1)	7681(1)	33(1)
O(2)	408(2)	-2255(1)	7194(1)	30(1)
O(3)	4751(2)	1532(1)	7544(1)	23(1)
O(4)	8248(2)	1689(1)	8139(1)	28(1)
C(1)	1349(3)	-582(1)	7744(1)	30(1)
C(2)	2331(3)	252(1)	7384(1)	27(1)
C(3)	4293(3)	689(1)	7916(1)	22(1)
C(4)	3707(3)	835(1)	8817(1)	28(1)
C(5)	2870(3)	-32(1)	9171(1)	33(1)
C(6)	845(3)	-446(1)	8655(1)	37(1)
C(7)	2300(3)	-2045(1)	7437(1)	19(1)
C(8)	4208(3)	-2647(1)	7544(1)	18(1)
C(9)	4700(2)	-2745(1)	8476(1)	17(1)
C(10)	6852(3)	-2539(1)	8821(1)	24(1)
C(11)	7336(3)	-2635(1)	9666(1)	29(1)
C(12)	5678(3)	-2938(1)	10166(1)	25(1)
C(13)	3542(3)	-3142(1)	9832(1)	26(1)
C(14)	3044(3)	-3043(1)	8991(1)	24(1)
C(15)	3785(3)	-3518(1)	7054(1)	18(1)
C(16)	1803(3)	-4048(1)	7088(1)	22(1)
C(17)	1494(3)	-4833(1)	6625(1)	25(1)
C(18)	3156(3)	-5103(1)	6119(1)	28(1)
C(19)	5146(3)	-4592(1)	6095(1)	28(1)
C(20)	5458(3)	-3806(1)	6559(1)	23(1)
C(21)	6769(3)	1960(1)	7708(1)	20(1)
C(22)	6908(2)	2818(1)	7265(1)	19(1)
C(23)	8339(2)	2750(1)	6506(1)	19(1)
C(24)	10344(3)	2337(1)	6520(1)	22(1)
C(25)	11571(3)	2277(1)	5813(1)	27(1)
C(26)	10835(3)	2638(1)	5084(1)	30(1)
C(27)	8877(3)	3066(1)	5066(1)	31(1)
C(28)	7632(3)	3114(1)	5768(1)	24(1)

C(29)	7675(2)	3590(1)	7860(1)	18(1)
C(30)	9808(3)	3681(1)	8257(1)	21(1)
C(31)	10446(3)	4396(1)	8789(1)	24(1)
C(32)	8962(3)	5036(1)	8939(1)	25(1)
C(33)	6847(3)	4958(1)	8547(1)	26(1)
C(34)	6211(3)	4239(1)	8013(1)	22(1)
C(7S)	2822(18)	494(6)	4112(8)	55(3)
C(1S)	4192(8)	88(4)	4763(3)	42(1)
C(2S)	3529(17)	-744(5)	5004(7)	40(2)
C(3S)	4767(8)	-1154(3)	5596(3)	44(1)
C(4S)	6640(20)	-790(6)	5935(9)	49(2)
C(5S)	7430(9)	63(4)	5705(4)	55(2)
C(6S)	6170(18)	468(6)	5131(7)	52(2)

Table 3. Bond lengths [Å] and angles [°] for tomk_tomaz.

O(1)-C(7)	1.336(2)
O(1)-C(1)	1.4662(19)
O(2)-C(7)	1.1961(18)
O(3)-C(21)	1.3396(19)
O(3)-C(3)	1.4629(19)
O(4)-C(21)	1.2055(18)
C(1)-C(6)	1.517(3)
C(1)-C(2)	1.518(2)
C(1)-H(1)	1.0000
C(2)-C(3)	1.517(2)
C(2)-H(2A)	0.9900
C(2)-H(2B)	0.9900
C(3)-C(4)	1.515(2)
C(3)-H(3)	1.0000
C(4)-C(5)	1.530(2)
C(4)-H(4A)	0.9900
C(4)-H(4B)	0.9900
C(5)-C(6)	1.519(3)
C(5)-H(5A)	0.9900
C(5)-H(5B)	0.9900
C(6)-H(6A)	0.9900

C(6)-H(6B)	0.9900
C(7)-C(8)	1.525(2)
C(8)-C(15)	1.520(2)
C(8)-C(9)	1.529(2)
C(8)-H(8)	1.0000
C(9)-C(14)	1.383(2)
C(9)-C(10)	1.386(2)
C(10)-C(11)	1.390(2)
C(10)-H(10)	0.9500
C(11)-C(12)	1.372(2)
C(11)-H(11)	0.9500
C(12)-C(13)	1.371(2)
C(12)-H(12)	0.9500
C(13)-C(14)	1.386(2)
C(13)-H(13)	0.9500
C(14)-H(14)	0.9500
C(15)-C(20)	1.389(2)
C(15)-C(16)	1.392(2)
C(16)-C(17)	1.384(2)
C(16)-H(16)	0.9500
C(17)-C(18)	1.385(2)
C(17)-H(17)	0.9500
C(18)-C(19)	1.379(2)
C(18)-H(18)	0.9500
C(19)-C(20)	1.385(2)
C(19)-H(19)	0.9500
C(20)-H(20)	0.9500
C(21)-C(22)	1.523(2)
C(22)-C(29)	1.519(2)
C(22)-C(23)	1.524(2)
C(22)-H(22)	1.0000
C(23)-C(24)	1.393(2)
C(23)-C(28)	1.394(2)
C(24)-C(25)	1.382(2)
C(24)-H(24)	0.9500
C(25)-C(26)	1.384(2)
C(25)-H(25)	0.9500

C(26)-C(27)	1.381(2)
C(26)-H(26)	0.9500
C(27)-C(28)	1.380(2)
C(27)-H(27)	0.9500
C(28)-H(28)	0.9500
C(29)-C(34)	1.392(2)
C(29)-C(30)	1.393(2)
C(30)-C(31)	1.381(2)
C(30)-H(30)	0.9500
C(31)-C(32)	1.388(2)
C(31)-H(31)	0.9500
C(32)-C(33)	1.380(2)
C(32)-H(32)	0.9500
C(33)-C(34)	1.387(2)
C(33)-H(33)	0.9500
C(34)-H(34)	0.9500
C(7S)-C(1S)	1.484(11)
C(7S)-H(7S1)	0.9800
C(7S)-H(7S2)	0.9800
C(7S)-H(7S3)	0.9800
C(1S)-C(6S)	1.376(12)
C(1S)-C(2S)	1.385(9)
C(2S)-C(3S)	1.379(11)
C(2S)-H(2S)	0.9500
C(3S)-C(4S)	1.301(11)
C(3S)-H(3S)	0.9500
C(4S)-C(5S)	1.429(10)
C(4S)-H(4S)	0.9500
C(5S)-C(6S)	1.361(11)
C(5S)-H(5S)	0.9500
C(6S)-H(6S)	0.9500
C(7)-O(1)-C(1)	116.77(13)
C(21)-O(3)-C(3)	118.28(12)
O(1)-C(1)-C(6)	108.26(14)
O(1)-C(1)-C(2)	107.09(14)
C(6)-C(1)-C(2)	111.97(16)

O(1)-C(1)-H(1)	109.8
C(6)-C(1)-H(1)	109.8
C(2)-C(1)-H(1)	109.8
C(3)-C(2)-C(1)	112.84(14)
C(3)-C(2)-H(2A)	109.0
C(1)-C(2)-H(2A)	109.0
C(3)-C(2)-H(2B)	109.0
C(1)-C(2)-H(2B)	109.0
H(2A)-C(2)-H(2B)	107.8
O(3)-C(3)-C(4)	109.69(13)
O(3)-C(3)-C(2)	104.28(13)
C(4)-C(3)-C(2)	112.02(14)
O(3)-C(3)-H(3)	110.2
C(4)-C(3)-H(3)	110.2
C(2)-C(3)-H(3)	110.2
C(3)-C(4)-C(5)	110.07(15)
C(3)-C(4)-H(4A)	109.6
C(5)-C(4)-H(4A)	109.6
C(3)-C(4)-H(4B)	109.6
C(5)-C(4)-H(4B)	109.6
H(4A)-C(4)-H(4B)	108.2
C(6)-C(5)-C(4)	110.71(15)
C(6)-C(5)-H(5A)	109.5
C(4)-C(5)-H(5A)	109.5
C(6)-C(5)-H(5B)	109.5
C(4)-C(5)-H(5B)	109.5
H(5A)-C(5)-H(5B)	108.1
C(1)-C(6)-C(5)	111.92(15)
C(1)-C(6)-H(6A)	109.2
C(5)-C(6)-H(6A)	109.2
C(1)-C(6)-H(6B)	109.2
C(5)-C(6)-H(6B)	109.2
H(6A)-C(6)-H(6B)	107.9
O(2)-C(7)-O(1)	123.98(15)
O(2)-C(7)-C(8)	126.66(15)
O(1)-C(7)-C(8)	109.35(13)
C(15)-C(8)-C(7)	113.45(13)

C(15)-C(8)-C(9)	113.20(13)
C(7)-C(8)-C(9)	108.62(13)
C(15)-C(8)-H(8)	107.1
C(7)-C(8)-H(8)	107.1
C(9)-C(8)-H(8)	107.1
C(14)-C(9)-C(10)	118.60(16)
C(14)-C(9)-C(8)	121.54(14)
C(10)-C(9)-C(8)	119.86(14)
C(9)-C(10)-C(11)	120.61(16)
C(9)-C(10)-H(10)	119.7
C(11)-C(10)-H(10)	119.7
C(12)-C(11)-C(10)	120.04(16)
C(12)-C(11)-H(11)	120.0
C(10)-C(11)-H(11)	120.0
C(13)-C(12)-C(11)	119.82(16)
C(13)-C(12)-H(12)	120.1
C(11)-C(12)-H(12)	120.1
C(12)-C(13)-C(14)	120.46(16)
C(12)-C(13)-H(13)	119.8
C(14)-C(13)-H(13)	119.8
C(9)-C(14)-C(13)	120.46(15)
C(9)-C(14)-H(14)	119.8
C(13)-C(14)-H(14)	119.8
C(20)-C(15)-C(16)	118.38(16)
C(20)-C(15)-C(8)	118.72(15)
C(16)-C(15)-C(8)	122.89(15)
C(17)-C(16)-C(15)	120.65(16)
C(17)-C(16)-H(16)	119.7
C(15)-C(16)-H(16)	119.7
C(16)-C(17)-C(18)	120.31(16)
C(16)-C(17)-H(17)	119.8
C(18)-C(17)-H(17)	119.8
C(19)-C(18)-C(17)	119.51(17)
C(19)-C(18)-H(18)	120.2
C(17)-C(18)-H(18)	120.2
C(18)-C(19)-C(20)	120.19(17)
C(18)-C(19)-H(19)	119.9

C(20)-C(19)-H(19)	119.9
C(19)-C(20)-C(15)	120.92(16)
C(19)-C(20)-H(20)	119.5
C(15)-C(20)-H(20)	119.5
O(4)-C(21)-O(3)	124.11(15)
O(4)-C(21)-C(22)	125.75(15)
O(3)-C(21)-C(22)	110.13(13)
C(29)-C(22)-C(21)	111.83(13)
C(29)-C(22)-C(23)	113.10(13)
C(21)-C(22)-C(23)	110.74(13)
C(29)-C(22)-H(22)	106.9
C(21)-C(22)-H(22)	106.9
C(23)-C(22)-H(22)	106.9
C(24)-C(23)-C(28)	118.28(16)
C(24)-C(23)-C(22)	122.49(14)
C(28)-C(23)-C(22)	119.23(14)
C(25)-C(24)-C(23)	120.60(16)
C(25)-C(24)-H(24)	119.7
C(23)-C(24)-H(24)	119.7
C(24)-C(25)-C(26)	120.30(16)
C(24)-C(25)-H(25)	119.9
C(26)-C(25)-H(25)	119.9
C(27)-C(26)-C(25)	119.75(17)
C(27)-C(26)-H(26)	120.1
C(25)-C(26)-H(26)	120.1
C(28)-C(27)-C(26)	119.98(17)
C(28)-C(27)-H(27)	120.0
C(26)-C(27)-H(27)	120.0
C(27)-C(28)-C(23)	121.07(16)
C(27)-C(28)-H(28)	119.5
C(23)-C(28)-H(28)	119.5
C(34)-C(29)-C(30)	118.24(16)
C(34)-C(29)-C(22)	119.18(14)
C(30)-C(29)-C(22)	122.57(14)
C(31)-C(30)-C(29)	120.75(15)
C(31)-C(30)-H(30)	119.6
C(29)-C(30)-H(30)	119.6

C(30)-C(31)-C(32)	120.33(16)
C(30)-C(31)-H(31)	119.8
C(32)-C(31)-H(31)	119.8
C(33)-C(32)-C(31)	119.66(17)
C(33)-C(32)-H(32)	120.2
C(31)-C(32)-H(32)	120.2
C(32)-C(33)-C(34)	119.92(16)
C(32)-C(33)-H(33)	120.0
C(34)-C(33)-H(33)	120.0
C(33)-C(34)-C(29)	121.09(15)
C(33)-C(34)-H(34)	119.5
C(29)-C(34)-H(34)	119.5
C(6S)-C(1S)-C(2S)	116.4(8)
C(6S)-C(1S)-C(7S)	124.3(7)
C(2S)-C(1S)-C(7S)	119.3(7)
C(3S)-C(2S)-C(1S)	121.4(9)
C(3S)-C(2S)-H(2S)	119.3
C(1S)-C(2S)-H(2S)	119.3
C(4S)-C(3S)-C(2S)	121.6(7)
C(4S)-C(3S)-H(3S)	119.2
C(2S)-C(3S)-H(3S)	119.2
C(3S)-C(4S)-C(5S)	119.6(9)
C(3S)-C(4S)-H(4S)	120.2
C(5S)-C(4S)-H(4S)	120.2
C(6S)-C(5S)-C(4S)	118.2(8)
C(6S)-C(5S)-H(5S)	120.9
C(4S)-C(5S)-H(5S)	120.9
C(5S)-C(6S)-C(1S)	122.8(7)
C(5S)-C(6S)-H(6S)	118.6
C(1S)-C(6S)-H(6S)	118.6

Symmetry transformations used to generate equivalent atoms:

Table 4. Anisotropic displacement parameters ($\text{\AA}^2 \times 10^3$) for tomk_tomaz. The anisotropic displacement factor exponent takes the form: $-2\pi^2 [h^2 a^{*2} U^{11} + \dots + 2 h k a^* b^* U^{12}]$

	U ¹¹	U ²²	U ³³	U ²³	U ¹³	U ¹²
O(1)	25(1)	13(1)	58(1)	1(1)	-14(1)	1(1)
O(2)	21(1)	23(1)	44(1)	-5(1)	-6(1)	1(1)
O(3)	21(1)	16(1)	30(1)	7(1)	-4(1)	-1(1)
O(4)	22(1)	27(1)	34(1)	13(1)	-3(1)	2(1)
C(1)	22(1)	15(1)	53(1)	2(1)	-11(1)	2(1)
C(2)	27(1)	18(1)	35(1)	2(1)	-10(1)	3(1)
C(3)	24(1)	13(1)	28(1)	5(1)	-2(1)	0(1)
C(4)	29(1)	22(1)	31(1)	0(1)	1(1)	-2(1)
C(5)	35(1)	31(1)	33(1)	8(1)	2(1)	-7(1)
C(6)	30(1)	24(1)	59(2)	11(1)	2(1)	-5(1)
C(7)	23(1)	18(1)	16(1)	6(1)	1(1)	-2(1)
C(8)	18(1)	16(1)	20(1)	5(1)	2(1)	-2(1)
C(9)	19(1)	12(1)	20(1)	1(1)	1(1)	1(1)
C(10)	19(1)	29(1)	24(1)	-2(1)	3(1)	-2(1)
C(11)	19(1)	37(1)	28(1)	-4(1)	-6(1)	1(1)
C(12)	31(1)	26(1)	19(1)	2(1)	-3(1)	6(1)
C(13)	27(1)	30(1)	22(1)	6(1)	4(1)	-2(1)
C(14)	18(1)	29(1)	25(1)	6(1)	-2(1)	-4(1)
C(15)	21(1)	17(1)	16(1)	6(1)	-2(1)	2(1)
C(16)	26(1)	21(1)	19(1)	4(1)	2(1)	1(1)
C(17)	30(1)	19(1)	26(1)	6(1)	-6(1)	-3(1)
C(18)	40(1)	19(1)	25(1)	-2(1)	-7(1)	6(1)
C(19)	33(1)	32(1)	21(1)	-1(1)	1(1)	11(1)
C(20)	22(1)	26(1)	21(1)	4(1)	-1(1)	4(1)
C(21)	19(1)	21(1)	21(1)	1(1)	1(1)	4(1)
C(22)	16(1)	20(1)	21(1)	4(1)	-2(1)	3(1)
C(23)	21(1)	14(1)	20(1)	2(1)	-1(1)	-2(1)
C(24)	23(1)	20(1)	23(1)	5(1)	-2(1)	2(1)
C(25)	26(1)	24(1)	30(1)	2(1)	3(1)	3(1)
C(26)	36(1)	32(1)	23(1)	3(1)	9(1)	-1(1)
C(27)	41(1)	30(1)	22(1)	7(1)	-2(1)	3(1)
C(28)	26(1)	22(1)	26(1)	5(1)	-4(1)	4(1)

C(29)	20(1)	18(1)	18(1)	7(1)	3(1)	-1(1)
C(30)	21(1)	23(1)	22(1)	5(1)	4(1)	5(1)
C(31)	22(1)	29(1)	21(1)	5(1)	1(1)	-3(1)
C(32)	35(1)	21(1)	20(1)	2(1)	5(1)	-3(1)
C(33)	32(1)	20(1)	28(1)	5(1)	7(1)	7(1)
C(34)	21(1)	23(1)	23(1)	7(1)	1(1)	3(1)
C(7S)	57(6)	54(7)	52(5)	-8(5)	-13(4)	14(5)
C(1S)	40(3)	49(3)	38(3)	-4(3)	-3(2)	11(3)
C(2S)	30(3)	43(5)	45(4)	-14(3)	1(2)	2(3)
C(3S)	60(3)	38(3)	33(2)	-4(2)	4(2)	-3(2)
C(4S)	56(5)	44(5)	45(4)	2(4)	-16(3)	5(3)
C(5S)	44(3)	48(3)	69(4)	-9(3)	-21(3)	-7(3)
C(6S)	59(5)	34(5)	60(5)	1(4)	-10(4)	-4(4)

Table 5. Hydrogen coordinates ($\times 10^4$) and isotropic displacement parameters ($\text{\AA}^2 \times 10^3$) for tomk_tomaz.

	x	y	z	U(eq)
H(1)	-53	-803	7414	36
H(2A)	2840	112	6818	32
H(2B)	1141	666	7329	32
H(3)	5630	333	7882	26
H(4A)	2526	1255	8852	33
H(4B)	5052	1087	9151	33
H(5A)	4089	-437	9171	40
H(5B)	2455	72	9755	40
H(6A)	375	-1017	8881	45
H(6B)	-419	-65	8702	45
H(8)	5576	-2341	7322	22
H(10)	8008	-2329	8478	29
H(11)	8816	-2491	9896	34
H(12)	6009	-3006	10743	30
H(13)	2395	-3352	10178	32
H(14)	1556	-3182	8766	29
H(16)	652	-3868	7433	26

H(17)	135	-5190	6655	30
H(18)	2928	-5635	5792	34
H(19)	6306	-4780	5759	34
H(20)	6835	-3460	6538	27
H(22)	5349	2916	7054	23
H(24)	10873	2094	7020	27
H(25)	12925	1987	5827	32
H(26)	11675	2591	4597	36
H(27)	8386	3327	4571	37
H(28)	6272	3400	5747	29
H(30)	10835	3246	8161	26
H(31)	11908	4451	9053	29
H(32)	9399	5524	9310	30
H(33)	5829	5396	8643	32
H(34)	4751	4190	7746	26
H(7S1)	2347	55	3666	82
H(7S2)	3720	977	3882	82
H(7S3)	1493	718	4360	82
H(2S)	2193	-1037	4756	48
H(3S)	4237	-1716	5760	53
H(4S)	7486	-1090	6333	59
H(5S)	8794	340	5945	66
H(6S)	6679	1037	4978	62

Table 6. Torsion angles [°] for tomk_tomaz.

C(7)-O(1)-C(1)-C(6)	100.99(17)
C(7)-O(1)-C(1)-C(2)	-138.10(15)
O(1)-C(1)-C(2)-C(3)	-68.12(19)
C(6)-C(1)-C(2)-C(3)	50.40(19)
C(21)-O(3)-C(3)-C(4)	79.40(17)
C(21)-O(3)-C(3)-C(2)	-160.47(14)
C(1)-C(2)-C(3)-O(3)	-171.25(14)
C(1)-C(2)-C(3)-C(4)	-52.70(19)
O(3)-C(3)-C(4)-C(5)	171.17(13)
C(2)-C(3)-C(4)-C(5)	55.88(18)
C(3)-C(4)-C(5)-C(6)	-57.7(2)

O(1)-C(1)-C(6)-C(5)	65.35(19)
C(2)-C(1)-C(6)-C(5)	-52.47(19)
C(4)-C(5)-C(6)-C(1)	56.5(2)
C(1)-O(1)-C(7)-O(2)	7.6(3)
C(1)-O(1)-C(7)-C(8)	-170.88(14)
O(2)-C(7)-C(8)-C(15)	19.0(2)
O(1)-C(7)-C(8)-C(15)	-162.59(14)
O(2)-C(7)-C(8)-C(9)	-107.82(19)
O(1)-C(7)-C(8)-C(9)	70.59(17)
C(15)-C(8)-C(9)-C(14)	-70.43(19)
C(7)-C(8)-C(9)-C(14)	56.5(2)
C(15)-C(8)-C(9)-C(10)	109.01(17)
C(7)-C(8)-C(9)-C(10)	-124.03(16)
C(14)-C(9)-C(10)-C(11)	0.3(2)
C(8)-C(9)-C(10)-C(11)	-179.12(15)
C(9)-C(10)-C(11)-C(12)	0.1(3)
C(10)-C(11)-C(12)-C(13)	-0.2(3)
C(11)-C(12)-C(13)-C(14)	-0.1(3)
C(10)-C(9)-C(14)-C(13)	-0.6(3)
C(8)-C(9)-C(14)-C(13)	178.80(15)
C(12)-C(13)-C(14)-C(9)	0.5(3)
C(7)-C(8)-C(15)-C(20)	130.67(15)
C(9)-C(8)-C(15)-C(20)	-104.95(17)
C(7)-C(8)-C(15)-C(16)	-50.3(2)
C(9)-C(8)-C(15)-C(16)	74.07(18)
C(20)-C(15)-C(16)-C(17)	-1.4(2)
C(8)-C(15)-C(16)-C(17)	179.57(15)
C(15)-C(16)-C(17)-C(18)	-0.1(2)
C(16)-C(17)-C(18)-C(19)	1.5(2)
C(17)-C(18)-C(19)-C(20)	-1.4(2)
C(18)-C(19)-C(20)-C(15)	-0.1(3)
C(16)-C(15)-C(20)-C(19)	1.5(2)
C(8)-C(15)-C(20)-C(19)	-179.43(15)
C(3)-O(3)-C(21)-O(4)	0.7(2)
C(3)-O(3)-C(21)-C(22)	180.00(13)
O(4)-C(21)-C(22)-C(29)	-52.5(2)
O(3)-C(21)-C(22)-C(29)	128.26(14)

O(4)-C(21)-C(22)-C(23)	74.6(2)
O(3)-C(21)-C(22)-C(23)	-104.61(15)
C(29)-C(22)-C(23)-C(24)	84.41(19)
C(21)-C(22)-C(23)-C(24)	-42.0(2)
C(29)-C(22)-C(23)-C(28)	-95.42(18)
C(21)-C(22)-C(23)-C(28)	138.15(15)
C(28)-C(23)-C(24)-C(25)	-1.3(2)
C(22)-C(23)-C(24)-C(25)	178.90(15)
C(23)-C(24)-C(25)-C(26)	0.9(3)
C(24)-C(25)-C(26)-C(27)	0.6(3)
C(25)-C(26)-C(27)-C(28)	-1.6(3)
C(26)-C(27)-C(28)-C(23)	1.2(3)
C(24)-C(23)-C(28)-C(27)	0.2(3)
C(22)-C(23)-C(28)-C(27)	-179.93(16)
C(21)-C(22)-C(29)-C(34)	-115.67(16)
C(23)-C(22)-C(29)-C(34)	118.48(16)
C(21)-C(22)-C(29)-C(30)	65.00(19)
C(23)-C(22)-C(29)-C(30)	-60.8(2)
C(34)-C(29)-C(30)-C(31)	0.2(2)
C(22)-C(29)-C(30)-C(31)	179.50(15)
C(29)-C(30)-C(31)-C(32)	0.3(3)
C(30)-C(31)-C(32)-C(33)	-0.7(3)
C(31)-C(32)-C(33)-C(34)	0.6(3)
C(32)-C(33)-C(34)-C(29)	-0.2(3)
C(30)-C(29)-C(34)-C(33)	-0.2(2)
C(22)-C(29)-C(34)-C(33)	-179.59(15)
C(6S)-C(1S)-C(2S)-C(3S)	1.6(17)
C(7S)-C(1S)-C(2S)-C(3S)	178.9(8)
C(1S)-C(2S)-C(3S)-C(4S)	-2.1(15)
C(2S)-C(3S)-C(4S)-C(5S)	1.3(18)
C(3S)-C(4S)-C(5S)-C(6S)	-0.1(18)
C(4S)-C(5S)-C(6S)-C(1S)	-0.4(17)
C(2S)-C(1S)-C(6S)-C(5S)	-0.3(18)
C(7S)-C(1S)-C(6S)-C(5S)	-177.5(9)

Symmetry transformations used to generate equivalent atoms:

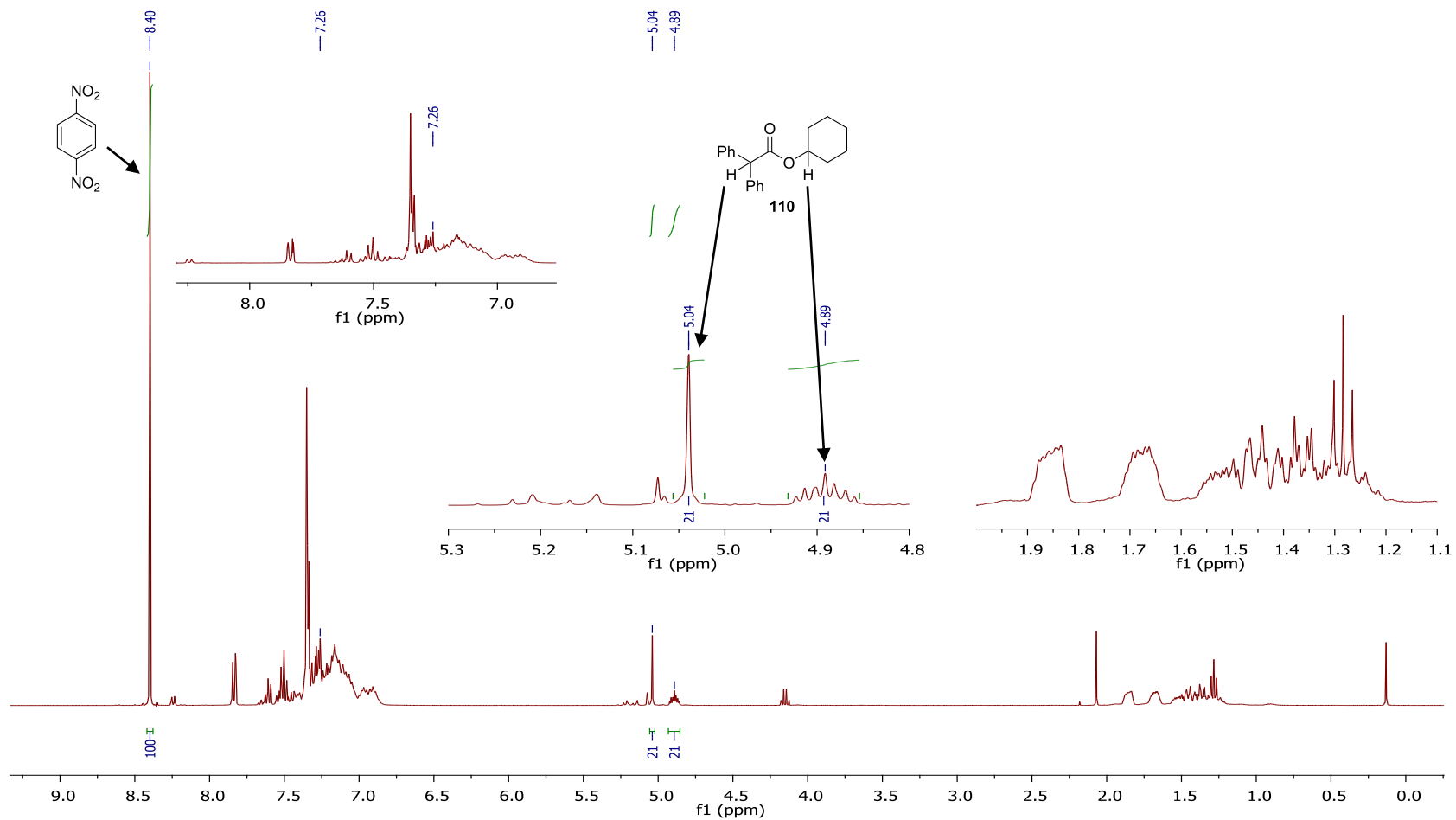
5.2. Selected ^1H NMR Spectrometric Data

Figure 5.1. ^1H NMR spectrum of the crude reaction mixture resulting from the reaction of diphenylketene **120** and cyclohexane **3** under standard reaction conditions.

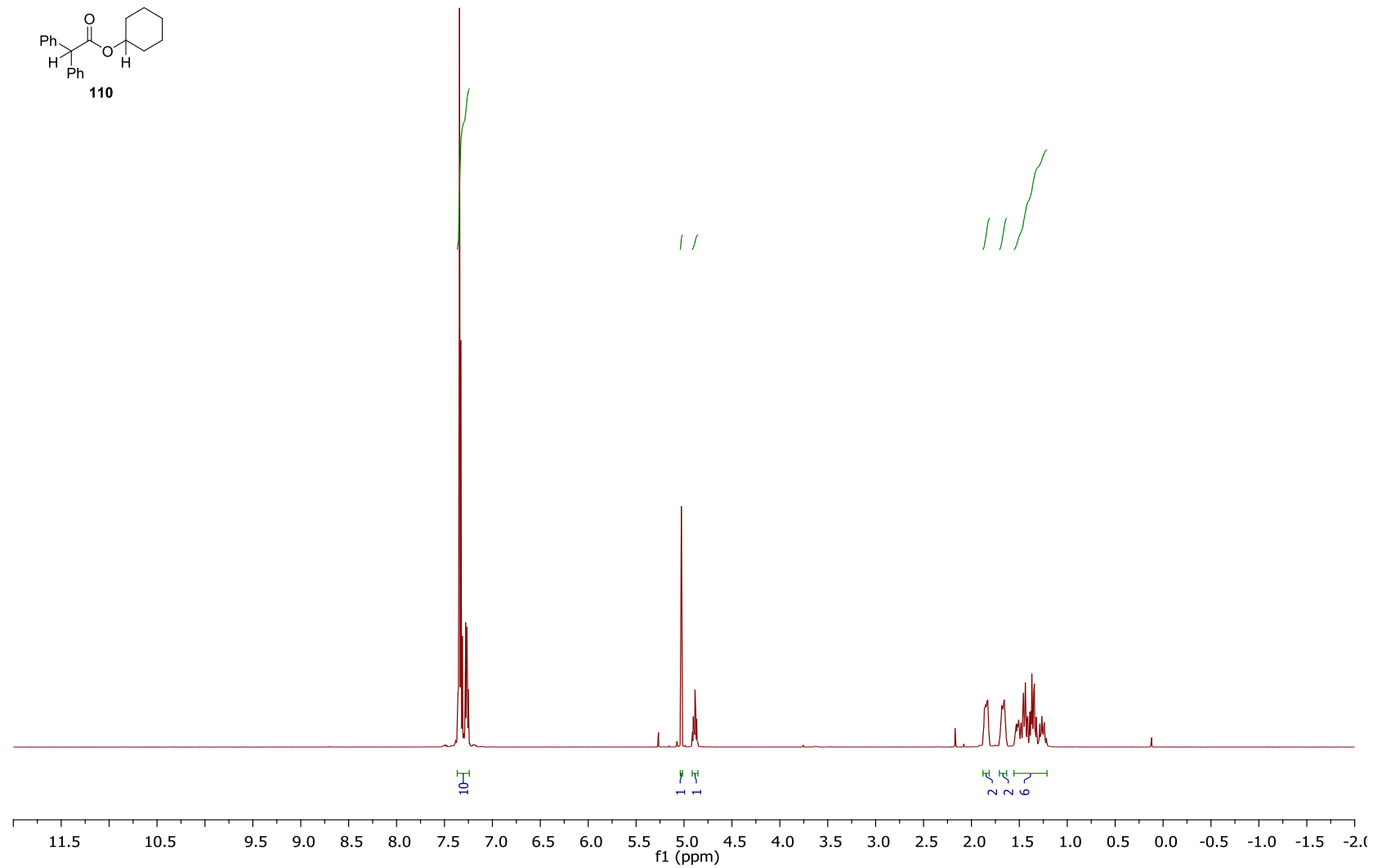


Figure 5.2. ¹H NMR spectrum of cyclohexyl 2,2-diphenylacetate **110** after purification by silica-gel flash chromatography.

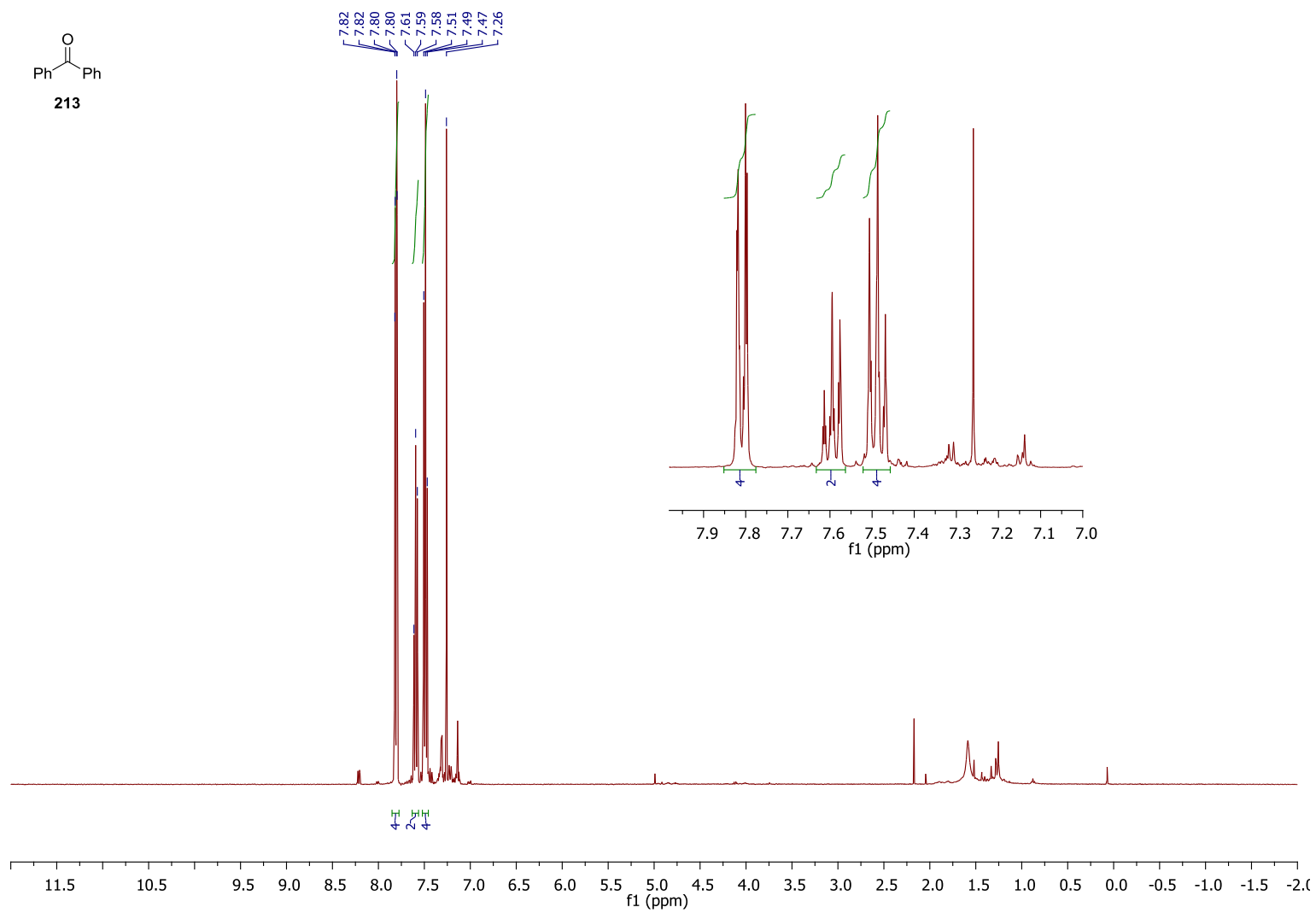


Figure 5.3. ¹H NMR spectrum of benzophenone **213** after purification by silica-gel flash chromatography.

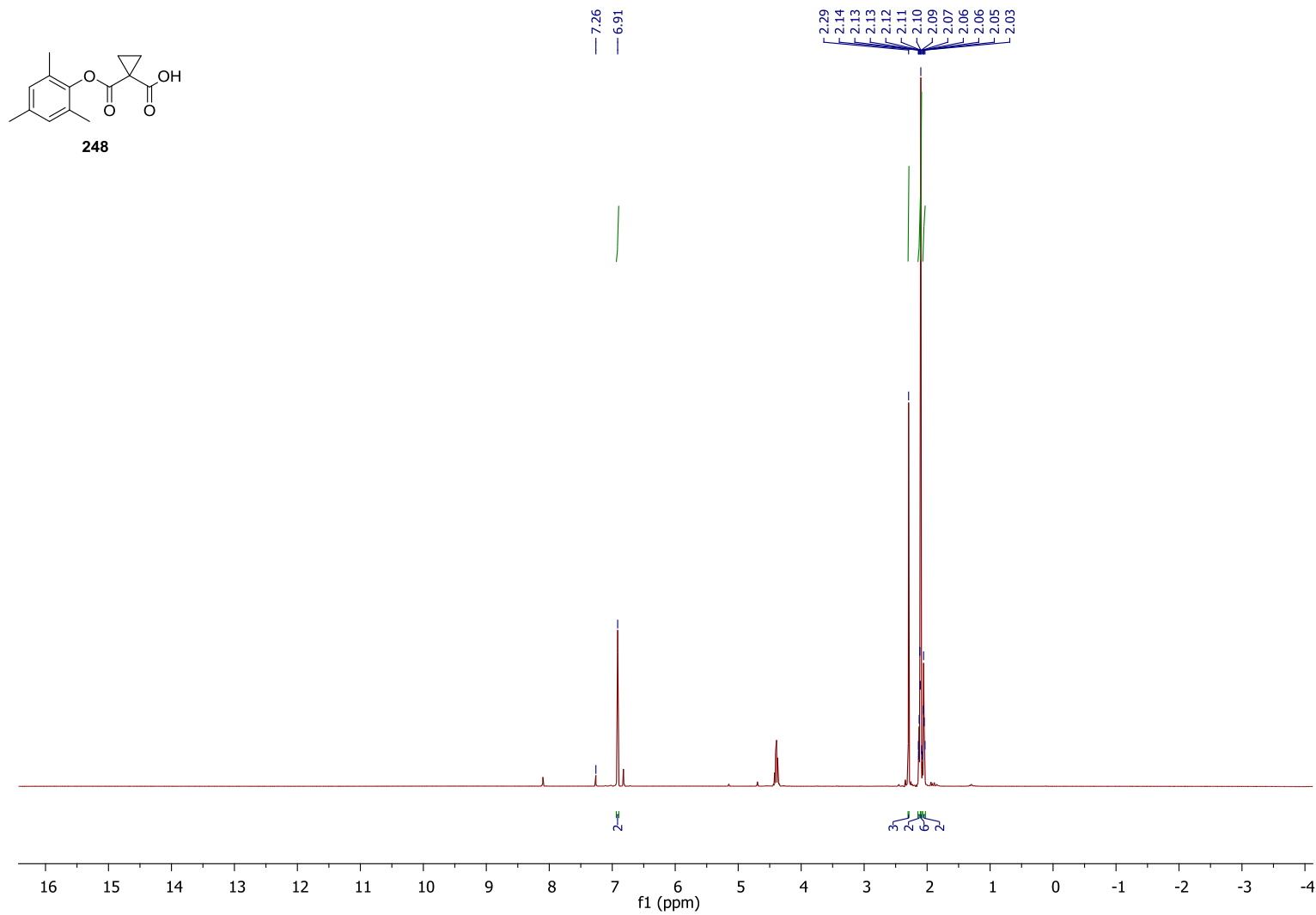


Figure 5.4. ¹H NMR spectrum of the crude reaction mixture resulting from the reaction of mesitylene **238** and peroxide **241** under standard reaction conditions.

5.3. Selected Mass Spectrometric Data

Print of window 80: MS Spectrum

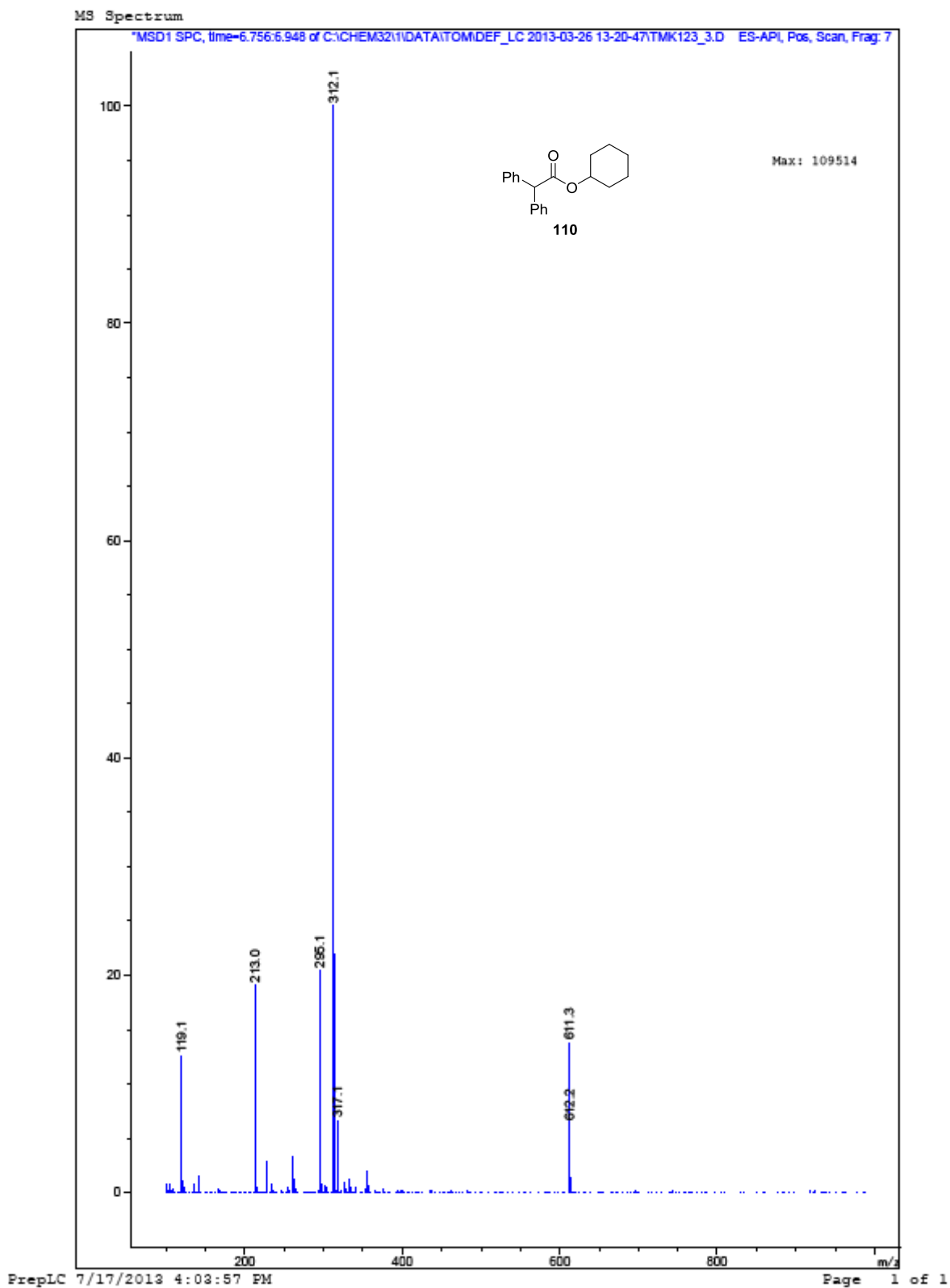


Figure 5.5. Mass spectrum of cyclohexyl 2,2-diphenylacetate **110**.

Print of window 80: MS Spectrum

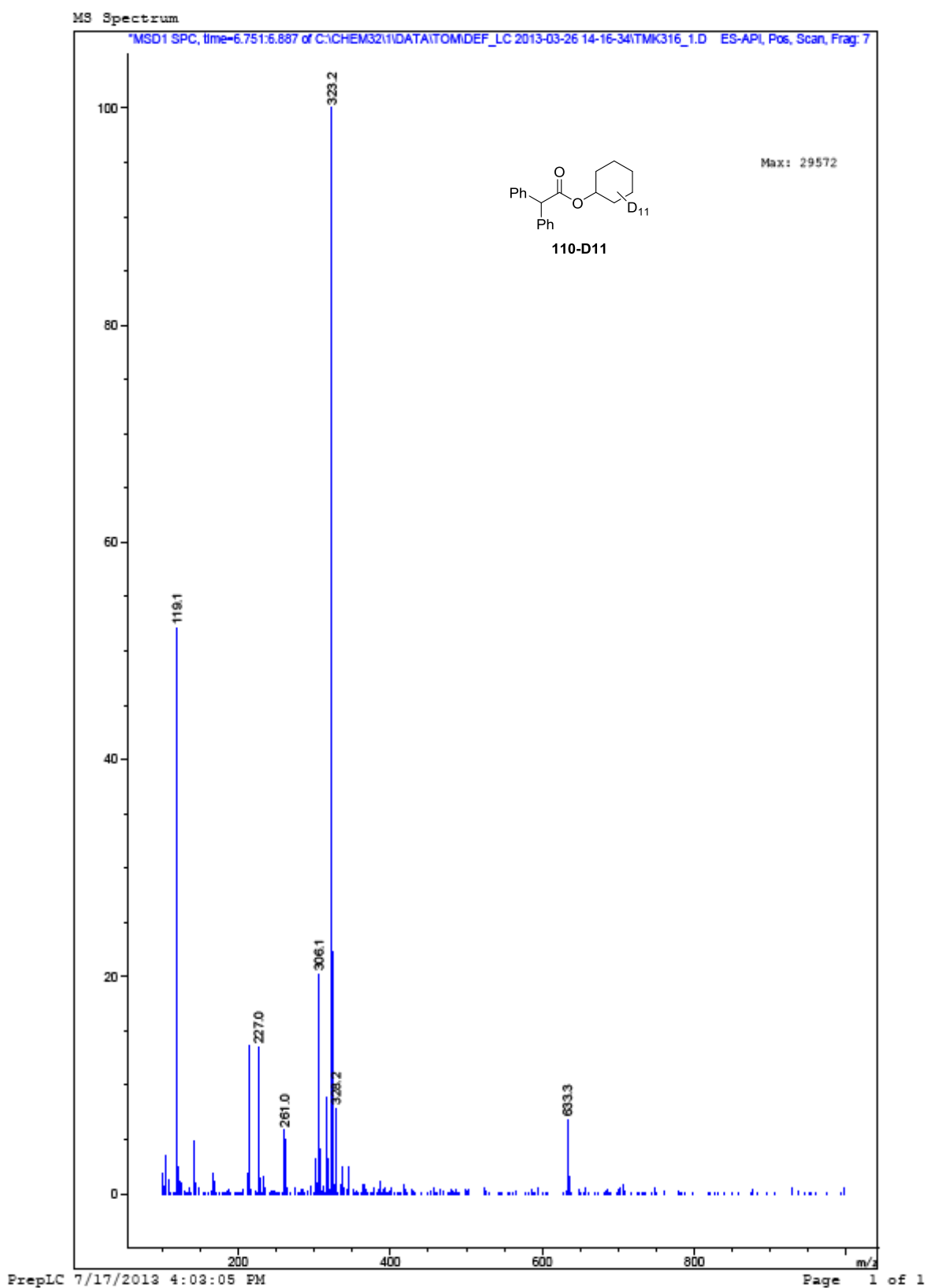


Figure 5.6. Mass spectrum of cyclohexyl 2,2-diphenylacetate 110-D11.

Print of window 80: MS Spectrum

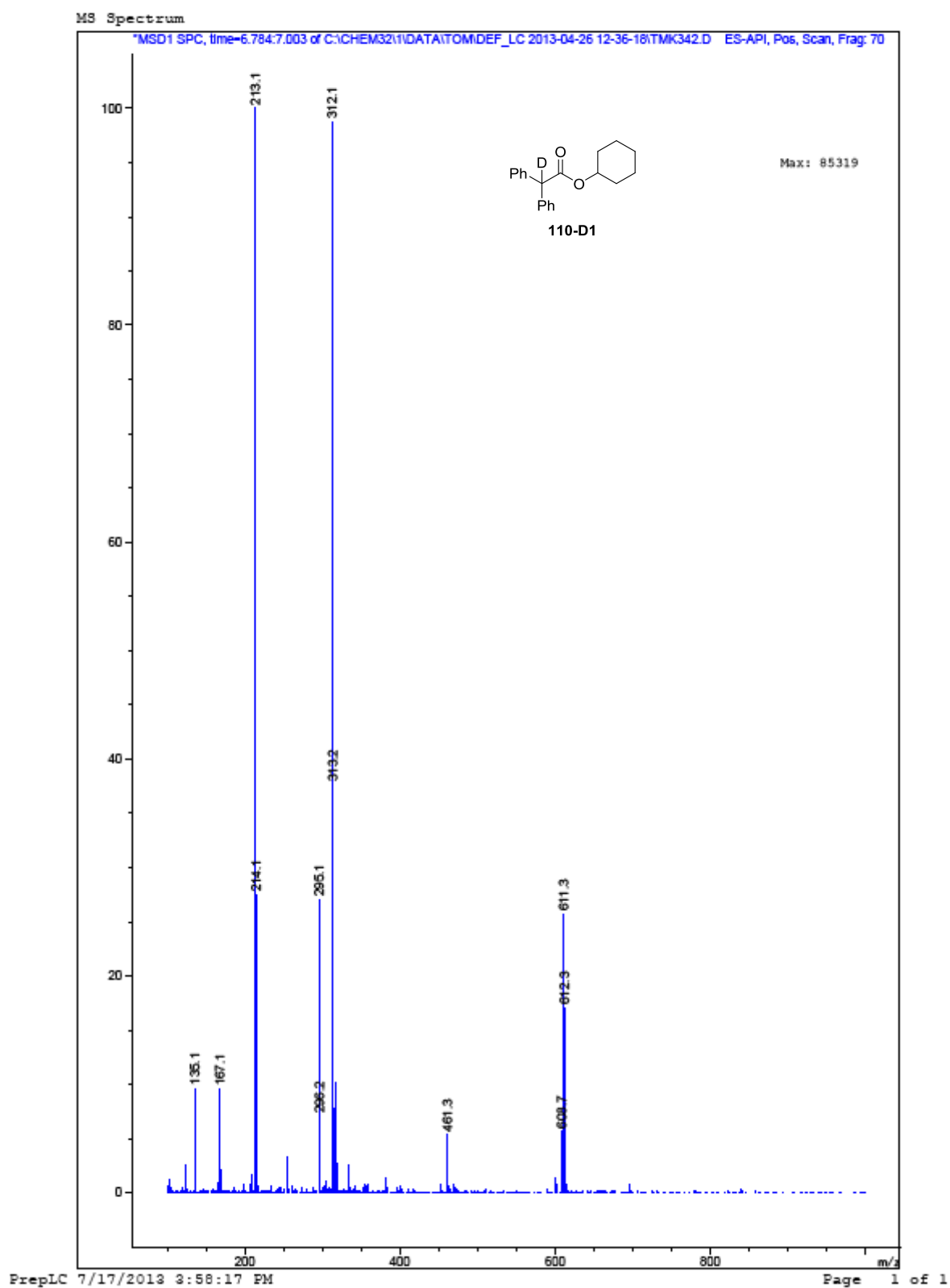


Figure 5.7. Mass spectrum of cyclohexyl 2,2-diphenylacetate **110-D1** from the reaction with D_2O_2 .

Print of window 80: MS Spectrum

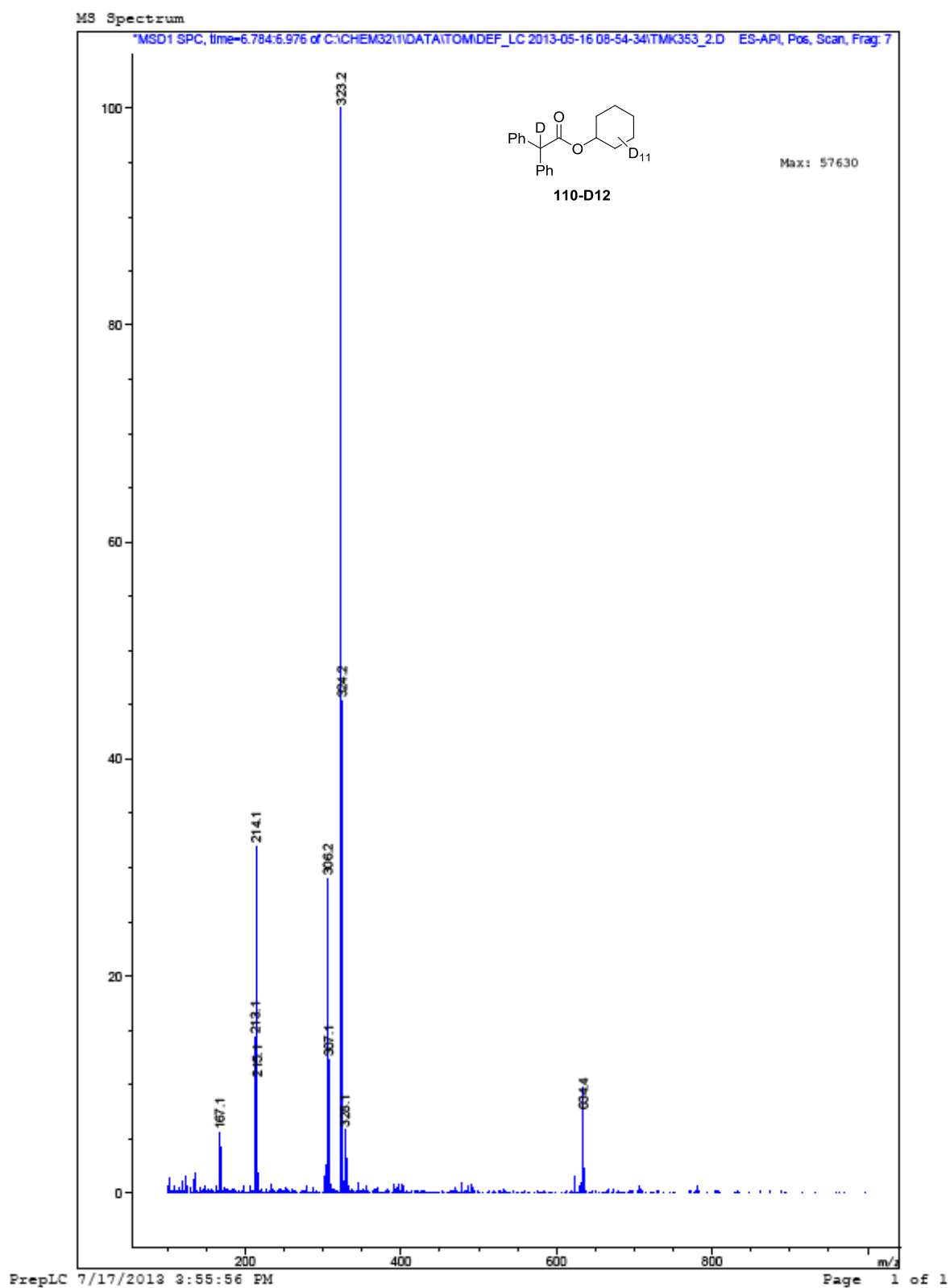
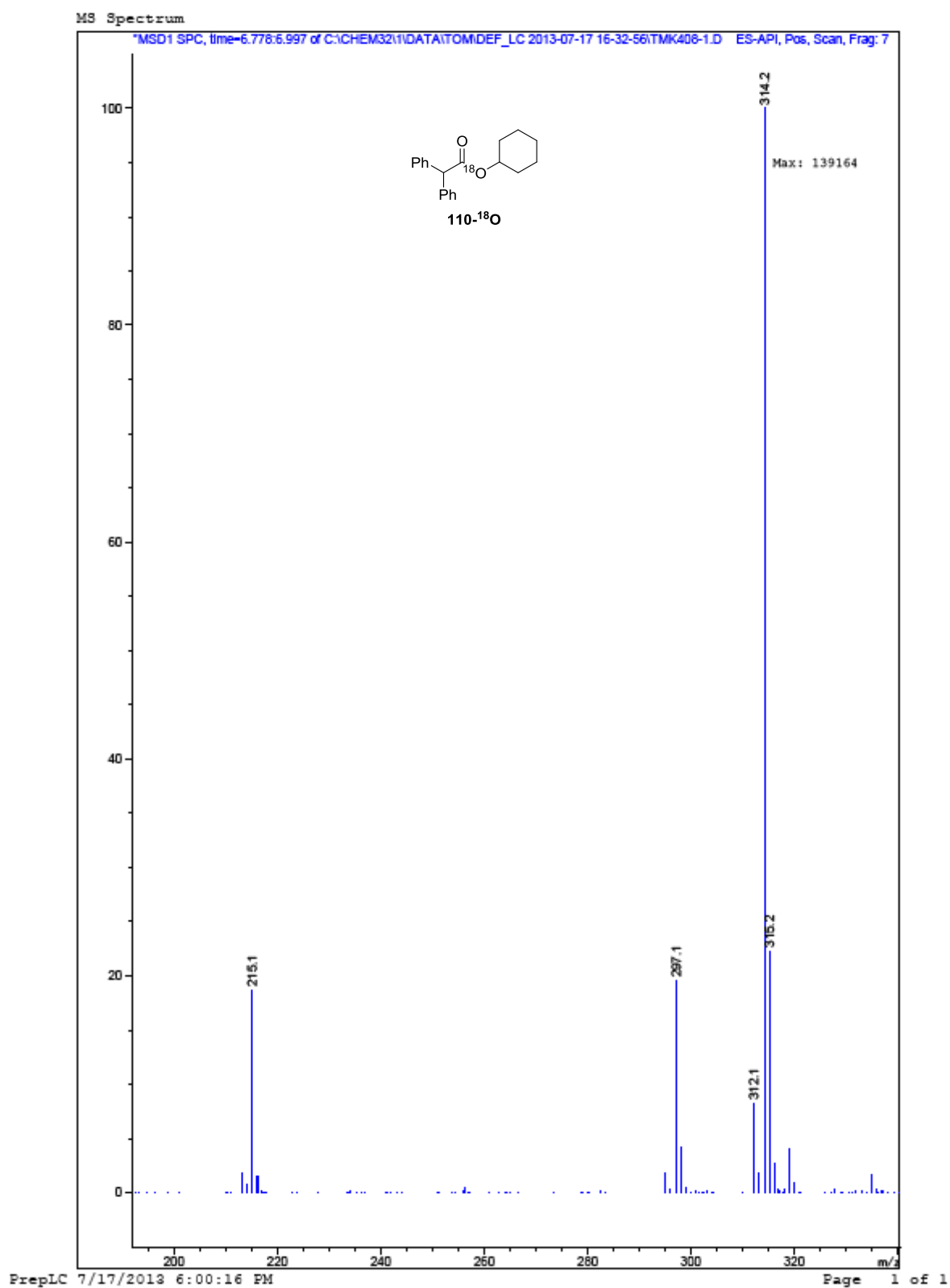


Figure 5.8. Mass spectrum of cyclohexyl 2,2-diphenylacetate **110-D12** from the reaction with D₂O₂.

Print of window 80: MS Spectrum

**Figure 5.9.** Mass spectrum of ¹⁸O-labelled cyclohexyl 2,2-diphenylacetate **110-¹⁸O**.

Print of window 80: MS Spectrum

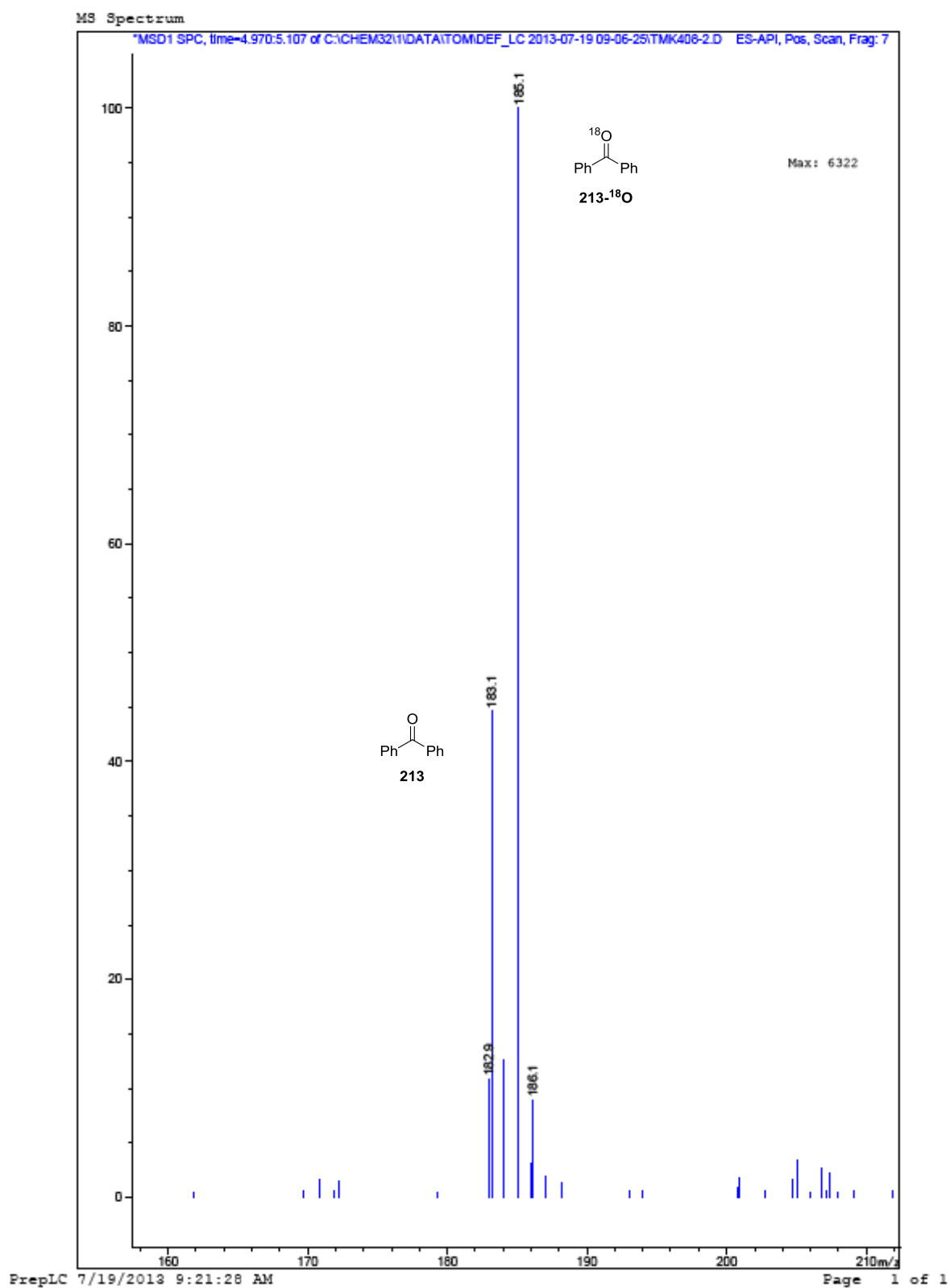
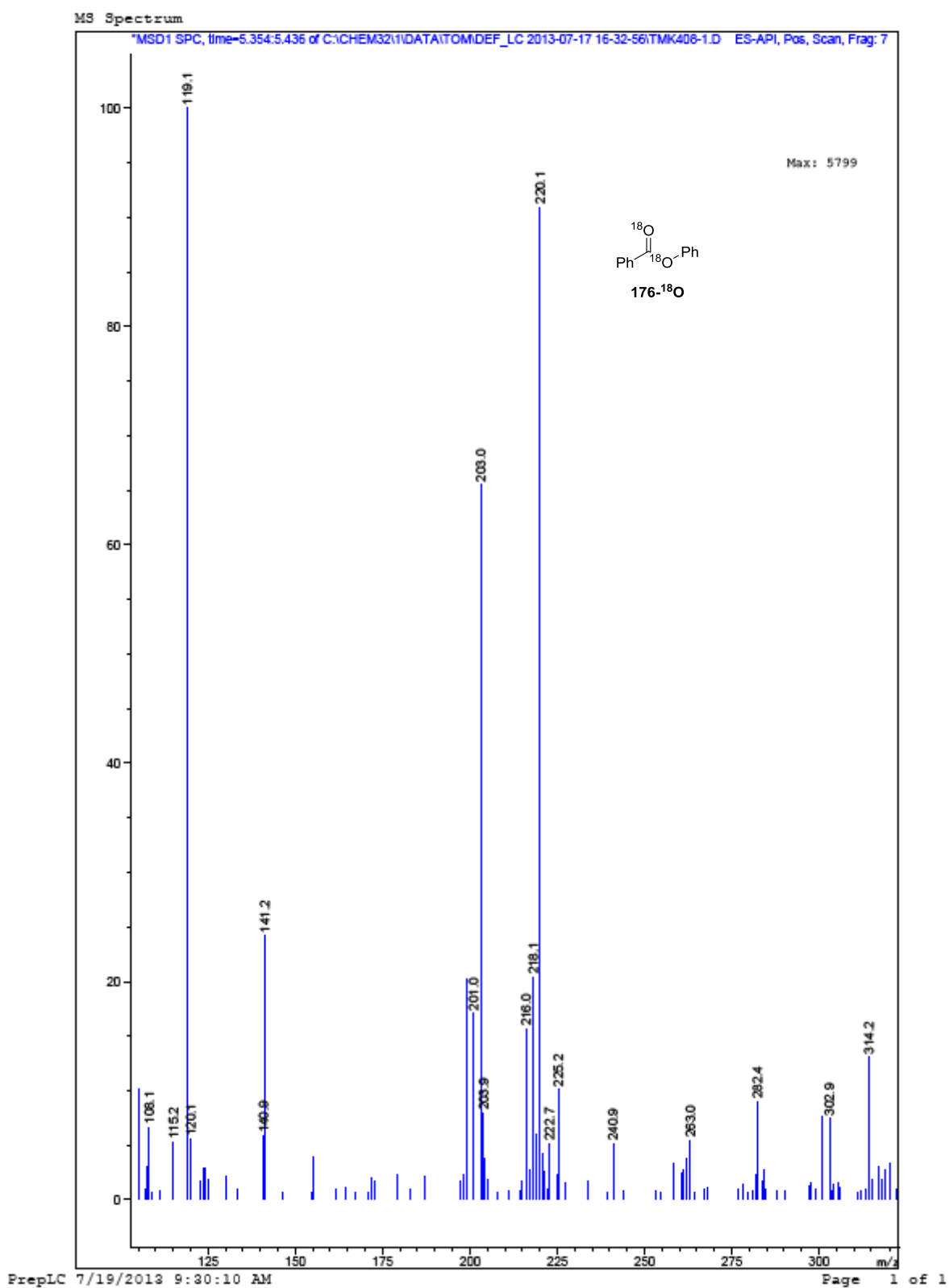


Figure 5.10. Mass spectrum of a mixture of ¹⁶O- and ¹⁸O-labelled benzophenone.

Print of window 80: MS Spectrum

Figure 5.11. Mass spectrum of ¹⁸O-labelled phenyl benzoate 176-¹⁸O.

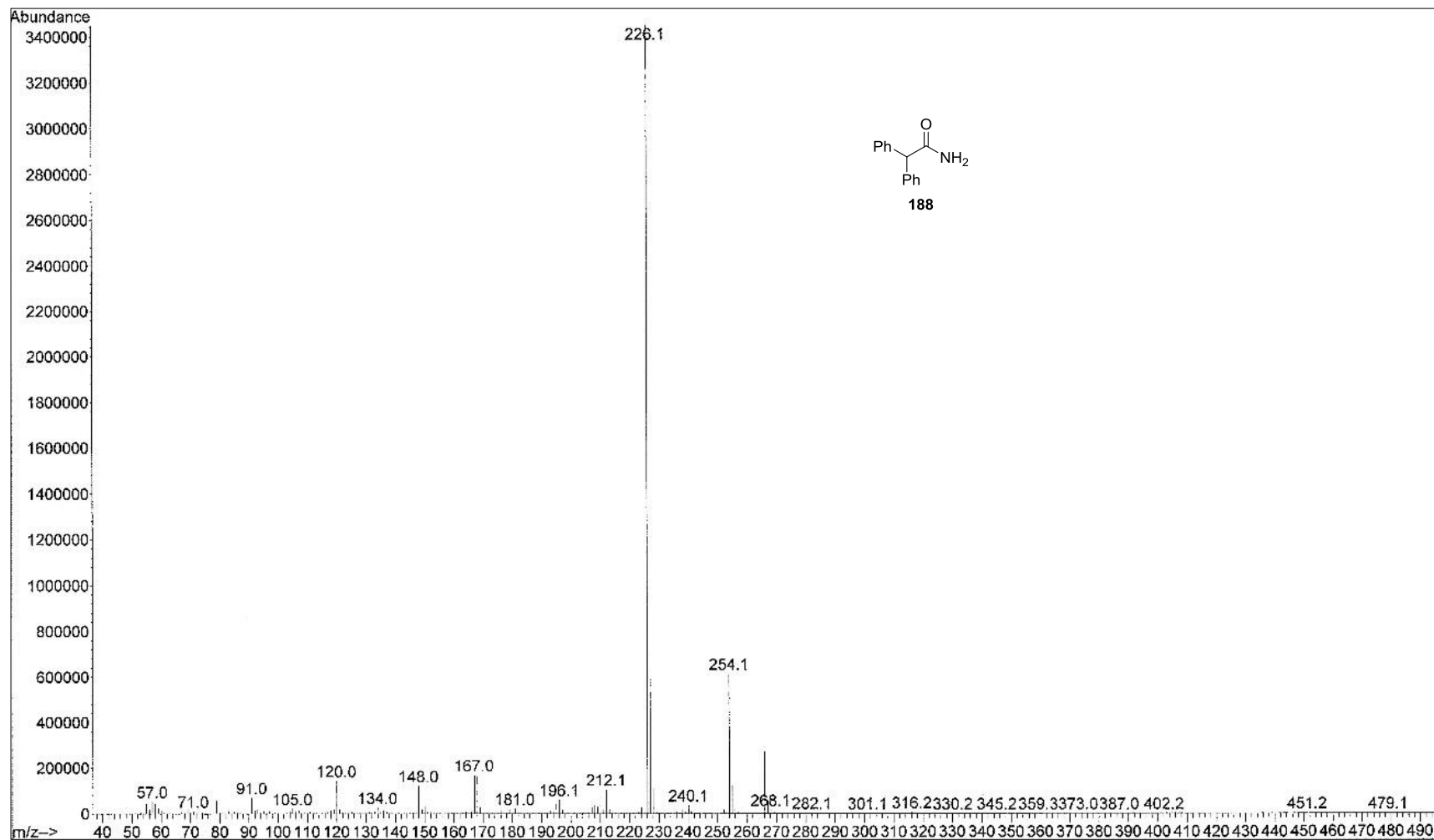


Figure 5.12. Mass spectrum of *N*-methyl-2,2-diphenylacetamide **188** after derivatisation of **110-¹⁸O**.

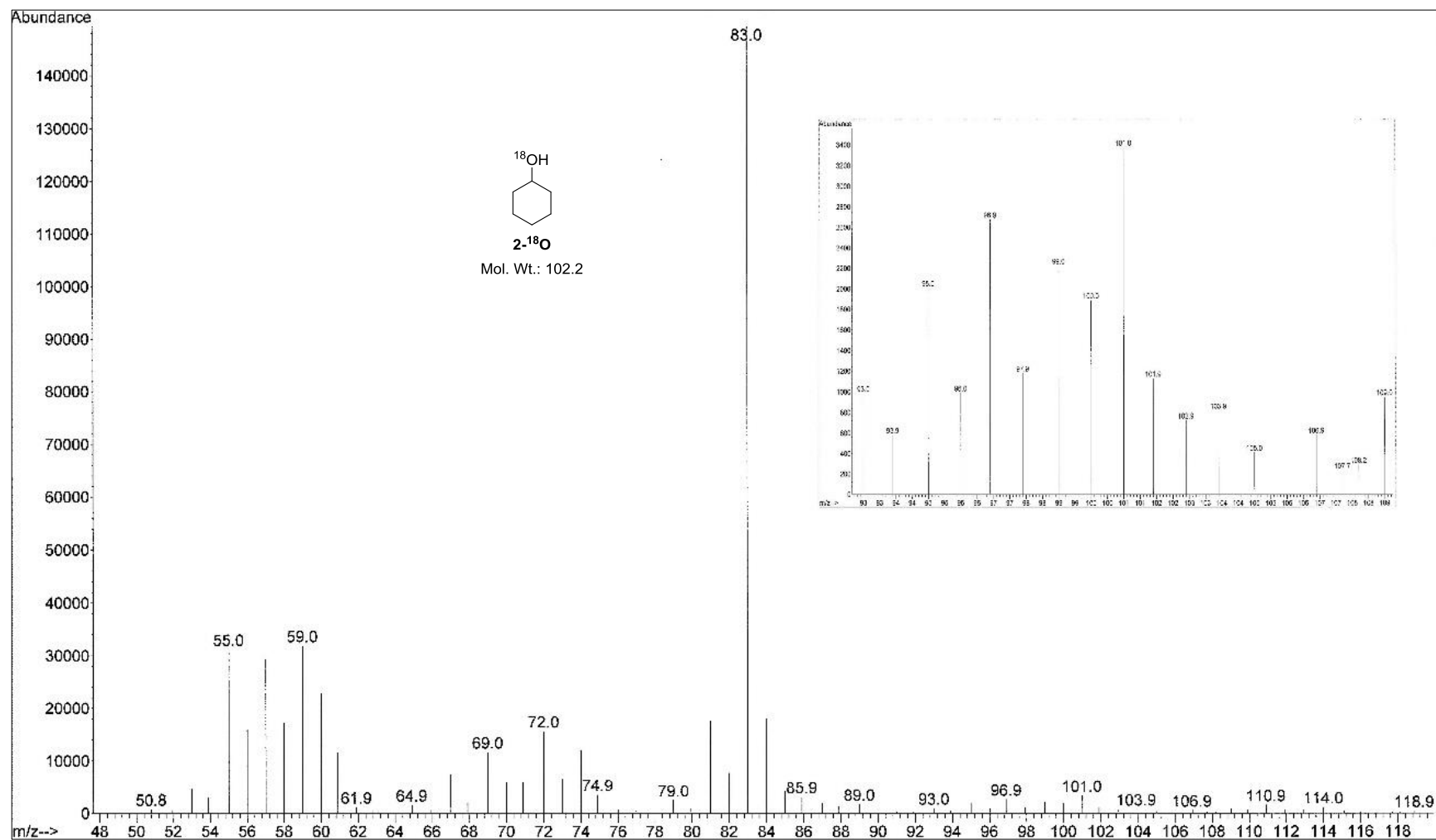


Figure 5.13. Mass spectrum of ¹⁸O-labelled cyclohexanol 2.

Chapter 6: References

6. References

1. F. A. Carey, *Organic Chemistry*. 4 ed.; McGraw-Hill: 2000.
2. B. M. Trost, *Science*, **1991**, *254*, 1471-1477.
3. A. W. Hofmann, *Ber. Dtsch. Chem. Ges.*, **1883**, *16*, 558-560.
4. S. J. Blanksby; G. B. Ellison, *Acc. Chem. Res.*, **2003**, *36*, 255-263.
5. R. Mas-Ballesté; L. Que Jr, *Science (New York, NY)*, **2006**, *312*, 1885.
6. M. Sono; M. P. Roach; E. D. Coulter; J. H. Dawson, *Chem. Rev.*, **1996**, *96*, 2841-2888.
7. A. B. Reiss; K. A. Siller; M. M. Rahman; E. S. Chan; J. Ghiso; M. J. de Leon, *Neurobiol. Aging*, **2004**, *25*, 977-989.
8. J. P. Bartek; J. R. Brazdil; A. M. Ebner. Process for oxidation of propane. 5,198,580, 1993.
9. Y. Koyasu; H. Nakamura; T. Ushikubo; S. Wajiki. Method for producing an unsaturated carboxylic acid. 5,380,933, 1995.
10. (a) M. M. Lin, *Appl. Catal., A*, **2001**, *207*, 1-16; (b) M. Lin; M. W. Linsen. A process for preparing a multi-metal oxide catalyst. EP 0 962 253 A2, 1999.
11. T. Ushikubo; K. Oshima; T. Umezawa; K. Kiyono. Process for producing nitriles. 0 529 853 A2, 1993.
12. Y. Moro-Oka; W. Ueda, Partial oxidation and ammoxidation of propane: Catalysts and processes. In *Catalysis: Volume 11*, J. J. Spivey; S. K. Agarwal, Eds. The Royal Society of Chemistry: 1994; Vol. 11, pp 223-245.
13. M.-J. Cheng; W. A. Goddard, *J. Am. Chem. Soc.*, **2013**, *135*, 4600-4603.
14. P. M. Michalakos; K. Birkeland; H. H. Kung, *J. Catal.*, **1996**, *158*, 349-353.
15. K. Inumaru; A. Ono; H. Kubo; M. Misono, *J. Chem. Soc., Faraday Trans.*, **1998**, *94*, 1765-1770.
16. N. Mizuno; M. Tateishi; M. Iwamoto, *Appl. Catal., A*, **1995**, *128*, L165-L170.
17. N. Mizuno; H. Ishige; Y. Seki; M. Misono; D.-J. Suh; W. Han; T. Kudo, *Chem. Commun.*, **1997**, 1295-1296.
18. H. Arakawa; M. Aresta; J. N. Armor; M. A. Barteau; E. J. Beckman; A. T. Bell; J. E. Bercaw; C. Creutz; E. Dinjus; D. A. Dixon; K. Domen; D. L. DuBois; J. Eckert; E. Fujita; D. H. Gibson; W. A. Goddard; D. W. Goodman; J. Keller; G. J. Kubas; H. H.

Kung; J. E. Lyons; L. E. Manzer; T. J. Marks; K. Morokuma; K. M. Nicholas; R. Periana; L. Que; J. Rostrup-Nielson; W. M. H. Sachtler; L. D. Schmidt; A. Sen; G. A. Somorjai; P. C. Stair; B. R. Stults; W. Tumas, *Chem. Rev.*, **2001**, *101*, 953-996.

19. (a) M. M. Díaz-Requejo; P. J. Pérez, *Chem. Rev.*, **2008**, *108*, 3379-3394; (b) J. A. Labinger; J. E. Bercaw, *Nature*, **2002**, *417*, 507-514.

20. H. Chen; S. Schlecht; T. C. Semple; J. F. Hartwig, *Science*, **2000**, *287*, 1995-1997.

21. N. Barros; O. Eisenstein; L. Maron; T. D. Tilley, *Organometallics*, **2008**, *27*, 2252-2257.

22. T. R. Cundari; T. R. Klinckman; P. T. Wolczanski, *J. Am. Chem. Soc.*, **2002**, *124*, 1481-1487.

23. B. B. Wayland; S. Ba; A. E. Sherry, *J. Am. Chem. Soc.*, **1991**, *113*, 5305-5311.

24. A. S. Goldman; K. I. Goldberg In *Activation and functionalization of C-H bonds*, ACS Symp. Ser., 2004; pp 1-43.

25. A. Sen; M. Lin; L. C. Kao; A. C. Hutson, *J. Am. Chem. Soc.*, **1992**, *114*, 6385-6392.

26. R. H. Crabtree, *J. Chem. Soc., Dalton Trans.*, **2001**, 2437-2450.

27. (a) H. J. H. Fenton, *J. Chem. Soc., Trans.*, **1894**, *65*, 899-910; (b) C. Walling, *Acc. Chem. Res.*, **1975**, *8*, 125-131.

28. B. Meunier; S. P. De Visser; S. Shaik, *Chem. Rev.*, **2004**, *104*, 3947-3980.

29. J. C. Lewis; P. S. Coelho; F. H. Arnold, *Chem. Soc. Rev.*, **2011**, *40*, 2003-2021.

30. F. Hollmann; I. W. Arends; K. Buehler; A. Schallmeyer; B. Bühler, *Green Chem.*, **2011**, *13*, 226-265.

31. J. T. Groves; T. E. Nemo; R. S. Myers, *J. Am. Chem. Soc.*, **1979**, *101*, 1032-1033.

32. (a) H. Lu; X. P. Zhang, *Chem. Soc. Rev.*, **2011**, *40*, 1899-1909; (b) W. Nam; I. Kim; Y. Kim; C. Kim, *Chem. Commun.*, **2001**, 1262-1263.

33. (a) P. A. Grieco; T. L. Stuk, *J. Am. Chem. Soc.*, **1990**, *112*, 7799-7801; (b) J. T. Groves; R. Neumann, *J. Am. Chem. Soc.*, **1989**, *111*, 2900-2909; (c) R. F. Moreira; P. M. Wehn; D. Sames, *Angew. Chem. Int. Ed.*, **2000**, *39*, 1618-1621.

34. (a) T. D. Bugg, *Tetrahedron*, **2003**, *59*, 7075-7101; (b) M. Costas; M. P. Mehn; M. P. Jensen; L. Que, *Chem. Rev.*, **2004**, *104*, 939-986.

35. M. S. Chen; M. C. White, *Science*, **2007**, *318*, 783-787.

36. R. Hage; J. E. Iburg; J. Kerschner; J. H. Koek; E. L. Lempers; R. J. Martens; U. S. Racherla; S. W. Russell; T. Swarthoff; M. R. P. van Vliet, *Nature*, **1994**, *369*, 637-639.
37. J. L. Smith; G. B. Shul'pin, *Tetrahedron Lett.*, **1998**, *39*, 4909-4912.
38. (a) T. Tano; M. Z. Ertem; S. Yamaguchi; A. Kunishita; H. Sugimoto; N. Fujieda; T. Ogura; C. J. Cramer; S. Itoh, *Dalton Trans.*, **2011**, *40*, 10326-10336; (b) P. Vanelderren; R. G. Hadt; P. J. Smeets; E. I. Solomon; R. A. Schoonheydt; B. F. Sels, *J. Catal.*, **2011**, *284*, 157-164.
39. H. M. Davies; X. Dai; M. S. Long, *J. Am. Chem. Soc.*, **2006**, *128*, 2485-2490.
40. (a) B. J. Li; S. L. Tian; Z. Fang; Z. J. Shi, *Angew. Chem. Int. Ed.*, **2008**, *47*, 1115-1118; (b) P. Gandeepan; K. Parthasarathy; C.-H. Cheng, *J. Am. Chem. Soc.*, **2010**, *132*, 8569-8571; (c) B. Xiao; Y. Fu; J. Xu; T.-J. Gong; J.-J. Dai; J. Yi; L. Liu, *J. Am. Chem. Soc.*, **2009**, *132*, 468-469; (d) G. Cai; Y. Fu; Y. Li; X. Wan; Z. Shi, *J. Am. Chem. Soc.*, **2007**, *129*, 7666-7673; (e) D.-H. Wang; T.-S. Mei; J.-Q. Yu, *J. Am. Chem. Soc.*, **2008**, *130*, 17676-17677; (f) Y. Lu; D.-H. Wang; K. M. Engle; J.-Q. Yu, *J. Am. Chem. Soc.*, **2010**, *132*, 5916-5921; (g) C. Huang; B. Chattopadhyay; V. Gevorgyan, *J. Am. Chem. Soc.*, **2011**, *133*, 12406-12409; (h) M. Yu; Z. Liang; Y. Wang; Y. Zhang, *J. Org. Chem.*, **2011**, *76*, 4987-4994.
41. E. M. Simmons; J. F. Hartwig, *Nature*, **2012**, *483*, 70-73.
42. A. A. Fokin; P. R. Schreiner, *Chem. Rev.*, **2002**, *102*, 1551-1594.
43. B. Wang, *Oxidation of Unfunctionalized Olefins Involving Three-membered Heterocycles and Its Related Applications*. ProQuest: 2008; p 2.
44. N. Sawwan; A. Greer, *Chem. Rev.*, **2007**, *107*, 3247-3285.
45. W. Adam; C. R. Saha-Möller; P. A. Ganeshpure, *Chem. Rev.*, **2001**, *101*, 3499-3548.
46. P. Bovicelli; P. Lupattelli; E. Mincione; T. Prencipe; R. Curci, *J. Org. Chem.*, **1992**, *57*, 5052-5054.
47. A. Arnone; M. Cavicchioli; V. Montanari; G. Resnati, *J. Org. Chem.*, **1994**, *59*, 5511-5513.
48. N. C. Deno; L. A. Messer, *J. Chem. Soc., Chem. Commun.*, **1976**, 1051a-1051a.
49. S.-I. Murahashi; N. Komiya; Y. Oda; T. Kuwabara; T. Naota, *J. Org. Chem.*, **2000**, *65*, 9186-9193.

50. B. Carpenter; N. C. O. Tomkinson, Cardiff University: 2011; Unpublished Results.
51. J. E. Dubois; M. El-Alaoui; J. Toullec, *J. Am. Chem. Soc.*, **1981**, *103*, 5393-5401.
52. J. Cerkovnik; B. Plesnicar; J. Koller; T. Tuttle, *J. Org. Chem.*, **2008**, *74*, 96-101.
53. B. Neises; W. Steglich, *Angew. Chem. Int. Ed. Engl.*, **1978**, *17*, 522-524.
54. (a) E. W. Francis; W. S. James. Process for the purification of organic peroxides. 1957, 1965; (b) W. E. Parker; C. Ricciuti; C. Ogg; D. Swern, *J. Am. Chem. Soc.*, **1955**, *77*, 4037-4041.
55. F. P. Greenspan, *J. Am. Chem. Soc.*, **1946**, *68*, 907-907.
56. J. K. Crandall; S. A. Sojka; J. B. Komin, *J. Org. Chem.*, **1974**, *39*, 2172-2175.
57. X.-b. Zhao; T. Zhang; Y.-j. Zhou; D.-h. Liu, *Chinese J. Chem. Eng.*, **2008**, *8*.
58. (a) J. Frey; Z. Rappoport, *J. Am. Chem. Soc.*, **1996**, *118*, 5169-5181; (b) J. Frey; Z. Rappoport, *J. Am. Chem. Soc.*, **1996**, *118*, 5182-5191.
59. E. Taylor; A. McKillop; G. Hawks, *Org. Synth.*, **1988**, *50*, 549-551.
60. C. W. Jones, *Applications of hydrogen peroxide and derivatives*. Royal Society of Chemistry: 1999; Vol. 2, p 39.
61. C.-S. Lu; E. Hughes; P. A. Giguère, *J. Am. Chem. Soc.*, **1941**, *63*, 1507-1513.
62. N. Kornblum, *Angew. Chem. Int. Ed. Engl.*, **1975**, *14*, 734-745.
63. A. Dias; C. Gonçalves; J. Legido; J. Coutinho; I. Marrucho, *Fluid Phase Equilib.*, **2005**, *238*, 7-12.
64. J.-P. Begue; D. Bonnet-Delpon; B. Crousse, *Synlett*, **2004**, *2004*, 18-29.
65. A. Búcsi; O. L. Malkina; V. G. Malkin; P. Mach, *Appl Magn Reson*, **2002**, *22*, 1-10.
66. S. D. Ross, *J. Am. Chem. Soc.*, **1946**, *68*, 1484-1485.
67. L. Ghosez; R. Montaigne; A. Roussel; H. Vanlierde; P. Mollet, *Tetrahedron*, **1971**, *27*, 615-633.
68. O. Grummitt; A. Buck; R. Egan, *Org. Synth.*, **1946**, *26*, 21.
69. W.-w. Huang; H. Henry-Riyad; T. T. Tidwell, *J. Am. Chem. Soc.*, **1999**, *121*, 3939-3943.
70. M. Alajarin; B. Bonillo; M.-M. Ortin; R.-A. Orenes; A. Vidal, *Org. Biomol. Chem.*, **2011**, *9*, 6741-6749.
71. D. R. Lide, *CRC Handbook of Chemistry and Physics*, **2005**, *89*, 9-71.

72. J. Clayden; N. Greeves; S. Warren, *Organic Chemistry*. OUP Oxford: 2001; p 1027.
73. D. H. Barton; D. Doller, *Acc. Chem. Res.*, **1992**, *25*, 504-512.
74. M. Pettersson; S. Tuominen; M. Räsänen, *J. Phys. Chem. A*, **1997**, *101*, 1166-1171.
75. I. Montgomery; A. F. Parsons; F. Ghelfi; F. Roncaglia, *Tetrahedron Lett.*, **2008**, *49*, 628-630.
76. C. Schweitzer; R. Schmidt, *Chem. Rev.*, **2003**, *103*, 1685-1758.
77. G. Tonachini; H. B. Schlegel; F. Bernardi; M. A. Robb, *J. Am. Chem. Soc.*, **1990**, *112*, 483-491.
78. S. Miyamoto; G. R. Martinez; M. H. G. Medeiros; P. Di Mascio, *J. Am. Chem. Soc.*, **2003**, *125*, 6172-6179.
79. R.-r. Cui; L.-z. Deng; W.-b. Shi; H.-p. Yang; G.-h. Sha; C.-h. Zhang, *Quant. Electron.*, **2011**, *41*, 139.
80. <http://www.hw.ac.uk/schools/engineering-physical-sciences/staff-directory/filipe-vilela.htm>.
81. K. Zhang; D. Kopetzki; P. H. Seeberger; M. Antonietti; F. Vilela, *Angew. Chem.*, **2013**, *125*, 1472-1476.
82. T. Nishimi; T. Kamachi; K. Kato; T. Kato; K. Yoshizawa, *Eur. J. Org. Chem.*, **2011**, *2011*, 4113-4120.
83. G. B. Payne; P. H. Deming; P. H. Williams, *J. Org. Chem.*, **1961**, *26*, 659-663.
84. S. Jankowski; R. Kamiński, *J. Label. Compd. Radiopharm.*, **1995**, *36*, 373-376.
85. I. Reile; A. Paju; A.-M. Müürisepp; T. Pehk; M. Lopp, *Tetrahedron*, **2011**, *67*, 5942-5948.
86. (a) F. G. Bordwell; A. Knipe, *J. Org. Chem.*, **1970**, *35*, 2956-2959; (b) D. Ballard; B. Tighe, *J. Chem. Soc. B*, **1967**, 976-980; (c) E. Grunwald; S. Winstein, *J. Am. Chem. Soc.*, **1948**, *70*, 841-846; (d) C. Walling; E. S. Savas, *J. Am. Chem. Soc.*, **1960**, *82*, 1738-1744; (e) J. E. Leffler; R. G. Zepp, *J. Am. Chem. Soc.*, **1970**, *92*, 3713-3718; (f) W. Adam; R. Rucktaeschel, *J. Am. Chem. Soc.*, **1971**, *93*, 557-559; (g) R. Wheland; P. D. Bartlett, *J. Am. Chem. Soc.*, **1970**, *92*, 6057-6058.
87. K. M. Jones. On the Metal-Free Dihydroxylation of Alkenes. PhD Thesis, Cardiff University, 2010.

88. P. D. Bartlett; R. E. McCluney, *J. Org. Chem.*, **1983**, *48*, 4165-4168.
89. R. Criegee, *Angew. Chem. Int. Ed. Engl.*, **1975**, *14*, 745-752.
90. (a) S. B. Said; J. Skarżewski; J. Młchowski, *Synth. Commun.*, **1992**, *22*, 1851-1862; (b) R. Zeng; H. Sheng; Y. Zhang; Y. Feng; Z. Chen; J. Wang; M. Chen; M. Zhu; Q. Guo, *J. Org. Chem.*, **2014**, *79*, 9246-9252.
91. N. J. Turro; M.-F. Chow; Y. Ito, *J. Am. Chem. Soc.*, **1978**, *100*, 5580-5582.
92. C. Kolano; G. Bucher; H. H. Wenk; M. Jäger; O. Schade; W. Sander, *J. Phys. Org. Chem.*, **2004**, *17*, 207-214.
93. C. Yuan; Y. Liang; T. Hernandez; A. Berriochoa; K. N. Houk; D. Siegel, *Nature*, **2013**, *499*, 192-196.
94. F. D. Greene, *J. Am. Chem. Soc.*, **1959**, *81*, 1503-1506.
95. M. Jones; M. R. DeCamp, *J. Org. Chem.*, **1971**, *36*, 1536-1539.
96. M. J. Rawling. Metal-Free *Syn*-Dihydroxylation of Alkenes using Malonoyl Peroxides. PhD Thesis, University of Strathclyde, 2013.
97. J. C. Griffith; K. M. Jones; S. Picon; M. J. Rawling; B. M. Kariuki; M. Campbell; N. C. O. Tomkinson, *J. Am. Chem. Soc.*, **2010**, *132*, 14409-14411.
98. M. B. Smith; J. March, *March's Advanced Organic Chemistry: Reactions, Mechanisms, and Structure*. 6th ed.; John Wiley & Sons: 2007; p 279.
99. K. Fujimori; Y. Oshibe; Y. Hirose; S. Oae, *J. Chem. Soc., Perkin Trans. 2*, **1996**, 413-417.
100. M. J. Rawling; J. H. Rowley; M. Campbell; A. R. Kennedy; J. A. Parkinson; N. C. Tomkinson, *Chem. Sci.*, **2014**, *5*, 1777-1785.
101. (a) M. J. Darmon; G. B. Schuster, *J. Org. Chem.*, **1982**, *47*, 4658-4664; (b) J. E. Porter; G. B. Schuster, *J. Org. Chem.*, **1985**, *50*, 4068-4071.
102. M. Khalid; S. P. Souza Jr; L. F. M. Ciscato; F. H. Bartoloni; W. J. Baader, *Photochem. Photobiol. Sci.*, **2015**.
103. D. R. Vij, *Luminescence of Solids*. Springer Science + Business Media New York: New York, 1998; p 393.
104. (a) S. Sarker; L. Nahar, *Chemistry for pharmacy students: general, organic and natural product chemistry*. John Wiley & Sons: 2007; p 76; (b) J. Murto, *Acta Chem. Scand.*, **1964**, *18*, 1043-1053; (c) B. Dyatkin; E. Mochalina; I. Knunyants, *Tetrahedron*, **1965**, *21*, 2991-2995.

105. (a) A. Sakakura; S. Nakagawa; K. Ishihara, *Nat. Protocols*, **2007**, 2, 1746-1751;
(b) T. T. Vo; D. A. Parrish; J. n. M. Shreeve, *J. Am. Chem. Soc.*, **2014**, 136, 11934-11937.
106. H. C. Brown; Y. Okamoto, *J. Am. Chem. Soc.*, **1958**, 80, 4979-4987.
107. P. Rys; P. Skrabal; H. Zollinger, *Angew. Chem. Int. Ed. Engl.*, **1972**, 11, 874-883.
108. M. B. Smith; J. March, *March's Advanced Organic Chemistry: Reactions, Mechanisms, and Structure*. 6th ed.; John Wiley & Sons: 2007; p 412.
109. S.-Y. Choi; P. H. Toy; M. Newcomb, *J. Org. Chem.*, **1998**, 63, 8609-8613.
110. R. Hollis; L. Hughes; V. W. Bowry; K. U. Ingold, *J. Org. Chem.*, **1992**, 57, 4284-4287.
111. Q. Zhao; J. Sun; J. Li; J. He, *Catal. Commun.*, **2013**, 36, 98-103.
112. H. Dalton; P. C. Wilkins; N. Deighton; I. D. Podmore; M. C. R. Symons, *Faraday Discuss.*, **1992**, 93, 163-171.
113. A. Dragan; T. M. Kubczyk; J. H. Rowley; S. Sproules; N. C. Tomkinson, *Org. Lett.*, **2015**.
114. G. Moussa; N. Eweiss, *J. App. Chem.*, **1970**, 20, 281-284.
115. F. F. Blicke; E.-P. Tsao, *J. Am. Chem. Soc.*, **1953**, 75, 5587-5590.
116. C. De Risi; L. Ferraro; G. P. Pollini; S. Tanganelli; F. Valente; A. C. Veronese, *Biorg. Med. Chem.*, **2008**, 16, 9904-9910.
117. C. Michejda; R. Comnick, *J. Org. Chem.*, **1975**, 40, 1046-1050.
118. G. Boyd; M. Harms, *J. Chem. Soc. C*, **1970**, 807-810.
119. S. D. Darling; R. L. Kidwell, *J. Org. Chem.*, **1968**, 33, 3974-3975.
120. T. Cohen; I. H. Song; J. H. Fager; G. L. Deets, *J. Am. Chem. Soc.*, **1967**, 89, 4968-4975.
121. P. Frøyen, *Phosphorus, Sulfur Silicon Relat. Elem.*, **1994**, 91, 145-151.
122. T. Kano; K. Sasaki; K. Maruoka, *Org. Lett.*, **2005**, 7, 1347-1349.
123. H. Dinçalp; O. Çimen; T. Ameri; C. J. Brabec; S. İçli, *Spectrochim. Acta Mol. Biomol. Spectros.*, **2014**, 128, 197-206.
124. F. S. Mancilha; B. A. DaSilveira Neto; A. S. Lopes; P. F. Moreira; F. H. Quina; R. S. Gonçalves; J. Dupont, *Eur. J. Org. Chem.*, **2006**, 2006, 4924-4933.
125. R. K. Singh; S. Danishefsky, *J. Org. Chem.*, **1975**, 40, 2969-2970.
126. A. M. Eliassen; R. P. Thedford; K. R. Claussen; C. Yuan; D. Siegel, *Org. Lett.*, **2014**, 16, 3628-3631.

127. C. C. Chan; Y. W. Chen; C. S. Su; H. P. Lin; C. F. Lee, *Eur. J. Org. Chem.*, **2011**, 2011, 7288-7293.
128. J. F. Cívicos; D. A. Alonso; C. Nájera, *Adv. Synth. Catal.*, **2013**, 355, 203-208.
129. S. Tanaka; A. Mori, *Eur. J. Org. Chem.*, **2014**, 2014, 1167-1171.
130. J. Cadogan; I. Sadler, *J. Chem. Soc. B*, **1966**, 1191-1205.
131. E. Cahard; F. Schoenebeck; J. Garnier; S. P. Cutulic; S. Zhou; J. A. Murphy, *Angew. Chem.*, **2012**, 124, 3733-3736.
132. S. L. Jain; V. B. Sharma; B. Sain, *J. Mol. Catal. A: Chem.*, **2005**, 239, 92-95.